

EEG signatures of schizophrenia: visual backward masking and microstates

Thèse N° 9507

Présentée le 21 juin 2019

À l'École Polytechnique Fédérale de Lausanne
à la Faculté des sciences de la vie
Laboratoire de psychophysique

et

À l'Instituto Superior Técnico (IST) da Universidade de Lisboa
Programme doctoral en neurosciences

et

Doutoramento em Engenharia Biomédica

pour l'obtention du grade de Docteur ès Sciences (PhD)

par

Janir Nuno RAMOS ANTUNES DA CRUZ

Acceptée sur proposition du jury

Prof. J. Gräff, président du jury
Prof. M. Herzog, Prof. P. Figueiredo, directeurs de thèse
Prof. C. Michel, rapporteur
Prof. T. Koenig, rapporteur
Prof. F. Hummel, rapporteur

2019



TÉCNICO
LISBOA



Pá nhas kretxeu...

Acknowledgments

First of all, I want to thank my supervisors Patrícia and Michael not only for accepting me as a Ph.D. student in their laboratories but also for their support, constant guidance and freedom to explore the research questions that I deemed interesting as well as setting boundaries to my “Dora, the explorer”-mode when my projects and ideas were going everywhere without focus. I truly enjoyed working with and learning from these two genuine people, who had complementary functions throughout my studies.

Many thanks to the great people of LPSY and LaSEEB, you guys need no *Bonferroni* at all. The atmosphere in both labs is so chill, supportive, and collaborative - a true life enriching experience. I learned a great deal from you and it was an honor to be part of such groups. I am sure every single one of you has a great future in front of you. A special *merci* to Ophélie. We did the hiring days together, our projects were so complementary to each other, we spent hours and hours discussing about science and problems, supporting each other, etc., and now we are graduating just a few weeks apart. Thank you for everything! A big thank you to Marc Repnow, the guy that keeps LPSY running. You are one of the smartest and most meticulous people I have ever met. We all look up to you.

Thank you to the great Georgian team lead by Maya and Eka, without whom this work would not have been possible. To the anonymous participants in our experiments, my most sincere thank you.

A special gratitude for Fundação para a Ciência e a Tecnologia (FCT) and the National Center of Competence in Research (NCCR) Synapsy for providing funding for the work.

I also want to thank Carmen and João for the fruitful collaboration and support during the writing and submission process of the dominance paper. After each “I regret to inform you...”, you were always there to keep the motivation high and ready to work hard to improve the paper and prepare for the next submission (How many of them? 15+?). Thanks a lot.

My sincere thanks to Noé. You are just amazing. From the day you went to pick me up at the Lausanne train station until today, you have been like a brother to me. Thank you for hosting me and helping me in every single aspect possible. Thank you for introducing me to your beautiful family and friends. You guys made me feel like home.

I want to thank my cousin/sister Isy for the beautiful year in Lisbon. I love your outgoing spirit and your positive attitude towards life, truly inspiring. I cannot thank you enough for being there for me every single day.

To my sister Jackye, thank you for everything. You have been a role model my whole life and I will always look up to you. Thank you for bringing Kemi, Dara, and Jacob into my life. To Jacob, thank you very, very much for always pushing me to aim for more and never settle for anything less than the best. If I am doing a Ph.D. it is largely because of you. You have been a great role model and mentor.

To Aline, my partner in crime and my most significant finding, thank you for making my life easier and for being so caring, loving, and supporting. You are a true blessing in my life. You and your family have been nothing but a source of joy. Thank you!

To my aunt, or better, second mom, Naná, thank you. You have the biggest heart in the whole world. I wish that I could be more like you.

To my mom and dad, I cannot thank you enough for everything you did to and for me. You have always been there for me even when I did not deserve it. I am the luckiest person on Earth for having such a beautiful family. I know that I do not say it enough but I love you!

Contents

Abstract	1
Résumé.....	3
Resumo.....	5
Preface.....	7
1 Introduction.....	9
1.1 Endophenotypes.....	10
1.2 EEG in schizophrenia	11
1.3 Visual backward masking deficits.....	13
1.4 Abnormal EEG microstates dynamics.....	17
1.5 Handling EEG artifacts	20
1.6 Aims of the present work	22
2 Results.....	23
2.1 Automatic EEG pre-processing pipeline.....	23
2.2 EEG correlates of visual backward masking in unaffected siblings of schizophrenia patients.....	27
2.3 Inter-trial variability in schizophrenia patients.....	32
2.4 Neural correlates of target enhancement	37
2.5 Resting-state EEG microstates in schizophrenia.....	42
3 General discussion	47
3.1 Visual backward masking.....	47
3.2 EEG microstates.....	52
3.3 Implications	54
3.4 Conclusions	55
3.5 Future work.....	58
Bibliography	59
Appendix A.....	73
Appendix B	95

Appendix C.....	109
Appendix D	161
Appendix E.....	205
Appendix F.....	223
Curriculum Vitae.....	243

Abstract

Schizophrenia is a complex and devastating mental disorder that influences how one behaves, feels, and thinks. It affects a little less than 1 % of the world population and it is understood to be partly genetically mediated. Several genetic risk factors of schizophrenia have been identified. However, efforts to functionally characterize the genetic risk of schizophrenia have not been successful. To link the genetic risk to schizophrenia phenotype, schizophrenia research has turned to quantifiable stable trait markers with a clear genetic connection, so-called endophenotypes. Endophenotypes research in schizophrenia has heavily relied on the use of electroencephalogram (EEG) to identify endophenotypes and to better understand the neural mechanisms of neuropsychological candidate endophenotypes for schizophrenia.

Here, I used high-density EEG to study two promising candidate endophenotypes of schizophrenia: visual backward masking (VBM) and EEG microstates. To cope with the heterogeneity of schizophrenia, I analyzed data from more than 300 participants (including schizophrenia patients, their unaffected siblings, healthy students scoring either high or low in schizotypal traits, patients with a first episode of psychosis, and healthy controls) performing a masking task or at rest. To deal with undesired signals that may affect the measurements and change the EEG signals of interest in a time-efficient manner and to minimize experts' subjectivity, I first proposed and validated an automatic pre-processing pipeline. This pipeline was subsequently used to pre-process all the analyzed EEG data.

In a VBM study, performance of siblings was in between the ones of patients and controls (endophenotype concept). In patients, masking deficits were associated with decreased EEG amplitudes. In siblings, contrary to expectation, EEG amplitudes were even higher than in controls, which I interpret as a compensation signal. Based on EEG source localization, I propose that siblings over-activate a network of brain areas, including the right insula as a key player, to compensate for the deficits.

In an EEG microstates study, schizophrenia patients, their siblings, and patients with a first episode of psychosis showed abnormal microstate dynamics compared to controls (endophenotype concept). Interestingly, siblings showed atypical dynamics of a particular microstate compared to patients, which I interpret also as a compensation signal. A similar result was also found in high schizotypes.

My findings suggest that, even if there are genetic risks for developing schizophrenia, the brain is somehow capable of compensating for them. A better understanding of these compensation mechanisms and their commonalities might help to explain why some siblings develop schizophrenia, while others do not, which might open new avenues for characterization of schizophrenia and possible treatments of the disorder.

Keywords: schizophrenia, siblings, EEG, endophenotypes, visual backward masking, microstates, compensation, first episode of psychosis, schizotypy, automatic pre-processing

Résumé

La schizophrénie est un trouble mental complexe et dévastateur qui influence la façon dont on se comporte, on se sent et on pense. Ce trouble affecte un peu moins de 1 % de la population mondiale et est supposé être partiellement expliqué par la génétique. Plusieurs facteurs de risque génétiques de la schizophrénie ont été identifiés. Cependant, les efforts pour caractériser le fonctionnement du risque génétique de la schizophrénie n'ont pas été concluants. Afin d'établir un lien entre le risque génétique et le phénotype de la schizophrénie, la recherche sur la schizophrénie s'est tournée vers des marqueurs de traits stables et quantifiables dotés d'un lien génétique clair, appelés endophénotypes. La recherche sur la schizophrénie a largement compté sur l'utilisation de l'électroencéphalogramme (EEG) pour identifier des endophénotypes et également pour mieux comprendre les mécanismes neuronaux des candidats neuropsychologiques aux endophénotypes de la schizophrénie.

Dans ma thèse, j'ai utilisé l'EEG de haute densité pour étudier deux candidats prometteurs aux endophénotypes de la schizophrénie: le masquage visuel rétrograde (*visual backward masking*; VBM) et les micro-états de l'EEG. Pour faire face à l'hétérogénéité de la schizophrénie, j'ai analysé les données de plus de 300 participants (y compris des patients schizophrènes, leurs frères et sœurs non affectés par la maladie, des étudiants en bonne santé présentant des traits schizotypiques élevés ou faibles, des patients présentant un premier épisode de psychose et des contrôles sains) alors qu'ils effectuaient une tâche de VBM ou lorsqu'ils se reposaient. Afin de traiter efficacement les signaux indésirables susceptibles d'affecter les mesures et de modifier les signaux d'intérêt de l'EEG et dans le but de minimiser la subjectivité des experts, j'ai d'abord proposé et validé une méthode de pré-traitement automatique des données de l'EEG. Cette méthode a ensuite été utilisée pour pré-traiter toutes les données EEG que j'ai analysées.

Dans une étude sur le VBM, la performance des frères et sœurs des patients schizophrènes se situait entre celles des patients et des contrôles (concept de l'endophénotype). Chez les patients, les déficits en VBM étaient associés à une diminution des amplitudes de l'EEG. Chez les frères et sœurs des patients schizophrènes, contrairement aux attentes, les amplitudes de l'EEG étaient encore plus élevées que chez les contrôles, ce que j'interprète comme un signal de compensation. Basé sur l'étude de la localisation de la source de l'EEG, je propose que les frères

et sœurs des patients schizophrènes suractivent un réseau de zones cérébrales, comprenant l'insula droite en tant qu'acteur clé, afin de compenser leurs déficits.

Dans une étude sur les micro-états de l'EEG, les patients schizophrènes, leurs frères et sœurs et les patients présentant un premier épisode de psychose ont montré une dynamique anormale des micro-états par rapport aux contrôles (concept de l'endophénotype). Fait intéressant, les frères et sœurs des patients schizophrènes ont présenté une dynamique atypique d'un micro-état spécifique par rapport aux patients, ce que j'interprète également comme un signal de compensation. Un résultat similaire a été observé chez les étudiants en bonne santé présentant des traits schizotypiques élevés.

Mes résultats suggèrent que même s'il existe des risques génétiques pour développer la schizophrénie, le cerveau est en quelque sorte capable de compenser ces risques. Une meilleure compréhension de ces mécanismes de compensation et de leurs points communs pourrait aider à expliquer pourquoi certains frères et sœurs développent la maladie tandis que d'autres ne la développent pas, ce qui pourrait ouvrir de nouvelles perspectives pour la caractérisation de la schizophrénie et le développement de traitements possibles de la maladie.

Mots-clés: schizophrénie, frères et sœurs, EEG, endophénotypes, masquage visuel rétrograde, micro-états, compensation, premier épisode de psychose, schizotypie, pré-traitement automatique

Resumo

A esquizofrenia é um distúrbio mental complexo e devastador que influencia o modo como o indivíduo se comporta, se sente e pensa. Este distúrbio afeta um pouco menos de 1 % da população mundial e julga-se que seja parcialmente mediado pela genética, tendo já sido identificados vários fatores de risco genéticos. No entanto, os esforços para caracterizar funcionalmente os riscos genéticos para a esquizofrenia não têm sido bem sucedidos. Tendo em vista associar o risco genético ao fenótipo da esquizofrenia, a investigação em esquizofrenia têm-se focado em estabelecer marcadores estáveis e quantificáveis, com uma conexão genética clara, chamados endofenótipos. A pesquisa de endofenótipos da esquizofrenia tem-se baseado fortemente no uso do eletroencefalograma (EEG) para identificar endofenótipos, assim como para entender melhor os mecanismos neuronais de potenciais endofenótipos neuropsicológicos da esquizofrenia.

Neste trabalho, utilizei EEG de alta densidade para estudar dois potenciais endofenótipos da esquizofrenia: o mascaramento visual retrógrado (*visual backward masking*; VBM) e os microestados de EEG. De modo a lidar com a heterogeneidade subjacente à esquizofrenia, analisei dados de mais de 300 participantes (incluindo: doentes com esquizofrenia, os seus irmãos e irmãs não afetados/as pela doença, estudantes saudáveis com valores elevados ou baixos em questionários sobre características esquizotípicas, doentes com um primeiro episódio de psicose e controlos saudáveis) enquanto executavam uma experiência de VBM ou em repouso. Com o objetivo de minimizar a presença de sinais indesejáveis nos registos de EEG que pudessem afetar as medições e adulterar os sinais de interesse, propus e validei uma metodologia de pré-processamento automático para sinais de EEG, com especial foco na eficiência computacional e na sistematização (minimizando a subjetividade inerente aos peritos tipicamente responsáveis por este passo). Este método foi posteriormente usado no pré-processamento de todos os dados de EEG analisados.

Num estudo de VBM, o desempenho dos irmãos e irmãs dos doentes com esquizofrenia situou-se entre o desempenho dos doentes com esquizofrenia e o dos controlos (conceito de endofenótipo). Nos doentes, o mau desempenho na experiência de VBM foi associado a uma diminuição da amplitude dos sinais de EEG. Nos irmãos e irmãs, ao contrário do esperado, a amplitude dos sinais de EEG foi maior do que nos controlos, o que interpreto como sendo um sinal de compensação. Com base em resultados de localização cortical das fontes do EEG

registado nos eléctrodos, proponho que os irmãos e irmãs dos doentes com esquizofrenia ativam uma rede de regiões cerebrais (na qual se inclui a ínsula direita), cujo papel será crucial para compensar os défices observados nos doentes.

Num estudo de microestados de EEG, demostrei que doentes com esquizofrenia e os seus irmãos e irmãs, assim como doentes com um primeiro episódio de psicose apresentaram microestados de EEG com dinâmicas anormais quando comparados com controlos (conceito de endofenótipo). Curiosamente, os irmãos e irmãs dos doentes com esquizofrenia mostraram uma dinâmica atípica de um determinado microestado em comparação com os doentes, o que eu interpreto também como um sinal de compensação. Um resultado semelhante foi também encontrado em estudantes saudáveis com valores elevados em questionários sobre características esquizotípicas.

Os meus resultados sugerem que, mesmo que existam riscos genéticos para o desenvolvimento da esquizofrenia, o cérebro é, de alguma forma, capaz de compensar estes riscos. Uma melhor compreensão desses mecanismos de compensação e as semelhanças entre eles podem ajudar a explicar a razão para a qual alguns irmãos desenvolvem esquizofrenia, enquanto outros não, podendo abrir novos caminhos para a caracterização da esquizofrenia e o desenvolvimento de possíveis tratamentos para este distúrbio.

Palavras-chave: esquizofrenia, irmãos e irmãs, EEG, endophenótipos, mascaramento visual retrógrado, microestados, compensação, primeiro episódio de psicose, esquizotípico, pré-processamento automático

Preface

In this thesis, I present a selection of the work conducted in the course of my doctoral studies. In a first project, I collaborated with Prof. Carmen Sandi from the Laboratory of Behavioral Genetics at EPFL to study the influence of social dominance in decision making. Our results show that dominant individuals are faster to respond in choice situations, regardless of social context, and highlight an electrical brain signal that may represent a biomarker for social dominance disposition.

In subsequent works, I focused on my main topic: application of electroencephalography (EEG) to better understand the neurophysiological and neuropsychological abnormalities in schizophrenia. Since my work is based on EEG data from large samples of participants, I first proposed and validated a novel automatic pipeline to pre-process EEG data. Second, I analyzed data from a task-related EEG experiment with schizophrenia patients as well as their unaffected siblings and showed that both patients and their siblings have deficits compared to healthy controls. However, siblings are able to compensate for these deficits by over-activating a network of brain regions. Third, I re-analyzed the EEG data of schizophrenia patients, focusing on the inter-trial variability of the data, to better understand their task-related EEG deficits. Fourth, I conducted an EEG experiment in healthy participants to explore a neural mechanism that might be the cause of the above-mentioned deficits in schizophrenia patients. Last, I analyzed the resting-state EEG data, in which participants are not engaged in any task, of schizophrenia patients, their unaffected siblings, individuals with either high or low schizotypal traits, and patients with a first episode of psychosis, with a technique termed microstates analysis, and found evidence that it might be used as an early marker to discriminate people at risk to develop schizophrenia.

At the time of writing, 3 articles are published, 3 manuscripts are under review, 2 are in preparation, and one project is ongoing. A list of these projects is provided below. Published articles and pre-prints of the submitted manuscripts are provided in the appendix with permission of the copyright holders.

1. da Cruz, J. R., Rodrigues, J., Thoresen, J. C., Chicherov, V., Figueiredo, P., Herzog, M. H., & Sandi, C. (2018). Dominant men are faster in decision-making situations and exhibit a distinct neural signal for promptness. *Cerebral Cortex*, 28(10), 3740-3751. (Appendix A)

- Planned and conducted part of experiments, analyzed the data, and participated in writing of the manuscript.
2. da Cruz, J. R., Chicherov, V., Herzog, M. H., & Figueiredo, P. (2018). An automatic pre-processing pipeline for EEG analysis (APP) based on robust statistics. *Clinical Neurophysiology*, 129(7), 1427-1437. (Appendix B)
Conceptualized the pipeline, analyzed the data, and wrote the manuscript.
 3. da Cruz, J. R., Shaqiri, A., Roinishvili, M., Chkonia, E., Brand, A., Figueiredo, P., & Herzog, M. H. (under review). Neural compensation mechanisms of siblings of schizophrenia patients as revealed by high-density EEG. (Appendix C)
Analyzed the data, interpreted the results, and wrote the manuscript.
 4. Increased intra-participant variability in schizophrenia: evidence from single-trial EEG analysis (in preparation, section 2.3).
Analyzed the data.
 5. Neural correlates of target enhancement (in preparation, section 2.4).
Planned and conducted the experiments, and analyzed the data.
 6. da Cruz, J. R., Favrod, O., Roinishvili, M., Chkonia, E., Brand, A., Mohr, C., Figueiredo, P., & Herzog, M. H. (under review). EEG microstates: a candidate endophenotype for schizophrenia. (Appendix D)
Analyzed the data, interpreted the results, and wrote the manuscript.
 7. Favrod, O., Roinishvili, M., da Cruz, J. R., Brand, A., Okruashvili, M., Gramkrelidze, T., Figueiredo, P., Herzog, M. H., Chkonia, E., & Shaqiri, A. (2018). Electrophysiological correlates of visual backward masking in patients with first episode psychosis. *Psychiatry Research: Neuroimaging*, 282, 64-72. (Appendix E)
Participated in the analysis of the data and writing of the manuscript.
 8. Favrod, O., da Cruz, J. R., Roinishvili, M., Brand, A., Figueiredo, P., Herzog, M. H., & Chkonia, E. (under review). Electrophysiological correlates of visual backward masking in patients with depression. (Appendix F)
Participated in the analysis of the data and writing of the manuscript.
 9. Multiverse analysis of EEG data (ongoing).
Analyzed the data.

1 Introduction

Schizophrenia is a complex neuropsychiatric disorder characterized by positive symptoms, e.g., abnormal perceptual experiences to an external source (hallucinations) and distorted thinking (delusions), negative symptoms, e.g., reduction in affect and behavior, and disorganization of thoughts and behavior. Schizophrenia is also associated with impairments in basic sensory and higher cognitive functions, including reasoning and language. Schizophrenia is one of the top 15 leading causes of disability worldwide (Vos et al., 2017), affecting around 0.33 to 0.75 % of the world population (Moreno-Küstner, Martín, & Pastor, 2018).

A combination of genetic and environmental factors is involved in the development of schizophrenia (Owen, Sawa, & Mortensen, 2016). Despite an estimated heritability of 70 to 85 % (Burmeister, McInnis, & Zöllner, 2008), the genetic architecture of schizophrenia is still poorly understood (Sullivan, Daly, & O'Donovan, 2012). Several genetic risk factors of schizophrenia have been identified through family-based linkage studies or large-scale population-based genome-wide association studies (GWAS). At the time of writing, at least 138 distinct susceptibility genetic loci have been localized for schizophrenia (Li et al., 2017; Ripke et al., 2014; Stefansson et al., 2009; The International Schizophrenia Consortium, 2009; The Schizophrenia Psychiatric Genome-Wide Association Study (GWAS) Consortium et al., 2011; Yue et al., 2011). However, efforts to validate and functionally characterize the genetic risk of this complex disorder were not successful. First, the identified trait loci only explain a small portion of the genetic variance predisposing to schizophrenia (So, Gui, Cherny, & Sham, 2011; The International Schizophrenia Consortium, 2009). Second, the identified genetic loci do not mean true gene identifications, since the causal functional variants are yet to be identified (Glahn et al., 2014). Last, there is limited replication of these genetic findings, mainly due to a large number of genetic and environmental factors contributing to the pathophysiology of schizophrenia (Burmeister et al., 2008; Sanders et al., 2008). Therefore, schizophrenia research has turned to stable markers, so-called endophenotypes, as a means to link genetic risk to schizophrenia phenotype in a mechanistic way (Braff, Freedman, Schork, & Gottesman, 2007).

1.1 Endophenotypes

Endophenotypes are biological or psychological tests that reflect the actions of genes predisposing an individual to a specific disorder, even if there is no diagnosable pathology (Gottesman & Gould, 2003). Endophenotypes serve as separated components of a complex disorder phenotype, reflecting the action of fewer genes, therefore reducing the complexity analysis required to identify contributing genes. These endophenotypes can be used to characterize symptoms and behaviors using quantitative units of analysis that can be assessed in laboratories. Since endophenotypes are genetically *simpler* and provide greater statistical power through quantitatively ranking patients within a diagnostic category, they may improve the power to localize disease-related genes than imposing an artificial ill vs. non-ill threshold (Glahn et al., 2014).

The term endophenotype is sometimes used indiscriminately to describe distinctive characteristics/biological markers that individuals suffering from a condition possess. However, these biological markers can be primarily environmental, epigenetic, or multifactorial rather than genetic. Endophenotypes are a special subset of these markers. Most researchers agree that a candidate endophenotype should: (1) be associated with the disorder; (2) be heritable; (3) be independent of clinical state; (4) be apparent in unaffected relatives at higher rates than general population; (5) have high test-retest reliability; (6) be practical; (7) reflect a well-understood neurobiological mechanism (Gottesman & Gould, 2003; Turetsky et al., 2007).

Schizophrenia patients exhibit robust “deficits” in multiple laboratory-based neurophysiological and neuropsychological tests, ranging from cognition to information processing, as well as abnormal resting-state neurological metrics (Braff & Light, 2005; Chkonia, Roinishvili, Makhatadze, et al., 2010; Rieger, Diaz, Baeninger, & Koenig, 2016; Turetsky et al., 2007; Uhlhaas & Singer, 2010). Neurophysiological and neuropsychological deficits are an important dimension of schizophrenia and may be related to a considerable portion of functional deficiencies in patients’ daily lives (an der Heiden & Häfner, 2011). The presence of these deficits in schizophrenia patients and their unaffected relatives, as well as in healthy population with schizotypal personality, gives researchers a crucial insight into the development and understanding of endophenotypes. To this end, non-invasive endophenotypes research in schizophrenia has heavily relied on the use of neuroimaging tools to identify endophenotypes, understand their neural functions and abnormalities associated with the disease.

1.2 EEG in schizophrenia

For many decades, electroencephalography (EEG) was widely used to study the underlying mechanisms of neurophysiological and neuropsychological deficits in schizophrenia (Niedermeyer & Lopes da Silva, 2005). With the development of function magnetic resonance (fMRI) in the 1990s, giving new insights into the disorder through the interpretation of the hemodynamic signal associated with neuronal activity with high spatial resolution, EEG slowly lost its space. However, recently, EEG has attracted increased interest for the development and understanding of endophenotypes and biomarkers in general (McLoughlin, Makeig, & Tsuang, 2014). This has been mainly due to three reasons: (1) advances in signals processing improved EEG spatial resolution; (2) relatively low cost of EEG data collection, allowing the study of large cohorts, which is important for highly heterogeneous disorders, such as schizophrenia; (3) ease of use, allowing portability and application in participants that usually would be excluded from MRI studies.

The scalp EEG is believed to reflect the summated postsynaptic potentials of underlying cortical pyramidal neurons due to their unique orientation, perpendicular to the cortical surface (Niedermeyer & Lopes da Silva, 2005). Pyramidal neurons form about two-thirds of all the neurons in the mammalian cerebral cortex (Bekkers, 2011), making them extremely important in cognitive processes. The EEG changes with time, in an oscillatory fashion, which reflects not only intrinsic neural activity but also responses to specific internal and external events. In contrast to other neuroimaging techniques, it provides a direct and real-time measure of neural activity with millisecond temporal resolution, making it possible to assess neural dynamics at early stages of information processing.

Traditionally, the use of EEG in schizophrenia research has been mainly focused on the assessment of evoked-related potentials (ERPs), which are voltage changes time-locked to a stimulus, reflecting a specific neural process (Luck & Kappenman, 2013). Several neurophysiological candidate endophenotypes for schizophrenia have been proposed based on ERPs: sensory gating and P50 amplitudes, mismatch negativity (MMN), N100 amplitudes, N200 amplitudes, and P300 amplitudes (Braff & Geyer, 1990; Umbricht & Krljes, 2005; Turetsky et al., 2008; Ethridge et al., 2015; Jeon & Polich, 2003). In schizophrenia research, apart from the P300 amplitudes deficits, which are studied using visual or auditory oddball stimuli, all the other above-mentioned potentials are elicited using auditory stimuli. These candidate endophenotypes have been studied extensively and have high translational value since they can be modelled in animals (Owens, Bachman, Glahn, & Bearden, 2016; Turetsky et al., 2007).

A complementary approach to ERPs is to assess how stimuli cause event-related spectral perturbations (ERSPs) that change the intrinsic neuronal oscillations, within and across functional brain networks (Winterer & McCarley, 2011). Neuronal oscillations are derived by transforming the time-series of the EEG signals into amplitude and phase at several frequencies using spectral power and decomposition techniques like Fourier Transform or Wavelet Analysis. Typically, the oscillations measured by EEG are divided into five frequency bands, with the range of each band being slightly different for different researchers, however, they fall around the following values: delta (1 to 4 Hz), theta (4 to 8 Hz), alpha (8 to 12 Hz), beta (12 to 30 Hz), and gamma (30 to 100 Hz). Several studies have shown evidence that schizophrenia patients and their unaffected relatives have reduced power and phase synchronization of steady-state auditory responses in gamma-band to clicks, tone pipes, and amplitude modulated tones presented at 40 Hz (van der Stelt & Belger, 2007), thus suggesting deficits in the gamma-band activity as potential endophenotypes for schizophrenia (Ethridge et al., 2015; Owens et al., 2016).

Another approach is to use ERPs and ERSPs to gain insights into the neural mechanisms of neuropsychological candidate endophenotypes for schizophrenia. This approach has been successfully applied to better understand patients' deficits in the Continuous Performance Test (CPT; Ryman et al., 2018)¹, the Wisconsin Card Sorting Test (WCST; González-Hernández et al., 2002), working memory tasks (Okruszek, Jarkiewicz, Gola, Cella, & Łojek, 2018), visual backward masking tasks (VBM; Plomp et al., 2013), antisaccade tasks (Kirenskaya, Tkachenco, & Novototsky-Vlasov, 2017), and so on. Among the neuropsychological candidate endophenotypes, the ones based on visual processing are of great interest because of their good reproducibility, language independence, and contributions to higher cognitive impairments (Silverstein & Keane, 2011). VBM (section 1.3) is one of such candidate endophenotypes for schizophrenia (Braff & Freedman, 2002), particularly the shine-through masking paradigm, which has a much higher sensitivity and specificity for schizophrenia than most other cognitive and perceptual paradigms (Chkonia, Roinishvili, Makhatadze, et al., 2010; Herzog, Roinishvili, Chkonia, & Brand, 2013).

Considering the broad range of task-related deficits associated with schizophrenia, most likely some of these deficits are related, independent of the tasks, and

¹ There is some controversy whether CPT is or is not a candidate endophenotype for schizophrenia since first-order relatives of schizophrenia patients do not show deficits (Chkonia, Roinishvili, Herzog, & Brand, 2010).

can be found before stimulus presentation or even when the participant is not engaged in any task, i.e., at rest. In fact, EEG literature has long reported resting-state abnormalities in schizophrenia patients (Boutros et al., 2008; Rieger et al., 2016). The simplest quantifiable resting-state EEG measure that has long been studied in schizophrenia is the spectral EEG (Uhlhaas & Singer, 2010). Similar to ERSPs, in spectral EEG, we quantify the neural oscillations of the EEG signal. Increased power of slow waves (delta and theta) have been consistently found in schizophrenia patients, their unaffected relatives, and patients with first-episode of psychosis (Alfimova & Uvarova, 2003; Boutros et al., 2008; Koenig et al., 2001), suggesting the power of these slow waves as a candidate endophenotype for schizophrenia. Another quantifiable resting-state EEG measure that shows great sensitivity to schizophrenia is the EEG microstates (section 1.4). Several studies have reported deviant EEG microstates patterns in schizophrenia patients for more than 15 years (Rieger et al., 2016). These abnormalities have been suggested to correspond to core symptoms of schizophrenia, e.g., deficits of attention and saliency, and to be potential endophenotypes for the disorder (Tomescu et al., 2014, 2015).

1.3 Visual backward masking deficits

In visual backward masking (VBM), a briefly presented target is followed shortly by a mask, which decreases performance in discriminating the target (Breitmeyer & Ögmen, 2006). There are two kinds of masking, termed A- and B-type masking. In A-type masking, performance decreases monotonically when the inter-stimulus interval (ISI) between the target and mask decreases. In B-type masking, the strongest deterioration of performance occurs for intermediate ISIs. It is unknown how the mask is able to disrupt the processing of the target. One initial theory is the *dual channel model*, in which each stimulus is processed in a slower but sustained channel (P-system) and a faster but transient channel (M-system; Breitmeyer & Ganz, 1976). B-type masking occurs when a fast M-system signal created by the mask is able to catch up and inhibit the slower P-system signal of the target. While A-type masking occurs mainly due to intra-channel inhibition in both M- and P-system. However, this theory has been heavily criticized and many other explanations for the deterioration of performance have been proposed throughout the years (Bridgeman, 1978; Di Lollo, Enns, & Rensink, 2000; Enns, 2004; Francis, 2003; Herzog, Roinishvili, Chkonia, & Brand, 2013).

VBM is a powerful experimental tool for schizophrenia research (Herzog & Brand, 2015). Patients show strong and reproducible masking deficits and these

deficits have been proposed as candidate endophenotypes for schizophrenia (Chkonia, Roinishvili, Herzog, & Brand, 2010; Kéri, Kelemen, Benedek, & Janka, 2001; Nuechterlein, Dawson, & Green, 1994; Rund, Landrø, & Ørbeck, 1993). One particular masking paradigm that has a much higher sensitivity and specificity for schizophrenia than most other cognitive and perceptual paradigms is the shine-through masking paradigm (Chkonia, Roinishvili, Makhatadze, et al., 2010; Herzog et al., 2013).

In the shine-through paradigm, a target vernier is presented, i.e., two vertical bars separated by a horizontal offset (Figure 1.1). The lower bar can be offset either to the left or to the right and participants need to indicate the offset direction. After target presentation, a masking grating follows, which decreases monotonically performance on the target with shorter ISIs (A-type masking). The grating comprises aligned verniers, i.e., without offset, of the same length and width as the target vernier. If the grating comprises more than seven elements, the target vernier appears to be superimposed on the grating - shining through the grating -, i.e., subjectively looking brighter and wider than the target vernier really is (shine-through effect; Herzog & Koch, 2001). However, if the grating comprises less elements, e.g., five elements, the target vernier remains largely invisible whereas the grating appears to inherit some of the target, such as its offset, orientation or motion. This phenomenon is called the feature inheritance effect (Herzog & Koch, 2001). In schizophrenia patients, performance is only slightly deteriorated, compared to healthy controls, when the target vernier is presented alone (Roinishvili, Chkonia, Brand, & Herzog, 2008). However, performance strongly deteriorates when the target vernier is masked. This deterioration is much stronger in chronic schizophrenia patients, about five times more, than in healthy controls (Herzog, Kopmann, & Brand, 2004).

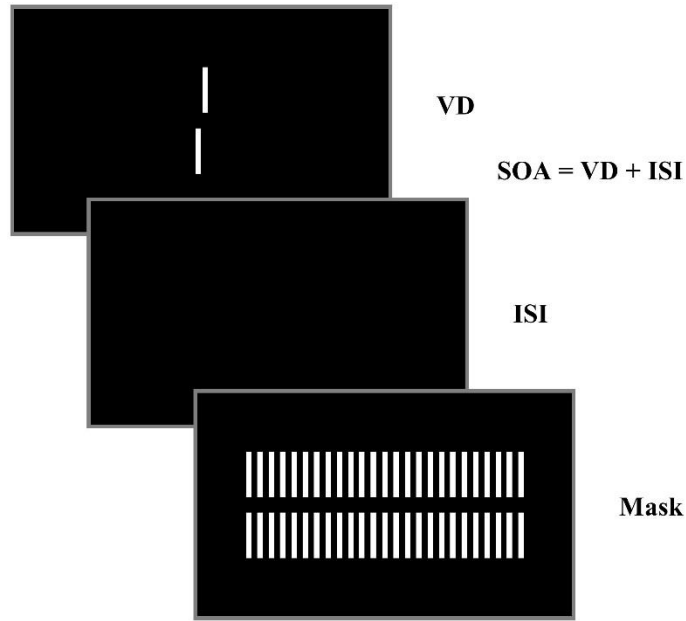


Figure 1.1 - Illustration of a typical shine-through masking trial. The paradigm is described in detail in Herzog et al. (2004). In short, for each participant, we determine the vernier duration (VD) for which the threshold of vernier discrimination is below 40" (arc seconds). In the next step, we present the vernier with the individual VD for each participant, followed by a blank screen during an inter-stimulus interval (ISI) and the mask (comprised of 25 aligned verniers) with a duration of 300 ms. We adaptively determine the target-mask stimulus-onset asynchrony ($SOA = VD + ISI$) such that it yields a performance level of 75 % correct responses, using Parametric Estimation by Sequential Testing (PEST; Taylor & Creelman, 1967). (Reprinted from da Cruz et al. (submitted b)).

The shine-through paradigm meets most of the main criteria of an endophenotype (Gottesman & Gould, 2003). First, unaffected first-order relatives (offspring, siblings, and parents) of schizophrenia patients show strong and reproducible deficits (Chkonia, Roinishvili, Makhatadze, et al., 2010; da Cruz et al., submitted b). Second, masking deficits do not change throughout one year in chronic schizophrenia patients (Chkonia, Roinishvili, Makhatadze, et al., 2010) and patients with first episodes of psychosis (Favrod et al., 2018), indicating that the shine-through paradigm is a trait rather than a state marker of the psychosis. Third, patients with functional psychosis, e.g., schizoaffective and bipolar patients, show similar masking deficits as schizophrenia patients, while abstinent alcoholics and depressive patients do not (Chkonia et al., 2012). Fourth, deficits are present already at early stages of the disorder since adolescents with psychosis also show masking

deficits (Holzer, Jaugey, Chinet, & Herzog, 2009). Fifth, students with high schizotypal traits, i.e., scoring high cognitive disorganization (CogDis), show masking deficits compared to with their peers with low schizotypal traits (Cappe, Herzog, Herzig, Brand, & Mohr, 2012). Finally, in schizophrenia patients, a single nucleotide polymorphism (SNP) related to the cholinergic nicotinic receptor ($\alpha 7$) was found to show a high correlation with masking deficits in the shine-through paradigm (Bakanidze et al., 2013).

The large behavioral deficits in chronic schizophrenia patients are associated with strongly decreased ERP amplitudes at around 200 ms after the target vernier presentation (Plomp et al., 2013). Similar results were found with a cohort of patients with first episode of psychosis (Favrod et al., 2018) as well as in students scoring high in CogDis compared to those scoring low (Favrod et al., 2017).

Summarizing all these findings, Herzog and colleagues proposed that masking deficits in schizophrenia are not visual deficits *per se* but are a manifestation of a general deficit of target enhancement and stabilization caused by dysfunctions of attention and/or the cholinergic system (Herzog et al., 2013). In *grosso modo*, whenever a target is presented for short durations or has a low contrast, only a weak neural response is elicited and target enhancement is needed to prevent overwriting by subsequently presented stimuli. The authors proposed that one potential mechanism of target enhancement might be attention. Attention deficits are core deficits in schizophrenia (Green, 2006). Without attention, performance is strongly deteriorated in weak and low contrast stimuli (Reynolds & Heeger, 2009) and attention can increase neuronal response in human primary visual cortex (Gandhi, Heeger, & Boynton, 1999). Based on the genetic findings (Bakanidze et al., 2013), the authors proposed that neuromodulation by the cholinergic nicotinic system as another potential mechanism of target enhancement, which might be deficient in patients. The cholinergic system, through acetylcholine release, is able to decrease responses to disturbing visual signals and also potentiate weak but important information (Picciotto, Higley, & Mineur, 2012), e.g., increase of neural responses to weak and low contrast target stimuli at the primary visual cortex (Disney, Aoki, & Hawken, 2007). In patients, the ERP amplitudes to the target are strongly diminished even when the mask is not presented (Plomp et al., 2013), which the authors relate to a diminished enhancement of neural activity. In other words, patients cannot translate the briefly presented target into stable neural representations, making the target more vulnerable to masking (Green, Lee, Wynn, & Mathis, 2011).

1.4 Abnormal EEG microstates dynamics

Multichannel EEG has evolved into a powerful tool capable of providing spatiotemporal information regarding brain (dys)function (Michel & Murray, 2012). One major advancement for characterizing the resting-state activity of the human brain, which has been shown to be particularly sensitive to schizophrenia, is microstate analysis (Khanna, Pascual-Leone, Michel, & Farzan, 2015; Michel & Koenig, 2018). Microstates are global patterns of scalp potential topographies that remain quasi-stable for around 60 to 120 ms before changing to a different topography that remains quasi-stable again, suggesting semi-simultaneity of activity among the nodes of large-scale brain networks (Lehmann, Ozaki, & Pal, 1987).

Four recurrent and dominant classes of microstates are observed in resting-state EEG (Figure 1.2), which explain around 65 to 84 % of the global variance of the data (Michel & Koenig, 2018). Several studies have attempted to identify the brain sources underlying these microstates (Britz, Van De Ville, & Michel, 2010; Custo et al., 2017; Milz, Pascual-Marqui, Achermann, Kochi, & Faber, 2017; Musso, Brinkmeyer, Mobascher, Warbrick, & Winterer, 2010; Pascual-Marqui et al., 2014; Yuan, Zotev, Phillips, Drevets, & Bodurka, 2012). It was found that these four EEG microstates classes were correlated with blood oxygenation level dependent (BOLD) fluctuations across brain regions overlapping with four of the resting-state networks (RSNs) commonly found in resting-state fMRI (Britz et al., 2010; Custo et al., 2017). The first microstate (class A) was associated with the auditory RSN, the second microstate (class B) with the visual RSN, the third microstate (class C) is with the salience RSN, and the last microstate (class D) with the attention RSN.

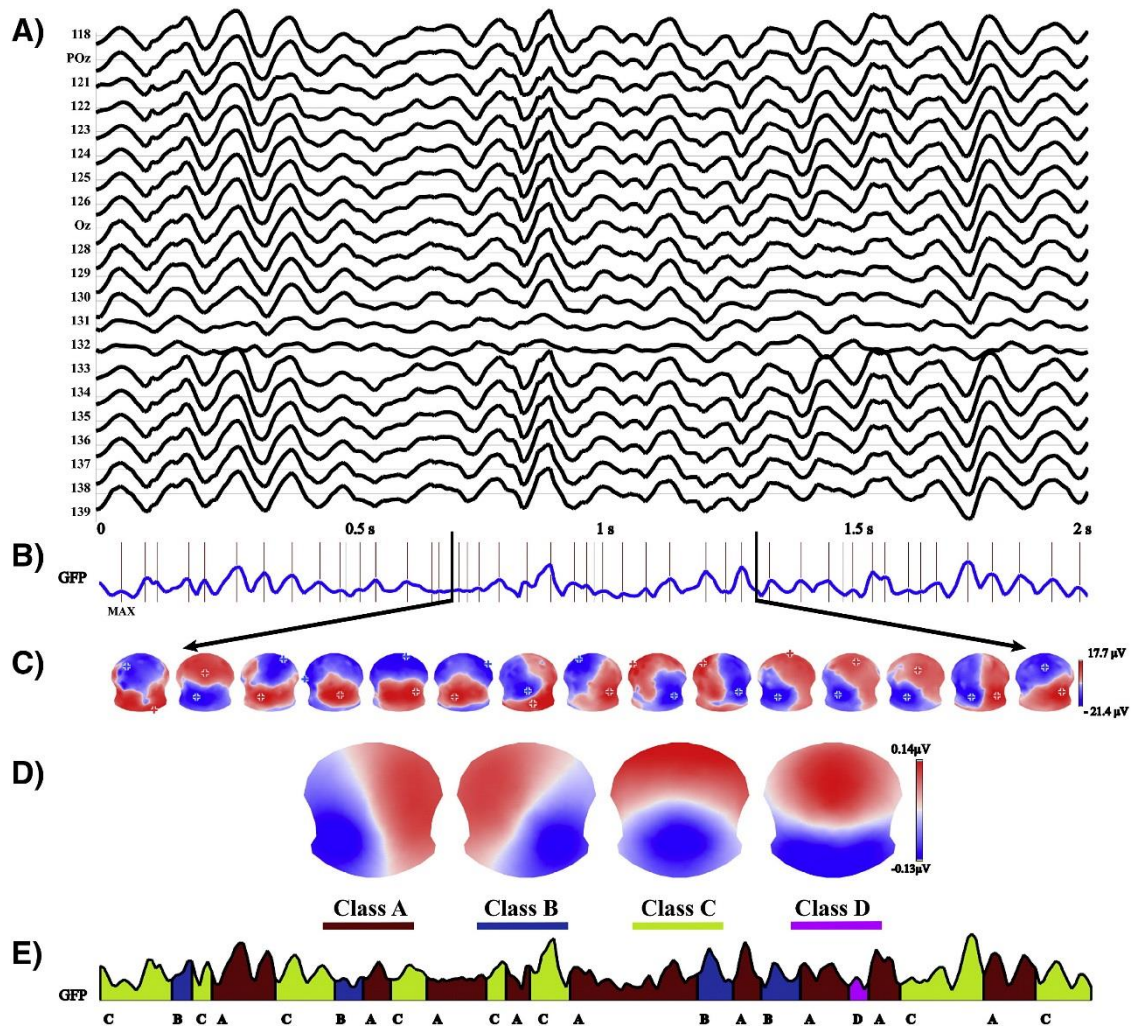


Figure 1.2 - Illustration of the EEG resting-state microstate analysis method. A) 2 s resting-state multichannel EEG signal. B) The Global Field Power (GFP) times series, which is a measure of the instantaneous field strength. The peaks of the GFP are marked by vertical lines, they represent instances of the highest field strength and are the best representatives of the topographic maps regarding signal-to-noise ratio (SNR). C) Topographic maps at consecutive GFP peaks. D) Spatial k -means cluster analysis of the GFP peaks of the whole EEG recording. Most studies of resting-state EEG microstates find the same microstates classes, traditionally labeled A to D. E) Each of the 4 maps is fitted back to the original EEG recording and each time point is labeled with the microstate class that it best correlates to. (Adapted from Tomescu et al. (2014). Reprinted with permission from Elsevier).

For almost 20 years, numerous studies have reported abnormalities in parameters characterizing the temporal dynamics of EEG microstates measured in schizophrenia patients compared to controls (Khanna et al., 2015; Michel & Koenig, 2018). Recently, a meta-analysis (Rieger et al., 2016) revealed that microstate class C occurred more frequently and for longer durations in schizophrenia patients than in controls. For microstate class D, it was found that it occurred less frequently and for shorter durations in patients compared to controls. Interestingly, the estimated effect sizes were larger than those typically found in spectral EEG. The same meta-analysis reported that microstate class B was shorter in patients than controls, but the effect was not significant after correction for multiple comparisons.

These aforementioned abnormal microstates dynamics are viewed as an imbalance between processes that load on saliency (microstates class C), which are increased, and processes that integrate contextual information (microstates class D), which are reduced (Rieger et al., 2016). This interpretation goes in line with the view of schizophrenia as a state of abnormal assignment of salience (Kapur, 2003) and a disorder affecting attentional processes, context update, and executive control (Fioravanti, Bianchi, & Cinti, 2012).

Similar abnormalities were also observed in medication-naïve schizophrenia patients (Irisawa et al., 2006), patients with first-episode of schizophrenia (Lehmann et al., 2005), and adolescents with 22q11.2 deletion syndrome, a population that has a 30 % risk of developing psychosis (Tomescu et al., 2014, 2015). These results have prompted researchers to suggest that abnormal parameters of EEG microstates may provide a potential endophenotype for schizophrenia.

Besides providing a potential endophenotype for schizophrenia, which could help to distinguish individuals at risk for developing the disorder, the abnormal microstates dynamics in schizophrenia might help to introduce new treatment options for the disorder. For example, it was shown that healthy participants can successfully up-regulate the duration of microstate class D in a neurofeedback experiment (Diaz, Rieger, Baenninger, Brandeis, & Koenig, 2016). Since shortening of microstates class D duration has been correlated with positive symptoms in schizophrenia patients (Kindler, Hubl, Strik, Dierks, & Koenig, 2011; Koenig et al., 1999), Diaz and colleagues (2016) proposed that using neurofeedback in patients may promote skills useful to reduce their positive symptoms. In addition, Sverak et al. (2018) showed that the application of intensive repetitive transcranial magnetic stimulation over the left dorsolateral prefrontal cortex decreased the oc-

currence of microstates class C in patients that showed positive effect to the treatment. In treatment responder patients, this occurrence of microstates class C was accompanied with a decrease of negative symptoms.

1.5 Handling EEG artifacts²

To cope with the heterogeneity of schizophrenia, increasingly larger samples of participants are being measured. In EEG experiments, this increasing volume of data becomes a problem, mainly due to the presence of artifacts. Artifacts are undesired signals that may affect the measurement and change the EEG signal of interest. These artifacts may arise from non-physiological noise sources that originate outside the participant, such as the grounding of the electrodes causing power line noise, interferences with other electrical devices, or imperfections in electrode settling. Artifacts may also arise from physiological noise sources originating within the participants, such as the ones produced by head, eye, or muscle movements (Urigüen & Garcia-Zapirain, 2015). Head movements may result in spikes and discontinuities due to a rapid change of impedance at one or several electrodes. Reflective eye movements occur frequently and are normally picked up by the frontal electrodes in the frequency range of the delta band. Blinking also contaminates the EEG signal, usually causing a more abrupt change in its amplitude than eye movements. Finally, every movement of the participant generates muscular artifacts that can be found everywhere on the scalp at frequencies higher than 20 Hz (within the beta and gamma bands range).

One simple way to deal with these artifacts is to remove segments of the data that exceed a certain level of artifact contamination, for example, signal amplitudes greater than ± 100 μ V. However, this approach may lead to the loss of a great amount of data that could still contain artifact-free information, therefore potentially compromising the subsequent analysis and interpretation of the data. This is true for both evoked-related potentials (ERPs) and resting-state (RS) signal fluctuations. Moreover, since participant generated artifacts may overlap in the spectral domain, and on many EEG channels, with the signal of interest, simple spatial and frequency band filtering approaches may be inefficient to remove this kind of artifacts (Tatum, Dworetzky, & Schomer, 2011). Another method that is commonly used to clean-up EEG data is independent component analysis (ICA;

² This section is based on the article “An automatic pre-processing pipeline for EEG analysis (APP) based on robust statistics”, da Cruz, J. R., Chicherov, V., Herzog, M. H., & Figueiredo, P., 2018, *Clinical Neurophysiology*, 129(7), 1427-1437 (Appendix B).

Makeig et al., 1996). Assuming that neuronal signals and noise recorded on the scalp are independent of each other, then the EEG signal can be described by their linear summation. The ICA is used to decompose the EEG data in statistically independent sources (ICs), so as to separate the neuronal and noise contributions to the signal. The artifactual ICs can then be identified and subsequently subtracted from the EEG data, yielding an artifact-free signal.

Usually, pre-processing of EEG data, including the classification of artifactual ICs, is performed under expert supervision. However, with the advent of both high-density EEG arrays (64-256 channels) and studies of large populations, yielding increasingly greater amounts of data, supervised methods have become excessively time consuming. To cope with this, and to minimize subjectivity, automatic methods have recently been presented (Abreu, Leite, Jorge, et al., 2016; Abreu, Leite, Leal, & Figueiredo, 2016; Bigdely-Shamlo, Mullen, Kothe, Su, & Robbins, 2015; Hatz et al., 2015; Nolan, Whelan, & Reilly, 2010). Fully automated statistical thresholding for EEG artifact rejection (FASTER; Nolan et al., 2010), for instance, enables a fully automated pre-processing of ERP data, based on computing z-scores of different signal metrics, and threshold them in order to detect bad channels, bad epochs and artifactual ICs. Tool for automated processing of EEG data (TAPEEG; Hatz et al., 2015) uses a similar approach for the automatic pre-processing of RS EEG data. However, because they are based on z-scores, these approaches are not robust to outliers and as a consequence they tend to have high rejection rates of artifact-free signal. A more promising approach is to use robust statistics instead. For example, the Prep pipeline (Bigdely-Shamlo et al., 2015) provides an automatic pre-processing pipeline including filtering and bad channels identification using the RANSAC (random sample consensus) algorithm. However, in this case the identified bad channels are assumed to be globally bad. Thus, if a channel contains artifactual periods, these are neglected and left in the pre-processed EEG data. Moreover, supervised inspection of pre-processed data for bad epochs is necessary since the Prep pipeline does not provide this feature.

In sum, multiple procedures for automatic pre-processing methods of EEG data have been developed in the last years. However, none of them stands out since there is a plethora of EEG artifacts contaminating the data, making it difficult to account for all of them, and most of proposed methods are adapted to specific scenarios.

1.6 Aims of the present work

As discussed in previous sections, several neurophysiological and neuropsychological candidate endophenotypes have been proposed for schizophrenia. Among these candidate endophenotypes, two of particular interest are VBM deficits and abnormal dynamics of resting EEG microstates. In schizophrenia patients, VBM deficits are associated with strongly decreased ERP amplitudes. However, it is still unknown whether unaffected siblings of schizophrenia patients share this reduction of amplitude, and if yes, to what extent. More importantly, the exact underlying mechanisms of this decreased ERP amplitudes are still unknown. Similarly, schizophrenia patients show abnormal dynamics of specific EEG microstate classes. However, we have no information on the resting EEG microstate dynamics in unaffected siblings of schizophrenia patients, which is important for an endophenotype. Therefore, the goal of this thesis is to address these major points by analyzing the behavioral and EEG data of patients, their unaffected siblings, and healthy controls while performing a VBM task and at rest.

The specific objectives comprise of the following:

1. EEG data quality improvement, by developing an automatic pre-processing and artifact rejection pipeline to handle large samples of both evoked and resting EEG data, which is needed to cope with the heterogeneity of schizophrenia. Details about the proposed pipeline and its validation are presented in section 2.1.
2. Investigate the EEG correlates of VBM deficits in unaffected siblings of schizophrenia patients. Results are presented in section 2.2.
3. Study the basis of the decreased VBM elicited ERP amplitudes in schizophrenia patients, by analyzing the inter-trial variability of the ERPs. Outcomes are presented in section 2.3.
4. Explore the neural mechanisms of target enhancement, an abnormality that might be at the core of schizophrenia patients' VBM deficits. Findings are presented in section 2.4.
5. Investigate whether abnormal EEG microstate dynamics are an endophenotype for schizophrenia, by testing schizophrenia patients, their unaffected siblings, students scoring high or low in schizotypal traits, and patients with a first episode of psychosis. Results are presented in section 2.5.

2 Results

2.1 Automatic EEG pre-processing pipeline

This section is based on the article “An automatic pre-processing pipeline for EEG analysis (APP) based on robust statistics”, da Cruz, J. R., Chicherov, V., Herzog, M. H., & Figueiredo, P., 2018, *Clinical Neurophysiology*, 129(7), 1427-1437 (Appendix B).

To cope with the heterogeneity in schizophrenia, we tested large samples of participants while recording their EEG signals with dense arrays. Precise artifact screening of such large amount of data becomes extremely time consuming. Here, I propose a novel automatic pre-processing EEG pipeline (APP) to handle large datasets (both evoked and resting data), which innovates relative to existing methods by not only following state-of-the-art guidelines but also further employing robust statistics.

APP consists of the following steps: (1) high-pass filtering, to eliminate signal low-frequency non stationarity (for example, slow drifts in the mean); (2) removal of power line noise, with minimum distortion; (3) re-referencing to a robust estimate of the mean of all channels; (4) removal and interpolation of bad channels; (5) removal of bad epochs; (6) removal of eye-movement, muscular-, and bad-channel related artifacts based on independent component analysis (ICA); and (7) removal of epoch artifacts. At each step of the pipeline, a number of relevant parameters are estimated from the data and outliers are detected based on a robust z-score and adjusted boxplot, chosen automatically depending on the distribution of the data, e.g., normality and skewness.

APP was tested on both ERP and RS data. ERP results were compared with FASTER (Nolan et al., 2010), a variant for automated ERP pre-processing, and supervised artifact detection by experts using CARTOOL (Brunet, Murray, & Michel, 2011). While RS results were compared with TAPEEG (Hatz et al., 2015), and Prep pipeline (Bigdely-Shamlo et al., 2015), as well as supervised artifact detection by experts using Cartool.

The ERP dataset consisted of data from 61 healthy controls and 44 schizophrenia patients performing a vernier discrimination task. This type of visual stimuli usually evokes a strong negative N1 component, around 200 ms after the stimulus onset, as measured by the global field power (GFP). Schizophrenia patients tend to have reduced amplitudes compared to healthy controls (Plomp et al., 2013). As shown in Figure 2.1, similar result, i.e., low N1 amplitudes for patients compared

to controls, were found using either APP, supervised inspection by experts, or FASTER. However, the N1 amplitudes obtained using APP were similar to the ones obtained using the supervised scheme but were significantly larger than the ones obtained using FASTER. Interestingly, the difference between the mean of the controls' N1 amplitudes and the mean of the patients' N1 amplitudes were larger for APP and the supervised scheme than the ones of FASTER.

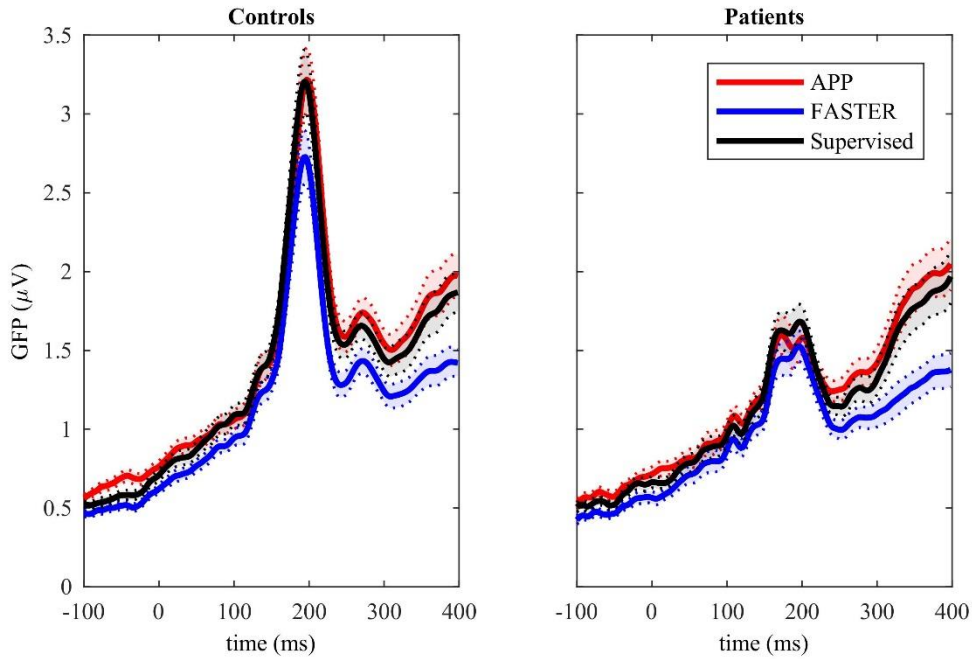


Figure 2.1 - The global field power (GFP) time series of the ERP data, for healthy controls (left) and patients (right), after pre-processing with APP (red), FASTER (blue), and the Supervised scheme (black). Solid lines represent the group mean and dashed lines represent plus or minus one standard error of the mean. (Adapted from da Cruz et al. (2018). Reprinted with permission from Elsevier).

As expected, patients had more bad trials than controls, for all pre-processing schemes, Figure 2.2. The supervised scheme rejected more trials than APP and FASTER. This might be the case because the experts did not use ICA to reduce artifacts nor interpolated channels that are bad just in specific trials, thus, considering those trials as bad overall. Considering, the two automatic methods, APP removed less bad trials than FASTER, however, the two methods removed similar amount of ICs. In terms of channels interpolated, APP interpolated similar num-

ber of channels as the supervised scheme, however, FASTER interpolated significantly more than the other two methods. In addition, FASTER interpolated more channels per trial than APP.

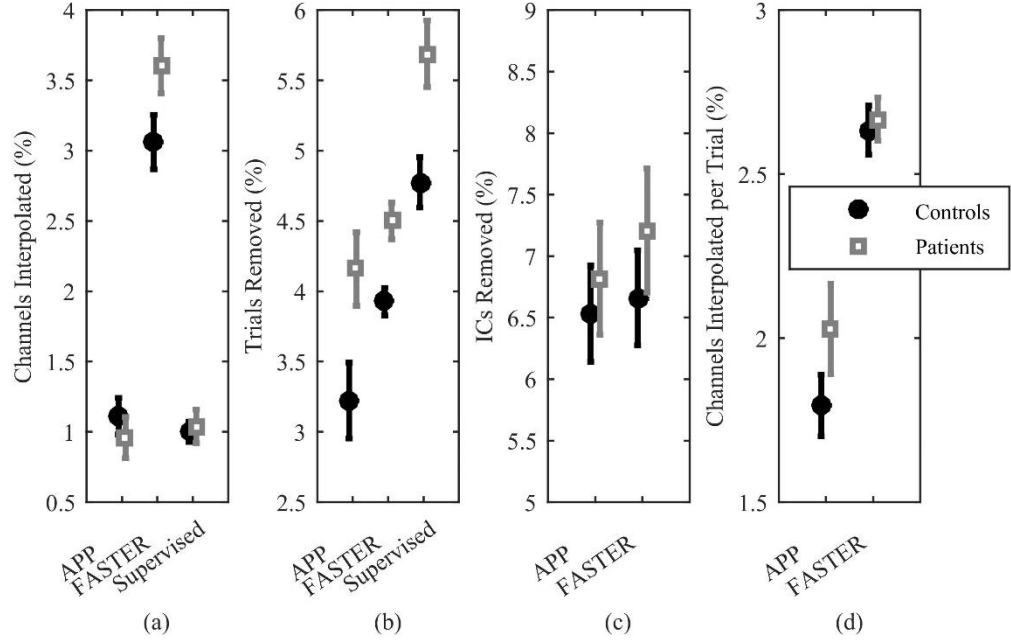


Figure 2.2 - Average percentage of channels interpolated (a), trials removed (b), independent components (ICs) removed (c), and channels interpolated per trial (d), for healthy controls and schizophrenia patients, using APP, FASTER, and Supervised artifact rejection (except for ICs removed and channels interpolated per trial). Error bars indicate the standard error of the mean. (Adapted from da Cruz et al. (2018). Reprinted with permission from Elsevier).

For the validation of APP on RS data pre-processing, data from 68 healthy participants *performing* a 5 min eyes-closed EEG recording was used. Similar levels of correlation were found for the power across multiple frequency bands between each of the three automatic pre-processing schemes (APP, TAPEEG, and Prep pipeline) and the expert supervision. In addition, as shown in Figure 2.3, APP removed and interpolated a similar number of channels as the supervised scheme and fewer than both TAPEEG and Prep pipeline. Regarding the amount of data segments rejected, EEG experts had to prune the data for artifactual segments, following Prep pipeline pre-processing, since this method does not incorporate such feature. Consequently, Prep pipeline and the supervised scheme rejected similar amount of data segments and significantly less than APP and TAPEEG. The

latter two methods use fixed epochs to prune the data for artifactual segments, which might cause the difference between the EEG experts supervision and the two fully automated methods. Considering only the two fully automated methods, APP removed significantly less epochs than TAPEEG but no statistically significant difference was found in terms of ICs removed. Additionally, TAPEEG interpolated more channels per epoch than APP.

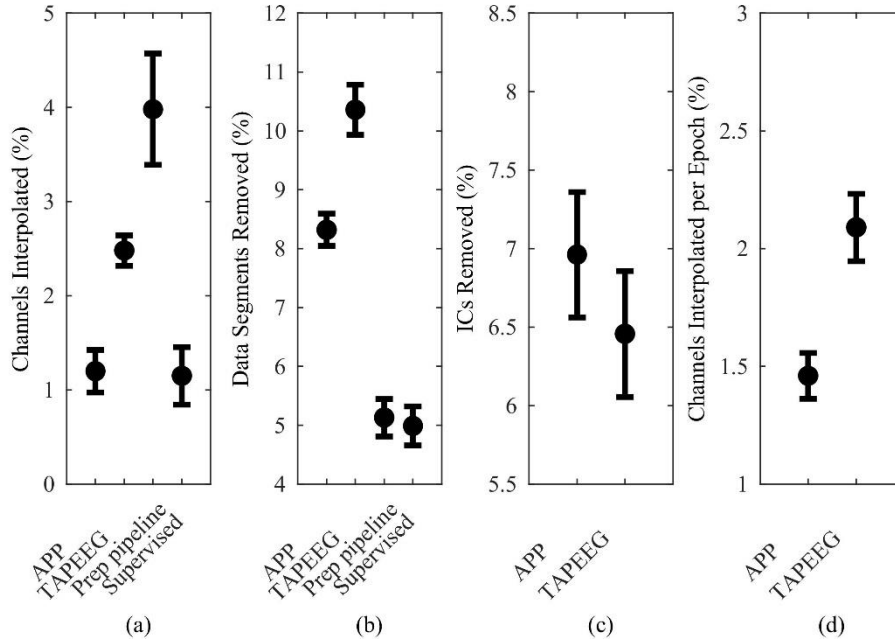


Figure 2.3 - Average percentage of channels interpolated (a), data segments removed (b), independent components (ICs) removed (c), and channels interpolated per epoch (d) using APP, TAPEEG, Prep pipeline, and Supervised artifact rejection (except for ICs removed and channels interpolated per epoch for the latter two methods). Error bars indicate the standard error of the mean. (Adapted from da Cruz et al. (2018). Reprinted with permission from Elsevier).

In conclusion, APP effectively removed EEG artifacts, performing similarly to the supervised scheme and outperforming existing automatic alternatives. Therefore, APP provides a reliable and efficient tool for pre-processing large datasets of both evoked and resting-state EEG, and was used in all subsequent works presented in this thesis.

2.2 EEG correlates of visual backward masking in unaffected siblings of schizophrenia patients

This section is based on the manuscript “Neural compensation mechanisms of siblings of schizophrenia patients as revealed by high-density EEG”, da Cruz, J. R., Shaqiri, A., Roinishvili, M., Chkonia, E., Brand, A., Figueiredo, P., & Herzog, M. H. (submitted, Appendix C).

Schizophrenia patients and, to a lesser extent, their unaffected relatives, show strong and reproducible masking deficits. In patients, masking deficits are associated with reduced ERP amplitudes, as measured by the GFP. Here, to unveil the neural mechanisms of VBM in schizophrenia, circumventing the illness specific confounds (e.g., medication, progression of the disease, and social situation), I investigated the EEG correlates of VBM in unaffected siblings of schizophrenia patients.

We tested 90 schizophrenia patients, 55 unaffected siblings of patients, and 76 healthy controls performing two variants of the shine-through masking paradigm. In experiment 1, we used the *classic* shine-through paradigm with subject-specific SOAs determined using PEST, as described in Figure 1.1. In experiment 2, we measured participants’ EEG while they performed another variant of the shine-through paradigm. We had to use exactly the same stimuli for all observers in order to study group differences in the EEG. To this end and to make sure that patients could do the task, we set the vernier duration (VD) to 30 ms, which was the average VD across patients in previous works (Chkonia, Roinishvili, Makhatadze, et al., 2010; Herzog et al., 2004). We had 4 stimulus conditions. In the simplest one, the Vernier Only condition, only the target was presented. In a slightly more difficult condition, the Long SOA condition, the mask followed the vernier with an SOA of 150 ms. In the hardest condition, the Short SOA condition, the target vernier was followed immediately by the mask, for an SOA of 30 ms. To ensure that our effects were due to the processing of the target, we included a control, the Mask Only, in which only the mask was presented.

In experiment 1, I replicated previous findings (Chkonia, Roinishvili, Makhatadze, et al., 2010), where the mean SOA of the siblings was in between the ones of patients and controls (Figure 2.4A). In experiment 2, performance of patients was inferior in the 3 conditions that contained the target vernier, while siblings and controls achieved similar performance (Figure 2.4B). As mentioned before, unlike in experiment 1, where we explored the individual differences with

an adaptive procedure, in the EEG experiment, we had the same stimuli for all participants and fixed the VD as the mean VD across patients. Likely for these reasons, the task was not challenging enough to bring out the group differences between siblings and controls.

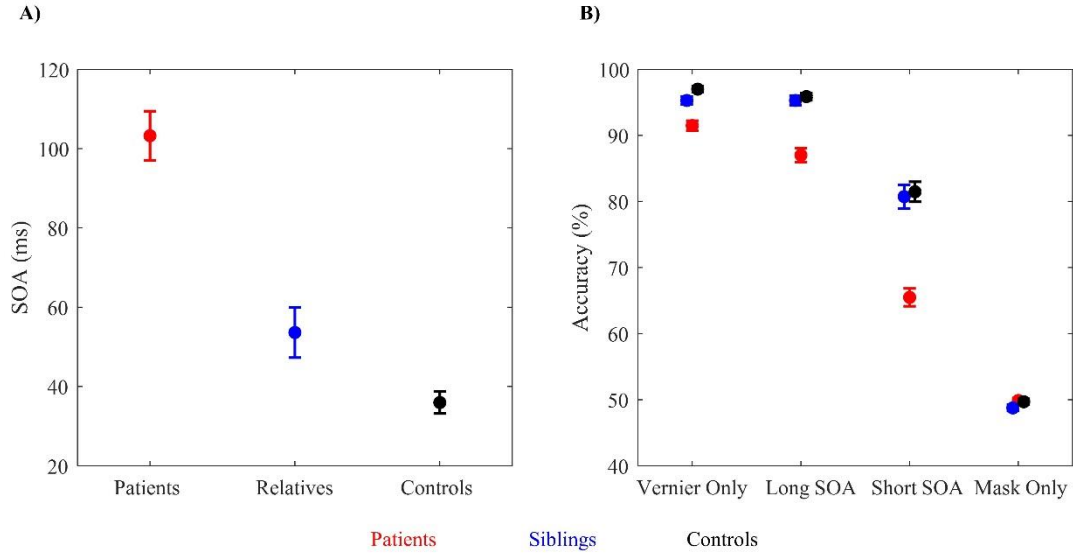


Figure 2.4 - Behavioral Results. A) Experiment 1. Mean SOA (stimulus onset asynchrony) for each group. Performance of siblings was significantly in between controls and patients. B) Experiment 2. Mean accuracy for each group for the 4 conditions. Patients were less accurate at discriminating the vernier offset compared to both siblings and controls. This difference in performance increased with task difficulty (Vernier Only < Long SOA < Short SOA). Siblings and controls performed at the same level. Error bars indicated standard error of the mean. (Reprinted from da Cruz et al. (submitted b)).

The GFP time course for patients, siblings, and controls in the 4 conditions are shown in Figure 2.5A. The GFP peak amplitudes of patients were lower than those of controls and siblings, for all conditions with the target vernier (Figure 2.5B). Interestingly, GFP peak amplitudes were higher in siblings compared to controls for the Vernier Only and Long SOA conditions. For siblings, GFP peak amplitudes were roughly at the same level in all the 3 conditions with the target vernier. For controls and patients, GFP peak amplitudes increased with task difficulty, i.e., from Vernier Only to Long SOA and to Short SOA conditions. Last, GFP peak amplitudes correlated positively with the behavioral performance.

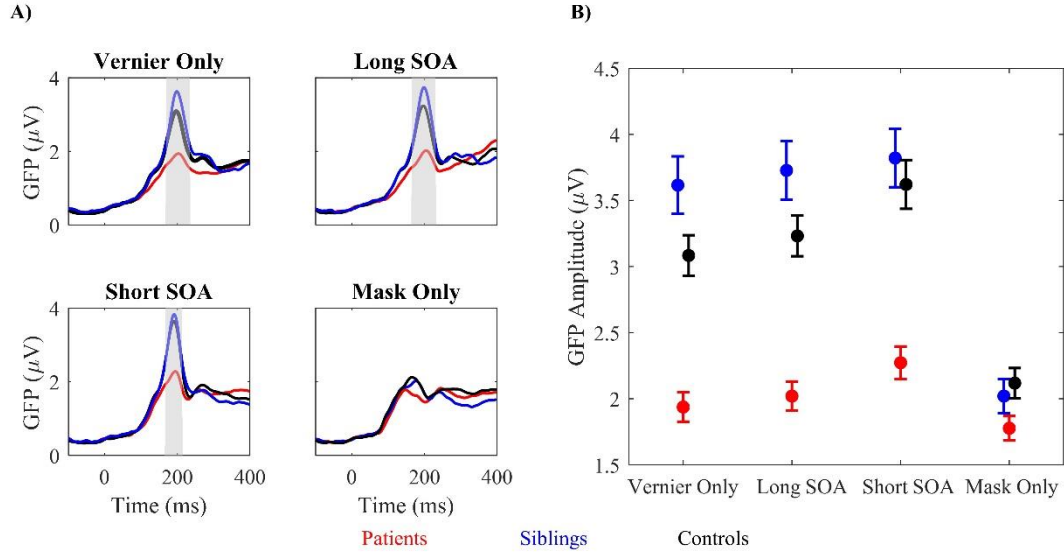


Figure 2.5 - A) Group average global field power (GFP) time series for patients, siblings, and controls, in the 4 conditions. GFP amplitudes were significantly different for the 3 groups at around 200 ms after stimulus onset for conditions with the target vernier (grey region). B) Group average GFP amplitudes at the peak latencies for all groups and conditions. Patients have decreased GFP peak amplitudes in all conditions with the target. Siblings have higher amplitudes than controls in the Vernier Only and Long SOA conditions. For patients and controls, GFP amplitudes are lower for the Long SOA than the Short SOA condition. For the siblings, the GFP amplitudes remained on a high level. Error bars indicate standard error of the mean. (Reprinted from da Cruz et al. (submitted b)).

Next, to identify the brain areas generating the GFP effects, from the individual averaged ERPs, we estimated current densities (CDs) throughout the brain's grey matter using a Local Auto-Regressive Average (LAURA; Grave de Peralta Menendez, Murray, Michel, Martuzzi, & Gonzalez Andino, 2004). I identified six EEG source clusters exhibiting statistically significant Group \times Condition interaction effects, as well as the corresponding average CD in each group (Figure 2.6). The clusters were located bilaterally in the middle temporal gyrus and insula, as well as in the precentral gyrus and the right precuneus.

I computed separated multiple linear regressions to predict the behavioral performance based on the estimated CDs of the center of mass of the six EEG source clusters. For the Vernier Only and Short SOA conditions, activity of the right insula predicted accuracy. For the Long SOA condition, activity of the right insula as well as the left precentral gyrus predicted accuracy.

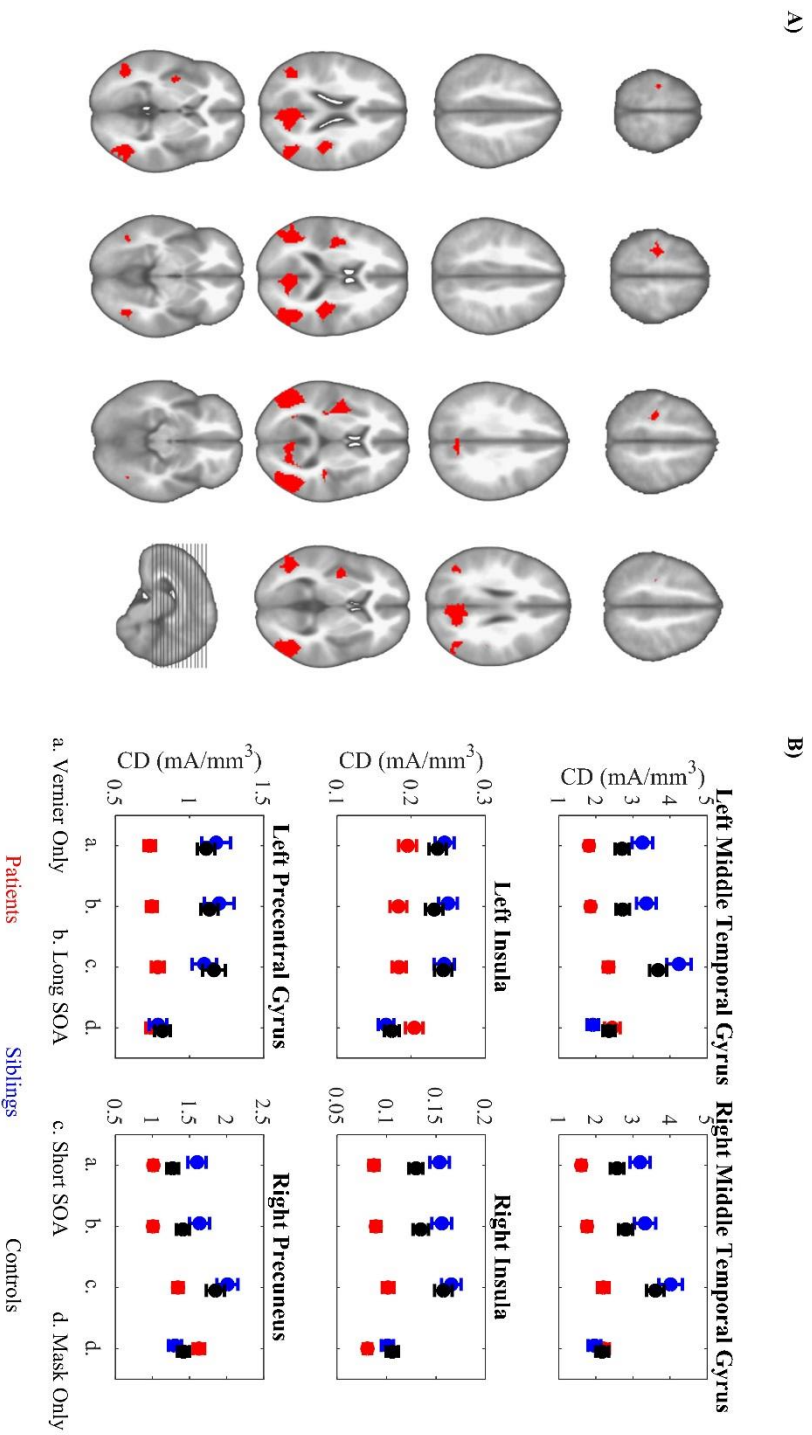


Figure 2.6 - A) Clusters of significant Group \times Condition effects are indicated in red. B) Average current density (CD) at the centers of mass for the six clusters, indicating the direction of the interaction effects. In general group differences are larger in the three conditions with the target vernier compared with the Mask Only condition. Error bars indicate standard error of the mean. (Reprinted from da Cruz et al. (submitted b)).

I interpret these results as a compensation signal. To process the target vernier, whose neural correlates are indexed by the ERP component at around 200 ms (Herzog et al., 2013), siblings might need to engage available neural resources in all conditions, independently of task difficulty. Indeed, the fact that ERP amplitudes in siblings remained stable across the 3 conditions with the target suggests that their ERP amplitudes were at ceiling. ERP amplitudes at around 200 ms have been shown to be susceptible to task difficulty (Philiastides, Ratcliff, & Sajda, 2006) and to engagement of attention (Eason, Harter, & White, 1969; Luck, Woodman, & Vogel, 2000). All these effects observed were specific to the target vernier and did not occur when only the mask was presented, suggesting that top-down processes are responsible for these effects. Since conditions were randomized, differences in attention are not expected.

The lack of behavioral differences between siblings and controls in the EEG experiment, suggests that by over-enhancing the neural responses to the target, i.e., increasing the activity of a network of brain regions, siblings, unlike patients, can partially compensate for their VBM deficits. In this network, the right insula, as a *center* that regulates the interaction between selective attention and arousal to keep focused on the target (Eckert et al., 2009), might play a key role. Too little activity of the right insula, as in patients, would probably lead to an impairment in collecting evidence for decision making. Too much activity of the right insula, as in siblings, might indicate that participants need to engage more to achieve a good performance. Nonetheless, by pushing the visual system to its limits, this compensation mechanism is too weak to fully compensate for the VBM deficits.

2.3 Inter-trial variability in schizophrenia patients

Single-trial ERPs have an extremely low signal-to-noise ratio (SNR) due to background brain activity as well as other physiological and instrumental noise. To increase ERP SNR, researchers average many trials measured under the same conditions, causing the background activity to be averaged out. This approach is very effective for early ERP components, which mainly reflect the properties of the stimulus, and whose latencies are very stable. However, for later components, which reflect complex brain information processing, latencies are more variable across trials (Kutas, McCarthy, & Donchin, 1977). If this latency variability is excessively large, it might lead to substantial distortion of the computed averaged ERP and subsequently biased results with limited interpretability.

In schizophrenia, it has been shown that patients tend to have increased ERP inter-trial variability, e.g., P50, P300, and MMN, compared to healthy controls (Jansen, Hu, & Boutros, 2010; Jordanov et al., 2011; Roth, Roesch-Ely, Bender, Weisbrod, & Kaiser, 2007; Shin et al., 2015). Computational models have suggested that this increased intra-individual variability might be due to increased *neural noise* in schizophrenia patients' brains, caused by randomly spiking neurons (Rolls, Loh, Deco, & Winterer, 2008). Since increased latency variability may result in a blurring of the ERP amplitudes, I investigated whether the decreased VBM-elicited N1 amplitudes in schizophrenia patients (da Cruz et al., submitted b; Plomp et al., 2013) arise from reduced neuronal activity or increased variability at the peak latencies.

I re-analyzed the ERP data from patients and controls from section 2.2, focusing on the latency variability of single-trial ERP. Single-trial ERP analysis remains a scientific challenge, mainly due to low ERP SNR (da Cruz, Wang, Wong, & Wan, 2014). One way to deal with the low SNR, at the single-trial level, is to use blind source separation (BSS) methods, e.g., independent component analysis (ICA). Contrasting to section 2.1, where I used ICA to estimate and remove activity of artifactual sources, here, ICA is used to estimate and extract the brain activity of interest, i.e., the ERP (Delorme, Palmer, Onton, Oostenveld, & Makeig, 2012). The basic ICA model is usually applied to single participant data since it is assumed that brain sources and their spatial location vary from participant to participant. To allow inferences in multi-participants/conditions studies, group-level ICA (gICA) has been proposed (Cong et al., 2013; Eichele, Rachakonda, Brakedal,

Eikeland, & Calhoun, 2011). ICs that constantly appear across participants/conditions can be estimated using gICA computed on the aggregate data containing observations from multiple subjects and conditions.

I used the EEGIFT toolbox (Eichele et al., 2011) to perform temporal ICA on single-trial ERP for multiple participants and conditions simultaneously ((90 patients + 76 controls) \times 4 conditions = 664 observations). For each observation separately, the single-trial data were reduced via principal component analysis (PCA) to 20 principal components (PCs; EEGIFT default). Individual PCs were then concatenated into an aggregate group data. The group data were decomposed via ICA, to estimate ICs that were consistently expressed across participants and conditions, using the Infomax algorithm (Bell & Sejnowski, 1995). This allowed us to estimate a group-level IC whose topography and activation time-course resembled the ERP topography at around 200 ms and ERP time-course at the occipital electrodes (the minima of the ERP amplitude at 200 ms; Figure 2.7).

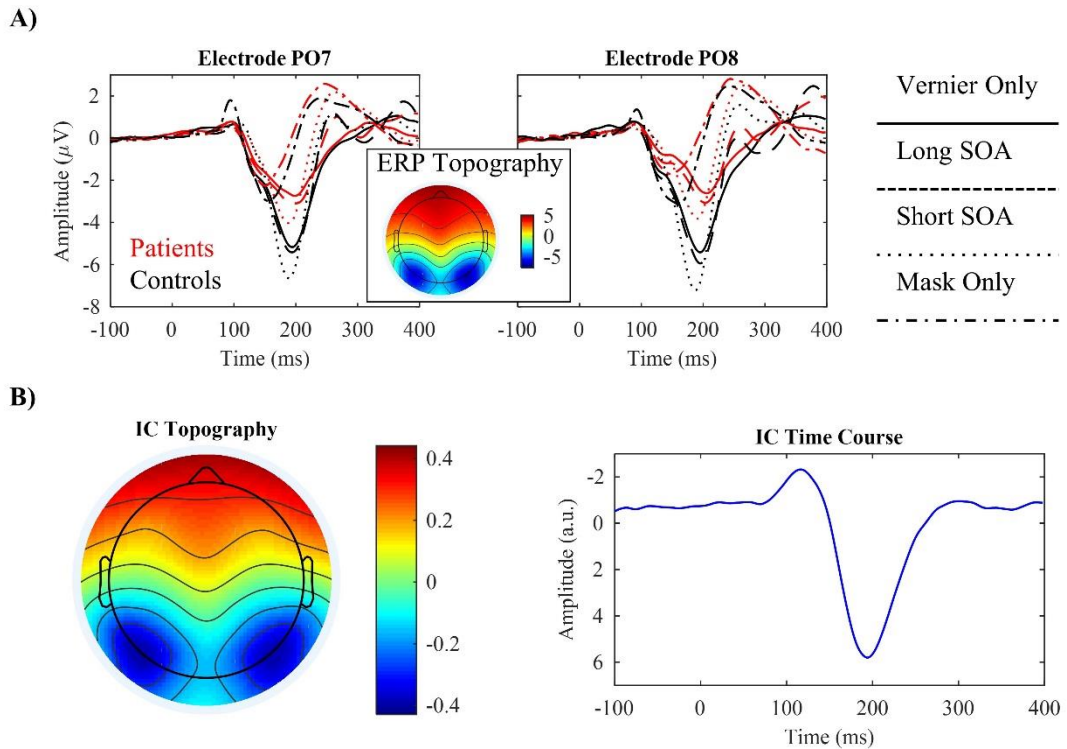


Figure 2.7 - A) Average ERP amplitudes at occipital electrodes for patients (in red) and controls (in black) in the 4 conditions. At around 200 ms, ERP topographies showed bilateral negativity resembling an N1 component. B) Group ICA across all participants and conditions identified an independent component (IC) with weight topography and activation time course resembling the N1 component.

The group-level IC of interest, shown in Figure 2.7B, was back-projected to each of individual data and the evoked-related IC N1 peak amplitude latency variability for each participant and condition was estimated using a graph-based method (Gramfort, Keriven, & Clerc, 2010). The method is comprised of two steps (Figure 2.8). First, the trials are sorted monotonically with respect to the latency using a manifold learning algorithm based on graph Laplacian. Second, the latencies are estimated using graph cuts. After the latencies estimation, the single-trial ICs are re-aligned according to the estimated mean latency of the N1 peak amplitude and the individual averaged evoked-related IC computed (Figure 2.9).

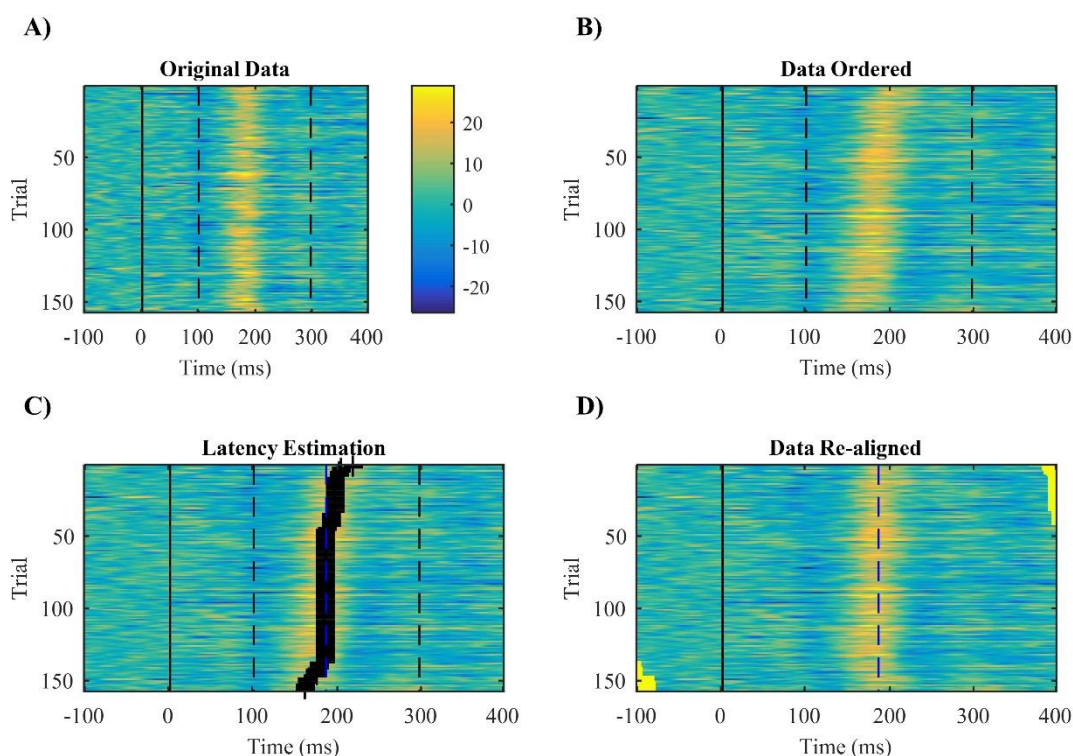


Figure 2.8 - The graph-based latency variability estimation method. A) Originally ordered trials of the evoked group-level independent component (IC) of interest back-projected to the individual data. B) Re-ordered trials based on graph Laplacian. C) Latency estimation based on graph cuts. D) Single-trial evoked-related ICs re-aligned to match the estimated mean latency of the N1 peak amplitude.

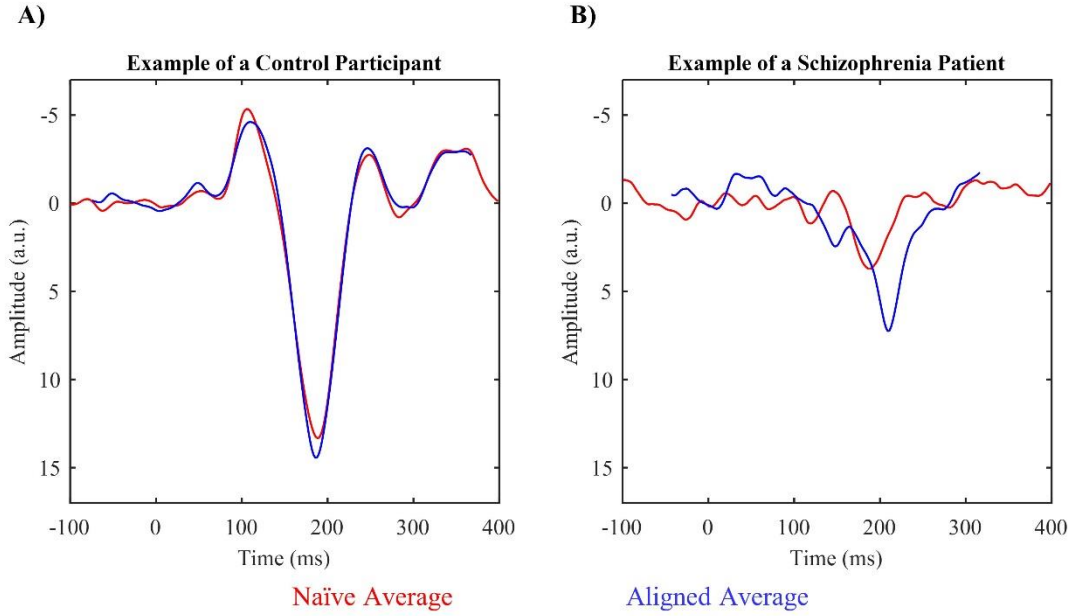


Figure 2.9 - Example of the difference between the naïve (red) and the mean N1 peak amplitude latency aligned (blue) evoked-related independent component (IC) for A) a healthy control, with low N1 peak latency variability, and B) a schizophrenia patient, with high N1 peak latency variability, for the Short SOA condition.

An ANOVA of the estimated N1 peak amplitude latency variability showed statistical significant main effects of Group ($F(1,164)=8.018$, $P=0.005$, $\eta^2=0.047$), Condition ($F(2.938,481.894)=41.301$, $P<0.001$, $\eta^2=0.198$), and an interaction effect ($F(2.938,481.894)=3.541$, $P=0.015$, $\eta^2=0.017$). Figure 2.10A displays this interaction, showing that patients had larger N1 peak amplitude latency variability than controls for all conditions with the target vernier; while in the Mask Only condition, patients' latency variability was comparable to controls ($p=0.584$, Bonferroni-Holm corrected for multiple comparisons).

After adjusting for the latency variability, patients still showed smaller N1 amplitudes compared to controls, for all the conditions with the target vernier (Figure 2.10B). An ANOVA of the re-aligned N1 peak amplitude showed statistical significant main effects of Group ($F(1,164)=7.863$, $P=0.006$, $\eta^2=0.046$), Condition ($F(2.457,402.906)=125.761$, $P<0.001$, $\eta^2=0.415$), and an interaction effect ($F(2.457,402.906)=12.924$, $P<0.001$, $\eta^2=0.043$). For the Mask Only condition, no significant difference was found between the two groups ($p=0.576$, Bonferroni-Holm corrected).

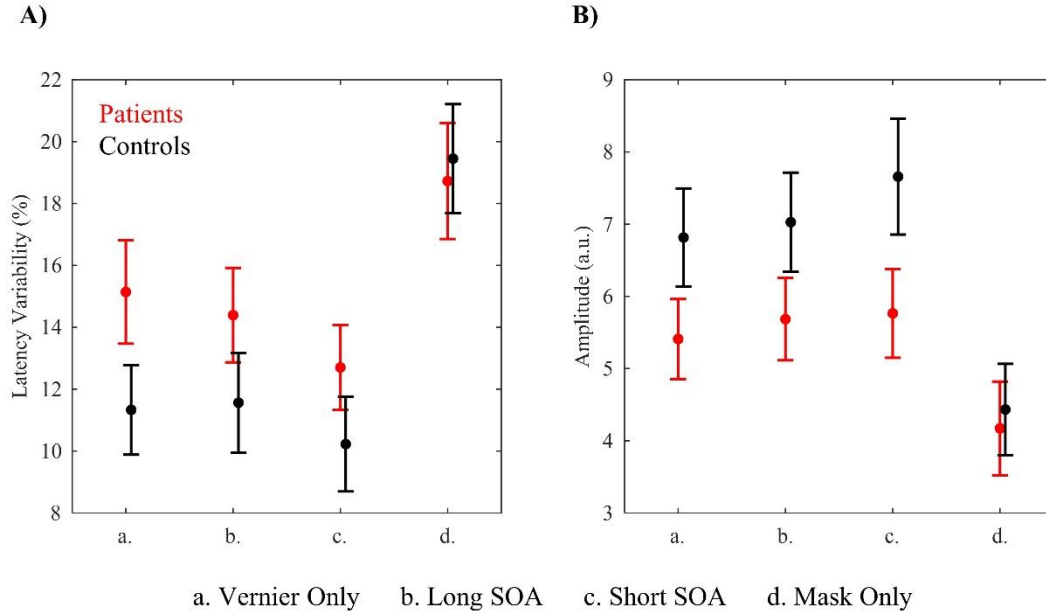


Figure 2.10 - A) N1 peak latency variability in terms of the individual mean latency of the N1 peak amplitude for schizophrenia patients (in red) and healthy controls (in black) in the 4 conditions. Patients had increased latency variability for all conditions with the target vernier. B) Mean N1 peak amplitude after correcting for the latency variability. Patients had decreased amplitudes compared to controls for all conditions with the target vernier. Error bars indicate the standard error of the mean.

My results suggest that the VBM-related ERP deficits observed in schizophrenia patients might be due to two mechanisms: decreased activity and higher variability. As in section 2.2, all the effects observed were specific to the target vernier and did not occur when only the mask was presented, suggesting that top-down processes are responsible for these effects. Thus, providing evidence for lack or deficient target enhancement.

2.4 Neural correlates of target enhancement

Visual backward masking (VBM) is a powerful tool to study schizophrenia and masking paradigms have been suggested as candidate endophenotypes for schizophrenia (Chkonia, Roinishvili, Herzog, & Brand, 2010; Kéri, Kelemen, Benedek, & Janka, 2001; Nuechterlein, Dawson, & Green, 1994; Rund, Landrø, & Ørbeck, 1993). As shown in Plomp et al. (2013) as well as in sections 2.2 and 2.3, in patients, masking deficits are associated with strongly reduced ERP amplitudes, compared to controls. These reduced amplitudes most likely result from deficient top-down processing since they were specific to conditions with the target vernier and did not occur when only the mask was presented. If bottom-up processing was impaired, we would expect differences in the mask only condition.

Herzog and colleagues (2013) proposed that these masking deficits are not visual deficits *per se* but a manifestation of a general deficit related to the enhancement of weak neural signals, which occur in all sorts of information processing. In essence, what is deficient in patients is processing of the stimulus as a *target*. When a task-relevant stimulus is presented for a brief duration or with low contrast, neural enhancement by recurrent processing, attention, and/or acetylcholine neuromodulation (cholinergic system) is needed to boost the weak responses to the target. Otherwise, the stimulus goes unnoticed, which is the default when the stimulus is task-irrelevant.

However, the neural mechanisms of target enhancement and how the mask interferes with them are still poorly understood. In previous works (da Cruz et al., submitted b; Favrod et al., 2018, 2017; Plomp et al., 2013), we inferred the neural mechanisms of target enhancement by comparing patients' and controls' ERPs in the conditions with the target vernier against the condition where only the mask was presented (see section 2.2). A more straightforward approach would be to investigate the neural correlates of the vernier when it is task-relevant compared to when it is task-irrelevant. The stimulus properties are the same, only the task relevance of the vernier is different. Also, to better understand how the mask disrupts target enhancement, a strong mask is needed. In most of our previous studies, we mainly used a 25 elements grating mask. However, due to the *shine-through* effect (the vernier appears superimposed on the grating), even if the mask follows the target with an inter-stimulus-interval (ISI) of 0 ms, healthy controls achieve, on average, more than 80 % of correct responses (Figure 2.4B).

To investigate the neural correlates of target enhancement and how masking disrupts target processing, I recorded the EEG of 14 healthy students while performing two tasks. In experiment 1 (Figure 2.11A), participants had to perform a color discrimination task. I presented a series of white, red, or green vernier stimuli with a duration of 20 ms (which was the average vernier duration (VD) across controls in previous work (da Cruz et al., submitted b)). Participants responded only to the green and red stimuli by pressing the appropriately colored button. In experiment 2 (Figure 2.11B), participants performed a VBM task. I fixed the VD to 20 ms and had 5 conditions. In the simplest condition, the Vernier Only condition, only the target vernier was presented. In the other conditions, the mask followed the target with an ISI of 0, 20, 40, or 60 ms. I used a 5 elements mask which leads to stronger masking as compared to the 25 elements mask used in the shine-through paradigm (Hermens, Luksys, Gerstner, Herzog, & Ernst, 2008; Herzog & Koch, 2001). Participants had to discriminate the vernier offset direction. Conditions were randomized. The order of experiment 1 and 2 was randomized for each participant.

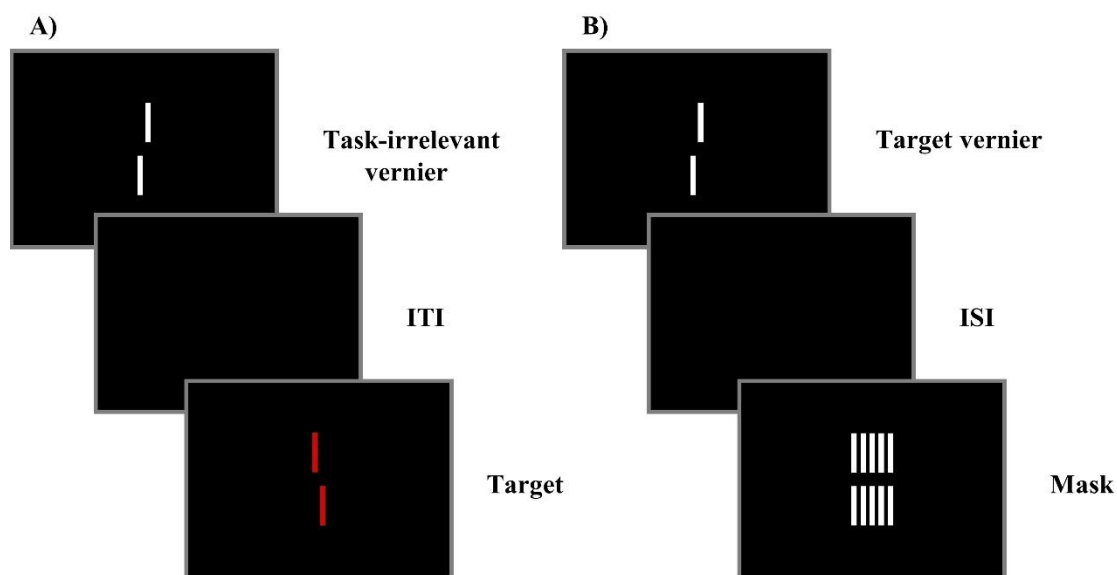


Figure 2.11 - A) Illustration of 2 trials for experiment 1. Participants had to discriminate the color of the target verniers, i.e., red vs. green (not shown), while ignoring the task-irrelevant white vernier. B) Sample trial of the VBM task (experiment 2). The target vernier was presented followed by the 5 element grating mask with a variable ISI. Participants had to discriminate the offset direction (here, left offset is shown). ITI, inter-trial interval; ISI, inter-stimulus interval.

I examined the progression of the evoked scalp topographies using topographic segmentation analysis (Murray, Brunet, & Michel, 2008) and determined the strength of elicited ERPs by computing the global field power (GFP; Lehmann & Skrandies, 1980) for each participant and each condition (Figure 2.12).

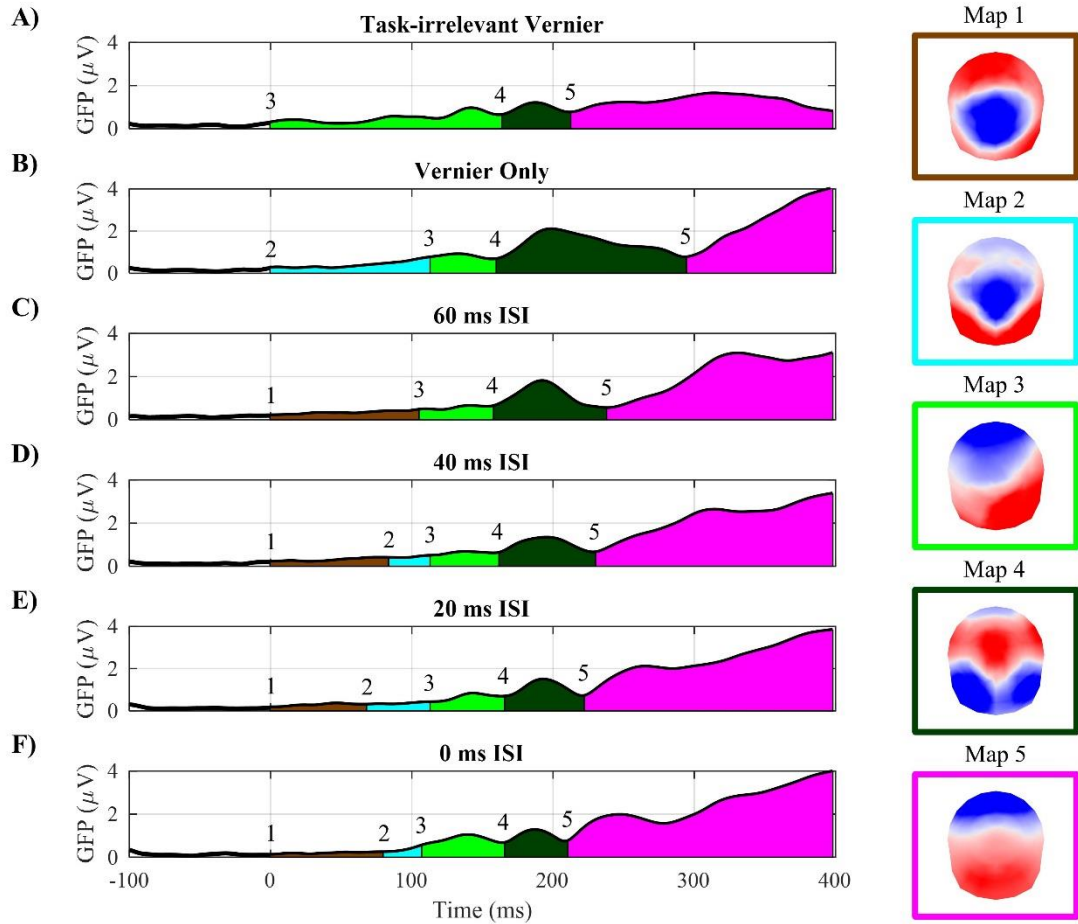


Figure 2.12 - Topography segmentation results for each of the 6 conditions, the GFP of the grand-average ERPs on the ordinate and time on the abscissa. The vertical lines represent the onset and offset of a given map. The numbers and colors correspond to the maps, which are presented on the right as voltage topographies. The target vernier elicited strong ERP amplitudes at ~ 200 ms with a bilateral negative occipital and positive fronto-central topography. These ERP amplitudes and the duration of its topography decreased with the inter-stimulus interval (ISI). When the ISI was 0 ms (F), ERP amplitudes and topography durations were similar to when the vernier was task-irrelevant (A).

First, I compared the ERPs elicited by the vernier when it was task-relevant (Vernier Only condition in experiment 2, Figure 2.12B) vs. task-irrelevant (white vernier in experiment 1, Figure 2.12A). When the vernier was task-relevant, it elicited strong ERP amplitudes at around 200 ms after stimulus-onset with a bilateral negative occipital and positive fronto-central topography (Map 4; average reference). This topography remained stable for around 140 ms (Figure 2.13A). When the vernier was task-irrelevant, similar ERPs were elicited but much weaker amplitudes (paired samples t -test: $t(13)=3.379$, $p=0.005$, $d=0.903$) and for shorter topography durations (paired samples t -test: $t(13)=3.808$, $p=0.002$, $d=1.018$).

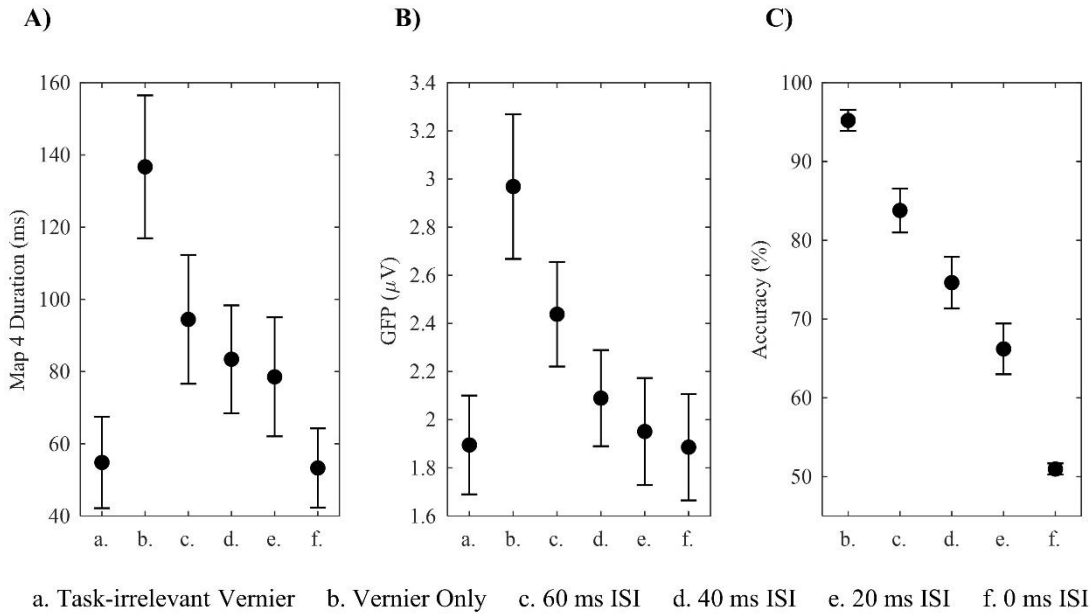


Figure 2.13 - A) Average durations of topographic map 4 and B) GFP peak amplitudes at around 200 ms after stimulus onset, for the 6 experimental conditions of interest. C) Mean accuracy for each of the 5 conditions in experiment 2. Map 4 durations, GFP peak amplitudes, and performance decreased with shorter inter-stimulus intervals (ISIs) between the target vernier and the mask. The task-irrelevant vernier, in experiment 1, elicited similar ERP amplitudes and map 4 durations as the 0 ms ISI condition.

For experiment 2, performance on the target decreased linearly with the ISI, i.e., the shorter the ISI, the worse the performance (Figure 2.13C; repeated measures ANOVA: $F(1.498,19.468)=113.800$, $P<0.001$, $\eta^2=0.897$). Interestingly, the ERP amplitudes and topography durations decreased with the ISI (Figure 2.12 and Figure 2.13; repeated measures ANOVA: $F(1.876,24.385)=10.817$, $P<0.001$,

$\eta^2=0.454$, and $F(2.156,28.025)=12.702$, $P<0.001$, $\eta^2=0.494$; for amplitudes and durations, respectively). When the ISI was 0 ms, performance was at chance level and ERP amplitudes and topography durations were similar to when the vernier was task-irrelevant (paired samples t -test: $t(13)=0.035$, $p=0.972$, $d=0.009$, and $t(13)=0.099$, $p=0.923$, $d=0.026$; for amplitudes and durations, respectively).

My results indicate that only when the vernier is task-relevant, mechanisms of target enhancement come into play to amplify the otherwise weak neural responses to the stimulus. I found evidence for two neural correlates of target enhancement: increased elicited ERP amplitudes and increased durations of the topographic map configuration of the elicited ERP. I, as in Herzog et al. (2013), attribute these mechanisms of target enhancement to an interplay between three factors: recurrent processing, attention, and acetylcholine neuromodulation. When no mask is presented (Vernier Only condition), long recurrent processing, as suggested by the increased Map 4 duration, may be sufficient to achieve good performance. This may explain why schizophrenia patients show similar performance as controls in the Vernier Only condition. However, when a mask is presented, this recurrent processing is interrupted, as suggested by the decreased Map 4 duration, and attention as well as acetylcholine neuromodulation become more relevant to achieve good performance. Since these two factors are deficient in patients, it may explain why patients decrease in performance due to masking is much stronger than controls.

Interestingly, my results also suggest that invisibility can come by either task irrelevance or strong masking, in our case $ISI = 0$ ms. Under these two conditions, ERPs amplitudes and topographies are identical, suggesting similar brain processing.

2.5 Resting-state EEG microstates in schizophrenia

This section is based on the manuscript “EEG microstates: a candidate endophenotype for schizophrenia”, da Cruz, J. R., Favrod, O., Roinishvili, M., Chkonia, E., Brand, A., Mohr, C., Figueiredo, P., & Herzog, M. H. (submitted, Appendix D).

EEG microstates are on-going scalp potential configurations that remain stable for around 90 ms (Lehmann et al., 1987). Four recurrent and dominant classes of microstates (labeled A-D) are observed in resting-state EEG, explaining around 65-84 % of the global variance of the data (Michel & Koenig, 2018). Several studies have reported abnormalities in the dynamics of EEG microstates in schizophrenia patients (Rieger et al., 2016). Similar abnormalities have also been observed in adolescents with 22q11.2 deletion syndrome, a population that has a 30% risk of developing psychosis (Tomescu et al., 2014). These results prompted researchers to suggest that the abnormal dynamics of EEG microstates is a potential endophenotype for schizophrenia (Tomescu et al., 2015). For an endophenotype, it is important that unaffected relatives also show deficits, suggesting a genetic component underpinning the marker (Gottesman & Gould, 2003). To the best of my knowledge, no study analyzed the resting dynamics of these four EEG microstate classes in relatives of schizophrenia patients.

Here, I examined 5 minutes resting-state EEG data of 38 unaffected siblings of schizophrenia patients, 89 schizophrenia patients, and 69 healthy controls, and estimated the dynamics of the four canonical EEG microstates using Cartool (Brunet et al., 2011). Siblings and patients showed similar microstates dynamics: increased presence of microstate class C and decreased presence of microstate class D, compared to controls (Figure 2.14). These results suggest that microstate classes C and D capture some genetic component shared by patients and their unaffected siblings, which might be related to schizophrenia. For microstates class B, patients showed decreased mean durations compared to controls. Surprisingly, microstate class B was more present in siblings compared to patients. I interpret this increased presence of microstate class B in siblings as a compensation signal. More specifically, even though patients and siblings share similar traits, e.g., dynamics of microstates class C and D, which might indicate vulnerability for schizophrenia, siblings can somehow counteract these traits by having an increased presence of microstate class B.

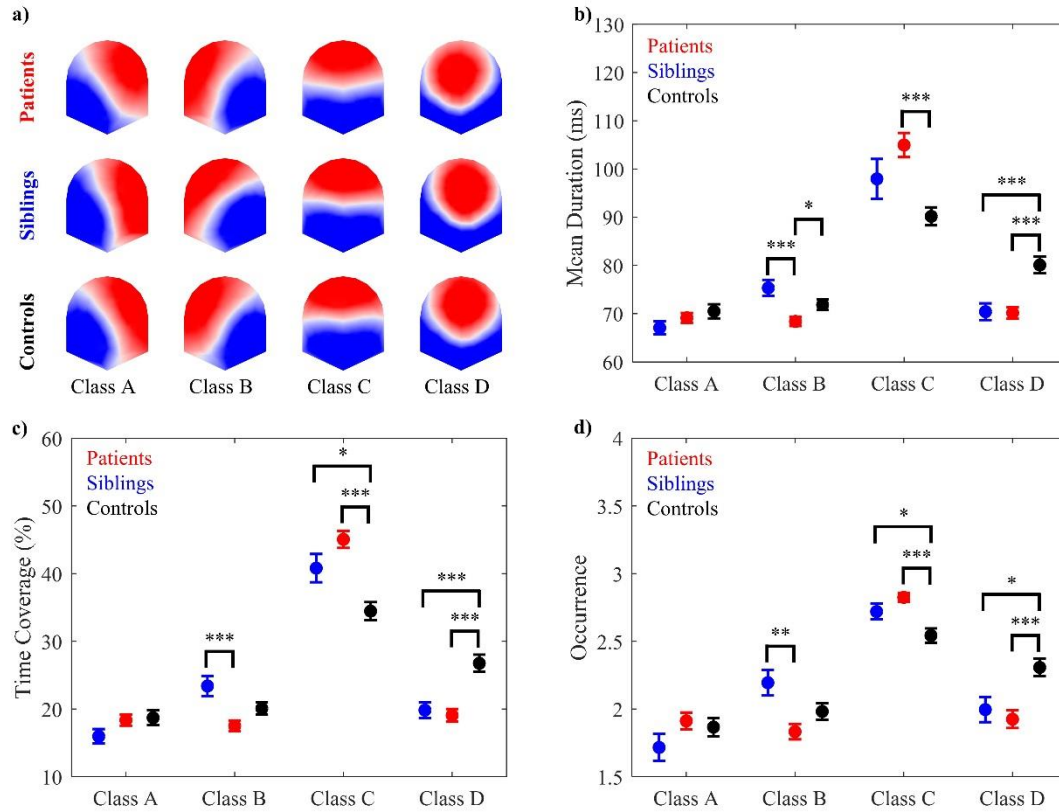


Figure 2.14 - Results of the EEG microstate analysis for patients (red), siblings (blue), and controls (black). a) The spatial configuration of the four microstate classes (A, B, C, D) for the three groups. Statistically significant group differences, Bonferroni-Holm corrected, were found for all computed microstates parameters: b) mean duration, c) time coverage, and d) occurrence. Error bars indicate standard error of the mean. (* $p < 0.05$, ** $p < 0.01$, *** $p < 0.001$). (Reprinted from da Cruz et al. (submitted a)).

These results motivated me to investigate microstates dynamics in healthy people scoring high in schizotypal traits. I hypothesized that if an increased prevalence of microstate class B is evidence for a compensation signal, participants scoring high in schizotypal traits might have increased values compared to the ones scoring low. I tested this hypothesis by analyzing microstates in healthy students scoring either high ($n = 22$) or low ($n = 20$) in the cognitive disorganization (CogDis) subscale of the Oxford-Liverpool Inventory of Feelings (O-LIFE questionnaire; Mason, Linney, & Claridge, 2005). My results indeed showed increased occurrence of microstate class B in students scoring high in CogDis scores, supporting the compensation signal hypothesis (Figure 2.15).

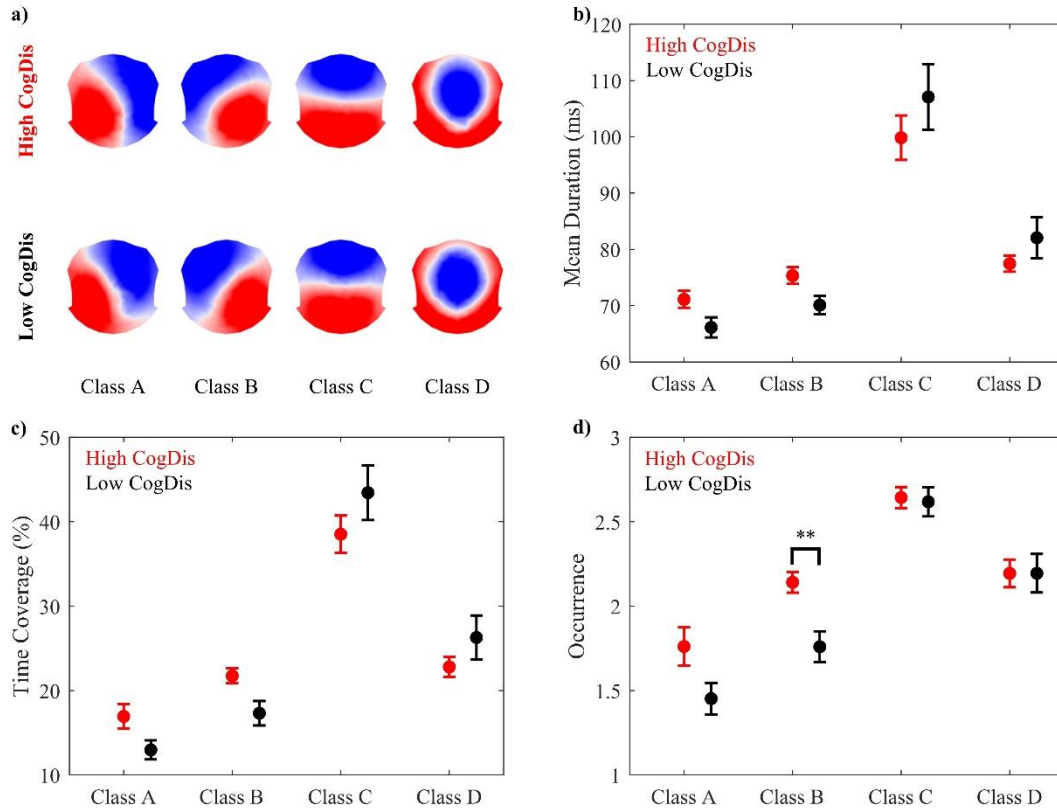


Figure 2.15 - Results of the EEG microstate analysis for students scoring either High (red) or Low (black) in cognitive disorganization (CogDis). a) The spatial configuration of the four microstate classes (A, B, C, D) for the two groups. Statistically significant group differences, Bonferroni-Holm corrected, were found in microstate class B for c) time coverage, and d) occurrence. No group differences were found for a) mean duration. Error bars indicate standard error of the mean. (** $p < 0.01$). (Reprinted from da Cruz et al. (submitted a)).

Considering the evidence for a compensation signal in siblings and high schizotypal students, I conjectured whether this increased presence of microstate class B existed in patients with a first episode of psychosis (FEP) since the disorder has not fully blown. I analyzed the EEG microstates of 22 FEP patients and a subset of 22 chronic schizophrenia patients (Patients_22), selected pseudo-randomly to match the FEP patients demographics as close as possible. As shown in Figure 2.16, I found no evidence for differences between the two groups in any of the computed microstates parameters. We re-tested FEP patients two other times, separated by six months, and found that the microstates dynamics remained stable throughout one year.

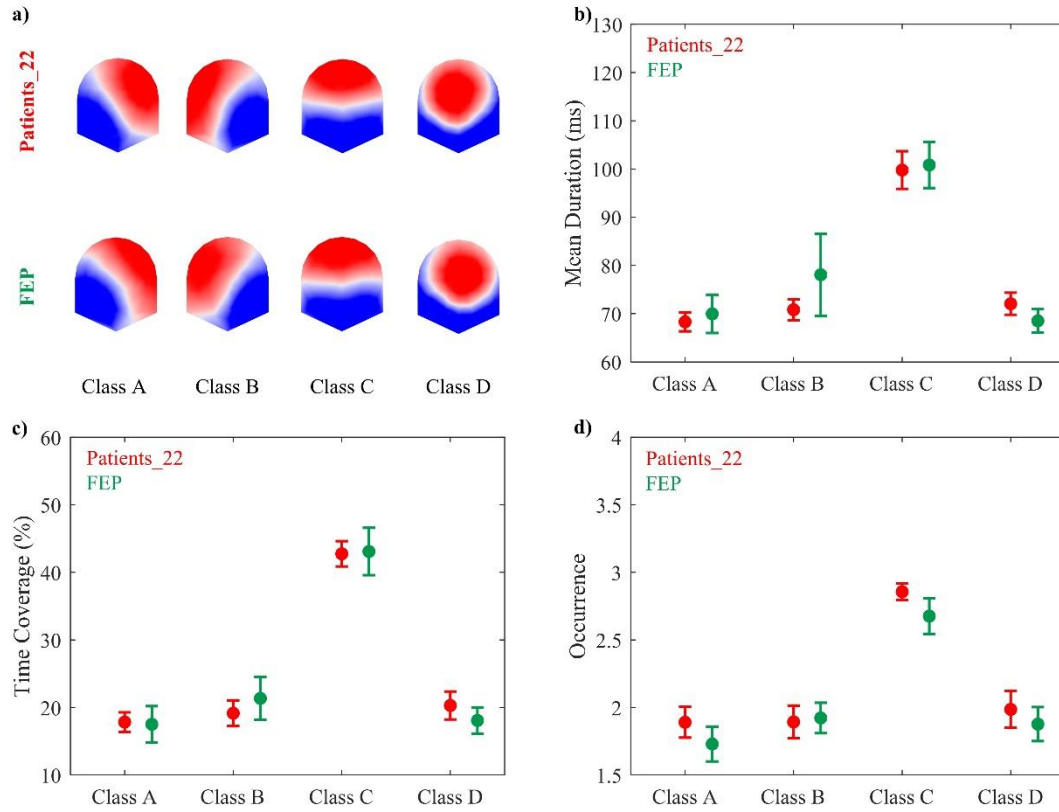


Figure 2.16 - Results of the EEG microstate analysis for patients with a first episode of psychosis (FEP, in green) and their matched schizophrenia patients (Patients_22, in red). A) The spatial configuration of the four microstate classes (A, B, C, D) for the two groups. No statistically significant group differences were found for any of the computed microstates parameters: b) mean duration, c) time coverage, and d) occurrence. Error bars indicate standard error of the mean. (Reprinted from da Cruz et al. (submitted a)).

My findings suggest that the dynamics of resting-state EEG microstates not only meet most of the requirements for an endophenotype for schizophrenia (Gottesman & Gould, 2003), particularly classes C and D, but they also reveal a potential compensation mechanism (increased presence of microstate class B) that unaffected siblings and healthy people with high schizotypal traits have that might prevent them from developing schizophrenia.

3 General discussion

Schizophrenia is a complex psychiatric disease strongly influenced by genetic disposition (Owen et al., 2016). To link genetic risk to schizophrenia phenotype in a mechanistic way, schizophrenia research has turned to stable trait markers with a clear genetic connection, so-called endophenotypes (Braff et al., 2007). Non-invasive endophenotypes research in schizophrenia has heavily relied on the use of EEG to identify endophenotypes and to better understand the neural mechanisms of neuropsychological candidate endophenotypes for schizophrenia.

In this thesis, I used EEG to gain insights into two very promising candidate endophenotypes for schizophrenia: visual backward masking (VBM) and EEG microstates. To cope with the heterogeneity of schizophrenia, I analyzed data from large samples of participants performing a masking task or at rest. Handling such large volumes of EEG data becomes a problem, mainly due to the presence of artifacts. To deal with this, in a time-efficient manner and to minimize experts' subjectivity, I proposed and validated an automatic pre-processing pipeline (APP; see section 2.1). APP effectively removed EEG artifacts, performing similarly to supervised artifact rejection by experts and outperforming existing automatic alternatives. Therefore, APP was subsequently used to pre-process all the measured EEG data.

3.1 Visual backward masking³

In my first study (see section 2.2), I investigated the EEG correlates of a VBM paradigm, the shine-through masking paradigm, which has a much higher sensitivity and specificity for schizophrenia than most other cognitive and perceptual paradigms (Chkonia, Roinishvili, Makhatadze, et al., 2010; Chkonia et al., 2012). In the shine-through masking paradigm, a target vernier is followed by a 25 element grating mask stimulus that deteriorates target perception (Herzog & Koch, 2001). Behaviorally, schizophrenia patients show strong and reproducible masking deficits. Importantly, performance of unaffected first-order relatives is in between the ones of patients and healthy controls (Chkonia, Roinishvili, Makhatadze, et

³ This section is based on the manuscript "Neural compensation mechanisms of siblings of schizophrenia patients as revealed by high-density EEG", da Cruz, J. R., Shaqiri, A., Roinishvili, M., Chkonia, E., Brand, A., Figueiredo, P., & Herzog, M. H. (submitted, Appendix C).

al., 2010), a result that I reproduced (Figure 2.4A). In patients, the large behavioral deficits are associated with large decreased ERP amplitudes, as measured by the GFP, at around 200 ms after stimulus presentation (Plomp et al., 2013). I hypothesized that, since the behavioral performance of relatives is in between the ones of patients and controls, their ERP amplitudes would also be in between the ones of patients and controls. Surprisingly, we found that, on the contrary, ERP amplitudes in siblings were even higher than in controls.

In this EEG experiment, to study group differences, we had to use the same stimulus for all participants. To this end, we had to fix the vernier duration (VD) and the target-to-mask inter-stimulus interval (ISI). For this reason, the EEG experiment was less challenging than the *classic* shine-through masking paradigm, where we explore the individual differences with an adaptive procedure (PEST). This was evident in the lack of behavioral differences between siblings and controls in the EEG experiment (Figure 2.4B). However, this also suggests that, if the task is not challenging enough, by over-enhancing the neural responses to the target, as implied by the extremely high ERP amplitudes, siblings can partially compensate for their masking deficits. Nonetheless, by pushing the visual system to its limits, like in *classic* shine-through masking paradigm, this compensation is too weak to fully counterbalance for the deficits.

In a second study (see section 2.3), I re-analyzed the above-mentioned ERP data from schizophrenia patients and controls focusing on the inter-trial variability. The goal was to investigate whether the decreased amplitudes in patients arise from reduced neuronal activity or increased variability at the peak latencies, since increased latency variability may result in a blurring of the average ERPs. As expected, I found that patients had larger ERP peak amplitude latency variability than matched controls. After correcting for the latency variability, patients still showed weaker amplitudes than controls. In other words, patients' weak VBM elicited ERP amplitudes result from decreased and highly variability neural activity.

Interestingly, all observed effects (i.e., increased variability of ERP peak amplitudes and decreased ERP amplitudes in patients as well as increased ERP amplitudes in siblings compared to controls) were specific to the target vernier and did not occur when only the mask was presented, suggesting that top-down processes are responsible for these effects. In other words, what is deficient in patients is processing of the stimulus as a *target*. Herzog et al. (2013) proposed that whenever a target is presented for short durations or has low contrast, only a weak neural response is elicited and target enhancement is needed for conscious percept and to

prevent overwriting by subsequently presented stimuli. Otherwise, if the stimulus is task-irrelevant, only a weak neural response is elicited and the stimulus goes unnoticed.

To better understand the mechanisms of target enhancement and how masking disrupts target processing, I conducted an EEG study on healthy participants (see section 2.4). First, I compared the ERPs elicited by the vernier when it was task-relevant vs. task-irrelevant. When the vernier was task-relevant, as in previous studies, it elicited strong ERP amplitudes peaking at around 200 ms after stimulus-onset with a bilateral negative occipital and positive fronto-central topography (average reference). This topography configuration remained stable for around 140 ms before changing to another configuration.⁴ When the vernier was task-irrelevant, similar ERPs were elicited but with much weaker amplitudes and with shorter topography configuration durations. In a second experiment, I presented a strong mask (5 elements grating; Figure 2.11B) after the target vernier, with varying ISIs. Performance on the target decreased linearly with the ISI, i.e., the shorter the ISI, the worse the performance. Interestingly, the ERP amplitudes and topography durations decreased with the ISI. When the ISI was 0 ms, performance was at chance level and ERP amplitudes and topography durations were very similar to when the vernier was task-irrelevant.

Topographic segmentation analysis, similar to the one done in section 2.4, of schizophrenia patients, their siblings, and controls elicited ERP data during the VBM task, revealed similar long-lasting topographic configurations with bilateral negative occipital and positive fronto-central topography for all groups in the Vernier Only condition (Figure 3.1). The elicited ERPs during the Vernier Only condition were much stronger, especially for controls and siblings, and for longer durations than when only the mask was presented (Mask Only condition). Similarly, when the mask was presented after the target vernier, the duration of the ERP topography of interest decreased with the ISI.

⁴ This change of topography configurations imply an alteration in the distribution of neuronal generators active in the brain (Lehmann et al., 1987), suggesting the end of an information processing step.

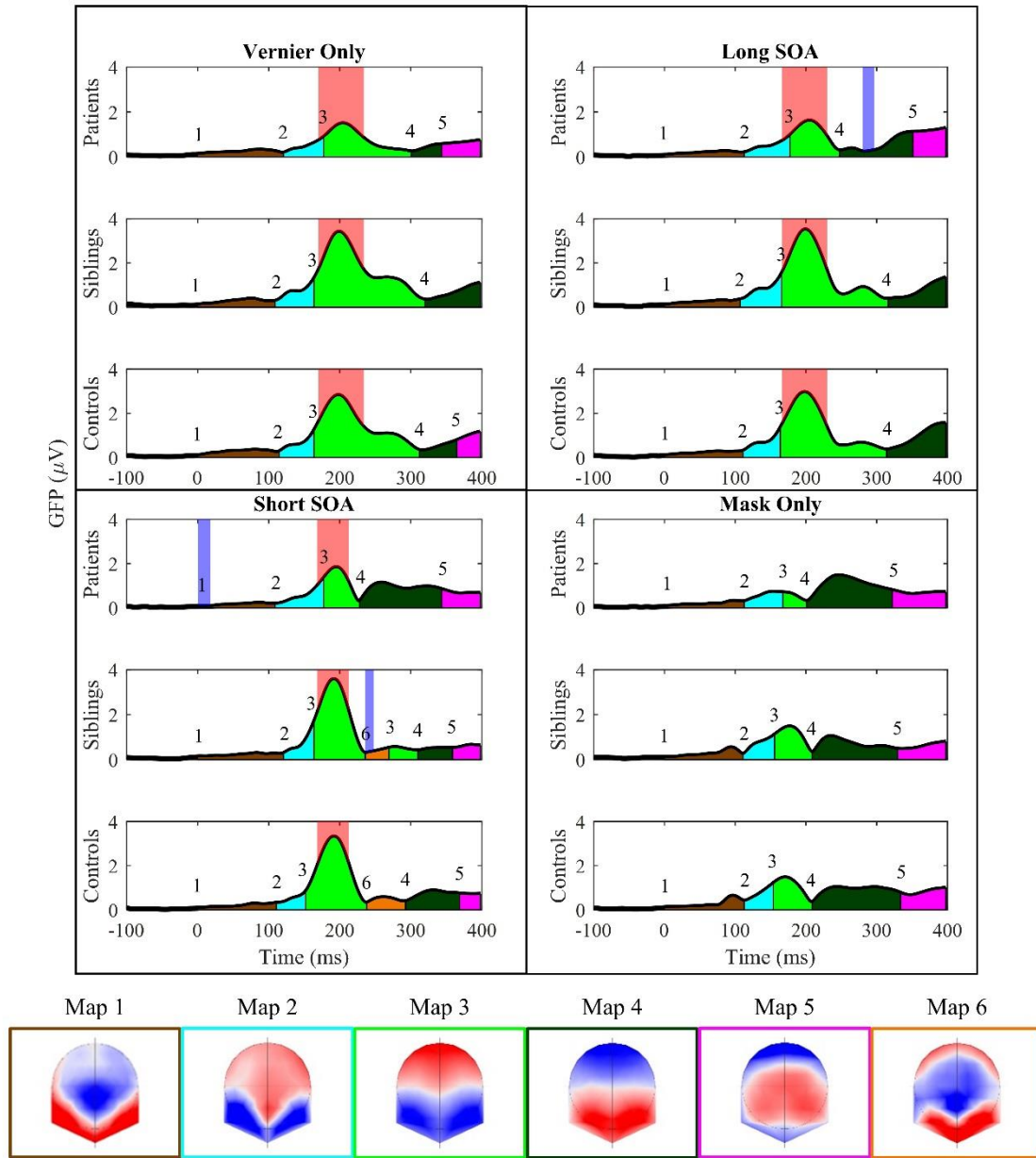


Figure 3.1 - Topographic segmentation results for patients, siblings, and controls for each of the 4 stimulus conditions, with the GFP of the grand-average ERPs on the ordinate and time on the abscissa. The vertical lines represent the onset and offset of a given topography map. The colors and numbers correspond to the maps, which are presented at the bottom. All groups followed similar sequences of maps for all the conditions. GFP amplitude group differences are indicated by the light red region. Topographic consistency test showed evidence of common ERP topographies, within each group for each condition, apart from time periods indicated in light blue region. (Reprinted from da Cruz et al. (submitted b)).

Based on these results, I propose that strong ERP amplitudes with a long-lasting topography configuration (bilateral negative occipital and positive fronto-central topography for average reference) peaking at around 200 ms after-stimulus onset is a neural signature of target enhancement. Importantly, the ERP amplitude, even though moderately correlated with performance, cannot be taken as a surrogate of performance. For example, even though patients show low amplitudes in the Vernier Only condition, they achieve good performance ($> 90\%$ correct responses; Figure 2.4B). I speculate that target enhancement is potentially a multifactorial construct. The first potential factor is recurrent processing between lower and higher visual areas and/or other brain areas. For conscious percept of target stimuli, it has been suggested that recurrent processing is indispensable (Lamme & Roelfsema, 2000). Since recurrent processing may lead to persistent neural signals even after target presentation is ceased, I hypothesize that the duration of the ERP topography configuration is a proxy of the recurrent processing. When no mask is presented, patients may achieve similar performance as controls after long enough recurrent processing.

This recurrent processing might be modulated, i.e., the amplitude of the neural response to the target, by other factors, e.g., attention and acetylcholine release. First, without attention, performance is strongly deteriorated in weak and low contrast stimuli (Reynolds & Heeger, 2009) and attention can increase neuronal response in human primary visual cortex (Gandhi et al., 1999). Second, acetylcholine release from cholinergic neurons is able to decrease responses to disturbing visual signals and also potentiate weak but important information (Picciotto et al., 2012), e.g., increase of neural responses to weak and low contrast target stimuli at the primary visual cortex (Disney et al., 2007). Both attention and the cholinergic system are known to be deficient in schizophrenia patients. Attention deficits are core deficits in schizophrenia (Green, 2006) and deficits in the cholinergic system has been found to play a key role in the pathogenesis of schizophrenia (Freedman, Hall, Adler, & Leonard, 1995; Severance & Yolken, 2007; Taly, Corringier, Guedin, Lestage, & Changeux, 2009). These deficits might explain the weak elicited ERPs in patients even in the absence of the mask.

When a mask follows the target, the mask interrupts the recurrent processing (Fahrenfort, Scholte, & Lamme, 2007) and performance on the target decreases. Then the deficits of attention and cholinergic system, which I propose to be reflected in the low ERP amplitudes, become relevant as the decrement of performance in patients is much stronger than in controls (Figure 2.4B). These deficits are also present in the unaffected siblings, indicating that VBM is a trait marker

for schizophrenia (endophenotype). I speculate that to compensate for these deficits, siblings engage more and this is reflected in their increased ERP amplitudes compared to controls. My electrical source imaging analysis complemented with multiple regression analyses pointed to the right insula as a key player in a network of brain regions that siblings, unlike patients, might over-activate to compensate for their behavior deficits. The insula is associated with several functions. One of special interest is the high-level integration from different modalities and brain areas (Craig, 2009). More specifically, it has been proposed that the right insula regulates the interaction between selective attention and arousal to keep focus on the target (Eckert et al., 2009). Too little activity of the right insula, as in patients, would probably lead to an impairment in collecting evidence for decision making. Too much activity of the right insula, as in siblings, might indicate that participants need to engage more to achieve a good performance in this challenging task. However, by pushing the visual system to its limits, e.g., exploring the individual differences as with the *classic* shine-through paradigm, this compensation mechanism is too weak to fully compensate for the deficits.

3.2 EEG microstates⁵

Besides masking deficits, deficits in several other behavioral tasks, such as Wisconsin Card Sorting Test (WCST), working memory tasks, antisaccade tasks, etc., have been proposed as candidate endophenotypes for schizophrenia (Braff & Light, 2005). Given the broad range of these deficits, some of these deficits might be related, independent of the tasks, and can be found even when the participant is not engaged in any task, i.e., at rest. EEG literature has indeed long reported resting-state abnormalities in schizophrenia patients (Boutros et al., 2008; Rieger et al., 2016). A quantifiable resting-state EEG measure that shows great sensitivity to schizophrenia is the EEG microstates (Michel & Koenig, 2018). A large body of literature has consistently identified abnormal temporal dynamics of EEG microstates in schizophrenia patients (Andreou et al., 2014; Giordano et al., 2018; Irisawa et al., 2006; Kikuchi et al., 2007; Koenig et al., 1999; Lehmann et al., 2005; Strelets et al., 2003; Tomescu et al., 2015). Similar patterns were also found in patients with 22q11.2 deletion syndrome, a population that has a 30 % risk of developing psychosis compared to less than 1 % in the general population

⁵ This section is based on the manuscript “EEG microstates: a candidate endophenotype for schizophrenia”, da Cruz, J. R., Favrod, O., Roinishvili, M., Chkonia, E., Brand, A., Mohr, C., Figueiredo, P., & Herzog, M. H. (submitted, Appendix D).

(Tomescu et al., 2014). Based on these findings, Tomescu and colleagues suggested that these alterations in the temporal dynamics of EEG microstates are a neurophysiological marker for developing schizophrenia (Tomescu et al., 2015).

In my last study (see section 2.5), I investigated whether abnormal EEG microstates dynamics are potential endophenotypes for schizophrenia. To this end I studied 5 minutes resting-state dynamics of the four canonical EEG microstates (labeled A to D) in unaffected siblings of schizophrenia patients, schizophrenia patients, healthy controls, healthy students scoring either high or low in the cognitive disorganization (CogDis) sub-scale of a schizotypal personality traits questionnaire, and patients with a first episodes of psychosis (FEP).

In line with previous studies, schizophrenia patients showed increased presence of the microstate class C and decreased presence of the microstate class D compared to controls (Figure 2.14). Siblings showed similar patterns of microstates classes C and D as patients. Surprisingly, siblings showed increased presence of the microstate class B compared to patients. A similar result was also found in students scoring high in schizotypal traits compared to the ones scoring low (Figure 2.15). No difference was found between FEP and matched chronic patients (Figure 2.16). Moreover, we re-tested FEP patients two other times, separated by six months, and found that the microstates dynamics remained stable throughout one year.

These results suggest that the dynamics of resting-state EEG microstates, particularly classes C and D, is a potential endophenotype for schizophrenia since it meets most of the major criteria proposed by Gottesman and Gould (2003) and further practicability and explicability criteria proposed by Turetsky and colleagues (2007), discussed one-by-one below. *Association with the disease*: abnormalities in the temporal metrics of microstate classes C and D have been associated with schizophrenia for almost 20 years, with meta-analyses yielding medium effect sizes (Rieger et al., 2016). *Relatives*: here, we showed that unaffected siblings show similar abnormalities as their ill relatives. *State independency*: here, we showed that FEP show similar microstates dynamics as chronic patients and that the dynamics remain stable throughout one year. I did not directly compare the FEP against healthy controls or the effects of medication, but several other studies have done so and found that FEP and un-medicated chronic patients also show similar microstates class C and D deviations (Irisawa et al., 2006; Kikuchi et al., 2007; Koenig et al., 1999; Lehmann et al., 2005; Nishida et al., 2013; Rieger et al., 2016; Strelets et al., 2003). *Practicability*: resting-state EEG is easily recorded in a 5 minutes session, and EEG montages with as low as 19 electrodes can be used for

microstates analysis (Koenig et al., 2002). *Explicability*: the abnormal microstates dynamics in schizophrenia are viewed as an imbalance between processes that load on saliency (microstate class C), which are increased, and processes that integrate contextual information (microstate class D), which are reduced (Rieger et al., 2016). This interpretation goes in line with the view of schizophrenia as a state of abnormal assignment of saliency (Kapur, 2003) and a disorder affecting attentional processes, context update, and executive control (Fioravanti et al., 2012). *Heritability*: I currently have no information on the heritability of the patterns of microstate dynamics.

Importantly, my results suggest that EEG microstates dynamics are not only a candidate endophenotype, but they also reveal a potential compensation signal that unaffected siblings and healthy people with high schizotypal traits have that might prevent them to develop the disorder. I associate this compensation signal with the increased duration of microstate class B present in these populations. Little is known about microstate class B. It has been related to a resting-state visual network in fMRI as well as activation of the right insular cortex (Britz et al., 2010; Custo et al., 2017). In healthy participants, it is the shortest and least frequent microstate from adolescence on (Koenig et al., 2002; Tomescu et al., 2018). Moreover, the visual network is expected to reach maturation much earlier than higher order cognitive networks (Gogtay et al., 2004). Combined together, these observations suggest that the dynamics of microstate class B might be an early marker to discriminate people that are at risk to develop schizophrenia from those that might compensate for their vulnerability.

3.3 Implications

Throughout this work, I gave special emphasis to the data of unaffected siblings of schizophrenia patients. First, for an endophenotype, it is important that unaffected relatives also show deficits, suggesting a genetic component underpinning the marker (Gottesman & Gould, 2003). Second, investigating the EEG in schizophrenia patients is confounded by the use of medication, progression of the disease, and social situation. Testing unaffected siblings of schizophrenia patients provides a way to bypass these confounds. These siblings do not have the disease but share, on average, 50 % of their genes with their siblings with schizophrenia (Gottesman & Gould, 2003; Meyer-Lindenberg & Weinberger, 2006), and have an empirical risk of approximately 10-fold higher to develop schizophrenia than the general population (Gottesman & Shields, 1982; Kendler & Diehl, 1993).

Following this approach, I found evidence for two potential compensation mechanisms in siblings of schizophrenia patients (increased ERP amplitudes during VBM tasks and increased presence of microstates class B) that might counteract for their “schizophrenia traits”-related behavioral deficits or genetic risk to develop schizophrenia.

Evidence for some sort of compensation mechanism in relatives of schizophrenia patients was presented earlier by Waldo et al. (1988). The authors reported that patients and about half of their relatives failed to suppress the P50 ERP component to the second click in a paired-click auditory experiment (sensory gating). More interestingly, the relatives with deficient sensory gating were found to have higher N100 amplitudes than the ones of healthy controls, suggesting that relatives can compensate for their early deficits at later information processing stages.

It has also been reported that first-degree relatives of patients with schizophrenia deploy compensatory neural resources to achieve good performance in working memory (WM) tasks (Stäblein et al., 2018).

Sensory gating dysfunctions and WM deficits, like VBM deficits and EEG microstates dynamics abnormalities, have been proposed as candidate endophenotypes for schizophrenia, suggesting that deployment of compensatory mechanisms might not be specific to the endophenotype but a more general phenomenon. Moreover, these findings also imply that even if there are genetic risks for developing schizophrenia, the brain is somehow capable of compensating for them. A better understanding of these compensation mechanisms and their commonalities might help to explain why some siblings develop schizophrenia, while others do not, which might open new avenues for characterization of schizophrenia and possible treatments of the disorder.

3.4 Conclusions

In this thesis, I used EEG to study two candidate endophenotypes for schizophrenia: VBM and EEG microstates. In a VBM study, I replicated the findings that schizophrenia patients and their siblings, to a lesser extent, have strong masking deficits. In patients, I showed that these deficits are associated not only with reduced ERP amplitudes but also highly variable ERP peak latencies. In siblings, contrary to expectation, ERP amplitudes were higher than controls, which I interpret as a compensation signal. Since genetic studies point to an association between abnormalities in the cholinergic system and VBM in schizophrenia, I propose that masking deficits are not caused by visual deficits *per se* but are related

to a more general target enhancement dysfunction. This dysfunction is, at least partially, associated with abnormalities in the cholinergic system, which is reflected in the deficient neural activity.

In a resting-stated EEG microstate study, I showed that schizophrenia patients and their siblings exhibit similar temporal dynamics of microstate classes C and D. Additionally, I found an increased presence of microstate class B in siblings of schizophrenia patients, as well as students scoring high schizotypal traits, which I also interpret as a compensation signal. These findings support the initial hypothesis that the temporal dynamics of EEG microstates, in particular microstate classes C and D, meet the requirements for an endophenotype of schizophrenia.

Finally, I only studied two of the many proposed candidate endophenotypes for schizophrenia. However, I do not claim that abnormal target enhancement or EEG microstates dynamics are necessary or sufficient conditions for developing schizophrenia. There are healthy participants with masking and/or microstates dynamics abnormalities as well as patients with no deficits in these two domains. Schizophrenia is a complex disease and there are possibly many systems and processes that contribute to the pathology and most likely a combination of these mechanisms need to be abnormal to develop schizophrenia. Therefore, studying not one or two deficits but several features that are known to be deficient in patients might better reflect the common genotype that is supposedly associated with schizophrenia, increasing the ability to identify sub-groups of patients, improving our neurobiological and genetic understanding of schizophrenia. Following this approach, EEG may be particularly useful. A plethora of features can be extracted from the EEG data and many of these metrics are deemed to be abnormal in schizophrenia. In an ongoing project (Figure 3.2), I am analyzing some of these EEG metrics by quantifying their efficiency in differentiating schizophrenia patients and their unaffected siblings from healthy controls, as well as combining these features to better understand their aspects in common and differences as a means to improve our knowledge about schizophrenia.

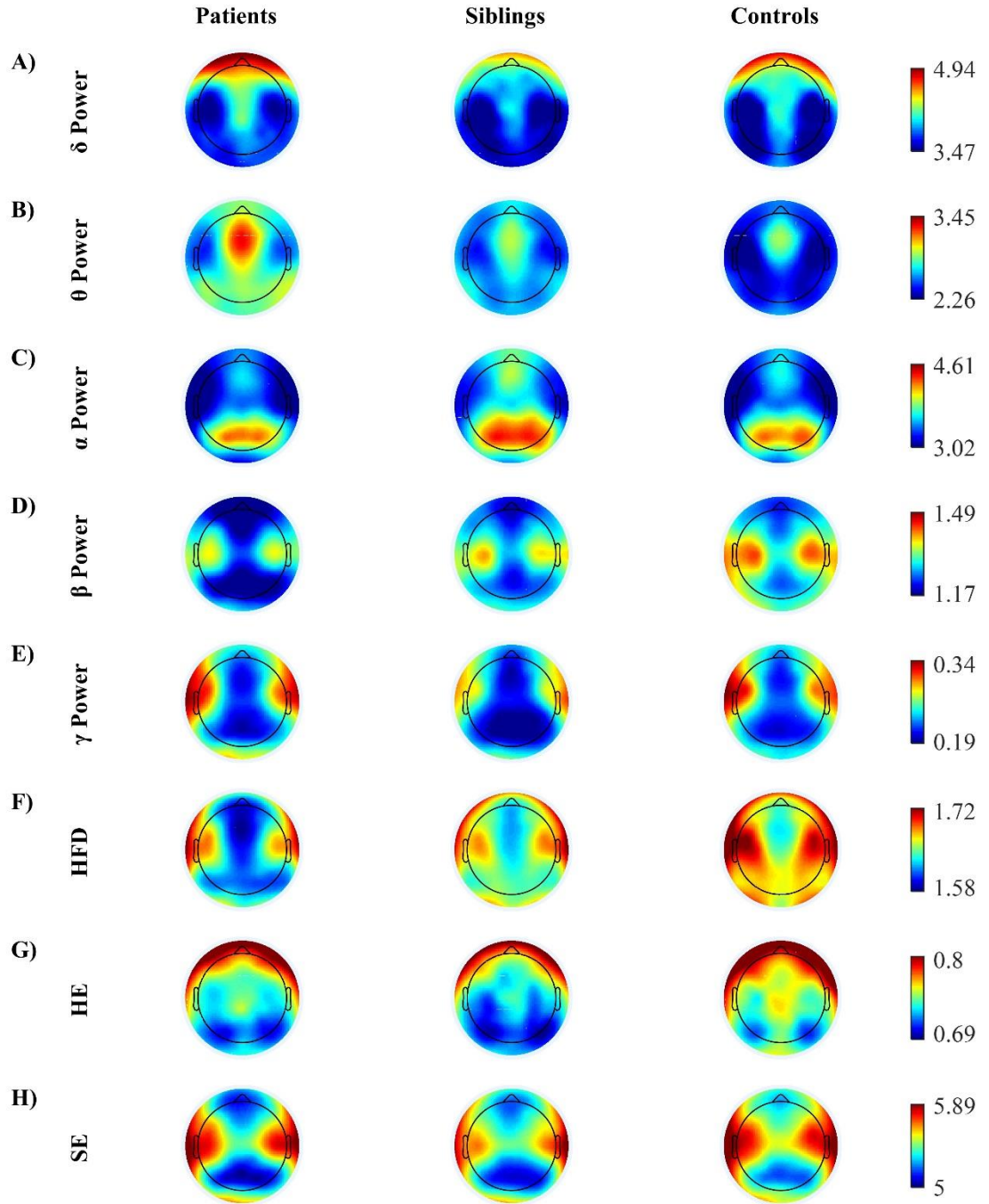


Figure 3.2 - Subset of preliminary results of an ongoing project to analyze multiple EEG features of schizophrenia patients, their siblings, and healthy controls. Features analyzed include the relative power in the A) delta (δ), B) theta (θ), C) alpha (α), beta (β), and E) gamma (γ) frequency bands, as well as F) Higuchi fractal dimension (HFD), G) Hurst exponent (HE), and H) spectral entropy (SE).

3.5 Future work

First, in the study of the EEG correlates of VBM with siblings of schizophrenia patients (section 2.2), I observed increased neural responses to the target in siblings compared to controls but lack of behavioral deficits between the two groups. I interpreted these results as a potential compensation mechanism in siblings of schizophrenia patients that allows them to achieve good performance if the task is not challenging enough and that this compensation mechanism *breaks down* when the task is more challenging, e.g., during the *classic* shine-through masking paradigm. To better understand this potential compensation mechanism, I would need to conduct a more challenging EEG experiment, to investigate the differences of neural processing of siblings and controls under conditions of similar behavioral performance. To this end, the VD would be set to the median VD of the siblings and controls (20 ms) and not the one of patients (30 ms) and the SOAs set to reflect the mean SOAs of siblings (55 ms) and controls (30 ms).

Second, to study the neural correlates of target enhancement and how masking affects target processing (section 2.4), I used a strong mask comprising 5 elements. My results suggest that masking derives its effectiveness from interrupting recurrent processing and this is reflected in a decrease of ERP amplitudes at ~200 ms after target presentation and a decrease of the duration of the ERP topography configuration. However, in the shine-through masking paradigm (25 elements mask), I found that masking increases ERP amplitudes (from Long to Short SOA condition), while the topography configuration duration decreases (Figure 2.5 and Figure 3.1). I propose that how the mask interferes with the processing is similar in both cases, however, in the shine-through effect since the target appears superimposed on the mask, the brain tries to amplify/extract the target information by engaging more and this is reflected in the increase of ERP amplitudes. This is only speculative and future experiments will address this point.

Bibliography

Abreu, R., Leite, M., Jorge, J., Grouiller, F., van der Zwaag, W., Leal, A., & Figueiredo, P. (2016). Ballistocardiogram artifact correction taking into account physiological signal preservation in simultaneous EEG-fMRI. *NeuroImage*, *135*, 45–63.

Abreu, R., Leite, M., Leal, A., & Figueiredo, P. (2016). Objective selection of epilepsy-related independent components from EEG data. *Journal of Neuroscience Methods*, *258*, 67–78.

Alfimova, M., & Uvarova, L. (2003). Cognitive peculiarities in relatives of schizophrenic and schizoaffective patients: heritability and resting EEG-correlates. *International Journal of Psychophysiology*, *49*(3), 201–216.

an der Heiden, W., & Häfner, H. (2011). Course and Outcome. In D. R. Weinberger & P. J. Harrison (Eds.), *Schizophrenia* (pp. 104–141). Oxford, UK: Wiley-Blackwell.

Andreou, C., Faber, P. L., Leicht, G., Schoettle, D., Polomac, N., Hanganu-Opatz, I. L., ... Mulert, C. (2014). Resting-state connectivity in the prodromal phase of schizophrenia: Insights from EEG microstates. *Schizophrenia Research*, *152*(2), 513–520.

Bakanidze, G., Roinishvili, M., Chkonia, E., Kitzrow, W., Richter, S., Neumann, K., ... Puls, I. (2013). Association of the nicotinic receptor $\alpha 7$ subunit gene (CHRNA7) with schizophrenia and visual backward masking. *Molecular Psychiatry*, *4*, 133.

Bekkers, J. M. (2011). Pyramidal neurons. *Current Biology*, *21*(24), R975.

Bell, A. J., & Sejnowski, T. J. (1995). An Information-Maximization Approach to Blind Separation and Blind Deconvolution. *Neural Computation*, *7*(6), 1129–1159.

Bigdely-Shamlo, N., Mullen, T., Kothe, C., Su, K.-M., & Robbins, K. A. (2015). The PREP pipeline: standardized preprocessing for large-scale EEG analysis. *Frontiers in Neuroinformatics*, *9*, 16.

Boutros, N. N., Arfken, C., Galderisi, S., Warrick, J., Pratt, G., & Iacono, W. (2008). The status of spectral EEG abnormality as a diagnostic test for schizophrenia. *Schizophrenia Research*, *99*(1–3), 225–237.

Braff, D. L., & Freedman, R. (2002). Endophenotypes in studies of the genetics of schizophrenia. In K. Davis, D. Charney, J. Coyle, & C. Nemeroff (Eds.), *Neuropsychopharmacology: The Fifth Generation of Progress* (pp. 703–716). Philadelphia, PA: Lippincott, Williams & Wilkins.

Braff, D. L., Freedman, R., Schork, N. J., & Gottesman, I. I. (2007). Deconstructing Schizophrenia: An Overview of the Use of Endophenotypes in Order to Understand a Complex Disorder. *Schizophrenia Bulletin*, 33(1), 21–32.

Braff, D. L., & Geyer, M. A. (1990). Sensorimotor Gating and Schizophrenia: Human and Animal Model Studies. *Archives of General Psychiatry*, 47(2), 181–188.

Braff, D. L., & Light, G. A. (2005). The use of neurophysiological endophenotypes to understand the genetic basis of schizophrenia. *Dialogues in Clinical Neuroscience*, 7(2), 125–135.

Breitmeyer, B. G., & Ganz, L. (1976). Implications of sustained and transient channels for theories of visual pattern masking, saccadic suppression, and information processing. *Psychological Review*, 83(1), 1–36.

Breitmeyer, B., & Ögmen, H. (2006). *Visual Masking: Time Slices Through Conscious and Unconscious Vision*. OUP Oxford.

Bridgeman, B. (1978). Distributed sensory coding applied to simulations of iconic storage and metacontrast. *Bulletin of Mathematical Biology*, 40(5), 605–623.

Britz, J., Van De Ville, D., & Michel, C. M. (2010). BOLD correlates of EEG topography reveal rapid resting-state network dynamics. *NeuroImage*, 52(4), 1162–1170.

Brunet, D., Murray, M. M., & Michel, C. M. (2011). Spatiotemporal Analysis of Multichannel EEG: CARTOOL. *Intell. Neuroscience*, 2011, 2:1–2:15.

Burmeister, M., McInnis, M. G., & Zöllner, S. (2008). Psychiatric genetics: progress amid controversy. *Nature Reviews Genetics*, 9(7), 527–540.

Cappe, C., Herzog, M. H., Herzig, D. A., Brand, A., & Mohr, C. (2012). Cognitive disorganisation in schizotypy is associated with deterioration in visual backward masking. *Psychiatry Research*, 200(2–3), 652–659.

Chkonia, E., Roinishvili, M., Herzog, M. H., & Brand, A. (2010). First-order relatives of schizophrenic patients are not impaired in the Continuous Performance Test. *Journal of Clinical and Experimental Neuropsychology*, 32(5), 481–486.

- Chkonia, E., Roinishvili, M., Makhatadze, N., Tsverava, L., Stroux, A., Neumann, K., ... Brand, A. (2010). The Shine-Through Masking Paradigm Is a Potential Endophenotype of Schizophrenia. *PLoS ONE*, 5(12), e14268.
- Chkonia, E., Roinishvili, M., Reichard, L., Wurch, W., Puhlmann, H., Grimsen, C., ... Brand, A. (2012). Patients with functional psychoses show similar visual backward masking deficits. *Psychiatry Research*, 198(2), 235–240.
- Cong, F., He, Z., Hämäläinen, J., Leppänen, P. H. T., Lyytinen, H., Cichocki, A., & Ristaniemi, T. (2013). Validating rationale of group-level component analysis based on estimating number of sources in EEG through model order selection. *Journal of Neuroscience Methods*, 212(1), 165–172.
- Craig, A. D. (Bud). (2009). How do you feel — now? The anterior insula and human awareness. *Nature Reviews Neuroscience*, 10(1), 59–70.
- Custo, A., Van De Ville, D., Wells, W. M., Tomescu, M. I., Brunet, D., & Michel, C. M. (2017). Electroencephalographic Resting-State Networks: Source Localization of Microstates. *Brain Connectivity*, 7(10), 671–682.
- da Cruz, J. N., Wang, Z., Wong, C. M., & Wan, F. (2014). Single-Trial Detection of Error-Related Potential by One-Unit SOBI-R in SSVEP-Based BCI. In Z. Zeng, Y. Li, & I. King (Eds.), *Advances in Neural Networks – ISNN 2014* (Vol. 8866, pp. 524–532). Cham: Springer International Publishing.
- da Cruz, J. R., Chicherov, V., Herzog, M. H., & Figueiredo, P. (2018). An automatic pre-processing pipeline for EEG analysis (APP) based on robust statistics. *Clinical Neurophysiology*, 129(7), 1427–1437.
- da Cruz, J. R., Favrod, O., Roinishvili, M., Chkonia, E., Brand, A., Mohr, C., ... Herzog, M. H. (submitted a). EEG microstates: a candidate endophenotype for schizophrenia.
- da Cruz, J. R., Shaqiri, A., Roinishvili, M., Chkonia, E., Brand, A., Figueiredo, P., & Herzog, M. H. (submitted b). Neural compensation mechanisms of siblings of schizophrenia patients as revealed by high-density EEG.
- Delorme, A., Palmer, J., Onton, J., Oostenveld, R., & Makeig, S. (2012). Independent EEG Sources Are Dipolar. *PLoS ONE*, 7(2), e30135.
- Diaz, L. H., Rieger, K., Baenninger, A., Brandeis, D., & Koenig, T. (2016). Towards Using Microstate-Neurofeedback for the Treatment of Psychotic Symptoms in Schizophrenia. A Feasibility Study in Healthy Participants. *Brain Topography*, 29(2), 308–321.

Di Lollo, V., Enns, J. T., & Rensink, R. A. (2000). Competition for consciousness among visual events: the psychophysics of reentrant visual processes. *Journal of Experimental Psychology. General*, 129(4), 481–507.

Disney, A. A., Aoki, C., & Hawken, M. J. (2007). Gain modulation by nicotine in macaque v1. *Neuron*, 56(4), 701–713.

Eason, R. G., Harter, M. R., & White, C. T. (1969). Effects of attention and arousal on visually evoked cortical potentials and reaction time in man. *Physiology & Behavior*, 4(3), 283–289.

Eckert, M. A., Menon, V., Walczak, A., Ahlstrom, J., Denslow, S., Horwitz, A., & Dubno, J. R. (2009). At the heart of the ventral attention system: The right anterior insula. *Human Brain Mapping*, 30(8), 2530–2541.

Eichele, T., Rachakonda, S., Brakedal, B., Eikeland, R., & Calhoun, V. D. (2011). EEGIFT: Group Independent Component Analysis for Event-Related EEG Data. *Computational Intelligence and Neuroscience*, 2011, 1–9.

Enns, J. T. (2004). Object substitution and its relation to other forms of visual masking. *Vision Research*, 44(12), 1321–1331.

Ethridge, L. E., Hamm, J. P., Pearlson, G. D., Tamminga, C. A., Sweeney, J. A., Keshavan, M. S., & Clementz, B. A. (2015). Event-Related Potential and Time-Frequency Endophenotypes for Schizophrenia and Psychotic Bipolar Disorder. *Biological Psychiatry*, 77(2), 127–136.

Fahrenfort, J. J., Scholte, H. S., & Lamme, V. A. F. (2007). Masking Disrupts Reentrant Processing in Human Visual Cortex. *Journal of Cognitive Neuroscience*, 19(9), 1488–1497.

Favrod, O., Roinishvili, M., da Cruz, J. R., Brand, A., Okruashvili, M., Gamkrelidze, T., ... Shaqiri, A. (2018). Electrophysiological correlates of visual backward masking in patients with first episode psychosis. *Psychiatry Research: Neuroimaging*, 282, 64–72.

Favrod, O., Sierro, G., Roinishvili, M., Chkonia, E., Mohr, C., Herzog, M. H., & Cappe, C. (2017). Electrophysiological correlates of visual backward masking in high schizotypic personality traits participants. *Psychiatry Research*, 254, 251–257.

Fioravanti, M., Bianchi, V., & Cinti, M. E. (2012). Cognitive deficits in schizophrenia: an updated metanalysis of the scientific evidence. *BMC Psychiatry*, 12(1), 64.

- Francis, G. (2003). Developing a new quantitative account of backward masking. *Cognitive Psychology*, 46(2), 198–226.
- Freedman, R., Hall, M., Adler, L. E., & Leonard, S. (1995). Evidence in post-mortem brain tissue for decreased numbers of hippocampal nicotinic receptors in schizophrenia. *Biological Psychiatry*, 38(1), 22–33.
- Gandhi, S. P., Heeger, D. J., & Boynton, G. M. (1999). Spatial attention affects brain activity in human primary visual cortex. *Proceedings of the National Academy of Sciences*, 96(6), 3314–3319.
- Giordano, G. M., Koenig, T., Mucci, A., Vignapiano, A., Amodio, A., Di Lorenzo, G., ... Maj, M. (2018). Neurophysiological correlates of Avolition-apathy in schizophrenia: A resting-EEG microstates study. *NeuroImage: Clinical*, 20, 627–636.
- Glahn, D. C., Knowles, E. E. M., McKay, D. R., Sprooten, E., Raventós, H., Blangero, J., ... Almasy, L. (2014). Arguments for the sake of endophenotypes: Examining common misconceptions about the use of endophenotypes in psychiatric genetics. *American Journal of Medical Genetics Part B: Neuropsychiatric Genetics*, 165(2), 122–130.
- Gogtay, N., Giedd, J. N., Lusk, L., Hayashi, K. M., Greenstein, D., Vaituzis, A. C., ... Thompson, P. M. (2004). Dynamic mapping of human cortical development during childhood through early adulthood. *Proceedings of the National Academy of Sciences of the United States of America*, 101(21), 8174–8179.
- González-Hernández, J. A., Pita-Alcorta, C., Cedeño, I., Bosch-Bayard, J., Galán-García, L., Scherbaum, W. A., & Figueredo-Rodríguez, P. (2002). Wisconsin card sorting test synchronizes the prefrontal, temporal and posterior association cortex in different frequency ranges and extensions: EEG WCST-Related Changes and Cortical Sources. *Human Brain Mapping*, 17(1), 37–47.
- Gottesman, I. I., & Gould, T. D. (2003). The Endophenotype Concept in Psychiatry: Etymology and Strategic Intentions. *American Journal of Psychiatry*, 160(4), 636–645.
- Gottesman, I. I., & Shields, J. (1982). The Epigenetic Puzzle. In *Schizophrenia, the epigenetic puzzle*. Cambridge ; New York: Cambridge University Press.
- Gramfort, A., Keriven, R., & Clerc, M. (2010). Graph-Based Variability Estimation in Single-Trial Event-Related Neural Responses. *IEEE Transactions on Biomedical Engineering*, 57(5), 1051–1061.

Grave de Peralta Menendez, R., Murray, M. M., Michel, C. M., Martuzzi, R., & Gonzalez Andino, S. L. (2004). Electrical neuroimaging based on biophysical constraints. *NeuroImage*, 21(2), 527–539.

Green, M. F. (2006). Cognitive impairment and functional outcome in schizophrenia and bipolar disorder. *The Journal of Clinical Psychiatry*, 67 Suppl 9, 3–8; discussion 36–42.

Green, M. F., Lee, J., Wynn, J. K., & Mathis, K. I. (2011). Visual Masking in Schizophrenia: Overview and Theoretical Implications. *Schizophrenia Bulletin*, 37(4), 700–708.

Hatz, F., Hardmeier, M., Bousleiman, H., Rüegg, S., Schindler, C., & Fuhr, P. (2015). Reliability of fully automated versus visually controlled pre- and post-processing of resting-state EEG. *Clinical Neurophysiology*, 126(2), 268–274.

Hermens, F., Luksys, G., Gerstner, W., Herzog, M. H., & Ernst, U. (2008). Modeling spatial and temporal aspects of visual backward masking. *Psychological Review*, 115(1), 83–100.

Herzog, M. H., & Koch, C. (2001). Seeing properties of an invisible object: Feature inheritance and shine-through. *Proceedings of the National Academy of Sciences*, 98(7), 4271–4275.

Herzog, H., & Brand, A. (2015). Visual masking & schizophrenia. *Schizophrenia Research: Cognition*, 2(2), 64–71.

Herzog, H., Kopmann, S., & Brand, A. (2004). Intact figure-ground segmentation in schizophrenia. *Psychiatry Research*, 129(1), 55–63.

Herzog, H., Roinishvili, M., Chkonia, E., & Brand, A. (2013). Schizophrenia and visual backward masking: a general deficit of target enhancement. *Frontiers in Psychology*, 4.

Holzer, L., Jaugey, L., Chinet, L., & Herzog, M. H. (2009). Deteriorated visual backward masking in the shine-through effect in adolescents with psychosis. *Journal of Clinical and Experimental Neuropsychology*, 31(6), 641–647.

Irisawa, S., Isotani, T., Yagyu, T., Morita, S., Nishida, K., Yamada, K., ... Kinoshita, T. (2006). Increased Omega Complexity and Decreased Microstate Duration in Nonmedicated Schizophrenic Patients. *Neuropsychobiology*, 54(2), 134–139.

Jansen, B. H., Hu, L., & Boutros, N. N. (2010). Auditory evoked potential variability in healthy and schizophrenia subjects. *Clinical Neurophysiology*, 121(8), 1233–1239.

- Jeon, Y.-W., & Polich, J. (2003). Meta-analysis of P300 and schizophrenia: Patients, paradigms, and practical implications. *Psychophysiology*, 40(5), 684–701.
- Jordanov, T., Popov, T., Weisz, N., Elbert, T., Paul-Jordanov, I., & Rockstroh, B. (2011). Reduced mismatch negativity and increased variability of brain activity in schizophrenia. *Clinical Neurophysiology*, 122(12), 2365–2374.
- Kapur, S. (2003). Psychosis as a State of Aberrant Salience: A Framework Linking Biology, Phenomenology, and Pharmacology in Schizophrenia. *American Journal of Psychiatry*, 160(1), 13–23.
- Kendler, K. S., & Diehl, S. R. (1993). The Genetics of Schizophrenia: A Current, Genetic-epidemiologic Perspective. *Schizophrenia Bulletin*, 19(2), 261–285.
- Kéri, S., Kelemen, O., Benedek, G., & Janka, Z. (2001). Different trait markers for schizophrenia and bipolar disorder: a neurocognitive approach. *Psychological Medicine*, 31(05).
- Khanna, A., Pascual-Leone, A., Michel, C. M., & Farzan, F. (2015). Microstates in resting-state EEG: Current status and future directions. *Neuroscience & Biobehavioral Reviews*, 49(Supplement C), 105–113.
- Kikuchi, M., Koenig, T., Wada, Y., Higashima, M., Koshino, Y., Strik, W., & Dierks, T. (2007). Native EEG and treatment effects in neuroleptic-naïve schizophrenic patients: Time and frequency domain approaches. *Schizophrenia Research*, 97(1), 163–172.
- Kindler, J., Hubl, D., Strik, W. K., Dierks, T., & Koenig, T. (2011). Resting-state EEG in schizophrenia: Auditory verbal hallucinations are related to shortening of specific microstates. *Clinical Neurophysiology*, 122(6), 1179–1182.
- Kirenskaya, A. V., Tkachenco, A. A., & Novototsky-Vlasov, V. Y. (2017). The Study of the Antisaccade Performance and Contingent Negative Variation Characteristics in First-Episode and Chronic Schizophrenia Patients. *The Spanish Journal of Psychology*, 20.
- Koenig, T., Lehmann, D., Merlo, M. C. G., Kochi, K., Hell, D., & Koukkou, M. (1999). A deviant EEG brain microstate in acute, neuroleptic-naïve schizophrenics at rest. *European Archives of Psychiatry and Clinical Neuroscience*, 249(4), 205–211.
- Koenig, T., Lehmann, D., Saito, N., Kuginuki, T., Kinoshita, T., & Koukkou, M. (2001). Decreased functional connectivity of EEG theta-frequency activity in first-

episode, neuroleptic-naïve patients with schizophrenia: preliminary results. *Schizophrenia Research*, 50(1), 55–60.

Koenig, T., Prichet, L., Lehmann, D., Sosa, P. V., Braeker, E., Kleinlogel, H., ... John, E. R. (2002). Millisecond by Millisecond, Year by Year: Normative EEG Microstates and Developmental Stages. *NeuroImage*, 16(1), 41–48.

Kutas, M., McCarthy, G., & Donchin, E. (1977). Augmenting mental chronometry: the P300 as a measure of stimulus evaluation time. *Science*, 197(4305), 792–795.

Lamme, V. A. F., & Roelfsema, P. R. (2000). The distinct modes of vision offered by feedforward and recurrent processing. *Trends in Neurosciences*, 23(11), 571–579.

Lehmann, D., Ozaki, H., & Pal, I. (1987). EEG alpha map series: brain microstates by space-oriented adaptive segmentation. *Electroencephalography and Clinical Neurophysiology*, 67(3), 271–288.

Lehmann, D., & Skrandies, W. (1980). Reference-free identification of components of checkerboard-evoked multichannel potential fields. *Electroencephalography and Clinical Neurophysiology*, 48(6), 609–621.

Lehmann, Dietrich, Faber, P. L., Galderisi, S., Herrmann, W. M., Kinoshita, T., Koukkou, M., ... Koenig, T. (2005). EEG microstate duration and syntax in acute, medication-naïve, first-episode schizophrenia: a multi-center study. *Psychiatry Research: Neuroimaging*, 138(2), 141–156.

Li, Z., Chen, J., Yu, H., He, L., Xu, Y., Zhang, D., ... Shi, Y. (2017). Genome-wide association analysis identifies 30 new susceptibility loci for schizophrenia. *Nature Genetics*, 49(11), 1576–1583.

Luck, S. J., & Kappenman, E. S. (2013). *The Oxford Handbook of Event-Related Potential Components*. Oxford University Press.

Luck, S. J., Woodman, G. F., & Vogel, E. K. (2000). Event-related potential studies of attention. *Trends in Cognitive Sciences*, 4(11), 432–440.

Mason, O., Linney, Y., & Claridge, G. (2005). Short scales for measuring schizotypy. *Schizophrenia Research*, 78(2), 293–296.

McLoughlin, G., Makeig, S., & Tsuang, M. T. (2014). In search of biomarkers in psychiatry: EEG-based measures of brain function. *American Journal of Medical Genetics Part B: Neuropsychiatric Genetics*, 165(2), 111–121.

- Meyer-Lindenberg, A., & Weinberger, D. R. (2006). Intermediate phenotypes and genetic mechanisms of psychiatric disorders. *Nature Reviews Neuroscience*, 7(10), 818–827.
- Michel, C. M., & Koenig, T. (2018). EEG microstates as a tool for studying the temporal dynamics of whole-brain neuronal networks: A review. *NeuroImage*, 180, 577–593.
- Michel, C. M., & Murray, M. M. (2012). Towards the utilization of EEG as a brain imaging tool. *NeuroImage*, 61(2), 371–385.
- Milz, P., Pascual-Marqui, R. D., Achermann, P., Kochi, K., & Faber, P. L. (2017). The EEG microstate topography is predominantly determined by intracortical sources in the alpha band. *NeuroImage*, 162, 353–361.
- Moreno-Küstner, B., Martín, C., & Pastor, L. (2018). Prevalence of psychotic disorders and its association with methodological issues. A systematic review and meta-analyses. *PLOS ONE*, 13(4), e0195687.
- Murray, M. M., Brunet, D., & Michel, C. M. (2008). Topographic ERP Analyses: A Step-by-Step Tutorial Review. *Brain Topography*, 20(4), 249–264.
- Musso, F., Brinkmeyer, J., Mobascher, A., Warbrick, T., & Winterer, G. (2010). Spontaneous brain activity and EEG microstates. A novel EEG/fMRI analysis approach to explore resting-state networks. *NeuroImage*, 52(4), 1149–1161.
- Niedermeyer, E., & Lopes da Silva, F. H. (2005). *Electroencephalography: Basic Principles, Clinical Applications, and Related Fields*. Lippincott Williams & Wilkins.
- Nishida, K., Morishima, Y., Yoshimura, M., Isotani, T., Irisawa, S., Jann, K., ... Koenig, T. (2013). EEG microstates associated with salience and frontoparietal networks in frontotemporal dementia, schizophrenia and Alzheimer’s disease. *Clinical Neurophysiology*, 124(6), 1106–1114.
- Nolan, H., Whelan, R., & Reilly, R. B. (2010). FASTER: Fully Automated Statistical Thresholding for EEG artifact Rejection. *Journal of Neuroscience Methods*, 192(1), 152–162.
- Nuechterlein, K. H., Dawson, M. E., & Green, M. F. (1994). Information-processing abnormalities as neuropsychological vulnerability indicators for schizophrenia. *Acta Psychiatrica Scandinavica*, 90(s384), 71–79.

Okruszek, Ł., Jarkiewicz, M., Gola, M., Cella, M., & Łojek, E. (2018). Using ERPs to explore the impact of affective distraction on working memory stages in schizophrenia. *Cognitive, Affective, & Behavioral Neuroscience*, 18(3), 437–446.

Owen, M. J., Sawa, A., & Mortensen, P. B. (2016). Schizophrenia. *The Lancet*, 388(10039), 86–97.

Owens, E. M., Bachman, P., Glahn, D. C., & Bearden, C. E. (2016). Electrophysiological Endophenotypes for Schizophrenia. *Harvard Review of Psychiatry*, 24(2), 129–147.

Pascual-Marqui, R. D., Lehmann, D., Faber, P., Milz, P., Kochi, K., Yoshimura, M., ... Kinoshita, T. (2014). The resting microstate networks (RMN): cortical distributions, dynamics, and frequency specific information flow. *ArXiv:1411.1949 [q-Bio]*. Retrieved from <http://arxiv.org/abs/1411.1949>

Philiastides, M. G., Ratcliff, R., & Sajda, P. (2006). Neural Representation of Task Difficulty and Decision Making during Perceptual Categorization: A Timing Diagram. *Journal of Neuroscience*, 26(35), 8965–8975.

Picciotto, M. R., Higley, M. J., & Mineur, Y. S. (2012). Acetylcholine as a neuromodulator: cholinergic signaling shapes nervous system function and behavior. *Neuron*, 76(1), 116–129.

Plomp, G., Roinishvili, M., Chkonia, E., Kapanadze, G., Kereselidze, M., Brand, A., & Herzog, M. H. (2013). Electrophysiological Evidence for Ventral Stream Deficits in Schizophrenia Patients. *Schizophrenia Bulletin*, 39(3), 547–554.

Reynolds, J. H., & Heeger, D. J. (2009). The Normalization Model of Attention. *Neuron*, 61(2), 168–185.

Rieger, K., Diaz Hernandez, L., Baenninger, A., & Koenig, T. (2016). 15 Years of Microstate Research in Schizophrenia – Where Are We? A Meta-Analysis. *Frontiers in Psychiatry*, 7.

Ripke, S., Neale, B. M., Corvin, A., Walters, J. T. R., Farh, K.-H., Holmans, P. A., ... O'Donovan, M. C. (2014). Biological insights from 108 schizophrenia-associated genetic loci. *Nature*, 511(7510), 421.

Roinishvili, M., Chkonia, E., Brand, A., & Herzog, M. H. (2008). Contextual suppression and protection in schizophrenic patients. *European Archives of Psychiatry and Clinical Neuroscience*, 258(4), 210–216.

Rolls, E. T., Loh, M., Deco, G., & Winterer, G. (2008). Computational models of schizophrenia and dopamine modulation in the prefrontal cortex. *Nature Reviews Neuroscience*, 9(9), 696–709.

Roth, A., Roesch-Ely, D., Bender, S., Weisbrod, M., & Kaiser, S. (2007). Increased event-related potential latency and amplitude variability in schizophrenia detected through wavelet-based single trial analysis. *International Journal of Psychophysiology*, 66(3), 244–254.

Rund, B. R., Landrø, N. I., & Ørbeck, A. L. (1993). Stability in Backward Masking Performance in Schizophrenics, Affectively Disturbed Patients, and Normal Subjects: *The Journal of Nervous and Mental Disease*, 181(4), 233–237.

Ryman, S. G., Cavanagh, J. F., Wertz, C. J., Shaff, N. A., Dodd, A. B., Stevens, B., ... Mayer, A. R. (2018). Impaired Midline Theta Power and Connectivity During Proactive Cognitive Control in Schizophrenia. *Biological Psychiatry*, 84(9), 675–683.

Sanders, A. R., Duan, J., Levinson, D. F., Shi, J., He, D., Hou, C., ... Gejman, P. V. (2008). No Significant Association of 14 Candidate Genes With Schizophrenia in a Large European Ancestry Sample: Implications for Psychiatric Genetics. *American Journal of Psychiatry*, 165(4), 497–506.

Severance, E. G., & Yolken, R. H. (2007). Novel alpha7 nicotinic receptor isoforms and deficient cholinergic transcription in schizophrenia. *Genes, Brain and Behavior*, 7(1), 37–45.

Shin, K. S., Kim, J. S., Kim, S. N., Hong, K. S., O'Donnell, B. F., Chung, C. K., & Kwon, J. S. (2015). Intraindividual neurophysiological variability in ultra-high-risk for psychosis and schizophrenia patients: single-trial analysis. *Npj Schizophrenia*, 1, 15031.

Silverstein, S. M., & Keane, B. P. (2011). Vision Science and Schizophrenia Research: Toward a Re-view of the Disorder Editors' Introduction to Special Section. *Schizophrenia Bulletin*, 37(4), 681–689.

So, H.-C., Gui, A. H. S., Cherny, S. S., & Sham, P. C. (2011). Evaluating the heritability explained by known susceptibility variants: a survey of ten complex diseases. *Genetic Epidemiology*, 35(5), 310–317.

Stäblein, M., Storchak, H., Ghinea, D., Kraft, D., Knöchel, C., Prvulovic, D., ... Oertel-Knöchel, V. (2018). Visual working memory encoding in schizophrenia and first-degree relatives: neurofunctional abnormalities and impaired consolidation. *Psychological Medicine*, 1–9.

Stefansson, H., Ophoff, R. A., Steinberg, S., Andreassen, O. A., Cichon, S., Rujescu, D., ... Collier, D. A. (2009). Common variants conferring risk of schizophrenia. *Nature*, 460(7256), 744–747.

Strelets, V., Faber, P. L., Golikova, J., Novototsky-Vlasov, V., Koenig, T., Gianotti, L. R. R., ... Lehmann, D. (2003). Chronic schizophrenics with positive symptomatology have shortened EEG microstate durations. *Clinical Neurophysiology*, 114(11), 2043–2051.

Sullivan, P. F., Daly, M. J., & O'Donovan, M. (2012). Genetic architectures of psychiatric disorders: the emerging picture and its implications. *Nature Reviews Genetics*, 13(8), 537–551.

Sverak, T., Albrechtova, L., Lamos, M., Rektorova, I., & Ustohal, L. (2018). Intensive repetitive transcranial magnetic stimulation changes EEG microstates in schizophrenia: A pilot study. *Schizophrenia Research*, 193, 451–452.

Taly, A., Corringer, P.-J., Guedin, D., Lestage, P., & Changeux, J.-P. (2009). Nicotinic receptors: allosteric transitions and therapeutic targets in the nervous system. *Nature Reviews Drug Discovery*, 8(9), 733–750.

Tatum, W. O., Dworetzky, B. A., & Schomer, D. L. (2011). Artifact and Recording Concepts in EEG: *Journal of Clinical Neurophysiology*, 28(3), 252–263.

Taylor, M. M., & Creelman, C. D. (1967). PEST: Efficient Estimates on Probability Functions. *The Journal of the Acoustical Society of America*, 41(4A), 782–787.

The International Schizophrenia Consortium. (2009). Common polygenic variation contributes to risk of schizophrenia and bipolar disorder. *Nature*, 460(7256), 748–752.

The Schizophrenia Psychiatric Genome-Wide Association Study (GWAS) Consortium, Ripke, S., Sanders, A. R., Kendler, K. S., Levinson, D. F., Sklar, P., ... Gejman, P. V. (2011). Genome-wide association study identifies five new schizophrenia loci. *Nature Genetics*, 43(10), 969–976.

Tomescu, M. I., Rihs, T. A., Rochas, V., Hardmeier, M., Britz, J., Allali, G., ... Michel, C. M. (2018). From swing to cane: Sex differences of EEG resting-state temporal patterns during maturation and aging. *Developmental Cognitive Neuroscience*, 31, 58–66.

Tomescu, Miralena I., Rihs, T. A., Becker, R., Britz, J., Custo, A., Grouiller, F., ... Michel, C. M. (2014). Deviant dynamics of EEG resting state pattern in

22q11.2 deletion syndrome adolescents: A vulnerability marker of schizophrenia? *Schizophrenia Research*, 157(1), 175–181.

Tomescu, Miralena I., Rihs, T. A., Roinishvili, M., Karahanoglu, F. I., Schneider, M., Menghetti, S., ... Cappe, C. (2015). Schizophrenia patients and 22q11.2 deletion syndrome adolescents at risk express the same deviant patterns of resting state EEG microstates: A candidate endophenotype of schizophrenia. *Schizophrenia Research: Cognition*, 2(3), 159–165.

Turetsky, B. I., Calkins, M. E., Light, G. A., Olincy, A., Radant, A. D., & Swerdlow, N. R. (2007). Neurophysiological Endophenotypes of Schizophrenia: The Viability of Selected Candidate Measures. *Schizophrenia Bulletin*, 33(1), 69–94.

Turetsky, B. I., Greenwood, T. A., Olincy, A., Radant, A. D., Braff, D. L., Cadenhead, K. S., ... Calkins, M. E. (2008). Abnormal Auditory N100 Amplitude: A Heritable Endophenotype in First-Degree Relatives of Schizophrenia Probands. *Biological Psychiatry*, 64(12), 1051–1059.

Uhlhaas, P. J., & Singer, W. (2010). Abnormal neural oscillations and synchrony in schizophrenia. *Nature Reviews Neuroscience*, 11(2), 100–113.

Umbricht, D., & Krljes, S. (2005). Mismatch negativity in schizophrenia: a meta-analysis. *Schizophrenia Research*, 76(1), 1–23.

Urigüen, J. A., & Garcia-Zapirain, B. (2015). EEG artifact removal—state-of-the-art and guidelines. *Journal of Neural Engineering*, 12(3), 031001.

van der Stelt, O., & Belger, A. (2007). Application of Electroencephalography to the Study of Cognitive and Brain Functions in Schizophrenia. *Schizophrenia Bulletin*, 33(4), 955–970.

Vos, T., Abajobir, A. A., Abate, K. H., Abbafati, C., Abbas, K. M., Abd-Allah, F., ... Murray, C. J. L. (2017). Global, regional, and national incidence, prevalence, and years lived with disability for 328 diseases and injuries for 195 countries, 1990–2016: a systematic analysis for the Global Burden of Disease Study 2016. *The Lancet*, 390(10100), 1211–1259.

Waldo, M. C., Adler, L. E., & Freedman, R. (1988). Defects in auditory sensory gating and their apparent compensation in relatives of schizophrenics. *Schizophrenia Research*, 1(1), 19–24.

Winterer, G., & McCarley, R. W. (2011). Electrophysiology of Schizophrenia. In D. R. Weinberger & P. J. Harrison (Eds.), *Schizophrenia* (pp. 311–333). Oxford, UK: Wiley-Blackwell.

Yuan, H., Zotev, V., Phillips, R., Drevets, W. C., & Bodurka, J. (2012). Spatiotemporal dynamics of the brain at rest — Exploring EEG microstates as electrophysiological signatures of BOLD resting state networks. *NeuroImage*, *60*(4), 2062–2072.


Yue, W.-H., Wang, H.-F., Sun, L.-D., Tang, F.-L., Liu, Z.-H., Zhang, H.-X., ... Zhang, D. (2011). Genome-wide association study identifies a susceptibility locus for schizophrenia in Han Chinese at 11p11.2. *Nature Genetics*, *43*(12), 1228–1231.

Appendix A


da Cruz, J. R., Rodrigues, J., Thoresen, J. C., Chicherov, V., Figueiredo, P., Herzog, M. H., & Sandi, C. (2018)

ORIGINAL ARTICLE

Dominant men are faster in decision-making situations and exhibit a distinct neural signal for promptness

Janir da Cruz^{1,2}, João Rodrigues³, John C. Thoresen³, Vitaly Chicherov¹, Patrícia Figueiredo², Michael H. Herzog¹ and Carmen Sandi ³

¹Laboratory of Psychophysics, Brain Mind Institute, School of Life Sciences, Swiss Federal Institute of Technology Lausanne (EPFL), CH-1015 Lausanne, Switzerland, ²Institute for Systems and Robotics – Lisboa, Department of Bioengineering, Instituto Superior Técnico, Universidade de Lisboa, 1049-001 Lisbon, Portugal and ³Laboratory of Behavioral Genetics, Brain Mind Institute, School of Life Sciences, Swiss Federal Institute of Technology Lausanne (EPFL), CH-1015 Lausanne, Switzerland

Address correspondence to Carmen Sandi, Laboratory of Behavioral Genetics, Brain Mind Institute, School of Life Sciences, Swiss Federal Institute of Technology Lausanne (EPFL), CH-1015 Lausanne, Switzerland. Email: carmen.sandi@epfl.ch  orcid.org/0000-0001-7713-8321

Janir da Cruz, João Rodrigues, and John C. Thoresen contributed equally to this work
Michael H. Herzog and Carmen Sandi contributed equally to this work

Abstract

Social dominance, the main organizing principle of social hierarchies, facilitates priority access to resources by dominant individuals. Throughout taxa, individuals are more likely to become dominant if they act first in social situations and acting fast may provide evolutionary advantage; yet whether fast decision-making is a behavioral predisposition of dominant persons outside of social contexts is not known. Following characterization of participants for social dominance motivation, we found that, indeed, men high in social dominance respond faster—without loss of accuracy—than those low in dominance across a variety of decision-making tasks. Both groups did not differ in a simple reaction task. Then, we selected a decision-making task and applied high-density electroencephalography (EEG) to assess temporal dynamics of brain activation through event related potentials. We found that promptness to respond in the choice task in dominant individuals is related to a strikingly amplified brain signal at approximately 240 ms post-stimulus presentation. Source imaging analyses identified higher activity in the left insula and in the cingulate, right inferior temporal and right angular gyri in high than in low dominance participants. Our findings suggest that promptness to respond in choice situations, regardless of social context, is a biomarker for social disposition.

Key words: High-density electroencephalography, Leadership, Reaction time, Social hierarchy

Introduction

Social hierarchies are pervasive across social species (van der Kooij and Sandi 2015). Although individuals' rank in social hierarchies can be reshuffled with changing circumstances (Knight

and Mehta 2017), there are drastic differences in the predisposition of individuals to attain or strive for dominance (Ellyson and Dovidio 1985; Johnson et al. 2012). Socially dominant individuals show consistently elevated motivation and directed behaviors to

control others (Hall et al. 2005). In social encounters, dominant individuals talk more (Schmid Mast 2002), interrupt others frequently (Ferguson 1977; Goldberg 1990), and are more likely to initiate social interactions, a behavior already observed in dominant children (Johnson et al. 2012). Even though humans use also other strategies (e.g., prestige) to navigate their way through social hierarchies (Maner and Case 2016), dominance is a strong predictor of peer ratings of competence (Anderson and Kilduff 2009) even when an individual actually lacks competence (Wiggins 1979; Buss and Craik 1980; Anderson and Kilduff 2009). Dominance is also the trait that most predicts who emerges as the leader in groups (Guinote 2017), even more so than intelligence (Judge et al. 2002).

Current knowledge about dominant people is mainly derived from their behavior in social, particularly competitive, contexts; little is known about their individual traits. Perhaps dominant people present specific traits, not necessarily depending on social contexts—though also manifested in them—that help them gather the referred social influence. In competitive settings, high dominance individuals have been shown to be faster in decision-making than low dominance ones (Santamaría-García et al. 2014, 2015; Balconi and Vanutelli 2016). Here, we hypothesized that a trait of dominant individuals is fast speed of acting as a general cognitive style. Being the fastest to take control of resources or to ensure survival could provide an evolutionary advantage and facilitate the emergence of dominant behaviour. According to the simple leader-follower decision rule “follow the one who moves first” (Van Vugt et al. 2008), being capable of deciding and consequently acting first in relevant social contexts increases the likelihood of becoming dominant and attaining leadership (Rands et al. 2008; King et al. 2009; Johnson et al. 2012). Despite the known evolutionary advantage redeemed by acting fast in social situations, it is not known whether dominant individuals respond faster as a cognitive style during decision-making, regardless of social context.

To test the hypothesis that trait dominance in humans relates to promptness of action, we first characterized individuals' social dominance motivation through the commonly used Personality Research Form dominance subscale [PRF-d (Jackson 1974)]. People who score high on PRF-d frequently attempt to control both, their environment and other people, and are forceful, decisive, authoritative and domineering (Buss and Craik 1980). They also tend to be considered high in leadership by their peers (Bateman and Crant 1993). Our hypothesis was that whereas high dominance individuals would have shorter latencies to respond when taking decisions on tasks involving cognitive challenges, they would not differ from low dominance individuals when performing a simple reaction task (SRT). Given the well-known sex differences in dominance (Helgeson and Fritz 1999; Dykiert et al. 2012), we focused on men. Thus, we set a series of experiments to assess if people scoring high or low in dominance motivation would differ in their promptness to respond across tasks involving different decision-making processes and in a SRT. Finally, we selected experimental conditions revealing group differences in response time to carry out an event related potentials (ERP) study with high-density electroencephalography (EEG) study to analyze potential differences in temporal dynamics of brain activation.

Materials and Methods

Participants

We recruited students from the Swiss Federal Institute of Technology in Lausanne (EPFL) and the University of Lausanne

(UNIL). Two-hundred and forty male participants were assigned to one of five different experiments included in the study. Participants were classified as either high or low in social dominance, depending on whether their score in the PRF-d (see Personality measurements) was below (low dominance) or above (high dominance) PRF-d = 9 (the median PRF-d score obtained from 412 students to the questionnaire). All participants were in good physical health with no current medical illnesses and had no neurological or psychiatric history. In addition, participants were tested for ocular dominance and completed a standardized handedness questionnaire (Oldfield 1971). We verified that all participants had good visual acuity of at least 1.0, as measured by the Freiburg Visual Acuity Test using both eyes (Bach 1996). Group characteristics and statistical analysis comparing demographic information between the five experiments as well as between the two dominance groups within each experiment are presented in Table 1. Participants gave informed written consent prior to the experiment, after receiving detailed written information. They obtained financial compensation of 20 CHF per hour. Experimental sessions were scheduled between 1 PM and 7 PM. All procedures complied with the Declaration of Helsinki. The Brain Mind Institute Ethics Committee for human behavior approved experiments 1-4, and the Cantonal Ethics Committee from Canton de Vaud the EEG experiment. The experimenters were male and were blind to the participants' personality scores.

Personality measurements

Social dominance motivation was assessed using the Personality Research Form dominance subscale [PRF-d (Jackson 1974)] through an online questionnaire (www.qualtrics.com) that was administered individually to participants several days before the experiment. The PRF-d is a 16-item true/false questionnaire that asserts motivation for social dominance with positive and negative items such as “The ability to be a leader is very important to me” and “I am not very insistent in an argument,” respectively. PRF-d scores are strongly and positively correlated with the frequency of self-reported prototypical social dominance acts such as “issuing orders that got the group organized” (Buss and Craik 1980) and with peer-nominations for leadership (Bateman and Crant 1993).

Spielberger's State-Trait Anxiety Inventory (STAI) (Spielberger et al. 1983) has two components designed to measure trait (STAI-T; e.g., “I worry too much over something that really doesn't matter”) and state (STAI-S; e.g., “I am presently worrying over possible misfortunes”) anxiety, independently. Each questionnaire includes 20-items to which participants respond on a 4-point Likert-type scale from 1 – completely disagree to 4 – completely agree. Scores range from 20 (very low anxiety) to 80 (very high anxiety). Since trait anxiety can correlate with social dominance and predict behavioral outcomes, we assessed STAI-T to control for this variable in statistical analyses.

Behavioral Experiments

We assessed the impact of dominance motivation on latency to respond in three choice tasks involving different cognitive processes and demands and a fourth one consisting of a simple reaction time (RT).

Custom-made E-prime scripts (version 2.0; Psychology Software Tools, Pittsburgh, PA) were used to program the behavioral experiments. In all experiments, participants sat comfortably with their heads approximately 50 cm apart from a

Table 1 Summary of participants' personal information

	Experiment 1	Experiment 2	Experiment 3	Experiment 4	Experiment 5	Between Experiments Analyses
Number of Participants						
High Dominance	16	20	45	26	13	
Low Dominance	16	20	45	26	13	
High Dominance	21.19 ± 2.26	20.55 ± 2.24	20.29 ± 2.61	21.35 ± 2.37	21.15 ± 2.30	
Age ± SD						
Low Dominance	21.38 ± 2.99	21.40 ± 1.79	21.31 ± 2.60	20.85 ± 1.93	21.92 ± 3.95	$F_{4,235} = 0.548, p = .701$
Analysis	$t(30) = 0.200, p = .843$	$t(38) = 1.328, p = .192$	$t(88) = 1.862, p = .066$	$t(50) = 0.835, p = .408$	$t(24) = 0.607, p = .550$	
High Dominance	12.50 ± 2.00	12.85 ± 1.60	11.64 ± 1.63	12.58 ± 1.33	12.23 ± 1.83	
PRF-d ± SD						
Low Dominance	6.00 ± 1.41	4.90 ± 1.55	5.98 ± 1.75	4.73 ± 1.93	5.23 ± 2.09	$F_{4,235} = 0.129, p = .972$
Analysis	$t(30) = 10.614, p < .001$	$t(38) = 15.955, p < .001$	$t(88) = 15.906, p < .001$	$t(50) = 17.062, p < .001$	$t(24) = 9.085, p < .001$	
High Dominance	35.19 ± 7.28	38.60 ± 37.55	39.49 ± 6.91	38.27 ± 10.01	40.08 ± 10.47	
STAI-T ± SD						
Low Dominance	42.63 ± 8.16	37.55 ± 8.68	41.91 ± 7.97	39.23 ± 9.94	42.77 ± 11.40	$F_{4,235} = 1.125, p = .345$
Analysis	$t(30) = 2.720, p = .011$	$t(38) = 0.404, p = .688$	$t(88) = 1.541, p = .127$	$t(50) = 0.348, p = .730$	$t(24) = 0.627, p = .537$	
Handedness (Right/ Left)						
High Dominance					12/1	
Low Dominance					10/3	
Analysis					$\chi^2(1) = 1.182, p = .277$	

Note that handedness was not collected in Experiments 1–4.

computer's screen. In choosing the tasks, we aimed at exploring in a non-parametric manner potential boundaries for findings in response latencies by covering different sensory processing, cognitive load and decision-making processes in each task. We also aimed at including different instructions and time demands across tasks so that in case of finding task-related differences in response latencies, we could explore whether time constraints or lack of them could play a role in our findings.

Experiment 1 involved a facial emotion discrimination task. The stimuli were greyscale pictures of male faces (72 identities) with a frontal profile acquired from the databases FACES (Ebner et al. 2010), Nimstim Set of Facial Expressions (Tottenham et al. 2009), Radboud Faces Database (Langner et al. 2010) and The Karolinska Directed Emotional Faces (Lundqvist et al. 1998). No clothes or jewelry were visible and we took care to avoid features that attracted attention (e.g., scars, moles, facial hair, and unusual haircuts). Adobe Photoshop CS5 software (version 12.0) was used for image adjustment by converting the pictures to greyscale, equalizing contrast, rescaling to 860 × 600 pixels, and then manually standardizing the distance between the eyes and the chin while preserving the original aspect ratio. The picture background was set to grey, and luminance was equalized using the Matlab® Shine Toolbox (Willenbockel et al. 2010). Participants were shown 120 unique pictures: 20 different facial expressions per emotion (anger, happiness or neutral) in their original format and also in their flopped format (obtained by mirror-reversing the original image across the vertical axis). Participants were asked to fixate upon a central cross and to select which of the three emotions were presented by pushing a pre-assigned keyboard key. Participants were asked to be as fast and accurate as possible. The faces were presented in one out of five positions on the screen; either center or 20° or 35° rotated to either side of the center, and appeared for only 80 ms to avoid saccades towards the target. The next face was presented immediately after the participant's response (Fig. 1a). This experiment assessed latency to respond and accuracy in determining facial emotion.

Experiment 2 involved a facial recognition memory task comprising two phases, memorization and recognition. In the first phase, participants were asked to memorize 30 different faces, of which 15 had to be recognized among 15 novel faces in the second phase. We used the same images as in Experiment 1. Faces were displayed for 10 s each. In order to probe different time constraints than in the previous task (in which participants performed under time pressure), in this task participants could progress in the task, to some extent, at their pace. They could pass to the next face by pushing the spacebar in the memorization phase or by answering yes/no in the recognition phase (Fig. 1b). Immediately before the memorization phase, participants were instructed to memorize as many pictures as they could within 90 s and were told that their memory would be tested in the ensuing recognition phase. They were also informed that an average of 3 s per face was allowed because all 30 pictures had to be viewed within 90 s. The latency to pass to the next image was recorded. The second, recognition phase took place within 5 minutes after the memorization phase. Participants were presented with faces and they had to indicate whether they had visualized them during the previous phase. There was no time limit to answer, and participants were instructed to guess in case of doubt. Latency to respond and accuracy were recorded. Due to aberrant response times, data from one participant was removed from the analyses.

Experiment 3 aimed at assessing possible group-related differences in latency to respond in a task essentially different to

the previous ones, not involving faces and intermediate levels of time pressure. We selected a working memory map-based route-learning task, as previously described (Thoresen et al. 2016). This task tests visual working memory by presenting a map trajectory and then presents a test trajectory to which participants must respond as to whether the test trajectory was the same or different. The results presented here are a reanalysis from data reported in (Thoresen et al. 2016), with participants stratified according to the PRF-d questionnaire. For the experiment, 48 maps with similar route densities were created using Google Static Maps API (<https://developers.google.com/maps>). An area of 0.9 km² was shown, and a pixel resolution of 640 × 640 was used. Half the maps were cartographic road maps and half were satellite maps with roads superimposed. Participants viewed animations of a red marker following a set route. Each trial consisted of a learning stimulus and a test stimulus. In the learning stimulus, the marker was animated for approximately 17 s, and participants were instructed to learn the trajectory of the route. After the trajectory finished, the marker remained static for 2 s, and the same trajectory was repeated again. The test stimulus ensued immediately with the question “Is this the same route as before?” appearing in French for 1 s and accompanied by two repetitions of an animation, presented at double speed in a map with a size reduction of 27%. Evenly between trials, in a random order, this would be either the same trajectory as before or one with a subtle difference midcourse. Participants could respond as soon as the second trajectory appeared, but were told that after viewing the repeated trajectory, they would have 4 s to answer (“same” or “different”) using predefined keys of a standard keyboard. Participants were not asked to be fast and would always be able to respond to all trials, regardless of how long they took to respond. The task was preceded by four practice trials for which responses were not recorded. Data from the first block of 24 trials was analyzed for latency to respond and accuracy. A depiction of one trial can be seen in Fig. 1c.

Experiment 4 was a control experiment that assessed participants' performance in a simple reaction time task adapted from a crossed-uncrossed difference task (Fig. 2). At each trial, a grey square appeared either on the left or on the right of a cross displayed at the center of the screen. The inter-trial interval varied randomly between 0.15 and 1.5 s. Participants were asked to push the spacebar of the keyboard as soon as they perceived the square, regardless of the side on which it was presented. After 0.5 s, the stimulus disappeared even if no response had been entered. After a practice block of six trials, a block of 200 stimuli was presented. Breaks were introduced every 50 trials, and the entire task took approximately 10 minutes to complete.

EEG Experiment

Experiment 5 aimed at identifying neural signals related to differences in promptness to respond in high and low dominance participants. To this end, we used an adapted version of the task from Experiment 1. Stimuli included 40 male or female faces with happy, sad, angry, or neutral expressions presented in a randomized fashion. Happy and sad faces were obtained from Ekman and Friesen's Pictures of Facial Affect Series (Ekman and Friesen 1976), while angry and neutral faces were obtained from FACES (Ebner et al. 2010), Radboud Faces Database (Langner et al. 2010) and the Karolinska Directed Emotional Faces (Lundqvist et al. 1998). Using Adobe Photoshop CS5 software (version 12.0), the images were cropped to the

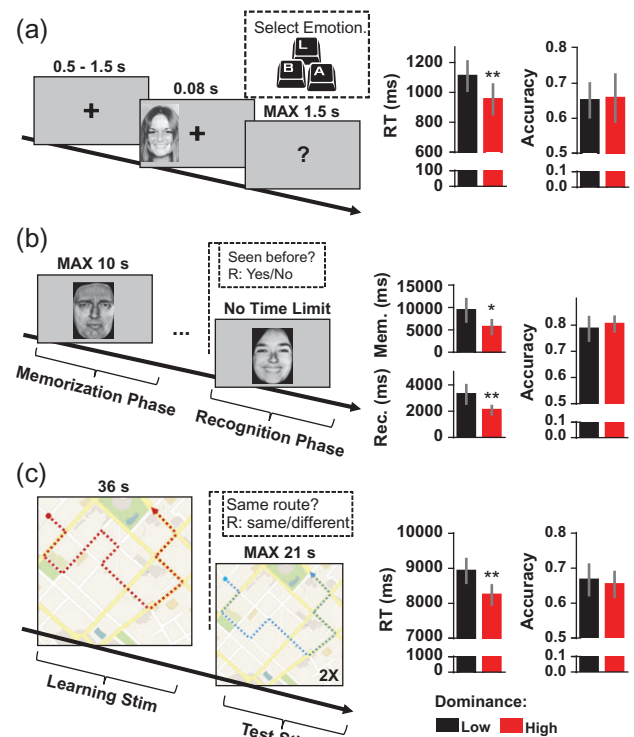


Figure 1. High dominance individuals respond faster but with the same accuracy as low dominance participants in a variety of choice decision-making tests. (a) Schematic representation of the emotion discrimination task included in experiment 1 (left panel) and corresponding RT and accuracy results for high and low dominance participants (right panel). Participants had to indicate the emotion (anger, happiness or neutral) depicted in the presented face, which could appear at different distances from the screen's center. (b) Schematic representation of the facial recognition memory task included in experiment 2 (left panel) and RT for both experimental phases, memorization and recognition, as well as accuracy data for the recognition phase (right panel). Participants learn faces (Mem., memorization phase) and indicated whether phases were familiar (i.e., presented in the memorization phase) or not (Rec., recognition phase) while responding at their own pace. (c) Schematic representation of the map-reading working memory task delivered in experiment 3 (left panel) and corresponding results (right panel). Participants had to indicate whether a route depicted by an animation in the screen was the same or different as the one just presented on a map. Data are presented as mean with 95% CI (* $p < 0.05$, ** $p < 0.01$). See also Table S1 for a summary of the statistical results.

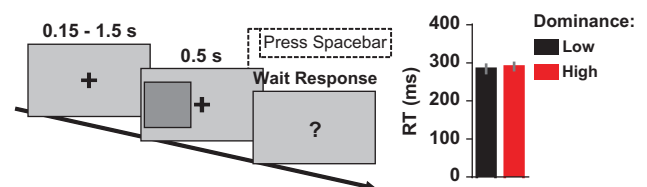


Figure 2. Schematic representation of the simple reaction time task delivered in experiment 4 (left panel) and corresponding results (right panel). Participants had to respond as soon as a grey square appeared on screen. Data are presented as mean with 95% CI (* $p < 0.05$, ** $p < 0.01$).

central portion of the face, regularized for luminosity and contrast, and transformed to the same size (346 × 543 pixels). All stimuli were presented on a grey background (RGB: 192, 192, 192). The images were displayed on an Asus VG248QE monitor with a resolution of 1920 × 1080 pixels and a refresh rate of 144 Hz. Participants sat 50 cm from the monitor in a dimly lit

Faraday cage. Background luminance was below 1 cd/m². Gaze was monitored by an eye tracker (The Eye Tribe ©) throughout the experiment. The head was fixed by a chin rest.

All participants completed two distinct experimental conditions, with the order of the conditions pseudo-randomly assigned to each participant. During the first condition, happy and sad faces (Happy vs. Sad) were used as stimuli, while in the second condition, angry and neutral faces (Angry vs. Neutral) were presented. Each condition began with one practice block with 10 trials followed by four experimental blocks with 80 trials each. Before each condition, participants were presented with onscreen instructions and after the practice block, they were allowed to ask any questions regarding the task. Experimental blocks were separated by a brief interval of 10 s. Participants were instructed to be as fast and accurate as possible, to keep their gaze on a fixation cross in the center of the screen, and to report the perceived emotion by pressing 1 of 2 buttons held in each hand or to guess when they were not sure. The association between response side and valence was counterbalanced across participants evenly within the high dominance and low dominance participants. During each trial, stimuli were presented in the observer's periphery either 26° left or right, during 0.1 s, followed by a 3 s period where the fixation cross was replaced with a question mark, prompting participants to respond. After each response, an inter-trial pause with a random duration from 0.5 to 1.5 s ensued. If a participant failed to respond, a short buzz sounded and the trial was repeated at the end of the presentation stack. For each condition, accuracy was calculated as the percentage of correct responses.

EEG Recording and Processing

Continuous EEG was recorded using a BioSemi Active 2 system (BioSemi) with 192 Ag-AgCl sintered active electrodes referenced to the common mode sense (CMS) electrode. The cap size and placement were adjusted individually: the Cz electrode was positioned halfway between the inion and nasion. The set of electrodes uniformly covered the entire scalp. The electrooculogram (EOG) was recorded with electrodes positioned 1 cm above and below the right eye and 1 cm lateral to the outer canthi. The recording sampling rate was 2048 Hz. Offline data were down sampled to 512 Hz and processed using an automatic pre-processing pipeline (da Cruz et al. 2018) that included the following steps: filtering via a bandpass of 1 – 40 Hz (3rd order Butterworth filter); removal of line-noise (CleanLine; www.nitrc.org/projects/cleanline); re-referencing to the bi-weight estimate of the mean of all channels (Hoaglin et al. 1982); removal and 3D spline interpolation of bad channels; removal of bad epochs; independent component analysis (ICA) to remove eye movement-, muscular- and bad channel-related artefacts; and removal of epoch artefacts. The proportion of interpolated electrodes was less than 5% for each subject. We extracted EEG epochs from 100 ms before stimulus onset (baseline) to 500 ms after stimulus onset. The averaged epochs for each participant were baseline corrected. The percent of rejected epochs was less than 10% for each subject.

Global Field Power Analysis

The global field power (GFP) is an instantaneous reference-independent measure of the neuronal response strength, and it is calculated as the standard deviation of the potentials across all electrodes (Lehmann and Skrandies 1980). To account for

temporal auto-correlation, 10 ms of contiguous significant effects ($p < 0.05$) is considered reliable (Guthrie and Buchwald 1991). The GFP was computed for each participant and each condition separately. Repeated-measures ANOVAs with the factors group (low and high dominance) and condition (Happy vs. Sad, Angry vs. Neutral) were conducted at each time point of the GFPs. Statistics were computed using the Statistical Toolbox for Electrical Neuroimaging (STEN) developed by Jean-François Knebel (<http://www.unil.ch/line/home/menuinst/about-the-line/software-analysis-tools.html>).

Distributed Electrical Source Imaging

Inverse solutions were computed for the time interval corresponding to the significant main effect of group in the GFP to estimate brain regions responsible for the group difference using the Local Auto Regressive Average inverse solution (Grave de Peralta Menendez et al. 2004; Plomp et al. 2010). A source space of 4022 points equally spaced throughout the grey matter of the Montreal Neurological Institute's (MNI) ICBM 152 non-linear atlas template brain (Fonov et al. 2011) was defined, and a model identical to (Plomp et al. 2009, 2010) was used. Source analysis was performed using Cartool software (Brunet et al. 2011). Repeated-measures ANOVAs with the factors group (low and high dominance) and condition (Happy vs. Sad, Angry vs. Neutral) were computed for each solution point on the current densities using STEN. Multiple comparisons for each solution point were partially corrected using the following spatial criterion: the clusters must contain at least 15 neighboring solution points showing significant effects ($p < 0.05$) (Knebel and Murray 2012). Current densities were averaged across the significant region for each cluster for the identification of each activation cluster center of mass (CoM). Activity in the solution point closest to each CoM was used to represent the corresponding brain region.

Salivary Cortisol Analyses

Saliva was collected three times: immediately after each participant had signed the informed consent form, at the beginning of the washout period, and 20 min after the end of the second condition. A sample of approximately 0.8 to 1.4 mL of saliva was obtained at each collection in 10 mL polypropylene tubes and frozen below -20°C until processed. Samples were then centrifuged at 3000 rpm for 15 minutes at room temperature, and salivary cortisol concentrations were measured by enzyme immunoassay according to the manufacturer's instructions (Salimetrics, Newmarket, Suffolk, United Kingdom). The samples were used to analyze cortisol baseline levels and hormonal changes taking place during the experiment. To control for the circadian rhythm of cortisol, all experimental sessions were scheduled between 1 PM and 7 PM. To estimate overall cortisol reactivity, we computed the area under the curve with respect to ground (AUC_g) and with respect to increase (AUC_i) indices (Pruessner et al. 2003). Due to sample contamination, data from 5 subjects had to be excluded resulting in 21 subjects (10 high dominance and 11 low dominance) with complete sets of 3 saliva samples proper for the cortisol AUC_g and AUC_i calculations.

Statistical Analyses

Behavioral data: Trials with latencies to respond values below 200 ms and above the stipulated time limits for each

experiment (c.f., see specific protocols above) were not considered valid and, hence, removed from the raw dataset. Trials with latencies three standard deviations away from each subject's mean latency were excluded (representing less than 5% of trials per subject). The effects of dominance group on latency and on accuracy were tested with ANCOVAs, or mixed-design ANCOVAs if a within-subject variable existed (in Experiment 1, within-subjects variables were used for emotion and difficulty; see Table S1). Accuracy was included as a covariate when latency was a dependent variable to account for possible trade-offs between these two variables (except in experiment 4 that involved a simple RT task in which accuracy is not relevant). Given that trait anxiety can affect individuals' reaction time (Etkin et al. 2004), ANCOVA included trait anxiety (evaluated with the STAI-T) as a covariate on analyses of the dependent variables latency and accuracy. Details concerning models and covariates can be consulted on Table S1. To account for random variation in latency to respond among participants in the EEG experiment, a mixed-effects model was used. The fixed effects were defined as an interaction model of "group" \times "condition" with additional predictors to control for STAI-T and accuracy, as in the previous ANCOVAs. Within-subjects variables differ from experiment 1 to accommodate the changes in the experimental designs: emotion and difficulty were used in experiment 1 while condition was used in experiment 5. Details concerning the fixed effects used in these models can be consulted on Tables S2 and S3. Random effects were the subjective intercept and slope, which respectively account for differences in individual baseline levels of latencies and for different latency changes due to condition. To study the overall effect of the PRF-d score in decision-making tasks' RT, we combined Experiments 1 to 5 in a mixed-effects model with an additional variable encoding decision-making experiments. RTs were standardized (z-scored) for each experiment to avoid comparing responses with different temporal scales. The fixed effects were defined as the interaction between PRF-d and the decision-making encoding variable, with additional predictors to control for STAI-T and accuracy (as done for all previous models). Details concerning the fixed effects used in these models can be consulted on Table S4. Random effects were a random intercept to account for the different experiments and a random slope to account for the two conditions in Experiment 2 (memorization and recognition). Satterthwaite's approximation for the degrees of freedom was used to compute mixed-effects models' p -values with the *lmerTest* package (Kuznetsova et al. 2017). The reported effect size statistics for the ANOVA-based methods were the Eta Square (η^2) for all experiments. Statistical analyses were performed with IBM® SPSS® Statistics Version 21 and in the R programming environment (R Core Team 2014).

Cortisol data: Cortisol AUC_g and AUC_i indices were used as dependent variables in ANOVAs to assess the effect of group on glucocorticoid reactivity in Experiment 5.

EEG data: To assess the effect of the activity in each brain region on RT or accuracy, significant CoM activations were used as independent variables in separate regressions for the dependent variables RT and accuracy. To account for the random variation in RT among participants, a mixed-effect model was used. The fixed effects were the CoM activations and the random effects were, as in the behavioral analysis, the subjective intercept and slope. Satterthwaite's approximation for the degrees of freedom was used to compute p -values. Inter-individual correlations between significant CoM activations were calculated with Pearson partial correlations using the *pcor* package (Kim 2015).

Results

High dominance individuals are faster to respond in choice tasks than low dominance ones

We assessed potential differences between high and low dominance individuals on latency to respond and accuracy in three choice tasks involving different cognitive demands and instructions (Experiments 1–3). We also tested them for latency to respond in a simple reaction time control task (Experiment 4).

In the emotion discrimination task (Experiment 1), high dominance participants had shorter latencies to respond than low dominance ones ($F_{1,28} = 9.06$, $p = 0.005$, $\eta^2 = 0.216$, 95% CI [0.044, 0.414]). The two groups did not differ in accuracy ($F_{1,29} = 0.02$, $p = 0.963$, $\eta^2 < 0.001$, 95% CI [<0.001 , <0.001]; Fig. 1a; Table S1). There were no significant effects for the task-related factors "emotion" and "difficulty", the latter related to the degree of rotation of stimulus presentation from fixation center (except for a significant effect of task difficulty on accuracy; $F_{1,58} = 3.45$, $p = 0.038$, $\eta^2 = 0.105$, 95% CI [0.003, 0.221]). There were no significant interactions between the different factors (see Table S1).

In the facial recognition memory task (Experiment 2; Fig. 1b), high dominance participants had shorter latencies to respond than low dominance ones in both, memorization ($F_{1,35} = 7.28$, $p = 0.011$, $\eta^2 = 0.169$, 95% CI [0.023, 0.333]) and recognition ($F_{1,35} = 9.64$, $p = 0.004$, $\eta^2 = 0.195$, 95% CI [0.043, 0.375]; Fig. 1b; Table S1) phases. In the recognition phase, both groups showed similar accuracy ($F_{1,36} = 0.57$, $p = 0.455$, $\eta^2 = 0.015$, 95% CI [< 0.001 , 0.128]). There was a positive correlation in participant's latencies across the two conditions (memorization and recall) ($r = 0.334$, $n = 40$, $p = 0.035$).

In the map-based route-learning task (Experiment 3; Fig. 1c), high dominance participants responded again faster than low dominance ones ($F_{1,86} = 9.56$, $p = 0.003$, $\eta^2 = 0.097$, 95% CI [0.021, 0.202]; Fig. 1c; Table S1). Here, again, both groups had similar accuracy levels ($F_{1,87} = 0.33$, $p = 0.567$, $\eta^2 = 0.004$, 95% CI [<0.001 , 0.051]).

In the simple reaction time task (Experiment 4), as hypothesized, there were no dominance-related differences in latency to respond ($F_{1,49} = 0.61$, $p = 0.439$, $\eta^2 = 0.012$, 95% CI [<0.001 , 0.101]; Fig. 2). This conclusion was further supported by a one-way Bayesian ANOVA that depicted a Bayesian factor (BF_{10}) for the main effect of group of 0.329 indicating around 3 times more evidence in favor of the null hypothesis (no difference between groups) as compared to the alternative (i.e., that there was a difference between groups).

High dominance individuals show a distinctive EEG signal

To identify brain activations linked with faster latency to respond, we performed an additional experiment (experiment 5) with high-density EEG while participants performed a slightly modified version of the emotion recognition task in experiment 1 (Fig. 3a). First, as in previous experiments, latencies to respond were shorter for high than low dominance participants (Fig. 3b; Table S2; $\beta = 127.57$ ms, $SE = 60.88$ ms, 95% CI [5.82, 250.89], $t(23.59) = 2.10$, $p = 0.047$). Groups did not differ in accuracy (Fig. 3b; Table S3). We also verified that the observed dominance-related effects on latencies to respond were observed across all performed decision-making experiments when PRF-d scores are considered as a continuous variable instead of using the dichotomous median-split approach used above (Fig. S1; Table S4).

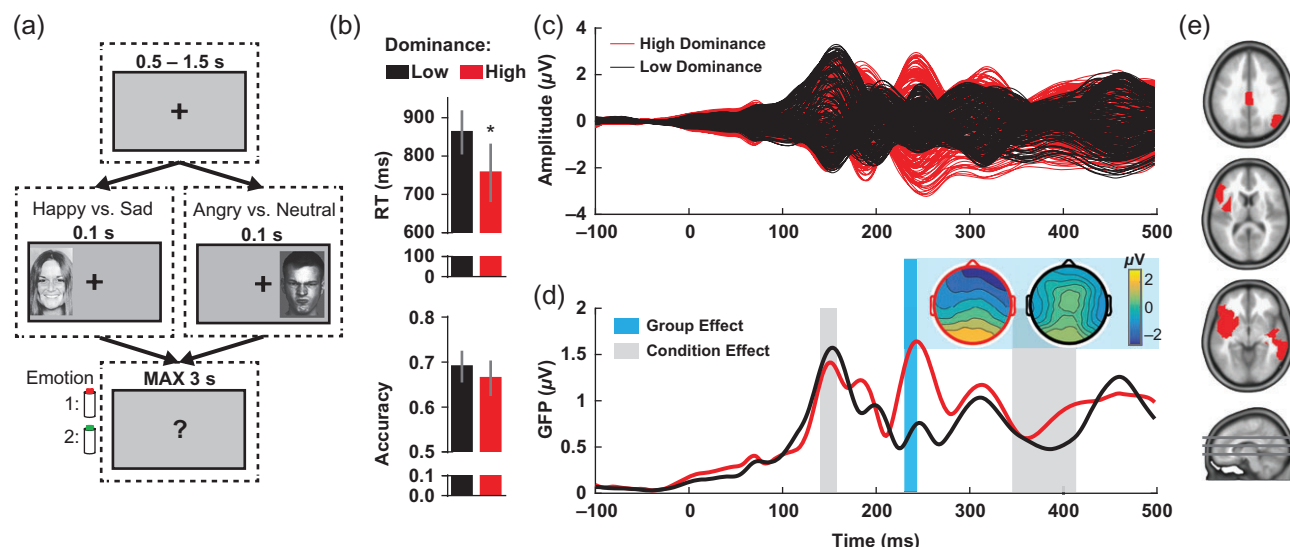


Figure 3. High dominance individuals show a distinctive EEG response related to faster reaction times. (a) Schematic representation of a single experimental trial for the Happy vs. Sad and Angry vs. Neutral conditions included in experiment 5. Following a fixation cross with a random duration from 0.5 to 1.5 s, one of the condition's facial stimuli is presented for 0.1 s. Participants then had 3 s to press the button corresponding to the identified emotion. (b) High dominance individuals performed faster but not less accurate in this task. Data are presented as mean with 95% CI (* $p < 0.05$). See also Table S2 and Table S3. (c) Butterfly plots of the grand average ERPs, where each line is the group grand average for a single electrode. (d) GFP, a measure of how much electrode amplitudes deviate from the mean activity and a good indicator of brain activity, is plotted for both dominance groups. GFP showed a large increase in N2/P2 amplitude at approximately 240 ms for high dominance compared to low dominance individuals (cyan region). Topographical maps for each dominance group are also shown for this period. Red contour, high dominance; black contour, low dominance; cyan region $p < 0.05$; first gray regions $p < 0.05$. See also Table S5. (e) EEG source imaging results of the main effect of dominance group from 230 to 243 ms. Regions of significant differences, $p < 0.05$, are indicated in red. High dominance participants showed increased activation of 4 regions: the cingulate gyrus, the right angular gyrus, the left insula, and the right inferior temporal gyrus. See also Fig. S2 and Table S6.

Given previous work indicating that enhanced glucocorticoid levels can affect the activation of neural circuits (Henckens et al. 2011, 2012; Vogel et al. 2016, 2017), we measured salivary cortisol at different time points of the experiment. We found no differences between the groups in cortisol levels throughout the experiment were (AUCg: $F_{1,19} = 0.23$, $p = 0.638$, $\eta^2 = 0.012$, 95% CI [<0.001 , 0.070]; AUCi: $F_{1,19} = 0.24$, $p = 0.633$, $\eta^2 = 0.012$, 95% CI [<0.001 , 0.072]).

EEG event-related potentials (ERP) in high dominance participants showed more prominent deflections, approximately at 210 to 280 ms from stimulus onset, i.e., for the anterior N2 and posterior P2 ERP components (see butterfly plot in Fig. 3c). Repeated measures ANOVA of the global field power (GFP, Materials and Methods for details) showed a significant effect of group between 230 and 243 ms after stimulus onset ($F_{1,24} = 4.87$, $p = 0.037$, $\eta^2 = 0.169$, 95% CI [0.006, 0.370], Fig. 3d). High dominance participants had larger deflections ($M = 2.36 \mu V$, $SD = 1.26$) than low dominance participants ($M = 1.48 \mu V$, $SD = 0.68$). There were significant effects for the block condition, but no "group" \times "condition" interaction (for details see Table S5).

During the identified group effect period (230 to 243 ms), EEG source imaging analyses revealed increased activity in the cingulate gyrus, the right angular gyrus, the left insula, and the right inferior temporal gyrus in high dominance participants compared to low dominance participants (Fig. 3e; Fig. S2; Table S6 for Talairach coordinates). In exploratory analyses, we examined the relationship between the cingulate gyrus activity and response latency (Fig. S3), as well as inter-individual correlations between the cingulate gyrus and the right angular gyrus and between the left insula and the right inferior temporal gyrus (see Supplement and Fig. S2).

Discussion

In this study, we show that individuals high in dominance motivation respond faster in a variety of tasks with high cognitive demands, without impairing their accuracy. This dominance-related difference was not observed in a simple, less demanding reaction time task. Importantly, promptness to respond in high dominance individuals is related to a marked brain signal at 240 ms post-stimulus presentation, which is virtually absent in low dominance ones. The neuronal generators of this signal identified several brain regions (i.e., left insula, cingulate gyrus, right inferior temporal gyrus, and right angular gyrus) that showed higher activation in high than in low dominance participants.

Therefore, we found support for our hypothesis that high dominance individuals were consistently faster than low dominance ones even when participants are not in social context. Our strategy was to test participants across several challenges to be able to cover a broad spectrum of situations and, therefore, we did not gather data on parametric manipulations of a specific aspect. This approach allowed us to reveal that promptness of response of high dominance individuals is consistently shown across a variety of tasks that require: i) matching faces to one of 2–3 emotions under a high difficulty level (stimuli presented unpredictably at different locations from the fixation cross for only 80 ms) and trying to be as fast and accurate as possible (Experiments 1 and 5); ii) memorizing faces at own pace with advice to move on every 3 s to allow enough time for the totality of faces (Experiment 2, part 1); iii) recognizing formerly seen vs. unseen faces at own pace, without time limit (Experiment 2, part 2); iv) identifying whether a dynamic

map trajectory was the same as another one just presented before, under slight time pressure (4 s to respond per trial) but no specific instructions to be fast (Experiment 3). Accordingly, high dominance individuals displayed faster latencies to respond in situations ranging from quite high to low degrees of time pressure, and including emotional recognition, facial learning and memory, and a map-reading working memory. Except for the memorization part of Experiment 2 (part 1) in which participants' responses signaled an internal process, in all other cases they had to provide an answer out of 2-3 given choices. Sometimes, the high demanding task conditions, such as in Experiments 1 and 5, participants might have even reacted to some trials by guessing the answer. Importantly, the fact that high dominance subjects did not have an advantage in the SRT (Experiment 4) suggests that their fast responding advantage is not due to a superiority in perception processes or execution of motor actions. Instead, the common factor across tasks in which they show faster responses is a decision-making processes that links choice selection with action.

Previously, a few studies examined performance in participants whose social status was manipulated "artificially" in a competitive setting. When the hierarchy was created before the competitive encounter (i.e., participants were told *a priori* whether they were going to play with a superior or inferior adversary), participants were faster performing a basic visual perceptual decision task than when facing superior players (i.e., when they were made artificially "subordinate") without increasing their error rates and independently of the difficulty level (Santamaría-García et al. 2014). Interestingly, the degree to which their reaction times were reduced when playing with a superior, as compared to an inferior player correlated positively with participants' trait social dominance, suggesting that these individuals are more sensitive to competitive hierarchical cues (Santamaría-García et al. 2015). Social dominance was a combined measure from the behavioral approach reward responsiveness (BAS-R) and drive (BAS-D) scales from the Behavioral Activation System (BAS) questionnaire (Carver and White 1994; Hortensius et al. 2014). The BAS is a motivational system that has been related to feelings of dominance (Gable et al. 2000; Hortensius et al. 2014). When the hierarchy was created during the task, following a first competitive session on a selective attention decision task (i.e., participants were told that their performance in the task immediately before was superior to their competitor, making them artificially "dominant"), participants reduced their latencies to respond in the follow up session though, in this case, their accuracy was also reduced. This effect was specifically observed in individuals that scored high in the BAS questionnaire (Balconi and Vanutelli 2016). These findings suggest a particular sensitivity of individuals high in social dominance to motivate their responses in competitive settings, particularly when competitively challenged or developing a general sense of dominance and superiority than others. However, our study did not involve social competition and we still found lower latencies to respond in choice decision-making tasks in high than in low dominance participants. One possible explanation for this discordance is that the challenge involved in our experimental settings (always involving male experimenters instructed to maintain a behavioral distance with participants) differentially affected the engagement of participants as a function of their dominance motivation. Alternatively, high dominance subjects defined by the BAS questionnaire (used in the studies discussed above) and by the PRF-d questionnaire (used in our study) might not totally overlap. With the PRF-d scale, we might have

captured subjects that show a particularly engaged cognitive style concerning promptness of action in decision-making situations, regardless of the contingent competitive nature. Future studies should include both dominance measurements to cross-validate findings through different studies.

Interestingly, our behavioral findings resonate with a literature in animals that indicates a positive relationship between proactive (bolder and more aggressive than reactive ones) behavioral types and both social dominance and competitive ability (Oortmerssen et al. 1984; David et al. 2011; Riebli et al. 2011). In striking parallelism with our findings in humans, bolder stickleback fish (*Gasterosteus aculeatus*) were found to be faster in the speed of decision-making (time to making a decision) than their shyer conspecifics, though not different in accuracy (Mamuneas et al. 2015). In the wild, bolder fish tend to emerge as leaders and shyer fish as followers (Harcourt et al. 2009; Nakayama et al. 2012).

In humans, dominance is also a strong predictor of leadership (Judge et al. 2002). Therefore, our results might have as well implications for the emergence of leadership. In line with the leader-follower decision rule "follow the one who moves first" that operates in many animal social structures (Van Vugt et al. 2008), the likelihood to become a leader is thought to depend on specific internal or social traits that increases probability of movement initiation (Rands et al. 2008; King and Cowlishaw 2009), what suggest response times to be an indicative psychometric variable in social dominance. Being the fastest to act in situations involving decision-making related to the control of resources or to ensure survival could provide an evolutionary advantage and facilitate the emergence of dominant behavior. The faster cognitive processing in dominant individuals without a speed-accuracy trade-off may help in guiding group decisions without jeopardizing accuracy. Recently, promptness of responding was shown to be related to increased perception of charisma by peers (von Hippel et al. 2015).

Although some studies have highlighted an association between cortisol and social dominance in competitive settings (Mehta et al. 2008; Mehta and Josephs 2010; Turan et al. 2015), high and low dominance groups in our study did not differ in their cortisol levels throughout the experiment. Given that our experiment did not involve competition, and each subject was tested in isolation for their behavioral reactions, the lack of social dominance-related differences in cortisol levels is fully aligned with the literature (Larrieu et al. 2017) indicating that cortisol differences are only revealed by social competitive challenges (Wirth et al. 2006; Mazur et al. 2015; Turan et al. 2015). Therefore, our findings preclude us from relating social dominance-related differences in brain activity with cortisol actions. However, we cannot exclude that other stress-related systems (e.g., brain norepinephrine) known to affect dynamics of brain activation (Hermans et al. 2011) could have been differentially engaged during task performance in the two dominance groups.

Our ERP data identified a time-window between 230-243 ms in which task processing highly differed between the two groups, at which high dominance participants showed large deflections that were virtually absent in the low dominance group. The amplitude modulation of these anterior N2 and posterior P2 components occurred much earlier than motor responses, thus, they do not reflect faster motor executions, as for example, the readiness potential does, but they are a precursor. This N2/P2 component in the EEG may reflect allocation of resources to the detection and categorization of the target stimulus and associated decision-making processes (Mudar

et al. 2016), as well as the intentional effort to carry out the task (Winterer et al. 2002). Therefore, the dominance-related difference in N2/P2 activation may reflect deficits in the mobilization of these resources. As a speculation, the marked increases in N2/P2 responses may be a general marker for social dominance. Intrinsic differences in the identified brain processes at approximately 240 ms may define key differences in cognitive style that, when operating in social contexts, set the basis for the emergence of dominance hierarchies and leader-follower relationships.

In particular, high dominance participants showed increased activations in four brain regions: left insula, cingulate gyrus, right inferior temporal gyrus, and right angular gyrus. Previous studies linked higher activation in the cingulate to faster reaction times (Paus 2001; Hahn et al. 2007; Mulert et al. 2008), particularly when the stimulus location is unpredictable, as in our experiment in which faces were presented either to the left or right of fixation. Cingulate activity was also related to increased efforts performed to excel in tasks (Winterer et al. 2002; Hillman and Bilkey 2012) to motor preparation (Isomura et al. 2003) and to allocation of attention (Winterer et al. 2002). Therefore, the higher activation in the cingulate cortex may reflect the greater ability of dominant individuals to recruit brain resources to facilitate response selection. In addition, high dominance participants showed increased recruitment of regions functionally engaged in the performed task. Specifically, the right inferior temporal gyrus contains the fusiform face area that is involved in face processing (Kanwisher et al. 1997; McCarthy et al. 1997; Gauthier et al. 2000), and activity in the left insula is observed during emotional perception and experience (Duerden et al. 2013).

Group differences in the EEG may have occurred for early, medium, or late components such as the P1, N1, P3 or the lateral readiness potential. Early differences could have been taken as evidence for faster sensory encoding and visual processing. Later difference in the P3 may have been taken as evidence for cognitive difference related to dominance and difference in the readiness potential for faster motor execution. As mentioned, we found only significant and large difference for the medium component indicating that people high in dominance translate sensory evidence faster into decision-making. Our findings raise several questions. First, it will be important to determine whether N2/P2 responses are susceptible to change, for example, when a dominant individual occupies a subordinate role similar to the above mentioned results (Santamaría-García et al. 2014). Second, social hierarchies are already observed in preschool children (Hay et al. 2004). Hence, it will be important to assess during which period of development the increased N2/P2 emerges. Third, it will be important to translate our findings to real life. For example, it will be relevant to assess whether even stronger signals are observed in groups known to be particularly dominant, such as CEOs. In this context, it is important to mention that several functional magnetic resonance imaging (fMRI) and EEG studies have shown a network of activated brain areas in relation to social ranking (Zink et al. 2008; Chiao et al. 2009; Marsh et al. 2009; Santamaría-García et al. 2015; Balconi and Vanutelli 2016; Ligneul et al. 2016). A further key question is whether female participants will show similar behavioral and EEG patterns? Finally, it will be important to determine whether we can find correlates between faster reaction times and increased activity in identified brain areas and everyday life parameters such as income, social status, or sports performance.

Importantly, our results are of correlational nature. Hence, we cannot make any conclusions about causality. For example, whereas faster responses may be beneficial for survival, they might just be an expression of dominance, similar to the observation that the dominant person expresses their opinion first in a group. Likewise, we do not exactly know whether the identified increases in brain activity are causal for faster reaction or just reflect other types of processing relate to dominance. In addition, we cannot exclude the possibility that the feeling of power and superiority, associated with dominance motivation, affects task engagement and, hence, ERPs and latency to respond, in resemblance to the recently discovered effect of artificial rank allocation on response latency and ERPs (Santamaría-García et al. 2014).

Processing speed, revealed through fast responses in laboratory tasks similar to those applied here, has been reported to be a strong predictor of survival (Roberts et al. 2009), and higher ranking individuals exhibit better health (Sapolsky 2005; Marmot 2006). Surprisingly, despite the numerous advantages for health and wellbeing associated with high rank, very little is known regarding the factors that predispose individuals to attain dominance. Our study raises the possibility that differences in promptness to respond in decision-making situations and the associated neural underpinnings are at the core of rank establishment and might link social rank with physical and mental health (Selten et al. 2017).

Supplementary Material

Supplementary material is available at *Cerebral Cortex* online.

Funding

This work was supported by grants from the Swiss National Science Foundation (CR2013-146431; NCCR Synapsy), the Oak Foundation, the EU FP7 project MATRICS (No 603016) and École Polytechnique Fédérale de Lausanne, and Fundação para a Ciência e a Tecnologia (Grant PD/BD/105785/2014). The funding sources had no additional role in study design, in the collection, analysis and interpretation of data, in the writing of the report or in the decision to submit the paper for publication. This paper reflects only the authors' views and the European Union is not liable for any use that may be made of the information contained therein.

Notes

The authors declare no competing financial interests. The authors would like to thank Rebecca Francelet for excellent contribution to the behavioural experiments. *Conflict of Interest:* Authors declare no conflict of interest.

References

- Anderson C, Kilduff GJ. 2009. Why do dominant personalities attain influence in face-to-face groups? The competence-signaling effects of trait dominance. *J Pers Soc Psychol.* 96: 491–503.
- Bach M. 1996. The Freiburg Visual Acuity test-automatic measurement of visual acuity. *Optom Vis Sci Off Publ Am Acad Optom.* 73:49–53.
- Balconi M, Vanutelli ME. 2016. Competition in the Brain. The Contribution of EEG and fNIRS Modulation and Personality Effects in Social Ranking. *Front Psychol.* 7:1587.

- Bateman TS, Crant JM. 1993. The proactive component of organizational behavior: A measure and correlates. *J Organ Behav*. 14:103–118.
- Brunet D, Murray MM, Michel CM. 2011. Spatiotemporal Analysis of Multichannel EEG: CARTOOL. *Comput Intell Neurosci*. 2011:e813870.
- Buss DM, Craik KH. 1980. The frequency concept of disposition: dominance and prototypically dominant acts. *J Pers*. 48: 379–392.
- Carver CS, White TL. 1994. Behavioral inhibition, behavioral activation, and affective responses to impending reward and punishment: The BIS/BAS Scales. *J Pers Soc Psychol*. 67: 319–333.
- Chiao JY, Harada T, Oby ER, Li Z, Parrish T, Bridge DJ. 2009. Neural representations of social status hierarchy in human inferior parietal cortex. *Neuropsychologia*. 47:354–363.
- R Core Team. 2014. R: A language and environment for statistical computing. Vienna (AT): R Foundation for Statistical Computing.
- da Cruz JR, Chicherov V, Herzog MH, Figueiredo P. 2018. An automatic pre-processing pipeline for EEG analysis (APP) based on robust statistics. *Clin Neurophysiol*. 129:1427–1437.
- David M, Auclair Y, Cézilly F. 2011. Personality predicts social dominance in female zebra finches, *Taeniopygia guttata*, in a feeding context. *Anim Behav*. 81:219–224.
- Duerden EG, Arsalidou M, Lee M, Taylor MJ. 2013. Lateralization of affective processing in the insula. *Neuroimage*. 78: 159–175.
- Dykier D, Der G, Starr JM, Deary IJ. 2012. Sex differences in reaction time mean and intraindividual variability across the life span. *Dev Psychol*. 48:1262–1276.
- Ebner NC, Riediger M, Lindenberger U. 2010. FACES—A database of facial expressions in young, middle-aged, and older women and men: Development and validation. *Behav Res Methods*. 42:351–362.
- Ekman P, Friesen WV. 1976. Pictures of Facial Affect. Palo Alto (CA): Consulting Psychologists Press.
- Ellyson SL, Dovidio JF. 1985. Power, Dominance, and Nonverbal Behavior: Basic Concepts and Issues. In: Ellyson SL, Dovidio JF, editors. *Power, Dominance, and Nonverbal Behavior*. Springer Series in Social Psychology. New York (NY): Springer New York. p. 1–27.
- Etkin A, Klemenhagen KC, Dudman JT, Rogan MT, Hen R, Kandel ER, Hirsch J. 2004. Individual Differences in Trait Anxiety Predict the Response of the Basolateral Amygdala to Unconsciously Processed Fearful Faces. *Neuron*. 44:1043–1055.
- Ferguson N. 1977. Simultaneous speech, interruptions and dominance. *Br J Soc Clin Psychol*. 16:295–302.
- Fonov V, Evans AC, Botteron K, Almli CR, McKinstry RC, Collins DL, Brain Development Cooperative Group. 2011. Unbiased average age-appropriate atlases for pediatric studies. *Neuroimage*. 54: 313–327.
- Gable SL, Reis HT, Elliot AJ. 2000. Behavioral activation and inhibition in everyday life. *J Pers Soc Psychol*. 78:1135–1149.
- Gauthier I, Tarr MJ, Moylan J, Skudlarski P, Gore JC, Anderson AW. 2000. The fusiform “face area” is part of a network that processes faces at the individual level. *J Cogn Neurosci*. 12: 495–504.
- Goldberg JA. 1990. Interrupting the discourse on interruptions: An analysis in terms of relationally neutral, power- and rapport-oriented acts. *J Pragmat*. 14:883–903.
- Grave de Peralta Menendez R, Murray MM, Michel CM, Martuzzi R, Gonzalez Andino SL. 2004. Electrical neuroimaging based on biophysical constraints. *Neuroimage*. 21:527–539.
- Guinote A. 2017. How Power Affects People: Activating, Wanting, and Goal Seeking. *Annu Rev Psychol*. 68:353–381.
- Guthrie D, Buchwald JS. 1991. Significance testing of difference potentials. *Psychophysiology*. 28:240–244.
- Hahn B, Ross TJ, Stein EA. 2007. Cingulate Activation Increases Dynamically with Response Speed under Stimulus Unpredictability. *Cereb Cortex*. 17:1664–1671.
- Hall JA, Coats EJ, LeBeau LS. 2005. Nonverbal behavior and the vertical dimension of social relations: a meta-analysis. *Psychol Bull*. 131:898–924.
- Harcourt JL, Ang TZ, Sweetman G, Johnstone RA, Manica A. 2009. Social Feedback and the Emergence of Leaders and Followers. *Curr Biol*. 19:248–252.
- Hay DF, Payne A, Chadwick A. 2004. Peer relations in childhood. *J Child Psychol Psychiatry*. 45:84–108.
- Helgeson VS, Fritz HL. 1999. Unmitigated Agency and Unmitigated Communion: Distinctions from Agency and Communion. *J Res Personal*. 33:131–158.
- Henckens MJ, van Wingen GA, Joëls M, Fernández G. 2011. Time-dependent corticosteroid modulation of prefrontal working memory processing. *PNAS*. 108:5801–5806.
- Henckens MJ, van Wingen GA, Joëls M, Fernández G. 2012. Time-dependent effects of cortisol on selective attention and emotional interference: a functional MRI study. *Front Integr Neurosci*. 6:66.
- Hermans EJ, van Marle HJ, Ossewaarde L, Henckens MJ, Qin S, van Kesteren MT, Schoots VC, Cousijn H, Rijpkema M, Oostenveld R, et al. 2011. Stress-Related Noradrenergic Activity Prompts Large-Scale Neural Network Reconfiguration. *Science*. 334: 1151–1153.
- Hillman KL, Bilkey DK. 2012. Neural encoding of competitive effort in the anterior cingulate cortex. *Nat Neurosci*. 15: 1290–1297.
- Hoaglin DC, Mosteller F, Tukey JW. 1982. Understanding Robust and Exploratory Data Analysis. 1st ed. New York (NY): Wiley.
- Hortensius R, van Honk J, de Gelder B, Terburg D. 2014. Trait dominance promotes reflexive staring at masked angry body postures. *PLoS One*. 9:e116232.
- Isomura Y, Ito Y, Akazawa T, Nambu A, Takada M. 2003. Neural Coding of “Attention for Action” and “Response Selection” in Primate Anterior Cingulate Cortex. *J Neurosci*. 23: 8002–8012.
- Jackson DN. 1974. Personality Research Form Manual. Goshen (NY): Research Psychologists Press.
- Johnson SL, Leedom LJ, Muhtadie L. 2012. The dominance behavioral system and psychopathology: Evidence from self-report, observational, and biological studies. *Psychol Bull*. 138:692–743.
- Judge TA, Bono JE, Ilies R, Gerhardt MW. 2002. Personality and leadership: A qualitative and quantitative review. *J Appl Psychol*. 87:765–780.
- Kanwisher N, McDermott J, Chun MM. 1997. The Fusiform Face Area: A Module in Human Extrastriate Cortex Specialized for Face Perception. *J Neurosci*. 17:4302–4311.
- Kim S. 2015. ppcor: An R Package for a Fast Calculation to Semi-partial Correlation Coefficients. *Commun Stat Appl Methods*. 22:665–674.
- King AJ, Cowlshaw G. 2009. Leaders, followers and group decision-making. *Commun Integr Biol*. 2:147–150.
- King AJ, Johnson DDP, Van Vugt M. 2009. The Origins and Evolution of Leadership. *Curr Biol*. 19:R911–R916.
- Knebel J-F, Murray MM. 2012. Towards a resolution of conflicting models of illusory contour processing in humans. *Neuroimage*. 59:2808–2817.

- Knight EL, Mehta PH. 2017. Hierarchy stability moderates the effect of status on stress and performance in humans. *Proc Natl Acad Sci USA*. 114:78–83.
- Kuznetsova A, Brockhoff PB, Christensen RHB. 2017. lmerTest Package: Tests in Linear Mixed Effects Models. *J Stat Softw*. 82:1–26.
- Langner O, Dotsch R, Bijlstra G, Wigboldus DHJ, Hawk ST, van Knippenberg A. 2010. Presentation and validation of the Radboud Faces Database. *Cogn Emot*. 24:1377–1388.
- Larrieu T, Cherix A, Duque A, Rodrigues J, Lei H, Gruetter R, Sandi C. 2017. Hierarchical Status Predicts Behavioral Vulnerability and Nucleus Accumbens Metabolic Profile Following Chronic Social Defeat Stress. *Curr Biol*. 27:2202–2210.e4.
- Lehmann D, Skrandies W. 1980. Reference-free identification of components of checkerboard-evoked multichannel potential fields. *Electroencephalogr Clin Neurophysiol*. 48:609–621.
- Ligneul R, Obeso I, Ruff CC, Dreher J-C. 2016. Dynamical Representation of Dominance Relationships in the Human Rostromedial Prefrontal Cortex. *Curr Biol*. 26:3107–3115.
- Lundqvist D, Flykt A, Öhman A. 1998. The Karolinska Directed Emotional Faces - KDEF. Psychology section, Karolinska Institutet.
- Mamuneas D, Spence AJ, Manica A, King AJ. 2015. Bolder stickleback fish make faster decisions, but they are not less accurate. *Behav Ecol*. 26:91–96.
- Maner JK, Case CR. 2016. Dominance and Prestige: Dual Strategies for Navigating Social Hierarchies. In: Olson JM, Zanna MP, editors. *Advances in Experimental Social Psychology*. San Diego (CA): Academic Press. p. 129–180.
- Marmot M. 2006. Health in an unequal world. *The Lancet*. 368:2081–2094.
- Marsh AA, Blair KS, Jones MM, Soliman N, Blair RJR. 2009. Dominance and submission: the ventrolateral prefrontal cortex and responses to status cues. *J Cogn Neurosci*. 21:713–724.
- Mazur A, Welker KM, Peng B. 2015. Does the Biosocial Model Explain the Emergence of Status Differences in Conversations among Unacquainted Men? *PLoS One*. 10:e0142941.
- McCarthy G, Puce A, Gore JC, Allison T. 1997. Face-specific processing in the human fusiform gyrus. *J Cogn Neurosci*. 9:605–610.
- Mehta PH, Jones AC, Josephs RA. 2008. The social endocrinology of dominance: Basal testosterone predicts cortisol changes and behavior following victory and defeat. *J Pers Soc Psychol*. 94:1078–1093.
- Mehta PH, Josephs RA. 2010. Testosterone and cortisol jointly regulate dominance: Evidence for a dual-hormone hypothesis. *Horm Behav*. 58:898–906.
- Mudar RA, Chiang H-S, Eroh J, Nguyen LT, Maguire MJ, Spence JS, Kung F, Kraut MA, Hart J. 2016. The Effects of Amnesic Mild Cognitive Impairment on Go/NoGo Semantic Categorization Task Performance and Event-Related Potentials. *J Alzheimers Dis JAD*. 50:577–590.
- Mulert C, Seifert C, Leicht G, Kirsch V, Ertl M, Karch S, Moosmann M, Lutz J, Möller H-J, Hegerl U, et al. 2008. Single-trial coupling of EEG and fMRI reveals the involvement of early anterior cingulate cortex activation in effortful decision making. *Neuroimage*. 42:158–168.
- Nakayama S, Harcourt JL, Johnstone RA, Manica A. 2012. Initiative, Personality and Leadership in Pairs of Foraging Fish. *PLoS One*. 7:e36606.
- Oldfield RC. 1971. The assessment and analysis of handedness: The Edinburgh inventory. *Neuropsychologia*. 9:97–113.
- Oortmerssen GAV, Benus I, Dijk DJ. 1984. Studies in Wild House Mice: Genotype-Environment Interactions for Attack Latency. *Neth J Zool*. 35:155–169.
- Paus T. 2001. Primate anterior cingulate cortex: Where motor control, drive and cognition interface. *Nat Rev Neurosci*. 2:417–424.
- Plomp G, Mercier MR, Otto TU, Blanke O, Herzog MH. 2009. Non-retinotopic feature integration decreases response-locked brain activity as revealed by electrical neuroimaging. *Neuroimage*. 48:405–414.
- Plomp G, Michel CM, Herzog MH. 2010. Electrical source dynamics in three functional localizer paradigms. *Neuroimage*. 53:257–267.
- Pruessner JC, Kirschbaum C, Meinlschmid G, Hellhammer DH. 2003. Two formulas for computation of the area under the curve represent measures of total hormone concentration versus time-dependent change. *Psychoneuroendocrinology*. 28:916–931.
- Rands SA, Cowlshaw G, Pettifor RA, Rowcliffe JM, Johnstone RA. 2008. The emergence of leaders and followers in foraging pairs when the qualities of individuals differ. *BMC Evol Biol*. 8:51.
- Riebel T, Avgan B, Bottini A-M, Duc C, Taborsky M, Heg D. 2011. Behavioural type affects dominance and growth in staged encounters of cooperatively breeding cichlids. *Anim Behav*. 81:313–323.
- Roberts BA, Der G, Deary IJ, Batty GD. 2009. Reaction time and established risk factors for total and cardiovascular disease mortality: Comparison of effect estimates in the follow-up of a large, UK-wide, general-population based survey. *Intelligence*. 37:561–566.
- Santamaría-García H, Burgaleta M, Sebastian-Galles N. 2015. Neuroanatomical Markers of Social Hierarchy Recognition in Humans: A Combined ERP/fMRI Study. *J Neurosci*. 35:10843–10850.
- Santamaría-García H, Pannunzi M, Ayneto A, Deco G, Sebastián-Gallés N. 2014. 'If you are good, I get better': the role of social hierarchy in perceptual decision-making. *Soc Cogn Affect Neurosci*. 9:1489–1497.
- Sapolsky RM. 2005. The Influence of Social Hierarchy on Primate Health. *Science*. 308:648–652.
- Schmid Mast M. 2002. Dominance as Expressed and Inferred Through Speaking Time. *Hum Commun Res*. 28:420–450.
- Selten JP, Booij J, Buwalda B, Meyer-Lindenberg A. 2017. Biological Mechanisms Whereby Social Exclusion May Contribute to the Etiology of Psychosis: A Narrative Review. *Schizophr Bull*. 43:287–292.
- Spielberger CD, Gorsuch RL, Lushene R, Vagg PR, Jacobs GA. 1983. Manual for the state-trait anxiety inventory. Palo Alto (CA): Consulting Psychologists Press.
- Thoresen JC, Francelet R, Coltekin A, Richter K-F, Fabrikant SI, Sandi C. 2016. Not all anxious individuals get lost: Trait anxiety and mental rotation ability interact to explain performance in map-based route learning in men. *Neurobiol Learn Mem*. 132:1–8.
- Tottenham N, Tanaka JW, Leon AC, McCarry T, Nurse M, Hare TA, Marcus DJ, Westerlund A, Casey B, Nelson C. 2009. The NimStim set of facial expressions: Judgments from untrained research participants. *Psychiatry Res*. 168:242–249.
- Turan B, Tackett JL, Lechtreck MT, Browning WR. 2015. Coordination of the cortisol and testosterone responses: A dual axis approach to understanding the response to social status threats. *Psychoneuroendocrinology*. 62:59–68.
- van der Kooij MA, Sandi C. 2015. The genetics of social hierarchies. *Curr Opin Behav Sci Behavioral genetics*. 2:52–57.

- Van Vugt M, Hogan R, Kaiser RB. 2008. Leadership, followership, and evolution: Some lessons from the past. *Am Psychol.* 63: 182–196.
- Vogel S, Fernández G, Joëls M, Schwabe L. 2016. Cognitive Adaptation under Stress: A Case for the Mineralocorticoid Receptor. *Trends Cogn Sci.* 20:192–203.
- Vogel S, Klumpers F, Schröder TN, Oplaat KT, Krugers HJ, Oitzl MS, Joëls M, Doeller CF, Fernández G. 2017. Stress Induces a Shift Towards Striatum-Dependent Stimulus-Response Learning via the Mineralocorticoid Receptor. *Neuropsychopharmacology.* 42:1262–1271.
- von Hippel W, Ronay R, Baker E, Kjelsaas K, Murphy SC. 2015. Quick Thinkers Are Smooth Talkers: Mental Speed Facilitates Charisma. *Psychol Sci.* 27:1–4.
- Wiggins JS. 1979. A psychological taxonomy of trait-descriptive terms: The interpersonal domain. *J Pers Soc Psychol.* 37:395–412.
- Willenbockel V, Sadr J, Fiset D, Horne GO, Gosselin F, Tanaka JW. 2010. Controlling low-level image properties: The SHINE toolbox. *Behav Res Methods.* 42:671–684.
- Winterer G, Adams CM, Jones DW, Knutson B. 2002. Volition to Action—An Event-Related fMRI Study. *Neuroimage.* 17:851–858.
- Wirth MM, Welsh KM, Schultheiss OC. 2006. Salivary cortisol changes in humans after winning or losing a dominance contest depend on implicit power motivation. *Horm Behav.* 49:346–352.
- Zink CF, Tong Y, Chen Q, Bassett DS, Stein JL, Meyer-Lindenberg A. 2008. Know your place: neural processing of social hierarchy in humans. *Neuron.* 58:273–283.

Supplementary Material for

Dominant men are faster in decision-making situations and exhibit a distinct neural signal for promptness

Janir R. da Cruz¹, João Rodrigues¹, John C. Thoresen¹, Vitaly Chicherov, Patrícia Figueiredo, Michael H. Herzog² and Carmen Sandi^{2*}

¹ Equal contribution

² Equal senior contribution

* Correspondence to: Carmen Sandi. E-mail: carmen.sandi@epfl.ch

This file includes:

Tables S1-7

Fig. S1 Association between PRF-d scores and decision speed across experiments

Fig. S2 EEG source imaging results of the Main effect of Group from 230 to 243ms

Fig. S3 Cingulate gyrus activity related to fast latency to respond

Table S1 (Related to Fig. 1). Summary of statistical results from the behavioral experiments 1-3 involving choice decision-making. *p*-values for significant effects are depicted in red. GGC: Greenhouse-Geisser corrected.

Experiment Number	N	Statistical test	Dependent variable	Independent variable	Test statistic	<i>p</i> -val	η^2
1	32	Mixed design ANCOVA	RT	Group	$F_{1,28}=9.06$	0.005	0.216, 95% CI [0.044, 0.414]
				Difficulty	$F_{1.62, 45.37}=1.24$ (GGC)	0.296	0.038, 95% CI [0.000, 0.151]
				Emotion	$F_{2,56}=0.06$	0.939	0.002, 95% CI [0.000, 0.007]
				Accuracy	$F_{1,28}=0.30$	0.589	0.011, 95% CI [0.000, 0.061]
				STAI-T	$F_{1,28}=4.50$	0.043	0.138, 95% CI [0.944, 0.261]
				Group x Emotion	$F_{2,56}=1.44$	0.245	0.048, 95% CI [0.000, 0.143]
				Group x Difficulty	$F_{1.62, 45.37}=2.00$ (GGC)	0.154	0.061, 95% CI [0.000, 0.188]
				Difficulty x Emotion	$F_{3.34, 93.43}=0.50$ (GGC)	0.703	0.018, 95% CI [0.000, 0.048]
				Group x Difficulty x Emotion	$F_{3.34, 93.43}=2.00$ (GGC)	0.114	0.067, 95% CI [0.000, 0.133]
				Difficulty x Accuracy	$F_{1.62, 45.37}=0.20$ (GGC)	0.777	0.007, 95% CI [0.000, 0.065]
				Difficulty x STAI-T	$F_{1.62, 45.37}=1.26$ (GGC)	0.287	0.043, 95% CI [0.000, 0.152]
				Emotion x Accuracy	$F_{2,56}=0.78$	0.463	0.007, 95% CI [0.000, 0.065]
				Emotion x STAI-T	$F_{2,56}=0.11$	0.900	0.004, 95% CI [0.000, 0.026]
				Emotion x Accuracy x Difficulty	$F_{3.34, 93.43}=0.39$ (GGC)	0.779	0.014, 95% CI [0.000, 0.037]
				Emotion x STAI-T x Difficulty	$F_{3.34, 93.43}=0.71$ (GGC)	0.561	0.025, 95% CI [0.000, 0.065]
			Accuracy	Group	$F_{1,29}=0.05$	0.946	0.000, 95% CI [0.000, 0.000]
				Difficulty	$F_{2,58}=3.45$	0.038	0.105, 95% CI [0.003, 0.221]

				Emotion	$F_{1,60,46.47}=1.46$ (GGC)	0.243	0.047, 95% CI [0.000, 0.159]
				STAI-T	$F_{1,29}=0.02$	0.963	0.000, 95% CI [0.000, 0.000]
				Group x Emotion	$F_{1,60,46.47}=0.17$ (GGC)	0.795	0.006, 95% CI [0.000, 0.058]
				Group x Difficulty	$F_{2,58}=0.59$	0.558	0.018, 95% CI [0.000, 0.087]
				Difficulty x Emotion	$F_{3,03,87.86}=0.32$ (GGC)	0.817	0.011, 95% CI [0.000, 0.034]
				Group x Difficulty x Emotion	$F_{3,03,87.86}=2.28$ (GGC)	0.084	0.073, 95% CI [0.000, 0.147]
				Difficulty x STAI-T	$F_{2,58}=0.09$	0.913	0.014, 95% CI [0.000, 0.018]
				Emotion x STAI-T	$F_{1,60,46.47}=0.41$ (GGC)	0.623	0.003, 95% CI [0.000, 0.090]
				STAI-T x Difficulty x Emotion	$F_{3,03,87.86}=0.84$ (GGC)	0.505	0.028, 95% CI [0.000, 0.076]
2	39	ANCOVA	Memorization time	Group	$F_{1,35}=7.28$	0.011	0.169, 95% CI [0.023, 0.333]
				Accuracy	$F_{1,35}=0.65$	0.425	0.018, 95% CI [0.000, 0.133]
				STAI-T	$F_{1,35}=0.08$	0.778	0.002, 95% CI [0.000, 0.073]
			Recall time	Group	$F_{1,35}=9.64$	0.004	0.195, 95% CI [0.043, 0.375]
				Accuracy	$F_{1,35}=3.89$	0.057	0.100, 95% CI [0.000, 0.254]
				STAI-T	$F_{1,35}=0.92$	0.345	0.026, 95% CI [0.000, 0.148]
			Accuracy	Group	$F_{1,36}=0.57$	0.455	0.015, 95% CI [0.000, 0.128]
				STAI-T	$F_{1,36}=0.95$	0.335	0.026, 95% CI [0.000, 0.150]
3	90	ANCOVA	RT	Group	$F_{1,86}=9.56$	0.003	0.097, 95% CI [0.021, 0.202]
				Accuracy	$F_{1,86}=3.31$	0.076	0.037, 95% CI [0.021, 0.118]
				STAI-T	$F_{1,86}=0.03$	0.855	0.000, 95% CI [0.000, 0.022]
			Accuracy	Group	$F_{1,87}=0.33$	0.567	0.004, 95% CI [0.000, 0.051]
				STAI-T	$F_{1,87}=0.29$		0.003, 95% CI [0.000, 0.049]

Table S2 (Related to Fig. 3b). Linear models applied to RT (experiment 5). *p*-values for significant effects are depicted in red.

Models 1 & 2: Effects of group and condition on RT								
Fixed Effect	Model 1; Mixed effects interaction model				Model 2: Mixed effects additive model			
	Coef. β	SE(β)	<i>t</i> (df)	<i>p</i> -val	Coef. β	SE(β)	<i>t</i> (df)	<i>p</i> -val
Condition	-49.90	38.48	<i>t</i> (27.28)=-1.30	0.206	-5.65	30.09	<i>t</i> (29.22)= -0.19	0.853
Group	71.168	68.84	<i>t</i> (23.12)=1.03	0.312	127.57	60.88	<i>t</i> (23.59)=2.10	0.047
Group x Condition	71.42	41.48	<i>t</i> (23.57)=1.72	0.098	n/a	n/a	n/a	n/a
Accuracy	-6.52	228.37	<i>t</i> (32.43)=-0.03	0.977	84.89	230.30	<i>t</i> (33.87)=0.37	0.715
STAI-T	-0.49	2.86	<i>t</i> (23.00)=-0.17	0.865	-0.60	2.85	<i>t</i> (23.06)=-0.21	0.835

Table S3 (Related to Fig. 3b). Linear model applied to Accuracy (experiment 5). *p*-values for significant effects are depicted in red.

Model 3: Effect of group and condition on Accuracy			
Independent variable	2 (Condition) by 2 (Group) mixed design ANCOVA		
	Stats	<i>p</i> -val	η^2
Condition	$F_{1,24}=32.51$	< 0.001	0.561
Group	$F_{1,23}=1.24$	0.277	0.050
Group x Condition	$F_{1,24}=1.41$	0.247	0.024
STAI-T	$F_{1,23}=0.32$	0.575	0.013

Table S4 (Related to Fig. S1). Linear mixed effects models applied to standardized RTs for all experiments using PRF-d scale scores and a decision making coding variable as predictors. *p*-values for significant effects are depicted in red.

Models 4 & 5: Effects of group and condition on RT								
Fixed Effect	Model 4; Mixed effects interaction model				Model 5: Mixed effects additive model			
	Coef. β	SE(β)	<i>t</i> (df)	<i>p</i> -val	Coef. β	SE(β)	<i>t</i> (df)	<i>p</i> -val
Decision	0.18	0.21	<i>t</i> (274)=-0.86	0.388	n/a	n/a	n/a	n/a
PRF-d	0.10	0.12	<i>t</i> (274)=0.88	0.382	-0.36	0.06	<i>t</i> (224)= -5.61	<0.001
PRF-d x Decision	-0.46	0.14	<i>t</i> (274)=-3.41	< 0.001	n/a	n/a	n/a	n/a
Accuracy	0.09	0.08	<i>t</i> (274)=1.16	0.248	0.10	0.08	<i>t</i> (224)= 1.22	0.225
STAI-T	-0.01	0.01	<i>t</i> (274)= -1.26	0.210	-0.60	-0.01	<i>t</i> (224)=- -0.67	0.504

Table S5 (Related to Fig. 3d). Significant results from the linear model applied to the GFP at different time points (experiment 5). *p*-values for significant effects are depicted in red.

Model 6: Effect of group and condition on the GFP				
Independent variable	2 (Condition) by 2 (Group) mixed design ANOVA ¹			
	Time (ms)	Stats	<i>p</i> -val	η^2
Condition	140-156	$F_{1,24}=9.06$	0.006	0.251
Condition	345-414	$F_{1,24}=5.96$	0.022	0.195
Group	230- 243	$F_{1,24}=4.87$	0.037	0.169

¹ To account for temporal auto-correlation, only significant effects ($p < 0.05$) lasting for at least 10 ms were considered reliable. For visualization reasons, only those effects are presented.

Table S6 (Related to Fig. 3e and Fig S2). Linear model applied to brain regions' evoked responses (experiment 5). *p*-values for significant effects are depicted in red.

Model 7: Effect of group on brain regions' evoked responses						
Dependent variable: center of mass activation	2 (Condition) by 2 (Group) mixed design ANOVA			Talairach coordinates		
	Stats	<i>p</i> -val	η^2	x	y	z
Left insula	$F_{1,24}=9.83$	0.005	0.291	-39	8	0
Cingulate gyrus	$F_{1,24}=7.12$	0.013	0.229	3	-22	35
Right Inferior temporal gyrus	$F_{1,24}=31.44$	< 0.001	0.567	51	-33	-13
Right angular gyrus	$F_{1,24}=8.58$	0.007	0.263	49	-62	34

Table S7 (Related to Fig. S3). Linear model applied to RT (experiment 5). *p*-values for significant effects are depicted in red.

Model 8: Effect of brain regions' evoked responses on RT				
Fixed Effect	Mixed effects additive model			
	Coef. β	SE(β)	<i>t</i> (df)	<i>p</i> -val
Left insula	-9.35	27.82	$t(42.09)=-0.34$	0.738
Cingulate gyrus	-57.87	23.03	$t(40.56)=-2.51$	0.016
Right Inferior temporal gyrus	21.68	21.68	$t(31.610)=1.00$	0.325
Right angular gyrus	25.68	23.25	$t(39.83)=1.10$	0.276

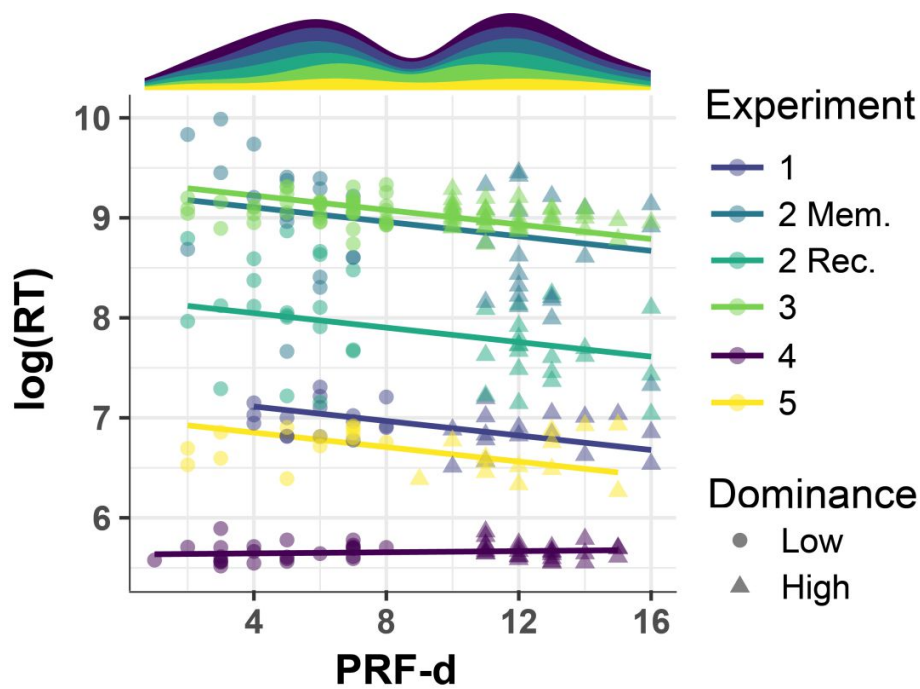


Fig. S1 (Related to Figs. 1-3 and Table S4) **Association between PRF-d scores and decision speed across experiments.** These analyses aimed at studying the relationship between the RT and PRF-d score as a continuous variable, beyond the median-split used in our main analyses when comparing results from individuals high vs. low in trait dominance. Note, however, that in order to account for the goal of the experiment subjects were recruited to ensure equivalent representation of high and low dominance individuals within each experiment. This can be appreciated on the stacked histogram displayed on the upper part of this graph depicting the distribution of subjects according to the median split approach used for group selection per experiment across PRF-d scores. For analyses purposes, we first combined all participants' responses in a mixed-effects model that accounts for the random variations within Experiments 1-5 and, besides having predictors for PRF-d, STAI-T and accuracy, it includes an interaction term between PRF-d and a coding variable for decision-making experiments (i.e., all experiments except Experiment 4). This model yielded a significant interaction effect between PRF-d and decision-making's RT ($\beta = -0.46$, $SE = 0.14$, 95% CI $[-0.73, -0.20]$, $t(274.00) = -3.41$, $p < .001$), while the effects of the remaining predictors were not significant (all $ps > 0.210$). Then, applying the same model to RT data from only the experiments that involve decision-making, the interaction between PRF-d scores is significant ($\beta = -0.36$, $SE = 0.063$, 95% CI $[-0.48, -0.23]$, $t(224.00) = -5.61$, $p < .001$), while the effects of the remaining predictors are not significant (all $ps > 0.225$). In this figure, the logarithm of RT is shown to facilitate visualization and comparison across experiments. Lines represent the model's prediction of RTs given PRF-d and the interaction between PRF-d and decision-making. Dominance groups are represented as either a full circle (low dominance) or triangle (high dominance). Experiments are color-coded.

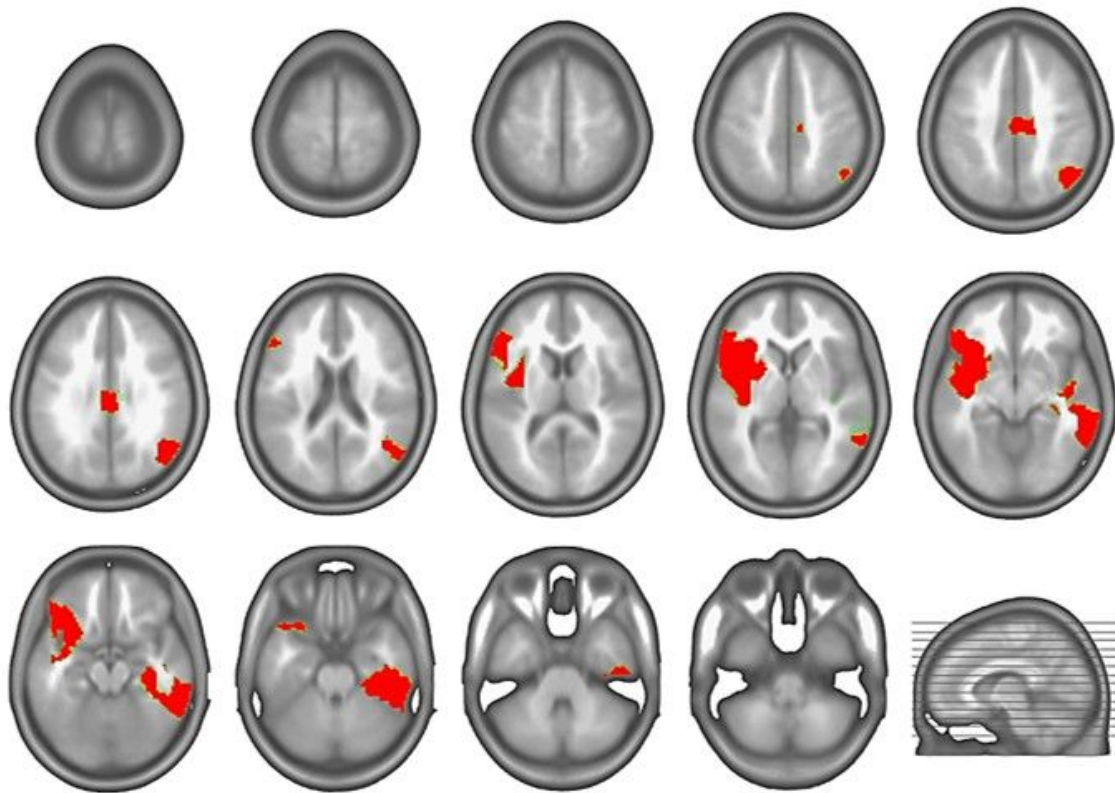


Fig. S2 (Related to Fig. 3e). **EEG source imaging results of the Main effect of Group from 230 to 243ms.** Regions of significant differences are indicated in red. High dominance participants showed increased activations in the 4 regions (center of mass at Table S5): left insula, cingulate gyrus, right inferior temporal gyrus, and right angular gyrus. **Inter-regional correlations in Experiment 5:** We identified significant inter-individual correlations between the cingulate gyrus and the right angular gyrus ($r(23) = 0.54$, $p = 0.006$) and between the left insula and the right inferior temporal gyrus ($r(23) = 0.45$, $p = 0.028$).

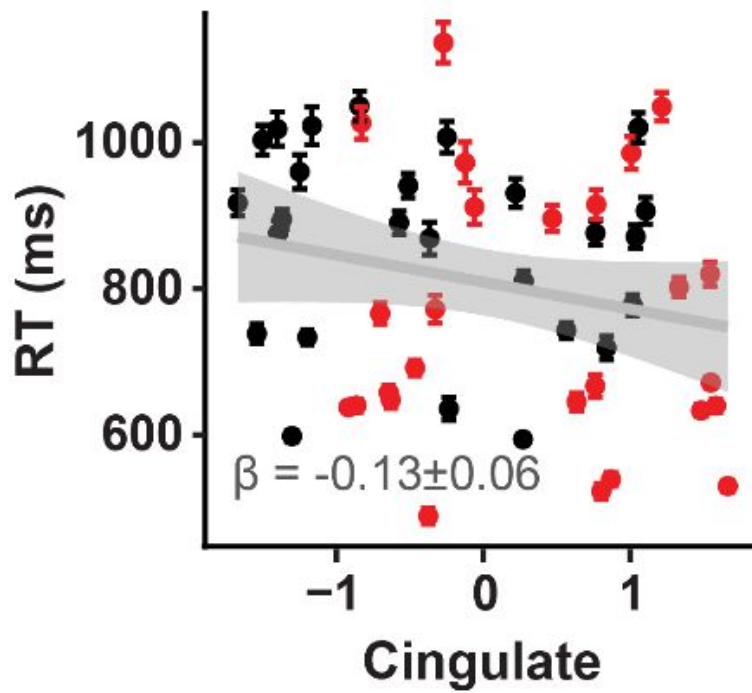
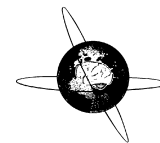


Fig. S3 (Related to Fig. 3; See also Table S7). **Cingulate gyrus activity predicted shorter latency to respond.** At the latency of the N2/P2 components, normalized activation of the cingulate gyrus linearly predicts shorter latency to respond ($\beta = -57.8$ ms, $SE = 23.03$ ms, $t(40.56) = -2.51$, $p = 0.016$). Data are presented as the mean RT \pm SEM for each subject at each condition.

Appendix B

da Cruz, J. R., Chicherov, V., Herzog, M. H., & Figueiredo, P. (2018)



An automatic pre-processing pipeline for EEG analysis (APP) based on robust statistics



Janir Ramos da Cruz^{a,b,*}, Vitaly Chicherov^b, Michael H. Herzog^b, Patrícia Figueiredo^a

^a Institute for Systems and Robotics – Lisbon (LARSys) and Department of Bioengineering, Instituto Superior Técnico, Universidade de Lisboa, Portugal

^b Laboratory of Psychophysics, Brain Mind Institute, École Polytechnique Fédérale de Lausanne, Switzerland

ARTICLE INFO

Article history:

Accepted 1 April 2018

Available online 23 April 2018

Keywords:

Electroencephalography

Automatic pre-processing

ERP

Resting-state

HIGHLIGHTS

- A novel automatic pre-processing pipeline for both resting state and evoked EEG data is proposed.
- The proposed automatic pipeline is tested in both clinical and healthy populations.
- The proposed automatic pipeline is as reliable as pre-processing by EEG experts.

ABSTRACT

Objective: With the advent of high-density EEG and studies of large numbers of participants, yielding increasingly greater amounts of data, supervised methods for artifact rejection have become excessively time consuming. Here, we propose a novel automatic pipeline (APP) for pre-processing and artifact rejection of EEG data, which innovates relative to existing methods by not only following state-of-the-art guidelines but also further employing robust statistics.

Methods: APP was tested on event-related potential (ERP) data from healthy participants and schizophrenia patients, and resting-state (RS) data from healthy participants. Its performance was compared with that of existing automatic methods (FASTER for ERP data, TAPEEG and Prep pipeline for RS data) and supervised pre-processing by experts.

Results: APP rejected fewer bad channels and bad epochs than the other methods. In the ERP study, it produced significantly higher amplitudes than FASTER, which were consistent with the supervised scheme. In the RS study, it produced spectral measures that correlated well with the automatic alternatives and the supervised scheme.

Conclusion: APP effectively removed EEG artifacts, performing similarly to the supervised scheme and outperforming existing automatic alternatives.

Significance: The proposed automatic pipeline provides a reliable and efficient tool for pre-processing large datasets of both evoked and resting-state EEG.

© 2018 International Federation of Clinical Neurophysiology. Published by Elsevier B.V. All rights reserved.

1. Introduction

The electroencephalogram (EEG) is a non-invasive tool for the investigation of human brain function, which has been continuously used for almost one century (Niedermeyer and Lopes da Silva, 2005). However, EEG data are typically contaminated with a number of artifacts. Artifacts are undesired signals that may affect the measurement and change the EEG signal of interest. These artifacts may arise from non-physiological noise sources that

originate outside the participant, such as the grounding of the electrodes causing power line noise at 50/60 Hz and at its harmonics, interferences with other electrical devices, or imperfections in electrode settling. Artifacts may also arise from physiological noise sources originating within the participants, such as the ones produced by head, eye, or muscle movements (Urigüen and Garcia-Zapirain, 2015). Head movements may result in spikes and discontinuities due to a rapid change of impedance at one or several electrodes. Reflective eye movements occur frequently and are normally picked up by the frontal electrodes in the frequency range of 1–3 Hz (within the delta wave range). Blinking also contaminates the EEG signal, usually causing a more abrupt change in its amplitude than eye movements. Finally, every movement

* Corresponding author at: Institute for Systems and Robotics – Lisbon (LARSys) and Department of Bioengineering, Instituto Superior Técnico, Universidade de Lisboa, Portugal.

E-mail address: janir.ramos@epfl.ch (J.R. da Cruz).

of the participant generates muscular artifacts that can be found everywhere on the scalp at frequencies higher than 20 Hz (within the beta and gamma waves range).

One simple way to deal with these artifacts is to remove segments of the data that exceed a certain level of artifact contamination, for example, signal amplitudes greater than $\pm 100 \mu\text{V}$. However, this coarse approach may lead to the loss of a great amount of data that could still contain artifact-free information, therefore potentially compromising the subsequent analysis and interpretation of the data. This is true for both evoked-related potentials (ERP) and resting-state (RS) signal fluctuations. Moreover, since participant generated artifacts may overlap in the spectral domain, and on many EEG channels, with the signal of interest, simple spatial and frequency band filtering approaches may be inefficient to remove this kind of artifacts (Tatum et al., 2011). Another method that is commonly used to clean-up EEG data is independent component analysis (ICA; Makeig et al., 1996). Assuming that neuronal signals and noise recorded on the scalp are independent of each other, then the EEG signal can be described by their linear summation. The ICA is used to decompose the EEG data in statistically independent sources (ICs), so as to separate the neuronal and noise contributions to the signal. The artifactual ICs can then be identified and subsequently subtracted from the EEG data, yielding an artifact-free signal.

Usually, pre-processing of EEG data, including the classification of artifactual ICs, is performed under expert supervision. However, with the advent of both high-density EEG arrays (64–256 channels) and studies of large populations, yielding increasingly greater amounts of data, supervised methods have become excessively time consuming. To cope with this, and to minimize subjectivity, automatic methods have recently been presented (Abreu et al., 2016a,b; Bigdely-Shamlo et al., 2015; Hatz et al., 2015; Nolan et al., 2010). Fully automated statistical thresholding for EEG artifact rejection (FASTER; Nolan et al., 2010), for instance, enables a fully automated pre-processing of ERP data, based on computing z-scores of different signal metrics, and threshold them in order to detect bad channels, bad epochs and artifactual ICs. Tool for automated processing of EEG data (TAPEEG; Hatz et al., 2015) uses a similar approach for the automatic pre-processing of RS EEG data. However, because they are based on z-scores, these approaches are not robust to outliers and as a consequence they tend to have high rejection rates of artifact-free signal. A more promising approach is to use robust statistics instead. For example, the Prep pipeline (Bigdely-Shamlo et al., 2015) provides an automatic pre-processing pipeline including filtering and bad channels identification using the RANSAC (random sample consensus) algorithm. However, in this case the identified bad channels are assumed to be globally bad. Thus, if a channel contains artifactual periods, these are neglected and left in the pre-processed EEG data. Moreover, supervised inspection of pre-processed data for bad epochs is necessary since the Prep pipeline does not provide this feature.

Here, we present APP, a novel Matlab® based fully automatic pipeline for pre-processing and artifact rejection of EEG data (including both ERP and RS data), which is based on state-of-the-art guidelines for EEG pre-processing, ICA decomposition, and robust statistics. APP consists of: (1) high-pass filtering; (2) power line noise removal; (3) re-referencing to a robust estimate of the mean of all channels; (4) removal and interpolation of bad channels; (5) removal of bad epochs; (6) ICA to remove eye-movement, muscular and bad-channel related artifacts; and (7) removal of epoch artifacts. At each step of the pipeline, a number of relevant parameters are estimated from the data and outliers are detected based on a robust data-driven outlier detection scheme.

APP was tested on ERP data from 61 healthy participants and 44 schizophrenia patients performing a visual discrimination task, and

on RS data from 68 healthy participants. The inclusion of patient data in the validation of APP is of particular interest since one of the primary applications of EEG is the study of clinical populations. Furthermore, many of these populations, schizophrenia patients in particular, are known to produce more artifacts than healthy volunteers, which is a challenge to automatic pre-processing. We compare APP to three state-of-the-art automatic artifact removal methods, FASTER, TAPEEG, and Prep pipeline, which have shown to be effective at removing a wide range of EEG artifacts. We also compared APP with supervised artifact removal by experts using the CARTOOL software (Brunet et al., 2011).

2. Methods

The proposed pre-processing and artifact removal method APP is first described, including a detailed description of each step. Then, the artifact removal methods FASTER, TAPEEG, and Prep pipeline, as well as the supervised artifact removal by experts, against which APP is compared, are described. Finally, the data acquisition and analysis methods used to validate the proposed method are presented.

2.1. Proposed EEG pre-processing and artifact removal method - APP

The APP pipeline consists of the following steps, which are described in detail in the respective sub-sections below:

- (1) High-pass filtering, to eliminate signal low-frequency non-stationarity (for example, slow drifts in the mean);
- (2) Removal of power line noise, with minimum distortion;
- (3) Robust re-referencing, to a robust estimate of the mean of all channels;
- (4) Detection, removal and interpolation of bad channels;
- (5) Detection and removal of bad epochs;
- (6) Detection and removal of eye movement-, muscular-, and bad channel-related artifacts based on ICA;
- (7) Detection, removal and interpolation of bad channels in epochs.

At every step, a number of relevant parameters are estimated from the data, and outliers are detected based on a scheme described below in the sub-section Outlier detection. Each step of APP is described in detail below.

2.1.1. High-pass filtering

The changes of the DC value of the EEG over time, called DC drift, can be corrected by high-pass filtering. In APP, in order to counteract the phase delay and to minimize distortion that are introduced by high-pass filtering (Lynn, 1989), we use a zero-phase 3rd order Butterworth filter, run both in forward and reverse directions (Picton et al., 2000). Usually, a cutoff frequency of 0.1 Hz suffices to remove these slow voltage shifts. However, when obtaining recordings from children or patients, which normally have excess body and head movements, which are a common source of sustained shifts in voltage, higher cutoff frequencies are advised (Luck, 2014). In order to make APP more robust to this kind of noise we use a 1 Hz cutoff frequency.

2.1.2. Power line noise removal

The removal of the power line interference (50/60 Hz noise and its harmonics) is usually accomplished using notch filters. However, these usually lead to several artifacts such as significant signal distortions around the notch filter frequencies, as well as phase distortions. In order to avoid such artifacts, in APP we apply the CleanLine plugin of EEGLAB which uses a multi-taper regression

method with a Thompson F-statistics for identifying sinusoidal power line noise from ICs (Delorme and Makeig, 2004; Mullen, 2012). In Fig. 1, an illustrative example of the EEG power spectrum before and after applying the CleanLine method, as desired the power line interference and its harmonics are greatly attenuated without distortion at the neighbor frequencies.

2.1.3. Robust re-referencing

In most EEG amplifiers, the full common-mode rejection ratio can only be achieved after re-referencing. Ideally, the average signal across mastoid and earlobes electrodes would be used as the reference, since they are close to the EEG electrodes but record less brain activity. However, many researchers do not record from mastoids nor earlobes. Instead, the Cz and FCz electrodes are typically used as references, since they do not introduce lateralization bias in the data. Nevertheless, in several experiments (e.g., when the response errors are of interest), these two electrodes are a poor choice of reference since the main effect is expected around those locations. A good compromise, when the number of electrodes is large enough (>32 electrodes), is to use the mean of all electrodes as the reference (Nunez et al., 1997).

The main disadvantage of using the channel average as the reference is that it is not resistant to outliers, namely those associated with bad channels and eye blinks. In the presence of such artifacts, the noise introduced in the reference will spread to the other scalp electrodes. In order to minimize this effect, in APP, we use the biweight estimates of the mean as an approximation of the true mean of the channels, since it offers high resistance to outliers and low sampling variability (Hoaglin et al., 1983, 1985). The biweight estimation is accomplished in two steps: first, the median and median absolute deviation (MAD) are used to assign a zero weight to extreme values; and second, a weighted mean is calculated by assigning decreasing weights nonlinearly to zero as going away from the center of the distribution (For more details, see Appendix A).

To demonstrate the behavior of the biweight estimate of the mean of the channels, we depict two illustrative cases in Fig. 2, one without bad channels and another with one bad channel. In the first case, the biweight mean behaves similarly to the ordinary

mean, with the two means having a high correlation. We also see that the biweight mean is less affected by the eye blinks (as captured by the spike like behavior in the waveform, which affects mainly the frontal electrodes). However, as we introduce the bad channel the biweight mean remains nearly unchanged while the mean of the electrodes is severely contaminated, which results in a decrease in the correlation between the two.

It should be noted that, although we could have performed re-referencing after steps 4 and 5 to avoid distribution of noise across all channels, early re-referencing is important to increase the common-rejection ratio and consequently the SNR, which improves the performance of the metrics used to detect bad channels (correlation and dispersion criteria) as well as bad epochs (mean global field power and mean deviation from channel biweight estimate of the channel means). Although such early re-referencing can cause problems, namely by distributing noise to all channels, we demonstrated that using the biweight estimate of the mean circumvents this problem.

2.1.4. Detection, removal and interpolation of bad channels

One of the most common artifacts in EEG recordings is the presence of bad channels, which often result from poor contact between the scalp and the electrode. In APP, the bad channel detection is accomplished in two stages, based on: (1) temporal features; and (2) ICA decomposition, described below in the subsection Detection and removal of artifacts based on ICA. The bad channel detection based on temporal features follows two criteria:

- (1) *Correlation criterion*: Due to volume conduction, the EEG signal recorded from each channel is highly correlated with the EEG signals from neighboring channels. Therefore, we compute the Pearson correlation between each EEG channel and all other channels, and take the mean of the 4 highest correlation coefficients. Under the high correlation assumption, bad channels are classified as the ones whose mean correlation departs significantly from the distribution of the mean correlation across channels.
- (2) *Dispersion criterion*: As a result of the poor contact, bad channels are more prone to additive Gaussian noise, exhibiting

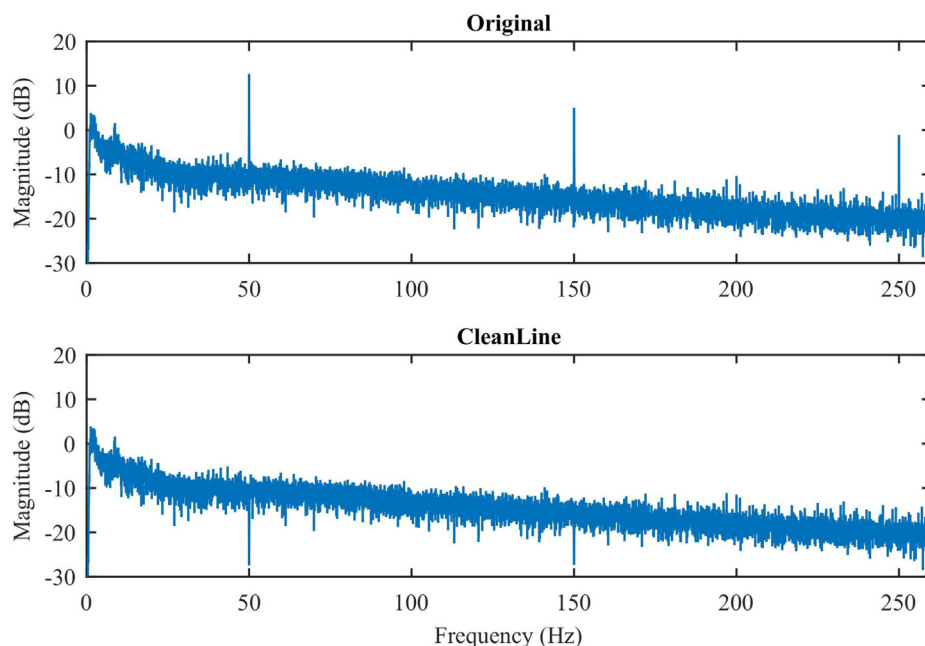


Fig. 1. Example of the EEG spectral power of a single channel (FCz) before (top) and after power line noise removal (bottom) using CleanLine (Mullen, 2012). The power line power (50 Hz) and its harmonics (150 and 250 Hz) are greatly reduced.

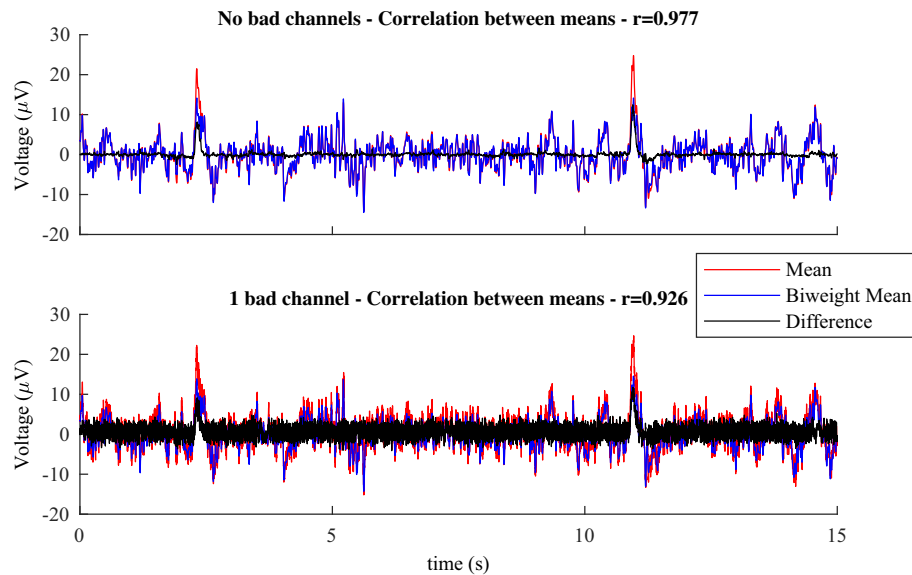


Fig. 2. Comparison of common mean reference (red) and the proposed biweight estimate of the mean (blue). In the case, with no bad channels (top), the two behave similarly, reflected by a small difference (black) and high correlation. However, when a bad channel is included (bottom), the common mean is greatly affected by the bad channel, while the biweight estimate of the mean remains the same, which is reflected in a large difference between them (black) as well as a lower correlation. (For interpretation of the references to colour in this figure legend, the reader is referred to the web version of this article.)

data dispersions spread over a larger range compared with good channels. To quantify the dispersion of the data in each channel, we use the biweight estimate of the standard deviation (see [Appendix A](#)). The rationale of using such robust measure is owing to the frontal electrodes being more susceptible to eye movement artifacts, which inflate their ordinary standard deviation. Under the high dispersion assumption, bad channels are classified as the ones whose biweight estimate of the standard deviation departs significantly from the respective distribution across channels.

A threshold on the number of bad channels is set to 5%, as suggested by ([Picton et al., 2000](#)). If the number of bad channels detected is above the threshold, the dataset is flagged and the pre-processing is stopped. If the number of bad channels is below the threshold, bad channels are removed. APP uses the spherical spline method to interpolate the missing data based on the neighboring channels ([Perrin et al., 1989](#)). It has been shown by Fletcher and colleagues, in an extensive study of interpolation errors in scalp topographic mapping that the spline class algorithms minimize interpolation errors ([Fletcher et al., 1996](#)).

2.1.5. Detection and removal of bad epochs

ICA decomposition can readily isolate in a few ICs typical EEG artifacts such as eye movements, bad channels and muscle tension, since these have stable scalp projections (as described below in sub-section Detection and removal of artifacts based on ICA). However, other kinds of artifacts affecting many or all electrodes simultaneously, such as head movements, are reflected in multiple (maybe hundreds of) ICs, with only a few ICs remaining to capture neuronal activity ([Onton et al., 2006](#)). Therefore, before submitting the EEG data to ICA, APP prunes the EEG data for epochs that deviate from the typical epoch ranges. In case of RS analysis, the data is split into epochs of 2 s, while for ERP analysis the data are epoched according to the respective event trials. To detect the bad epochs, APP computes two parameters:

- (1) *Mean global field power*: Electrode movements can inflate the impedance between electrodes and the scalp. This causes an increase in the electrode voltage offset resulting in high

amplitudes across the scalp. To quantify the overall scalp EEG strength for each epoch, APP uses the mean of the global field power (GFP), which is defined as the standard deviation of the EEG signal across all electrodes at a given time point ([Lehmann and Skrandies, 1980](#)):

$$GFP(t) = \sqrt{\frac{\sum_{i=1}^n (\mathbf{x}_i(t) - \bar{\mathbf{x}}(t))^2}{n}} \quad (1)$$

where $\mathbf{x}_i(t)$ is the signal at electrode i at time point t , $\bar{\mathbf{x}}(t)$ is the average signal across all electrodes at time t , and n is the number of electrodes.

- (2) *Mean deviation from channel biweight estimate of the channel means*: In certain cases, the electrodes movements do not produce high enough amplitudes to be detected using the mean GFP, although they still severely contaminate the respective epochs. In order to account for these, APP quantifies the mean deviation from the biweight estimate of the channel mean (MDCM) as:

$$MDCM(k) = \langle |\bar{\mathbf{x}}_{ik}| - \bar{\mathbf{x}}_{biweight_i} \rangle_n \quad (2)$$

where $\langle \dots \rangle_n$ is the mean operation across all n channels, $|\bar{\mathbf{x}}_{ik}|$ is the absolute value of the mean data in channel i within epoch k and $\bar{\mathbf{x}}_{biweight_i}$ is the biweight estimate of the means of the data in channel i .

In the case of visual stimulation using short presentation durations (e.g. 30 ms), we further apply a threshold of $\pm 100 \mu V$ to the vertical electrooculogram (EOG) signal within an interval of 100 ms before and after stimulus onset, in order to determine if the participant saw the stimulus or not. If the vertical EOG signal is above the threshold, the participant most likely blinked during stimulus presentation; in this case, the epoch is discarded. Moreover, in case the reaction times (RTs) are of interest, APP provides the option to discard responses that are too fast or too slow, according to thresholds specified by the user.

2.1.6. Detection and removal of artifacts based on ICA

EEG signals can be assumed as linear mixtures of electrical potentials originating from multiple brain sources propagating

instantaneously to the scalp, as well as artifacts (Sarvas, 1987). Formally, this can be described as:

$$\mathbf{X} = \mathbf{W}\mathbf{S} \quad (3)$$

where $\mathbf{X} = [\mathbf{x}(1), \dots, \mathbf{x}(N)] = [\mathbf{x}_i(j)]_{n \times N}$ are the EEG signals recorded from the scalp, where each row is one channel, n is the number of channels and N is the number of time samples; $\mathbf{S} = [\mathbf{s}(1), \dots, \mathbf{s}(N)] = [\mathbf{s}_i(j)]_{m \times N}$ is a matrix of unknown sources, in which the rows represent brain sources and artifacts, and \mathbf{W} is a $n \times m$ unknown mixing matrix.

ICA methods estimate the mixing matrix \mathbf{W} from the EEG by maximizing the statistical independence of the sources from each other (Hyvärinen and Oja, 2000). In this work, the second order blind source identification (SOBI) method is used, which is based on the simultaneous diagonalization of inter-signal correlation matrices over time (Belouchrani et al., 1997). The SOBI method was chosen based on its previously reported merits in terms of ability to separate the EEG neuronal sources from artifacts, insensitivity to the duration of the data segments and ability to preserve more brain activity than other ICA algorithms (Daly et al., 2013; Romero et al., 2008; Tang et al., 2005).

APP identifies ICs related with three major kinds of artifacts, as follows:

- (1) *Eye movements or blinks*: ICs exhibiting high temporal correlation with the EOG signals are selected. In order to improve the signal-to-noise ratio (SNR) of the EOG signals, the signal of the right EOG electrode is subtracted from the left one (HEOG) and the signal of lower EOG electrode is subtracted from the upper one (VEOG). It is worth noting that these ICs are usually ranked among the first few components because of their extreme amplitude and the fact that their topographies are essentially flat except for a few frontal electrodes (Chaumon et al., 2015).
- (2) *Muscle related artifacts*: Muscle activity from the jaw, facial muscles and neck movements often contaminate the EEG recordings. Muscular activity related components are easily spotted due to their high time-point-to-time-point variability. In APP, these ICs are detected by their low autocorrelation as a consequence of their noisy time course (Chaumon et al., 2015). The autocorrelation is defined at lag l (default set to 20 ms) for component \mathbf{x}_c by

$$\mathbf{A}_c = \sum_{t=l}^T \mathbf{x}_c(t) \times \mathbf{x}_c(t-l) \quad (4)$$

- (3) *Bad channels*: In order to cope with borderline cases that cannot be detected in the first step (described in Detection, removal and interpolation of bad channels), we include an extra step based on ICA in order to detect focal topographies typically associated with bad channels, we use the Generic Discontinuity Spatial Feature (GDSF) implemented in ADJUST (Mognon et al., 2011), which has been reported to perform better in identification of bad channels than existing alternatives (Chaumon et al., 2015), and it is measured by

$$\text{GDSF}_c = \max(|\mathbf{w}_{c_i} - \langle e^{\|\mathbf{r}_m - \mathbf{r}_i\|} \mathbf{w}_{c_i} \rangle_m|)_n \quad (5)$$

where \mathbf{w}_{c_i} is the topography weight of channel i in IC c , $\|\mathbf{r}_m - \mathbf{r}_i\|$ is the distance between channel \mathbf{r}_m and \mathbf{r}_i , $\langle \dots \rangle_m$ is the average of all channels $m \neq i$ and $\max(\dots)_n$ is the maximum over all channels; and n is the number of channels.

After the identification of the artifactual ICs, the EEG signal is reconstructed based on the remaining ICs, effectively removing the artifacts from the reconstructed signal.

2.1.7. Detection, removal and interpolation of bad channels in epochs

After the ICA step, most of the artifacts are already removed. However, some transient artifacts may still affect single channels in specific segments/epochs of the EEG data (e.g., electrodes that became faulty or lost connection in the middle of the recording). APP detects epochs affected by such transient artifacts based on two criteria, which are evaluated for each channel within each epoch:

- (1) *Dispersion criterion*: The biweight estimate of the temporal standard deviation within each channel is used to quantify the dispersion (similarly to sub-section Detection, removal and interpolation).
- (2) *High-frequency criterion*: The mean of the difference between two consecutive EEG signal time points of each channel within each epoch is used to quantify high-frequency activity.

Next, the bad channels within each epoch are interpolated using spherical splines. In the case of RS data, after interpolation of the bad channels within each epoch, epochs are concatenated with a 500 ms inverse Hanning window at the intersections.

2.1.8. Outlier detection

For each of the parameters computed in the previous steps, APP uses a general outlier detection and removal scheme based on the distribution of the data. First, the Shapiro-Wilk test is performed test for normality; if the data is Leptokurtic (kurtosis > 3), the Shapiro-Francia test is used instead, since it has been shown to outperform the Shapiro-Wilk test for high peaked data (Royston, 1993). If the data distribution is fairly normal distributed, the scheme uses a modified z-score, which is based on the median and the MAD, instead of the mean and standard deviation, respectively, in order to be robust to outliers (Iglewicz and Hoaglin, 1993). Following the recommendation by Iglewicz and Hoaglin, absolute modified z-scores larger than 3.5 are defined as outliers (as opposed to the more commonly used threshold of 3.0). If the data is not normal, then an adjusted boxplot is used to find outliers (Hubert and Vandervieren, 2008), which includes the medcouple, a robust measure of skewness, in the determination of the whiskers. This provides a more accurate representation of the data and avoids many data points to be considered as outliers as in the common boxplot. Data points outside the whiskers are defined as outliers.

2.2. Alternative EEG pre-processing and artifact removal methods

2.2.1. FASTER

For the ERP data analysis, APP is compared with the state-of-the-art artifact removal method “Fully Automated Statistical Thresholding for EEG artifact Rejection” (FASTER; Nolan et al., 2010), as implemented in the EEGLAB toolbox (Delorme and Makeig, 2004). FASTER performs the entire pre-processing from filtering to participants’ grand average, calculating multiple parameters at several steps, and using a threshold of 3 standard deviations from the average to detect outliers.

2.2.2. TAPEEG

For the RS data analysis, APP was compared with a state-of-the-art artifact removal method “Tool for Automated Processing of EEG data” (TAPEEG; Hatz et al., 2015), using our own implementation built onto routines from FASTER and FieldTrip (Oostenveld et al., 2011). Similarly to FASTER, TAPEEG also uses a stepwise procedure to calculate multiple parameters and a threshold of 3 standard deviations from the average as well as hard thresholds to detect outliers.

2.2.3. Prep pipeline

For the RS data analysis, APP was also compared with the Prep pipeline, another state-of-the-art standardized pre-processing method for large-scale EEG analysis (Bigdely-Shamlo et al., 2015). Prep pipeline is an EEG pre-processing pipeline that filters EEG data, re-references the data, and removes bad channels. Since the Prep pipeline does not prune the EEG data for bad epochs of the recording, visual inspection, by experts, was conducted to remove bad segments of the data in this case. The segments removed in this way do not correspond directly to the data epochs removed by APP or TAPEEG, as they are allowed to have variable durations. The plug-in of the algorithm for EEGLAB toolbox was used for comparison.

2.2.4. Supervised artifact identification

Finally, for both ERP and RS data analysis, APP was compared against supervised pre-processing and artifact identification by three researchers with experience in analyzing high-density EEG using CARTOOL (Brunet et al., 2011). Pre-processing of the raw EEG data included DC correction, band-pass filtered between 1 and 40 Hz, 50 Hz noise removal using notch filters. The data was then visually inspected for bad channels and bad epochs; in the case of RS data, data segments of variable duration were removed, which do not exactly match the epochs used in APP or TAPEEG. Bad channels were interpolated using 3D splines, and the data was re-referenced to the average reference.

2.3. Methods for EEG data acquisition and analysis

2.3.1. EEG recording apparatus

The EEG was recorded using a BioSemi Active 2 system (Biosemi) with 64 Ag-AgCl sintered active electrodes positioned in a cap according to the 10–20 system, referenced to the common mode sense (CMS) electrode. The EOG was recorded with electrodes positioned about 1 cm above and below the right eye and 1 cm lateral to the outer canthi. The recording sampling rate was 2048 Hz.

2.3.2. Participants and procedure

An ERP dataset was collected from 61 healthy participants and 44 schizophrenia patients (Table 1) performing a vernier offset discrimination. The vernier stimulus consisted of 2 vertical lines of 10' (arc minutes) separated by a gap of 1', with a fixed horizontal offset of about 1.2', and it was presented for 30 ms. Participants were requested to report the perceived offset direction by pushing a right or left button and to guess when they were not sure. A total of 160 trials were presented, with an inter-trial pause varying randomly between 1000 and 1500 ms. This type of visual stimuli evokes a strong negative ERP (N1 component) around 200 ms after

the stimulus onset in healthy participants, while schizophrenia patients tend to have reduced amplitudes (Plomp et al., 2013).

One RS dataset was collected from 68 healthy participants, Table 1, performing a 5 min eyes-closed EEG recording. No specific instructions were given to the participants besides avoiding head movements.

All participants had good visual acuity of at least 0.80, as measured by the Freiburg Visual Acuity Test using both eyes (Bach, 1996). Participants gave informed consent before the experiments. All procedures complied with the Declaration of Helsinki and were approved by the local ethics committee.

2.3.3. EEG data analysis

The ERP data were subjected to APP, FASTER or supervised pre-processing and artifact rejection. Epochs ranging from –100 to +400 ms around the stimulus onset were used for data segmentation. We then computed the average ERP and the respective GFP time series, for each participant, and subsequently obtained the grand-average GFP for each group (controls and patients), for each pre-processing and artifact rejection method.

In the RS study, the data were subjected to pre-processing and artifact rejection using APP, TAPEEG, Prep pipeline or the supervised method. Subsequently, the pre-processed data were split into epochs of 4 s in each participant. For each epoch, the relative amplitude of different frequency bands (delta: 1–4 Hz, theta: 4–8 Hz, low alpha: 8–10 Hz, high alpha: 10–13 Hz and beta: 13–30 Hz) was calculated as in (Wan et al., 2016), and the mean relative band amplitude across epochs was determined for each channel. In order to account for the different scalp distributions of the frequency bands, the relative amplitude of each band was averaged across the channels belonging to one of 5 scalp regions (frontal, left tempo-parietal, right tempo-parietal, central and parieto-occipital; for the definition of the regions see Supplementary Fig. S1). Furthermore, the peak alpha frequency (PAF) and the individual alpha band (IAB; PAF – 2 Hz to PAF + 2 Hz) were calculated and averaged across the parieto-occipital channels. In summary, we obtain 5 (frequency bands) × 5 (scalp regions) + 2 (IAB and PAF) = 27 parameters per participant, which were submitted to statistical analysis.

3. Results

The results obtained by applying the proposed data pre-processing and artifact removal pipeline APP, as well as its alternative pipelines, are presented here, first for the ERP data and then for the RS data.

3.1. ERP data analysis

3.1.1. GFP analysis

The grand-average GFP time series obtained for the control and patient groups, using each data pre-processing and artifact rejection method, are shown in Fig. 3. A GFP N1 peak around 200 ms after stimulus onset can be observed. The average GFP N1 amplitudes at the peak latencies for each Group (Controls and Patients), as a function of the pre-processing Method (APP, FASTER and Supervised) are shown in Fig. 4. A 2-way repeated measures ANOVA with a Greenhouse-Geisser correction on the peak N1 amplitudes showed significant main effects of Group ($F(1, 103) = 38.74$, $P < 0.001$) and Method ($F(1.699, 174.96) = 23.367$, $P < 0.001$), as well as a significant interaction effect between them ($F(1.699, 174.96) = 9.898$, $P < 0.001$). This interaction indicates that differences between groups depend on the pre-processing method used. The largest difference between patients and healthy participants' mean peak N1 amplitudes was obtained using APP ($1.59 \pm$

Table 1

Average statistics (mean \pm SD) of demographic and clinical data of all participants in the event-related potential (ERP) and resting-state (RS) datasets.

	ERP Participants		RS Participants
	Schizophrenia Patients	Healthy Controls	Healthy Participants
Gender (F/M)	11/33	29/32	29/39
Age	33.4 \pm 8.3	35.1 \pm 9.6	35.0 \pm 8.2
Education	13.4 \pm 2.7	15.0 \pm 2.8	14.1 \pm 2.7
Illness duration	9.2 \pm 7.1		
SANS*	10.4 \pm 5.1		
SAPS**	9.0 \pm 2.9		
Handedness (R/L)	43/1	56/5	64/4
Visual acuity	1.40 \pm 0.34	1.51 \pm 0.41	1.62 \pm 0.39

* SANS: Scale for the Assessment of Negative Symptoms.

** SAPS: Scale for the Assessment of Positive Symptoms.

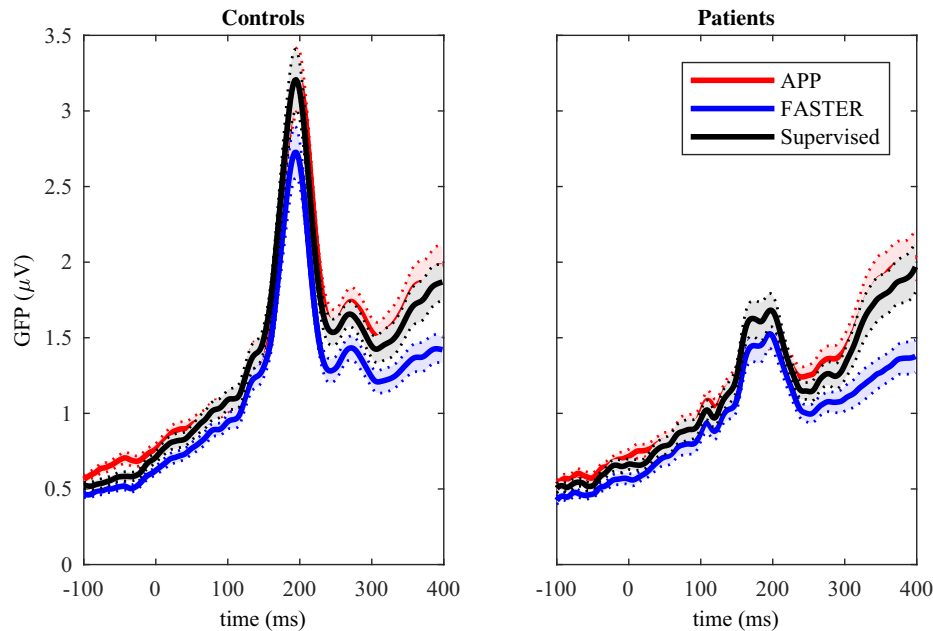


Fig. 3. The global field power (GFP) time series of the ERP data, for healthy controls (left) and patients (right), after pre-processing with APP (red), FASTER (blue) and the Supervised scheme (black). Solid lines represent the group mean and dashed lines represent plus or minus one standard error of the mean. (For interpretation of the references to colour in this figure legend, the reader is referred to the web version of this article.)

0.83 μV vs $3.21 \pm 1.55 \mu\text{V}$), followed by the supervised scheme ($1.68 \pm 0.72 \mu\text{V}$ vs $3.19 \pm 1.51 \mu\text{V}$), and FASTER ($1.53 \pm 0.65 \mu\text{V}$ vs $2.71 \pm 1.24 \mu\text{V}$). Moreover, post hoc tests using Bonferroni-Holm correction on the factor *Method* revealed that APP and the supervised scheme lead to similar N1 amplitudes for all participants ($2.53 \pm 1.53 \mu\text{V}$ and $2.56 \pm 1.46 \mu\text{V}$, respectively, $p = 1$). However, the mean N1 amplitudes for all participants after FASTER pre-processing had been reduced to $2.21 \pm 1.19 \mu\text{V}$, which was statistically significant different to APP ($p < 0.001$) and the supervised scheme ($p < 0.001$).

3.1.2. Channels interpolated

The percentage of channels interpolated using each pre-processing method, for both groups, is presented in Fig. 5(a). A

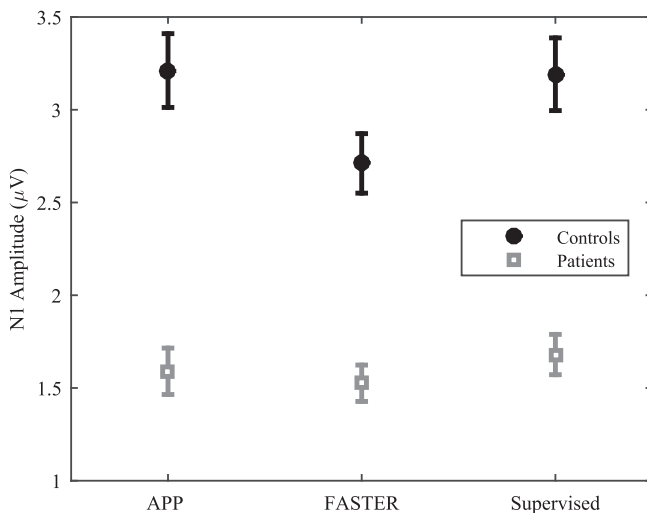


Fig. 4. Average GFP N1 amplitudes at the peak latencies for each Group (Controls and Patients), as a function of the pre-processing Method (APP, FASTER and Supervised). The interaction effect between Group and Method indicates that the GFP difference between patients and healthy controls is not as large when using FASTER compared to using APP or Supervised pre-processing. Error bars indicate the standard error of the mean.

2-way repeated measures ANOVA with a Greenhouse-Geisser correction showed a significant main effect of *Method* ($F(1.67, 172.38) = 153.126, P < 0.001$) but no significant effects of *Group* ($F(1, 103) = 1.44, P = 0.233$) nor a significant interaction ($F(1.67, 172.38) = 2.79, P = 0.074$). Post hoc tests using Bonferroni-Holm correction on the factor *Method* revealed that APP interpolated a similar amount of channels to the supervised scheme ($1.05 \pm 1.00\%$ and $1.02 \pm 0.66\%$, respectively, $p = 0.925$). However, FASTER interpolated around of $3.29 \pm 1.45\%$ channels, which was statistically significant more than APP ($p < 0.001$) and Supervised ($p < 0.001$).

3.1.3. Trials removed

The percentage of trials rejected using each pre-processing method, for both groups, is presented in Fig. 5(b). A 2-way repeated measures ANOVA with a Greenhouse-Geisser correction showed significant main effects of *Group* ($F(1, 103) = 17.85, P < 0.001$) and *Method* ($F(1.378, 141.93) = 32.94, P < 0.001$), but no statistically significant interaction ($F(1.378, 141.93) = 0.548, P = 0.515$). Patients in general had more trials rejected than healthy participants ($4.78 \pm 1.57\%$ and $3.97 \pm 1.64\%$, respectively). Post hoc tests using Bonferroni-Holm correction on the factor *Method* revealed that APP rejected significantly fewer trials than FASTER for all participants ($3.62 \pm 2.00\%$ and $4.17 \pm 0.85\%$, respectively, $p = 0.007$). Moreover, the supervised scheme rejected $5.16 \pm 1.53\%$ trials, which was significantly more than APP ($p < 0.001$) and FASTER ($p < 0.001$).

3.1.4. Independent components removed

The percentage of ICs removed using each pre-processing method (APP and FASTER), for both groups, is presented in Fig. 5(c). A 2-way repeated measures ANOVA yielded non-significant effects of *Method* ($F(1, 103) = 0.303, P = 0.583$) and *Group* ($F(1, 103) = 0.918, P = 0.340$) as well as non-significant interaction ($F(1, 103) = 0.078, P = 0.781$). On average, APP removed $6.65 \pm 3.03\%$ of ICs, while FASTER removed $6.89 \pm 3.44\%$.

3.1.5. Channels interpolated per trial

The percentage of channels interpolated per trial by each pre-processing method (APP and FASTER), for both groups, is presented

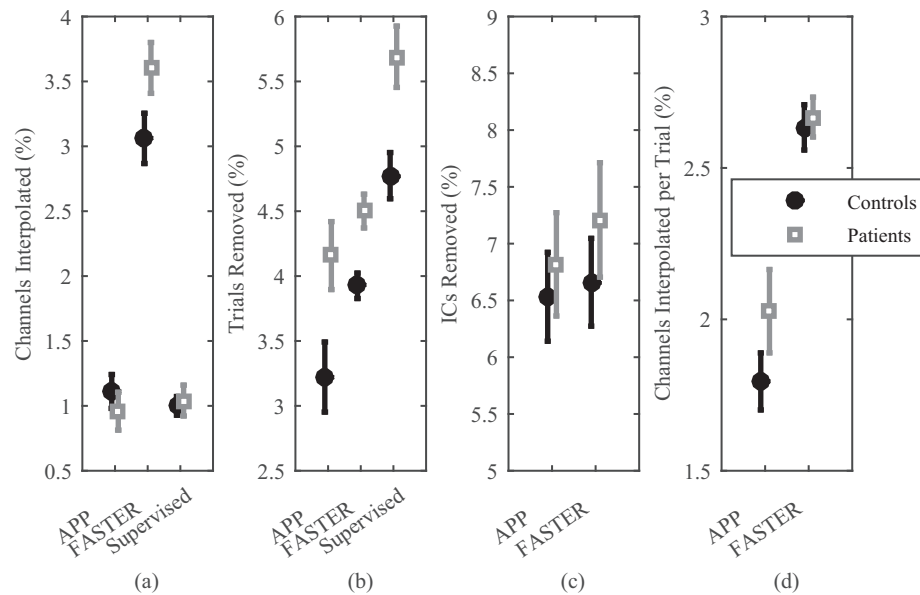


Fig. 5. Average percentage of channels interpolated (a), trials removed (b), independent components removed (c) and channels interpolated per trial (d), for healthy controls and schizophrenia patients, using APP, FASTER and supervised artifact rejection (except for channels interpolated per trial). Error bars indicate the standard error of the mean.

in Fig. 5(d). A 2-way repeated measures ANOVA showed a significant effect of *Method* ($F(1, 103) = 167.51, P < 0.001$) but no significant effect of *Group* ($F(1, 103) = 1.167, P = 0.282$) nor a significant interaction ($F(1, 103) = 3.022, P = 0.085$). APP interpolated fewer channels per trial than FASTER ($1.89 \pm 0.82\%$ and $2.65 \pm 0.52\%$, respectively).

3.2. RS data analysis

3.2.1. Frequency bands

A 3-way repeated measures ANOVA with a Greenhouse-Geisser correction was conducted on the main factors: *Method* (Supervised, APP, TAPEEG and Prep pipeline), *Region* (frontal, left temporo-parietal, right temporo-parietal, central and parieto-occipital), and *Band* (Delta, Theta, Low Alpha, High Alpha and Beta). The results showed a non-significant main effect of *Method* ($F(2.920, 195.609) = 0.357, P = 0.779$), but significant main effects of *Region* ($F(3.806, 255.025) = 22.488, P < 0.001$) and *Band* ($F(2.065, 138.327) = 1448.719, P < 0.001$), as well as a significant 3-way interaction ($F(17.110, 1146.356) = 1.790, P = 0.024$). The ANOVA yielded also a significant *Band* \times *Region* interaction ($F(7.495, 502.152) = 11.239, P < 0.001$), and non-significant interactions *Band* \times *Method* ($F(5.881, 394.053) = 1.010, P = 0.418$) and *Method* \times *Region* ($F(9.785, 655.585) = 0.916, P = 0.516$). Moreover, two 1-way repeated measures ANOVA's with a Greenhouse-Geisser correction were conducted to compare the effect of *Method* on PAF and IAB of the parieto-occipital region. For PAF, there was no significant effect of *Method* ($F(2.816, 188.657) = 1.859, P = 0.142$). Similarly, there was no significant of *Method* on IAB ($F(2.616, 175.282) = 0.943, P = 0.411$). In general, all the pre-processing methods yielded similar EEG relative amplitudes in each frequency band for all the 5 scalp regions, as well as similar PAF and IAB for the parieto-occipital region (for summary statistics, see [Supplementary Table S1](#)).

The Pearson correlation coefficients between the EEG relative amplitude in each frequency band, as well as the PAF and IAB, obtained using the automatic pipelines (APP, TAPEEG or Prep pipeline) and the ones obtained using the supervised scheme, are shown in [Table 2](#). On average, APP, TAPEEG, and Prep pipeline were found to correlate well with the supervised scheme ($r = 0.922 \pm 0.033$, $r = 0.923 \pm 0.046$, and $r = 0.928 \pm 0.035$, respectively).

3.2.2. Channels interpolated

The percentage of channels interpolated in the RS analysis, for each pre-processing method, is presented in [Fig. 6\(a\)](#). A one-way repeated measures ANOVA with a Greenhouse-Geisser correction showed a significant main effect of the pre-processing *Method* ($F(1.575, 105.527) = 15.49, P < 0.001$). Post hoc tests using Bonferroni-Holm correction revealed that APP interpolated a similar amount of channels as the supervised scheme ($1.20 \pm 1.87\%$ and $1.15 \pm 2.51\%$, respectively, $p = 0.924$), but significantly less than TAPEEG ($2.48 \pm 1.33\%$, $p = 0.018$) and Prep pipeline ($3.98 \pm 4.87\%$, $p < 0.001$). TAPEEG interpolated significantly fewer channels than Prep pipeline ($p = 0.008$) and significantly more than the supervised scheme ($p = 0.018$). Prep pipeline interpolated significantly more channels than the supervised scheme ($p < 0.001$).

3.2.3. Data segments removed

The percentage of RS data segments removed in the analysis, for each pre-processing method, is presented in [Fig. 6\(b\)](#). A one-way repeated measures ANOVA with a Greenhouse-Geisser correction yielded a significant main effect of the pre-processing *Method* ($F(2.720, 182.267) = 57.94, P < 0.001$). Post hoc tests using Bonferroni-Holm correction revealed that APP removed significantly more data segments than the supervised scheme ($8.32 \pm 2.24\%$ and $4.99 \pm 2.73\%$, $p < 0.001$) and Prep pipeline ($5.13 \pm 2.61\%$, $p < 0.001$) but significantly less than TAPEEG (10.36 ± 3.53 , $p < 0.001$). TAPEEG removed significantly more data than the supervised scheme ($p < 0.001$) and Prep pipeline ($p < 0.001$). Prep

Table 2

Pearson correlation coefficients of the EEG relative band amplitude in each frequency band, the individual alpha band (IAB) and the peak alpha frequency (PAF), between APP (left), TAPEEG (middle) or Prep Pipeline (right) and the supervised scheme.

	APP vs Supervised	TAPEEG vs Supervised	Prep pipeline vs Supervised
Delta	0.918	0.892	0.905
Theta	0.927	0.940	0.938
Low Alpha	0.960	0.969	0.976
High Alpha	0.949	0.967	0.947
Beta	0.952	0.971	0.966
IAB	0.870	0.861	0.882
PAF	0.878	0.864	0.885

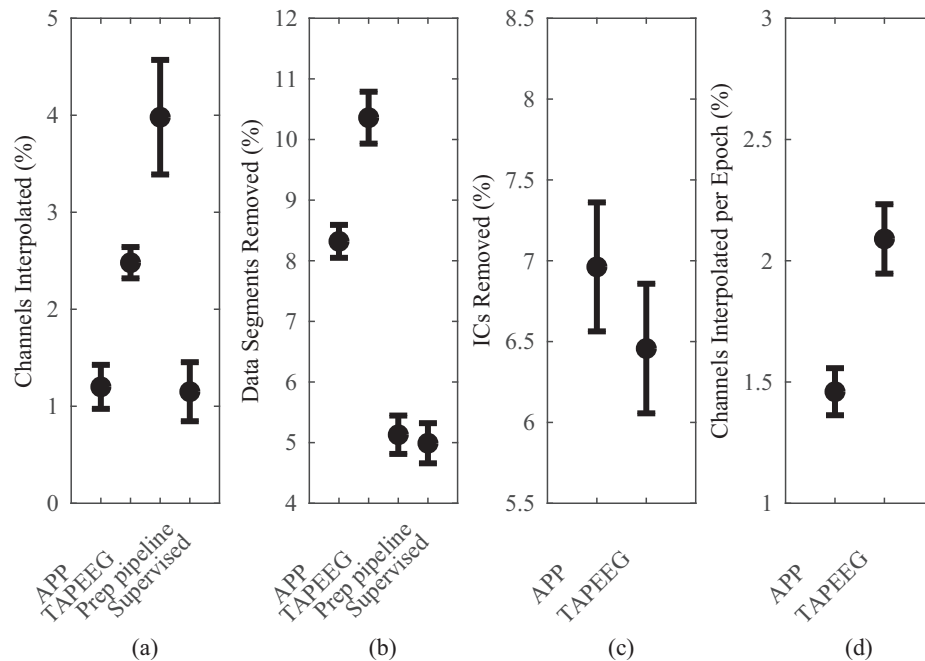


Fig. 6. Average percentage of channels interpolated (a), data segments removed (b), independent components removed (c) and channels interpolated per epoch (d) using APP, TAPEEG, Prep pipeline and supervised artifact reject (except channels interpolated per epoch for the latter two methods). Error bars indicate the standard error of the mean.

pipeline removed a similar amount of data segments as the supervised scheme ($p = 0.771$).

3.2.4. Independent components removed

The percentage of ICs removed by each pre-processing method (APP and TAPEEG) is presented in Fig. 6(c). A two-tailed paired-samples t -test showed that APP and TAPEEG removed similar number of ICs ($6.96 \pm 3.29\%$ and $6.46 \pm 3.31\%$, respectively); ($t(67) = 0.889$, $p = 0.377$).

3.2.5. Channels interpolated per epoch

The percentage of channels interpolated per epoch rejected by each pre-processing method (APP and TAPEEG) is presented in Fig. 6(d). A two-tailed paired-samples t -test showed that APP interpolated significantly less channels per epoch than TAPEEG ($1.46 \pm 0.80\%$ and $2.09 \pm 1.18\%$, respectively); ($t(67) = 4.125$, $p < 0.001$).

4. Discussion and Conclusion

EEG data are usually contaminated by numerous artifacts and require expert supervision for artifact identification and removal. However, with the increasing size of available datasets due to increasing numbers of EEG channels and study participants, supervised data pre-processing becomes impractical, paving the way for automatic pre-processing methods.

In this study, we propose a novel automatic pipeline (APP) for EEG pre-processing and artifact detection and removal, which makes use of state-of-the-art EEG signal processing techniques in a step-by-step manner to correct the EEG data for external and internal, i.e. participant generated, noise. First, APP filters the EEG data for non-stationarity and removes the power line noise with minimum distortion of the frequency spectrum. Second, it re-references the data to a robust estimate of the mean of all channels. Then, it detects and interpolates bad channels and removes bad epochs. After that, APP uses ICA to remove eye-movement, muscular and bad-channel related artifacts. Finally, it removes epoch artifacts. At each step, several parameters are estimated from the data and outliers are detected and removed based on a

robust data driven outlier detection scheme. APP was validated on two datasets containing real ERP and RS data.

4.1. ERP data

The ERP dataset consisted of data from healthy controls and schizophrenia patients performing a vernier discrimination task. This type of visual stimuli usually evokes a strong negative N1 component, around 200 ms after the stimulus onset, as measured by the GFP. However, schizophrenia patients tend to have reduced amplitudes compared to healthy controls (Plomp et al., 2013). The same result, i.e. low N1 amplitudes for patients compared to controls, were found using either APP, supervised inspection by experts, or FASTER (a previously proposed method of artifact detection in ERP data). However, the N1 amplitudes obtained using APP were similar to the ones obtained using the supervised scheme but were significantly larger than the ones obtained using FASTER. Interestingly, the difference between the mean of the controls' N1 amplitudes and the mean of patients' N1 amplitudes were larger for APP and the supervised scheme than the ones of FASTER.

Moreover, as expected, patients had more bad trials than controls, for all pre-processing schemes. The supervised scheme rejected more trials than APP and FASTER. This might be the case because the experts did not use ICA to reduce artifacts nor interpolated channels that are bad just in specific trials, thus, considering those trials as bad overall. Considering the two automatic methods, APP removed less bad trials than FASTER; however, the two methods removed similar amount of ICs. In terms of channels interpolated, APP interpolated similar number of channels as the supervised scheme; however, FASTER interpolated significantly more than the other two methods. In addition, FASTER interpolated more channels per trial than APP.

4.2. Resting-state data

For the validation of the proposed pipeline on RS data pre-processing, data from healthy participants performing a 5 min eyes-close EEG recording was used. Similar levels of correlation

were found for the power across multiple frequency bands, as well as the peak alpha frequency, between each of the three automatic pre-processing (APP, TAPEEG, and Prep pipeline) and the expert supervision. In addition, APP removed and interpolated a similar number of channels as the supervised scheme and fewer than both TAPEEG and Prep pipeline. Regarding the amount of data segments rejected, EEG experts had to prune the data for artifactual segments, following Prep pipeline pre-processing, since this method does not incorporate such feature. Consequently, Prep pipeline and the supervised scheme rejected similar amount of data segments and significantly less than APP and TAPEEG. The latter two methods use fixed epochs to prune the data for artifactual segments, which might cause the difference between the EEG experts supervision and the two fully automated methods. Considering only the two fully automated methods, APP removed significantly less epochs than TAPEEG but no statistically significant difference was found in terms of ICs removed. Additionally, TAPEEG interpolated more channels per epochs than APP.

Unlike FASTER and TAPEEG, APP does not assume a normal distribution of the parameters calculated at each step, which avoids that much data from skewed distributions be considered as outliers and therefore discarded. This is especially important when dealing with patient data, which by nature tend to be noisier but also more difficult to obtain so that we cannot afford to lose artifact-free information.

4.3. Limitations of the proposed pipeline

We only tested APP on 64-channels datasets. However, we expect the pipeline to work at least equally well for recordings with more channels, since each parameter computed at each step is treated statistically and more data therefore provide a better sampling of the parameter distribution. For the same reason, we do not recommend the use of APP for recordings with less than 32 channels without supervision. In such cases, APP can still be used, but only as an auxiliary tool to further support an informed decision on whether or not to classify a specific channel, trial or IC as artifactual.

The most challenging part of the proposed pipeline is the correct classification of ICs. So far, no metric can accurately classify artifactual ICs. Thus, in APP to avoid overcorrection, we relied on metrics that have low false alarm rates, while achieving satisfactory hit rates (for a comparison of the classification accuracy of different IC metrics, see Chaumon et al., 2015). Since Chaumon and colleagues used training sets to define thresholds for each metric, we conducted a small analysis to determine how these metrics would perform using APP's outlier detection scheme. Results were inspected by one EEG expert and the metrics reported in Chaumon et al. (2015) to have better results were found to yield satisfactory performance. Furthermore, in the absence of EOG signals the correction of eye-movement related artifacts cannot be performed, since APP uses EOG signal as a reference for the IC selection. Further work on APP could include metrics for improved IC classification, as well as metrics for the detection of eye-movement related ICs that do not resort on reference signals, such as the ADJUST eye movement detector. Finally, APP was only tested in laboratory conditions, in which artifacts are somehow mild and SNR is relatively high when compared to harsher environments, such as natural settings outside laboratories or inside magnetic resonance scanners. Therefore, we do not recommend the use of APP with EEG data acquired under such circumstances.

4.4. Summary

In sum, the aim of this paper was to propose and validate APP, a novel method for EEG pre-processing and artifact removal. Our

results show that APP performs at the same level as the pre-processing done by EEG experts, while outperforming existing alternatives in many aspects, namely the amount of data lost, and achieving higher ERP amplitudes. Currently, APP is a series of Matlab® scripts that can be obtained by contacting the corresponding author. However, our intention is to integrate APP as a plugin for EEGLAB, and to make the respective source code freely available online. The default parameters in this plugin will be the ones used in the present article; however, the users will have the option to change the parameters at their convenience. We hope that this method will contribute to the EEG research field by aiding researchers deal with the increased amount of data and improving the reproducibility of results.

Conflict of interest statement

None of the authors have declared any conflict of interest.

Acknowledgments

This work was partially funded by the Fundação para a Ciência e a Tecnologia under grants FCT UID/EEA/50009/2013 and FCT PD/BD/105785/2014, and the National Centre of Competence in Research (NCCR) Synapsy (The Synaptic Basis of Mental Diseases) under grant 51NF40-158776.

Appendix A

The biweight estimate (Hoaglin et al., 1983, 1985) is a weighted average, in which the weights decrease nonlinearly as going away from the center of the distribution. The weighting function returns zero after a certain distance from the center of the distribution and this distance is controlled by a censoring parameter c . First, the median M and the median absolute deviation MAD are determined. Second, a weight $u(i)$ is assigned to each of the N observations $x(i)$ as follows:

$$u(i) = \frac{x(i) - M}{c \times MAD}$$

To censor the extreme values, $\forall |u(i)| \geq 1, u(i) = 1$. In this study, c is set to 7.5, which censors values more than 5 standard deviations away from the center of the distribution.

Then, the biweight estimate of the mean is given by:

$$\bar{x}_{biweight} = M + \frac{\sum_{i=1}^N (x(i) - M)(1 - u(i)^2)^2}{\sum_{i=1}^N (1 - u(i)^2)^2}$$

The biweight estimate of the standard deviation is calculated in a similar fashion:

$$s_{biweight} = \frac{\sqrt{N \sum_{i=1}^N (x(i) - M)^2 (1 - u(i)^2)^4}}{\sum_{i=1}^N (1 - u(i)^2)(1 - 5u(i)^2)}$$

Appendix B. Supplementary material

Supplementary data associated with this article can be found, in the online version, at <https://doi.org/10.1016/j.clinph.2018.04.600>.

References

- Abreu R, Leite M, Jorge J, Grouiller F, van der Zwaag W, Leal A, Figueiredo P. Ballistocardiogram artifact correction taking into account physiological signal preservation in simultaneous EEG-fMRI. *NeuroImage* 2016a;135:45–63. <https://doi.org/10.1016/j.neuroimage.2016.03.034>.

- Abreu R, Leite M, Leal A, Figueiredo P. Objective selection of epilepsy-related independent components from EEG data. *J Neurosci Methods* 2016b;258:67–78. <https://doi.org/10.1016/j.jneumeth.2015.10.003>.
- Bach M. The Freiburg Visual Acuity test—automatic measurement of visual acuity. *Optom Vis Sci* 1996;73:49–53.
- Belouchrani A, Abed-Meraim K, Cardoso JF, Moulines E. A blind source separation technique using second-order statistics. *IEEE Trans Signal Process* 1997;45:434–44. <https://doi.org/10.1109/78.554307>.
- Bigdely-Shamlo N, Mullen T, Kothe C, Su K-M, Robbins KA. The PREP pipeline: standardized preprocessing for large-scale EEG analysis. *Front Neuroinform* 2015;9:16. <https://doi.org/10.3389/fninf.2015.00016>.
- Brunet D, Murray MM, Michel CM. Spatiotemporal Analysis of Multichannel EEG: CARTOOL. *Comput Intell Neurosci* 2011;2011(2011):813870. <https://doi.org/10.1155/2011/813870>.
- Chaumon M, Bishop DVM, Busch NA. A practical guide to the selection of independent components of the electroencephalogram for artifact correction. *J Neurosci Methods* 2015. <https://doi.org/10.1016/j.jneumeth.2015.02.025>.
- Daly I, Nicolaou N, Nasuto SJ, Warwick K. Automated Artifact Removal From the Electroencephalogram A Comparative Study. *Clin EEG Neurosci* 2013;44:291–306. <https://doi.org/10.1177/1550059413476485>.
- Delorme A, Makeig S. EEGLAB: an open source toolbox for analysis of single-trial EEG dynamics including independent component analysis. *J Neurosci Methods* 2004;134:9–21. <https://doi.org/10.1016/j.jneumeth.2003.10.009>.
- Fletcher EM, Kussmaul CL, Mangun GR. Estimation of interpolation errors in scalp topographic mapping. *Electroencephalogr Clin Neurophysiol* 1996;98:422–34. [https://doi.org/10.1016/0013-4694\(96\)95135-4](https://doi.org/10.1016/0013-4694(96)95135-4).
- Hatz F, Hardmeier M, Bousleiman H, Rüegg S, Schindler C, Fuhr P. Reliability of fully automated versus visually controlled pre- and post-processing of resting-state EEG. *Clin Neurophysiol* 2015;126:268–74. <https://doi.org/10.1016/j.clinph.2014.05.014>.
- Hoaglin DC, Mosteller F, Tukey JW, editors. *Exploring Data Tables, Trends, and Shapes*. 1 ed. New York: Wiley; 1985.
- Hoaglin DC, Mosteller F, Tukey JW, editors. *Understanding robust and exploratory data analysis*. New York: Wiley; 1983.
- Hubert M, Vandervieren E. An adjusted boxplot for skewed distributions. *Comput Stat Data Anal* 2008;52:5186–201. <https://doi.org/10.1016/j.csda.2007.11.008>.
- Hyvärinen A, Oja E. Independent component analysis: algorithms and applications. *Neural Netw* 2000;13:411–30. [https://doi.org/10.1016/S0893-6080\(00\)00026-5](https://doi.org/10.1016/S0893-6080(00)00026-5).
- Iglewicz B, Hoaglin DC. 1993. How to Detect and Handle Outliers. ASQC Quality Press.
- Lehmann D, Skrandies W. Reference-free identification of components of checkerboard-evoked multichannel potential fields. *Electroencephalogr Clin Neurophysiol* 1980;48:609–21. [https://doi.org/10.1016/0013-4694\(80\)90419-8](https://doi.org/10.1016/0013-4694(80)90419-8).
- Luck SJ. *An introduction to the event-related potential technique*. second ed. Cambridge, Massachusetts: The MIT Press; 2014.
- Lynn, P.A., 1989. *Introduction to the Analysis and Processing of Signals*, 3rd ed. Hemisphere Publishing Corporation.
- Makeig S, Bell AJ, Jung TP, Sejnowski TJ. Independent component analysis of electroencephalographic data. In *Advances in neural information processing systems*, 1996, 145–151.
- Mognon A, Jovicich J, Bruzzone L, Buiaiti M. ADJUST: An automatic EEG artifact detector based on the joint use of spatial and temporal features. *Psychophysiology* 2011;48:229–40. <https://doi.org/10.1111/j.1469-8986.2010.01061.x>.
- Mullen T, 2012. CleanLine. NITRC.
- Niedermeyer, E., Lopes da Silva, F.H., 2005. *Electroencephalography: Basic Principles, Clinical Applications, and Related Fields*. Lippincott Williams & Wilkins.
- Nolan H, Whelan R, Reilly RB. FASTER: Fully Automated Statistical Thresholding for EEG artifact Rejection. *J Neurosci Methods* 2010;192:152–62. <https://doi.org/10.1016/j.jneumeth.2010.07.015>.
- Nunez PL, Srinivasan R, Westdorp AF, Wijesinghe RS, Tucker DM, Silberstein RB, Cadusch PJ. EEG coherency: I: statistics, reference electrode, volume conduction, Laplacians, cortical imaging, and interpretation at multiple scales. *Electroencephalogr Clin Neurophysiol* 1997;103:499–515. [https://doi.org/10.1016/S0013-4694\(97\)00066-7](https://doi.org/10.1016/S0013-4694(97)00066-7).
- Onton J, Westerfield M, Townsend J, Makeig S. Imaging human EEG dynamics using independent component analysis. *Neurosci Biobehav Rev* 2006;30:808–22. <https://doi.org/10.1016/j.neubiorev.2006.06.007>.
- Oostenveld R, Fries P, Maris E, Schoffelen J-M. FieldTrip: Open Source Software for Advanced Analysis of MEG, EEG, and Invasive Electrophysiological Data. *Comput Intell Neurosci* 2011;2011(2011):156869. <https://doi.org/10.1155/2011/156869>.
- Perrin F, Pernier J, Bertrand O, Echallier JF. Spherical splines for scalp potential and current density mapping. *Electroencephalogr Clin Neurophysiol* 1989;72:184–7. [https://doi.org/10.1016/0013-4694\(89\)90180-6](https://doi.org/10.1016/0013-4694(89)90180-6).
- Picton TW, Bentin S, Berg P, Donchin E, Hillyard SA, Johnson R, Miller GA, Ritter W, Ruchkin DS, Rugg MD, Taylor MJ. Guidelines for using human event-related potentials to study cognition: Recording standards and publication criteria. *Psychophysiology* 2000;37:127–52. <https://doi.org/10.1016/j.psychphys.2000.03.001>.
- Plomp G, Rooinishvili M, Chkonia E, Kapanadze G, Kereselidze M, Brand A, Herzog MH. Electrophysiological Evidence for Ventral Stream Deficits in Schizophrenia Patients. *Schizophr Bull* 2013;39:547–54. <https://doi.org/10.1093/schbul/sbr175>.
- Romero S, Mañanas MA, Barbanoj MJ. A comparative study of automatic techniques for ocular artifact reduction in spontaneous EEG signals based on clinical target variables: A simulation case. *Comput Biol Med* 2008;38:348–60. <https://doi.org/10.1016/j.combiomed.2007.12.001>.
- Royston P. A Toolkit for Testing for Non-Normality in Complete and Censored Samples. *J Roy Stat Soc Ser Stat* 1993;42:37–43. <https://doi.org/10.2307/2348109>.
- Sarvas J. Basic mathematical and electromagnetic concepts of the biomagnetic inverse problem. *Phys Med Biol* 1987;32:11. <https://doi.org/10.1088/0031-9155/32/1/004>.
- Tang AC, Sutherland MT, McKinney CJ. Validation of SOBI components from high-density EEG. *NeuroImage* 2005;25:539–53. <https://doi.org/10.1016/j.neuroimage.2004.11.027>.
- Tatum WO, Dworetzky BA, Schomer DL. Artifact and Recording Concepts in EEG. *J Clin Neurophysiol* 2011;28:252–63. <https://doi.org/10.1097/WNP.0b013e31821c3c93>.
- Urigüen JA, García-Zapirain B. EEG artifact removal—state-of-the-art and guidelines. *J Neural Eng* 2015;12:031001. <https://doi.org/10.1088/1741-2560/12/3/031001>.
- Wan F, da Cruz JN, Nan W, Wong CM, Vai MI, Rosa A. Alpha neurofeedback training improves SSVEP-based BCI performance. *J Neural Eng* 2016;13:036019. <https://doi.org/10.1088/1741-2560/13/3/036019>.

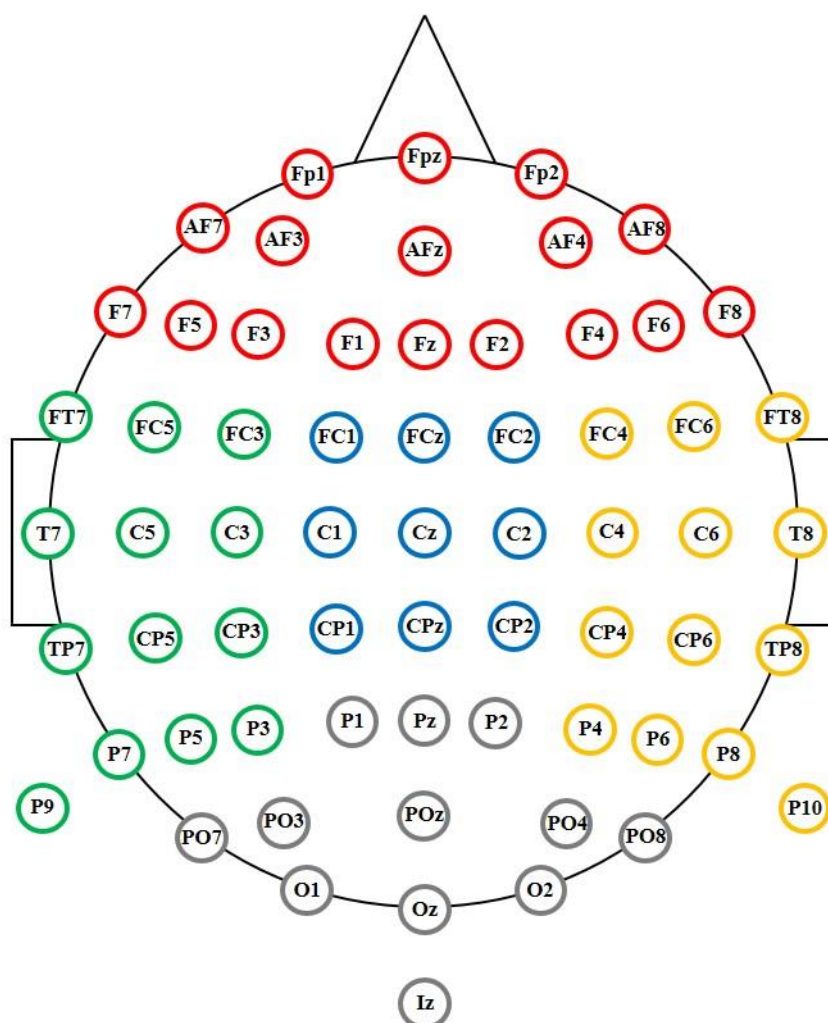


Figure S1 – Definition of the channels included in the 5 scalp regions used for frequency analysis of RS EEG data: frontal (red), left temporo-parietal (green), right temporo-parietal (yellow), central (blue), and parieto-occipital (grey).

Table S1 – Average Statistics (\pm SD) of the EEG relative band amplitude in each frequency band for each scalp region, the individual alpha band (IAB) and the peak alpha frequency (PAF) for different pre-processing methods (Supervised, APP, TAPEEG or Prep Pipeline). (TP: tempo-parietal; PO: parieto-occipital.)

	Region	Supervised	APP	TAPEEG	Prep Pipeline
Delta	Frontal	2.45 \pm 0.40	2.34 \pm 0.34	2.51 \pm 0.36	2.41 \pm 0.37
	Left TP	2.07 \pm 0.40	2.09 \pm 0.47	2.10 \pm 0.60	1.99 \pm 0.54
	Right TP	2.09 \pm 0.39	2.01 \pm 0.46	2.12 \pm 0.50	1.96 \pm 0.48
	Central	2.34 \pm 0.41	2.24 \pm 0.43	2.41 \pm 0.61	2.40 \pm 0.47
	PO	2.17 \pm 0.38	2.18 \pm 0.44	2.22 \pm 0.52	2.08 \pm 0.47
Theta	Frontal	1.50 \pm 0.21	1.45 \pm 0.22	1.54 \pm 0.19	1.50 \pm 0.19
	Left TP	1.37 \pm 0.23	1.41 \pm 0.30	1.33 \pm 0.30	1.32 \pm 0.34
	Right TP	1.38 \pm 0.24	1.42 \pm 0.35	1.31 \pm 0.33	1.37 \pm 0.33
	Central	1.55 \pm 0.22	1.54 \pm 0.32	1.64 \pm 0.31	1.51 \pm 0.33
	PO	1.42 \pm 0.23	1.42 \pm 0.33	1.33 \pm 0.39	1.43 \pm 0.31
Low Alpha	Frontal	2.45 \pm 1.16	2.44 \pm 1.13	2.63 \pm 1.07	2.23 \pm 0.93
	Left TP	2.38 \pm 1.02	2.26 \pm 1.07	2.17 \pm 1.09	2.61 \pm 0.97
	Right TP	2.45 \pm 1.02	2.25 \pm 1.08	2.37 \pm 1.07	2.65 \pm 0.86
	Central	2.55 \pm 1.08	2.70 \pm 1.24	2.46 \pm 1.06	2.57 \pm 1.46
	PO	2.80 \pm 1.24	3.04 \pm 1.22	2.75 \pm 1.41	2.77 \pm 1.40
High Alpha	Frontal	1.85 \pm 0.58	1.85 \pm 0.70	1.85 \pm 0.63	1.69 \pm 0.67
	Left TP	1.93 \pm 0.56	1.89 \pm 0.69	2.03 \pm 0.60	1.95 \pm 0.64
	Right TP	1.97 \pm 0.56	1.94 \pm 0.64	1.78 \pm 0.65	1.94 \pm 0.66
	Central	1.93 \pm 0.55	1.93 \pm 0.64	2.09 \pm 0.52	1.96 \pm 0.68
	PO	2.22 \pm 0.68	2.09 \pm 0.98	2.28 \pm 0.83	2.42 \pm 0.78
Beta	Frontal	0.72 \pm 0.10	0.70 \pm 0.24	0.69 \pm 0.29	0.78 \pm 0.31
	Left TP	0.79 \pm 0.11	0.78 \pm 0.28	0.80 \pm 0.29	0.89 \pm 0.31
	Right TP	0.78 \pm 0.10	0.73 \pm 0.27	0.79 \pm 0.33	0.78 \pm 0.31
	Central	0.74 \pm 0.11	0.71 \pm 0.32	0.70 \pm 0.39	0.68 \pm 0.29
	PO	0.73 \pm 0.10	0.74 \pm 0.29	0.79 \pm 0.41	0.77 \pm 0.25
IAB	PO	2.53 \pm 0.71	2.47 \pm 0.86	2.67 \pm 0.94	2.46 \pm 0.81
PAF	PO	10.39 \pm 0.93	10.30 \pm 0.89	10.20 \pm 0.71	10.53 \pm 0.72

Appendix C

da Cruz, J. R., Shaqiri, A., Roinishvili, M., Chkonia, E., Brand, A., Figueiredo, P., & Herzog, M. H. (under review)

Neural compensation mechanisms of siblings of schizophrenia patients as revealed by high-density EEG

Authors: Janir Ramos da Cruz^{1,2*}, Albulena Shaqiri¹, Maya Roinishvili^{3,4}, Eka Chkonia^{4,5}, Andreas Brand¹, Patrícia Figueiredo², and Michael H. Herzog¹

Affiliations:

¹ Laboratory of Psychophysics, Brain Mind Institute, École Polytechnique Fédérale de Lausanne (EPFL), Switzerland

² Institute for Systems and Robotics – Lisbon (LARSys) and Department of Bioengineering, Instituto Superior Técnico, Universidade de Lisboa, Portugal

³ Laboratory of Vision Physiology, Beritashvili Centre of Experimental Biomedicine, Tbilisi, Georgia

⁴ Institute of Cognitive Neurosciences, Free University of Tbilisi, Tbilisi, Georgia

⁵ Department of Psychiatry, Tbilisi State Medical University, Tbilisi, Georgia

***Corresponding author:**

Janir Ramos da Cruz, Laboratory of Psychophysics, Brain Mind Institute, School of Life Sciences, École Polytechnique Fédérale de Lausanne (EPFL), CH-1015 Lausanne, Switzerland

Phone number: +41 21 693 17 42

Email: janir.amos@epfl.ch

Running title: Compensation in siblings of schizophrenics (38 characters/ max 40)

Keywords: siblings, schizophrenia, compensation, GFP, EEG, insula

Number of words in abstract: 241 (max 400)

Number of words in the main text: 4836 (max 6000)

Number of figures: 4

Number of tables: 4

Number of supplementary materials: 1

Abstract

Visual backward masking (VBM) deficits are candidate endophenotypes of schizophrenia indexing genetic liability of the disorder. In VBM, a target is followed by a masking stimulus that deteriorates target perception. Schizophrenia patients and, to a lesser extent, their unaffected relatives, show strong and reproducible VBM deficits. In patients, VBM deficits are associated with strongly decreased amplitudes in evoked-related potentials (ERPs). Here, to unveil the neural mechanisms of VBM in schizophrenia, circumventing the illness specific confounds, we investigated the EEG correlates of VBM in unaffected siblings of schizophrenia patients. 90 schizophrenia patients, 55 siblings of schizophrenia patients, and 76 healthy controls performed two VBM experiments. In experiment 1, we used an adaptive inter-stimulus interval (ISI) paradigm. In experiment 2, we fixed the ISI and measured participants' EEG while they performed the VBM task. As in previous studies, patients showed strong behavioral deficits in experiments 1 and 2 as well as decreased ERP amplitudes compared to controls. In experiment 1, as in earlier works, performance of siblings was significantly in between the ones of patients and controls. In experiment 2, surprisingly, the ERP amplitudes of the siblings, at around 200 ms after stimulus onset, were even higher than the ones of controls. At this latency, activity of the right insula predicted participants' performance. This study suggests that VBM performance is strongly deteriorated in patients and siblings. However, siblings, unlike patients, can partially compensate for the deficits by over-activating a network of brain regions.

1. Introduction

Endophenotypes are trait rather than state markers of a disease supervening on the genetic makeup (Gottesman and Gould, 2003). Several candidate endophenotypes have been proposed for schizophrenia, with the ones based on visual processing being of great interest because of their good reproducibility, language independence, and contributions to higher cognitive impairments (Braff *et al.*, 1991, 2007; Yeap *et al.*, 2006; Chkonia *et al.*, 2010; Silverstein and Keane, 2011).

Visual backward masking (VBM) is one of such candidate endophenotypes of schizophrenia (Braff and Freedman, 2002), specially the shine-through paradigm, which has a much higher sensitivity and specificity for schizophrenia than most other cognitive and perceptual paradigms (Chkonia *et al.*, 2010; Herzog and Brand, 2015). In VBM, a briefly presented target is followed by a mask, which decreases performance in discriminating the target (Breitmeyer and Öğmen, 2006). This decrement of performance is much stronger in chronic schizophrenia patients, about five times more, than in healthy controls (Herzog *et al.*, 2004). Strong impairments are also found in adolescents with psychosis (Holzer *et al.*, 2009), dismissing the argument that such VBM deficits might be primarily due to long term medication and illness duration. Unaffected first-order relatives (offspring, siblings, and parents) of schizophrenia patients also show strong VBM deficits, as expected from an endophenotype (Green *et al.*, 1997; Chkonia *et al.*, 2010; Shaqiri *et al.*, 2015). Moreover, we identified abnormalities in a single nucleotide polymorphism (SNP) related to the cholinergic nicotinic receptor ($\alpha 7$), which correlated well with performance in the shine-through paradigm (Bakanidze *et al.*, 2013).

The large behavioral deficits in chronic patients are reflected in equally large deficits in electrophysiology correlates as measured by the electroencephalogram (EEG) (Plomp *et al.*, 2013). Patients have decreased N1 amplitudes at around 200 ms after stimulus presentation, as measured

by the Global Field Power (GFP). Similar results were found with a cohort of patients with first episode psychosis (Favrod *et al.*, 2018).

However, investigating the neural mechanisms of VBM in schizophrenia patients is confounded by the use of medication, progression of the disease, and social situation. One way to bypass these confounds is to test unaffected siblings of schizophrenia patients. These siblings do not have the disease but share, on average, 50 % of their genes with their siblings with the illness (Gottesman and Gould, 2003; Meyer-Lindenberg and Weinberger, 2006), and have an empirical risk of approximately 10-fold higher to develop schizophrenia than the general population (Gottesman and Shields, 1982; Kendler and Diehl, 1993). Therefore, here we investigated the EEG correlates of the shine-through masking paradigm in unaffected siblings of schizophrenia patients. Since the VBM performance of first-order relatives of schizophrenia patients is in between the one of schizophrenia patients and healthy controls (Chkonia *et al.*, 2010), we hypothesized that ERP amplitudes of the siblings would also be in between the one of patients and controls. However, to preface our results, we found that siblings had ERP amplitudes even higher than controls, which we interpret, post-hoc, as a compensation mechanism.

2. Materials and Methods

2.1. Participants

Three groups of participants joined the experiment: schizophrenia patients (n=102), unaffected siblings of schizophrenia patients (n=56), and healthy controls (n=77). We excluded 6 patients and 1 sibling because their vernier durations were too long as well as 3 other patients because their stimulus-onset asynchronies were too long (see subsection Experiment 1 – Adaptive Procedure). Three patients and 1 control were excluded due to excessive EEG artifacts (see subsection EEG

Recording and Data Processing). Thus, data from 90 patients, 55 siblings, and 76 controls were kept for further analyses. Schizophrenia patients and their siblings were recruited from the Tbilisi Mental Health Hospital or the psycho-social rehabilitation center. Patients were invited to participate in the study when they had recovered sufficiently. Thirty-two patients were inpatients; 58 were outpatients. Diagnosis was made according to the *Diagnostic and Statistical Manual of Mental Disorders Fourth Edition* (DSM-IV) criteria, based on the SCID-CV (Structured Clinical Interview for DSM-IV, Clinician Version), information from the staff, and study of patients' records. Psychopathology of the schizophrenia patients was assessed by an experienced psychiatrist using the Scales for the Assessment of Negative Symptoms (SANS) and Scales for the Assessment of Positive Symptoms (SAPS). Seventy-two out of the 90 patients were receiving neuroleptic medication. Chlorpromazine equivalents are indicated in **Table 1**. The siblings group consisted of siblings of the schizophrenia patients without any history of psychoses. Controls were recruited from the general population and were aimed to match patients and their siblings as closely as possible.

Participants were no older than 55 years. General exclusion criteria were alcohol or drug abuse, neurological or other somatic mind-altering illnesses. Family history of psychosis was an exclusion criterion for the control group. All participants had normal or corrected to normal visual acuity of at least 0.80, as measured by the Freiburg Visual Acuity Test using both eyes (Bach, 1996). Group characteristics are presented in **Table 1**. All procedures complied with the Declaration of Helsinki and were approved by the local ethics committee.

2.2. Stimuli and Apparatus

Stimuli were displayed on a cathode ray tube screen (Siemens Fujitsu P796-1) with a refresh rate of 100 Hz and screen resolution of 1024 x 768 pixels. Participants sat at 3.5 m from the monitor

in a dim lit room. With this distance a pixel comprised about 18" (arc seconds). Stimuli were white with a luminance of 100 cd/m² (measured with a GretagMacbeth Eye-One Display 2 colorimeter) on a black background of <1 cd/m².

The vernier stimulus consisted of 2 vertical line segments of 10' (arc minutes) length separated by a gap of 1'. The lower line was slightly offset randomly either to left or to the right compared to the upper one, with a fixed offset of about 1.2'. The mask consisted of 25 aligned verniers without horizontal offset, separated by 3.33'. Participants were asked to report the perceived horizontal offset direction by pushing one of two buttons and to guess when they were uncertain. Accuracy was emphasized over speed.

2.3. Experiment 1 – Adaptive Procedure

The paradigm is described in detail in (Herzog *et al.*, 2004). In short, for each participant, we determined the vernier duration (VD) for which the threshold of vernier discrimination was below 40". Verniers were presented for 150 ms in the first block for all participants. Afterwards, we reduced the VD when thresholds for offset discrimination were below 40" or increased it if otherwise. Participants with VD longer than 100 ms were excluded (6 patients and 1 sibling). In the next step, we presented the vernier with the individual VD for each participant, followed by a blank screen during an inter-stimulus interval (ISI) and the mask with a duration of 300 ms (**Fig. 1**). We adaptively determined the target-mask stimulus-onset asynchrony (SOA=VD+ISI) such that it yields a performance level of 75% correct responses, using Parametric Estimation by Sequential Testing (PEST) (Taylor and Creelman, 1967), making the task extremely challenging. The test was performed twice by each participant. Participants with mean SOAs longer than 300 ms were excluded at this stage (3 patients).

2.4. Experiment 2 – EEG

For the EEG experiment, we had to use exactly the same stimuli for all observers in order to study group differences. To this end and to make sure that patients could do the task, we set the VD to 30 ms, which was the average VD across patients in previous works (Herzog *et al.*, 2004; Chkonia *et al.*, 2010). We had 4 stimulus conditions, see also (Plomp *et al.*, 2013; Favrod *et al.*, 2017). In the simplest condition, the Vernier Only condition, only the target vernier was presented. In a slightly more difficult condition, the Long SOA condition, the mask followed the target vernier with an SOA of 150 ms. In the hardest condition, the Short SOA condition, the target vernier was followed immediately by the mask for an SOA=30 ms. The SOAs in the Long and Short SOA conditions were selected according to the mean SOA across patients and controls, respectively, in previous works (Herzog *et al.*, 2004; Chkonia *et al.*, 2010; Plomp *et al.*, 2013; Favrod *et al.*, 2018). To ensure that our effects were due to the processing of the target, we included a control, the Mask Only condition, in which only the mask was presented. In this particular case, accuracy was calculated by comparing the left/right offset response to a randomly chosen notional offset, which was not presented. The four conditions were presented interleaved in random order in blocks of 80 trials, in which each condition appeared 20 times. Each participant performed 8 blocks, totaling 160 trials per condition. The inter-trial pause varied randomly between 1000 and 1500 ms. The vernier offset direction was chosen pseudo-randomly so that half of the trials were offset either to the left or to the right.

2.4.1. EEG Recording and Data Processing

The EEG was recorded using a BioSemi Active 2 system (Biosemi) with 64 Ag-AgCl sintered active electrodes, referenced to the common mode sense (CMS) electrode. The sampling rate was 2048 Hz. Offline data were downsampled to 512 Hz and processed using an automatic pre-

processing pipeline (APP; da Cruz *et al.*, 2018) that included the following steps: filtering via a bandpass filter of 1 – 40 Hz; removal of line-noise (CleanLine; www.nitrc.org/projects/cleanline); re-referencing to the bi-weight estimate of the average of all electrodes; removal and 3D spline interpolation of bad electrodes; removal of bad epochs; independent component analysis (ICA) to remove artifacts related to eye movements, muscle activity and bad electrodes; and removal of epoch artefacts. Data from 3 patients and 1 control were excluded from further analysis due to excessive muscular artifacts or bad electrodes. The artefact-free EEG data were then re-referenced to the common average reference. The number of interpolated electrodes was similar for each group, as revealed by one-way ANOVA ($F(2,218)=1.184$, $P=0.308$, $\eta^2=0.011$): patients (1.30 ± 0.81), siblings (1.10 ± 0.74), and controls (1.25 ± 0.77). We extracted EEG epochs from 100 ms before (baseline) to 400 ms after stimulus onset. The averaged epochs for each participant were baseline corrected. A one-way ANOVA indicated a significant main effect of Group on the amount of rejected epochs ($F(2,218)=9.493$, $P<0.001$, $\eta^2=0.080$). Post hoc tests using Bonferroni-Holm correction revealed that we rejected significantly more epochs for patients (5.32 ± 3.34) compared to siblings (3.45 ± 1.88 ; $p<0.001$) and controls (4.01 ± 2.16 ; $p=0.004$). There was no significant difference between controls and relatives ($p=0.253$).

2.4.2. GFP Analysis

Signals from two occipital electrodes (PO7 and PO8) were extracted in order to visualize the negative and positive components of the ERPs ([Supplementary Fig. 2](#)). To avoid the pitfalls of reference-dependency of ERP analysis and arbitrarily selecting an electrode or group of electrodes for subsequent analyses, we determined the GFP for each participant and each condition. The GFP is a reference-independent measure of neural activity throughout the brain and it is computed as

the standard deviation of potentials across all electrodes at a given time point (Lehmann and Skrandies, 1980).

To make sure that the stimuli consistently activated a set of brain sources for each stimulus condition and that the 3 groups were not using different networks to process the stimuli, we conducted a Topographic Consistency Test and a Topographic Segmentation Analysis (see [Supplementary Material 1.2.1. and 1.2.2.](#)). The 3 groups have similar sequences of scalp topographies for all 4 conditions, indicating that the GFP differences occur because of differences in amplitudes rather than in different neural networks.

2.4.3. Electrical Source Imaging (ESI)

To identify the brain areas generating the GFP effects, we compared the estimated current densities (CDs) at the GFP peak latencies. Source analysis was performed using Cartool software (Brunet *et al.*, 2011). From the individually averaged ERPs data, we estimated CDs throughout the brain's grey matter using a Local Auto-Regressive Average (LAURA) inverse solution (Grave de Peralta Menendez *et al.*, 2004). In the gray matter of the Montreal Neurological Institute's (MNI) 152 non-linear atlas template brain model, we evenly distributed 4022 source points and used a three-shell spherical head model to calculate the lead field after transforming the volume to a best-fitting sphere (Spherical Model with Anatomical Constraints, SMAC). The model is described in details in (Plomp *et al.*, 2009, 2010).

2.5. Statistical analysis

Since the groups differed in terms of age and education (**Table 1**), these two items were inserted as covariates in all subsequent analysis. The reported effect size statistics for the ANOVA-based methods were the Eta Square (η^2) and Cohen's *d* for the *t*-tests. Statistical analyses were performed

with JASP (<https://jasp-stats.org/>, version 0.9.0.1) and in the R programming environment (R Core Team, 2017).

2.5.1. Experiment 1 – Adaptive Procedure

The result of the first and second testing were averaged and submitted to a one-way ANCOVA. Post hoc pairwise group comparisons were corrected using Bonferroni-Holm correction.

2.5.2. Experiment 2 – Behavior

A two-way repeated measures ANOVA with Greenhouse-Geisser was conducted to compare the effect Group (patients, siblings, and controls) and Condition (Vernier Only, Long SOA, and Short SOA) on the performance. Simple main effects of Group for each condition and post hoc pairwise group comparisons for each condition were corrected using Bonferroni-Holm correction.

2.5.3. Experiment 2 – GFP

The GFP amplitudes were analyzed in two ways. First, we compared the GFP amplitudes of the individual ERPs between groups with one-way ANOVAs for each time point between 0 and 400 ms (205 consecutive time points), for each of the four conditions separately. Multiple comparisons for each time point were corrected using Bonferroni-Holm correction. Since this preliminary analysis indicated that the GFP amplitude group differences appeared around the peak latencies of the GFP for each condition, and since the peak latencies differed because the mask onset latency depended on the condition, we compared the GFP amplitudes at the peak latencies across subjects with a two-way repeated measures ANOVA, with Greenhouse-Geisser correction, of the factors Group (patients, siblings, and controls) and Condition (Vernier Only, Long SOA, Short SOA, and Mask Only). Simple main effects of Group for each condition and post hoc pairwise group comparisons for each condition were corrected using Bonferroni-Holm correction.

2.5.4. Experiment 2 – ESI

Two-way repeated measures ANOVAs with factors Group (patients, siblings, and controls) and Condition (Vernier Only, Long SOA, Short SOA, and Mask Only) were computed on the CDs for each solution point using Statistical Toolbox for Electrical Neuroimaging (STEN; <http://www.unil.ch/line/home/menuinst/about-the-line/software--analysis-tools.html>). Multiple

comparisons across solution points were corrected using Bonferroni-Holm correction. For each cluster of statistically significant solution points, the average position of its solution points, weighted according to their effect sizes, was computed for the identification of its center of mass. CD of the solution point closest to each center of mass was used to represent the corresponding brain region.

To assess the effect of the estimated CDs in each of the identified clusters on the behavioral performance, the CDs of the centers of mass were used as predictors of the dependent variable accuracy, in separate multiple linear regressions for each of the 3 conditions containing the target vernier. Due to high multicollinearity, i.e., the predictors were correlated with each other, we used the best subsets regression analysis with the *leaps* R package (Lumley, 2017) with the Bayesian Information Criterion (BIC) model selection criterion to remove correlated factors.

2.6. Data availability

The data that support the findings of this study are available upon reasonable request.

3. Results

3.1. Experiment 1 – Adaptive Procedure

First, we replicated previous findings (Chkonia *et al.*, 2010), where the mean SOA of the siblings ($53.62 \text{ ms} \pm 47.04$) was in between the one of patients ($103.25 \text{ ms} \pm 58.89$) and controls ($35.96 \text{ ms} \pm 24.21$; **Fig. 2A**). A one-way ANCOVA, yielded a significant effect of Group ($F(2,216)=52.447$, $P<0.001$, $\eta^2=0.318$). Post hoc tests indicated significant pairwise differences between all groups: patients vs siblings ($t(143)=6.979$, $p<0.001$, $d=1.035$), patients vs controls ($t(164)=9.871$, $p<0.001$, $d=1.603$), and siblings vs controls ($t(129)=2.173$, $p=0.031$, $d=0.497$).

3.2. Experiment 2 – EEG

3.2.1. Behavior

Performance of the patients was inferior in the 3 conditions that contained the target vernier, while siblings and controls achieved similar performances (**Fig. 2B** and [Supplementary Table 1](#)). As mentioned before, unlike in experiment 1, where we explored the individual differences with an adaptive procedure (PEST), in the EEG experiment, we had the same stimuli for all participants and fixed the VD as the mean VD across patients. Likely for these reasons, the task was not challenging enough to bring out the group differences between siblings and controls. A two-way repeated measures ANOVA showed significant effects of Group ($F(2,216)=44.341$, $P<0.001$, $\eta^2=0.286$), Condition ($F(1,326,286.340)=20.993$, $P<0.001$, $\eta^2=0.072$) and a significant interaction effect ($F(2,651,286.340)=22.883$, $P<0.001$, $\eta^2=0.158$). The interaction indicates that Group differences depend on stimulus condition. Simple main effects of Group yielded significant effects of Group for all conditions: Vernier Only ($F(2,216)=23.809$, $P<0.001$, $\eta^2=0.180$), Long SOA ($F(2,216)=32.587$, $P<0.001$, $\eta^2=0.229$), and Short SOA ($F(2,216)=42.389$, $P<0.001$, $\eta^2=0.275$). Post hoc pairwise group comparisons for each Condition are shown in [Supplementary Table 2](#).

The SOAs in experiment 1 correlated with the performance in experiment 2, for each condition containing the target vernier ([Supplementary Table 3](#)). Participants with shorter SOAs were more accurate at discriminating the vernier offset in experiment 2.

3.2.2. GFP

The GFP time course for patients, siblings, and controls in the 4 stimulus conditions are shown in **Fig. 3A**. We found a significant main effect of group around 200 ms for all conditions containing the target vernier. A two-way repeated measures ANOVA of the peak GFP amplitudes showed

statistically significant main effects of Group ($F(2,216)=22.899$, $P<0.001$, $\eta^2=0.172$), Condition
 ($F(2,129,459.967)=11.445$, $P<0.001$, $\eta^2=0.043$), and a significant interaction
 ($F(4,259,459.967)=18.900$, $P<0.001$, $\eta^2=0.141$). This interaction is shown in **Fig. 3B** (see
[Supplementary Table 4](#) for summary statistics). Simple main effects of Group yielded significant
 effects of Group for the Vernier Only ($F(2,216)=27.091$, $P<0.001$, $\eta^2=0.197$), the Long SOA
 ($F(2,216)=28.303$, $P<0.001$, $\eta^2=0.205$), and the Short SOA ($F(2,216)=21.299$, $P<0.001$,
 $\eta^2=0.161$) conditions. No significant effect of Group for Mask Only condition was found
 ($F(2,216)=2.404$, $P=0.093$, $\eta^2=0.022$). Post-hoc pairwise comparisons between groups using
 Bonferroni-Holm correction were performed for each of the 3 simple main effects of Group that
 were significant (**Table 2**). In sum, the GFP peak amplitudes of patients were lower than those of
 controls and siblings, for all conditions with the target vernier. Interestingly, GFP peak amplitudes
 were higher in siblings compared to controls for the Vernier Only and Long SOA conditions. For
 siblings, GFP peak amplitudes were roughly at the same level in all the 3 conditions with the
 vernier target (one-way repeated measures ANOVA with Greenhouse-Geisser correction;
 $F(1.390,75.051)=1.842$, $P=0.176$, $\eta^2=0.033$). For controls and patients, GFP peak amplitudes
 increased with task difficulty, i.e., from Vernier Only to Long SOA and to Short SOA conditions
 (one-way repeated measures ANOVA with Greenhouse-Geisser correction; for controls:
 $F(1.364,102.303)=19.352$, $P<0.001$, $\eta^2=0.205$; for patients: $F(1.367,121.659)=11.871$, $P<0.001$,
 $\eta^2=0.118$). For post-hoc pairwise Condition comparisons for controls and patients, see
[Supplementary Table 5](#).

GFP amplitudes at the peak latencies correlated positively with the behavioral performance,
 when considering all participants ([Supplementary Table 6](#)). This was also the case for the siblings.

For patients and controls, while the individual groups' correlations were not statistically significant, they showed similar trends to the results considering all the participants.

3.2.3. ESI

Fig. 4 shows the six EEG source clusters exhibiting statistically significant Group x Condition interaction effects after Bonferroni-Holm correction for multiple comparisons, as well as the corresponding average CD in each group. The clusters were located bilaterally in the middle temporal gyrus and insula, as well as in the left precentral gyrus and the right precuneus. **Table 3** lists the Tailarach coordinates of the center of mass for these clusters and corresponding statistical results.

The results of the multiple linear regressions to predict the accuracy based on the estimated CDs of the center of mass of the 6 EEG source clusters are presented in **Table 4**. For the Vernier Only condition, activity of the right insula predicted accuracy. For the Long SOA condition, activity of the right insula as well as the left precentral gyrus predicted accuracy. Finally, for the Short SOA condition, again, activity of the right insula predicted accuracy. Similar results were found considering the 3 groups separately (see [Supplementary Table 10](#)).

Further analysis of the activity of the right insula, showed that, in siblings, as for the GFP peak amplitudes, the right insula activity was at the same level in all the 3 conditions with the vernier target (one-way repeated measures ANOVA with Greenhouse-Geisser correction; $F(1.633, 88.158)=3.024$, $P=0.064$, $\eta^2=0.053$). In contrast, for controls and patients, the right insula activity increased with task difficulty, i.e., from Vernier Only to Long SOA and Short SOA (one-way repeated measures ANOVA with Greenhouse-Geisser correction; for controls: $F(1.748, 131.114)=24.421$, $P<0.001$, $\eta^2=0.246$; for patients: $F(1.602, 142.540)=7.909$, $P=0.001$,

$\eta^2=0.082$). Lastly, the activity of the right insula correlated strongly with the GFP peak amplitudes, for each of the 4 conditions ([Supplementary Table 11](#)).

4. Discussion

VBM deficits are candidate endophenotypes for schizophrenia (Chkonia *et al.*, 2010). Importantly, not only patients show strong VBM deficits but also their unaffected first-order relatives (Green *et al.*, 1997). More specifically, performance of relatives is in between the ones of patients and healthy controls (Chkonia *et al.*, 2010), a result that we reproduced in our experiment 1.

In patients, the large behavioral deficits are associated with large decreased ERP amplitudes at around 200 ms after stimulus presentation (Plomp *et al.*, 2013). However, studying the neural mechanisms of VBM in patients is problematic due to confounding factors such as medication and secondary effects of the disease. To circumvent these confounds, here we tested 55 unaffected siblings of schizophrenia patients. These siblings do not have the disease but they share around 50% of their genes with their relatives with schizophrenia. We hypothesized that, since the behavioral performance of relatives is in between the ones of patients and controls, their ERP amplitudes would also be in between the ones of patients and controls. Surprisingly, we found that, on the contrary, ERP amplitudes in siblings were even higher than in controls. Interestingly, in siblings, these amplitudes remained almost constant across the 3 VBM conditions with the target vernier. In contrast, for patients and controls, the ERP amplitudes increased with task difficulty, i.e., from Vernier Only to Long and Short SOA.

We interpret these results as a compensation signal. To process the target vernier, whose neural correlates are indexed by the ERP component at around 200 ms (Herzog *et al.*, 2013), siblings

might need to engage relevant available neural resources in all the conditions, independently of task difficulty. Indeed, the fact that ERP amplitudes in siblings remained stable across the 3 conditions with the target suggests that their ERP amplitudes were at ceiling. ERP amplitudes around 200 ms have been shown to be susceptible to task difficulty (Philiastides *et al.*, 2006) and to engagement of attention (Eason *et al.*, 1969; Luck *et al.*, 2000). All the effects observed were specific to the target vernier and did not occur when only the mask was presented, suggesting that top-down processes are responsible for these effects. Since the conditions were randomized, differences in attention are not expected.

The lack of behavioral differences between siblings and controls in the EEG experiment, experiment 2, suggests that, by over-enhancing the neural responses to the target, siblings can partially compensate for their VBM deficits, if the task is not challenging enough. Nevertheless, if the visual system is pushed to its limits, as in experiment 1, this compensation mechanism is not sufficient for normal performance.

Evidence for some sort of compensation mechanism in relatives of schizophrenia patients was presented earlier by (Waldo *et al.*, 1988). Waldo and colleagues found that, as in patients, about half of relatives failed to suppress the P50 ERP component to the second click in a paired-click auditory experiment (sensory gating). More interestingly, the relatives with deficient sensory gating were found to have higher N100 amplitudes than the ones of healthy controls, suggesting that relatives can compensate for their early deficits at later information processing stages.

Both P50 sensory gating and VBM deficits in schizophrenia patients have been shown to be genetically linked to the $\alpha 7$ nicotinic receptor of the cholinergic system (Potter *et al.*, 2006; Martin and Freedman, 2007; Bakanidze *et al.*, 2013). Studies with nicotine agonists were found to improve sensory gating in patients and their relatives (Adler *et al.*, 1992, 1993; Zhang *et al.*, 2012).

Moreover, chronic nicotine consumption has a beneficial effect on VBM performance, especially with increasing age (Shaqiri *et al.*, 2015). Hence, the P50 sensory gating and VBM deficits might not be caused by auditory or visual deficits *per se* but by a more general deficit related, at least partially, to abnormalities in the cholinergic system (Herzog *et al.*, 2013).

Our electrical source imaging analysis indicated 6 brain regions where the 3 groups process the stimuli differently: left and right middle temporal gyrus, left and right insula, left precentral gyrus, and right precuneus. These results are similar to the ones reported by (Plomp *et al.*, 2013), who identified 7 regions where patients processed the stimuli differently from controls: left middle occipital gyrus, right middle temporal gyrus, left and right insula, left postcentral gyrus, and left and right precuneus. We attribute the small discrepancies between our studies to the intrinsically low spatial resolution of EEG source localization.

Among the 6 brain regions that we identified, one of special interest is the right insula. Our multiple regression analysis indicated that the activity of the right insula best predicted the behavioral differences. Furthermore, the activity of the right insula mimicked the ERP results: patients had decreased activations in all the conditions with the target, while siblings had higher activations than controls in the Vernier Only and Long SOA conditions. The insula is associated with several functions. One of special interest is the high-level integration of information from different modalities and brain areas (Craig, 2009). More specifically, it has been proposed that the right insula regulates the interaction between selective attention and arousal to keep focused on the target (Eckert *et al.*, 2009). Too little activity of the right insula, as in patients, would probably lead to an impairment in collecting evidence for decision making. Too much activity of the right insula, as in siblings, might indicate that participants need to engage more to achieve a good performance in this challenging task.

Dysregulation of the insular cortex is frequently reported in schizophrenia studies, see (Wylie and Tregellas, 2010) for a review. Interestingly, the insula seems to be susceptible to modulations by the cholinergic system through nicotine in patients. In prepulse inhibition of the startle response (PPI), a reduction in startle occurs when a startling stimulus is preceded by a weak stimulus (Graham, 1975). The PPI is deficient in schizophrenia patients and their relatives (Braff *et al.*, 1978; Cadenhead *et al.*, 2000). Interestingly, PPI responses improve in patients with direct subcutaneous nicotine treatment and this improvement is accompanied by increasing responses of the right insula (Postma *et al.*, 2006). Therefore, increased activations of the right insula might have positive effects in tasks related to the cholinergic system, such as VBM.

Here, we propose the following theory. When the target vernier is presented, strong ERP amplitudes are elicited at around 200 ms, after stimulus onset. Since the target is presented for a very short time (30 ms), only a weak neural response is elicited and target enhancement is needed to prevent overwriting by subsequently presented stimuli. We hypothesize that nicotinic cholinergic activation is one candidate of target enhancement, which might be deficient in schizophrenia patients (Bakanidze *et al.*, 2013; Herzog *et al.*, 2013). In patients, amplitudes are low in all 3 conditions with the target vernier, including the Vernier Only condition. This suggests that patients cannot translate the briefly presented target into stable neural representations, making the target more vulnerable to masking (Green *et al.*, 2011). These deficits are also present in the unaffected relatives, indicating that VBM is a trait marker for schizophrenia (endophenotype). We speculate that, to overcome these deficits, the siblings engage more or try harder. Their increased ERP amplitudes compared to controls support the hypothesis of a compensation mechanism, such that by increasing the activity of a network of brain regions, siblings, unlike patients, can successfully compensate for their behavior deficits. In this network, the right insula, with its

extensive connections to many areas of the cortex, might play a key role by integrating high-level sensory as well as perceptual information and subsequent decision making. Nonetheless, by pushing the visual system to its limits, this compensation mechanism is too weak to fully compensate for the deficits.

Our results suggest that even if there are genetic risks for schizophrenia, the brain is somehow capable of compensating for them. Better understanding of these compensation mechanisms might help to explain why some siblings develop schizophrenia and while others do not, which might open new avenues for characterization of schizophrenia and possible treatments of the disorder.

Funding

This work was partially funded by the Fundação para a Ciência e a Tecnologia under grant FCT PD/BD/105785/2014 and the National Centre of Competence in Research (NCCR) Synapsy (The Synaptic Basis of Mental Diseases) under grant 51NF40-158776.

Competing interests

The authors report no biomedical financial interests or potential conflicts of interest.

References

Adler LE, Hoffer LD, Wiser A, Freedman R. Normalization of auditory physiology by cigarette smoking in schizophrenic patients. *Am J Psychiatry* 1993; 150: 1856–1861.

Adler LE, Hoffer LJ, Griffith J, Waldo MC, Freedman R. Normalization by nicotine of deficient auditory sensory gating in the relatives of schizophrenics. *Biological Psychiatry* 1992; 32: 607–616.

Bach M. The Freiburg Visual Acuity test--automatic measurement of visual acuity. *Optom Vis Sci* 1996; 73: 49–53.

Bakanidze G, Roinishvili M, Chkonia E, Kitzrow W, Richter S, Neumann K, et al. Association of the nicotinic receptor $\alpha 7$ subunit gene (CHRNA7) with schizophrenia and visual backward masking. *Front. Psychiatry* 2013; 4: 133.

Braff D, Stone C, Callaway E, Geyer M, Glick I, Bali L. Prestimulus Effects on Human Startle Reflex in Normals and Schizophrenics. *Psychophysiology* 1978; 15: 339–343.

Braff DL, Freedman R. Endophenotypes in studies of the genetics of schizophrenia. In: Davis K, Charney D, Coyle J, Nemeroff C, editor(s). *Neuropsychopharmacology: The Fifth Generation of Progress*. Philadelphia, PA: Lippincott, Williams & Wilkins; 2002. p. 703–716.

Braff DL, Freedman R, Schork NJ, Gottesman II. Deconstructing Schizophrenia: An Overview of the Use of Endophenotypes in Order to Understand a Complex Disorder. *Schizophr Bull* 2007; 33: 21–32.

Braff DL, Saccuzzo DP, Geyer MA. Information processing dysfunctions in schizophrenia: Studies of visual backward masking, sensorimotor gating, and habituation. In: *Handbook of schizophrenia*. New York, NY, US: Elsevier Science; 1991. p. 303–334.

Breitmeyer B, Öğmen H. *Visual Masking: Time Slices Through Conscious and Unconscious Vision*. OUP Oxford; 2006.

Brunet D, Murray MM, Michel CM. Spatiotemporal Analysis of Multichannel EEG: CARTOOL. *Intell. Neuroscience* 2011; 2011: 2:1–2:15.

Cadenhead KS, Swerdlow NR, Shafer KM, Diaz M, Braff DL. Modulation of the Startle Response and Startle Laterality in Relatives of Schizophrenic Patients and in Subjects With Schizotypal Personality Disorder: Evidence of Inhibitory Deficits. *AJP* 2000; 157: 1660–1668.

Chkonia E, Roinishvili M, Makhatadze N, Tsverava L, Stroux A, Neumann K, et al. The Shine-Through Masking Paradigm Is a Potential Endophenotype of Schizophrenia. *PLoS ONE* 2010; 5: e14268.

Craig AD (Bud). How do you feel — now? The anterior insula and human awareness. *Nature Reviews Neuroscience* 2009; 10: 59–70.

da Cruz JR, Chicherov V, Herzog MH, Figueiredo P. An automatic pre-processing pipeline for EEG analysis (APP) based on robust statistics. *Clinical Neurophysiology* 2018; 129: 1427–1437.

Eason RG, Harter MR, White CT. Effects of attention and arousal on visually evoked cortical potentials and reaction time in man. *Physiology & Behavior* 1969; 4: 283–289.

Eckert MA, Menon V, Walczak A, Ahlstrom J, Denslow S, Horwitz A, et al. At the heart of the ventral attention system: The right anterior insula. *Human Brain Mapping* 2009; 30: 2530–2541.

Favrod O, Roinishvili M, da Cruz JR, Brand A, Okruashvili M, Gamkrelidze T, et al. Electrophysiological correlates of visual backward masking in patients with first episode psychosis. *Psychiatry Research: Neuroimaging* 2018; 282: 64–72.

Favrod O, Sierro G, Roinishvili M, Chkonia E, Mohr C, Herzog MH, et al. Electrophysiological correlates of visual backward masking in high schizotypic personality traits participants. *Psychiatry Research* 2017; 254: 251–257.

Gottesman II, Gould TD. The Endophenotype Concept in Psychiatry: Etymology and Strategic Intentions. *AJP* 2003; 160: 636–645.

Gottesman II, Shields J. The Epigenetic Puzzle. In: *Schizophrenia, the epigenetic puzzle*. Cambridge ; New York: Cambridge University Press; 1982.

Graham FK. The More or Less Startling Effects of Weak Prestimulation. *Psychophysiology* 1975; 12: 238–248.

Grave de Peralta Menendez R, Murray MM, Michel CM, Martuzzi R, Gonzalez Andino SL. Electrical neuroimaging based on biophysical constraints. *NeuroImage* 2004; 21: 527–539.

Green MF, Lee J, Wynn JK, Mathis KI. Visual Masking in Schizophrenia: Overview and Theoretical Implications. *Schizophr Bull* 2011; 37: 700–708.

Green MF, Nuechterlein KH, Breitmeyer B. Backward Masking Performance in Unaffected Siblings of Schizophrenic Patients: Evidence for a Vulnerability Indicator. *Arch Gen Psychiatry* 1997; 54: 465–472.

Herzog MH, Brand A. Visual masking & schizophrenia. *Schizophrenia Research: Cognition* 2015; 2: 64–71.

Herzog MH, Kopmann S, Brand A. Intact figure-ground segmentation in schizophrenia. *Psychiatry Research* 2004; 129: 55–63.

Herzog MH, Roinishvili M, Chkonia E, Brand A. Schizophrenia and visual backward masking: a general deficit of target enhancement [Internet]. *Front. Psychol.* 2013; 4[cited 2018 Jan 13] Available from: <https://www.frontiersin.org/articles/10.3389/fpsyg.2013.00254/full>

Holzer L, Jaugey L, Chinet L, Herzog MH. Deteriorated visual backward masking in the shine-through effect in adolescents with psychosis. *Journal of Clinical and Experimental Neuropsychology* 2009; 31: 641–647.

Kendler KS, Diehl SR. The Genetics of Schizophrenia: A Current, Genetic-epidemiologic Perspective. *Schizophr Bull* 1993; 19: 261–285.

Lehmann D, Skrandies W. Reference-free identification of components of checkerboard-evoked multichannel potential fields. *Electroencephalography and Clinical Neurophysiology* 1980; 48: 609–621.

Luck SJ, Woodman GF, Vogel EK. Event-related potential studies of attention. *Trends in Cognitive Sciences* 2000; 4: 432–440.

Lumley T. leaps: Regression Subset Selection [Internet]. 2017. Available from: <https://cran.r-project.org/web/packages/leaps/leaps.pdf>

Martin LF, Freedman R. Schizophrenia and the $\alpha 7$ Nicotinic Acetylcholine Receptor. In: *International Review of Neurobiology*. Academic Press; 2007. p. 225–246.

Meyer-Lindenberg A, Weinberger DR. Intermediate phenotypes and genetic mechanisms of psychiatric disorders. *Nature Reviews Neuroscience* 2006; 7: 818–827.

Philiastides MG, Ratcliff R, Sajda P. Neural Representation of Task Difficulty and Decision Making during Perceptual Categorization: A Timing Diagram. *J. Neurosci.* 2006; 26: 8965–8975.

Plomp G, Mercier MR, Otto TU, Blanke O, Herzog MH. Non-retinotopic feature integration decreases response-locked brain activity as revealed by electrical neuroimaging. *NeuroImage* 2009; 48: 405–414.

Plomp G, Michel CM, Herzog MH. Electrical source dynamics in three functional localizer paradigms. *NeuroImage* 2010; 53: 257–267.

Plomp G, Roinishvili M, Chkonia E, Kapanadze G, Kereselidze M, Brand A, et al. Electrophysiological Evidence for Ventral Stream Deficits in Schizophrenia Patients. *Schizophr Bull* 2013; 39: 547–554.

Postma P, Gray JA, Sharma T, Geyer M, Mehrotra R, Das M, et al. A behavioural and functional neuroimaging investigation into the effects of nicotine on sensorimotor gating in healthy subjects and persons with schizophrenia. *Psychopharmacology* 2006; 184: 589–599.

Potter D, Summerfelt A, Gold J, Buchanan RW. Review of Clinical Correlates of P50 Sensory Gating Abnormalities in Patients with Schizophrenia. *Schizophr Bull* 2006; 32: 692–700.

R Core Team. R: A Language and Environment for Statistical Computing [Internet]. Vienna, Austria: R Foundation for Statistical Computing; 2017. Available from: <https://www.r-project.org/>

Shaqiri A, Willemin J, Sierro G, Roinishvili M, Iannantuoni L, Rürup L, et al. Does chronic nicotine consumption influence visual backward masking in schizophrenia and schizotypy? *Schizophrenia Research: Cognition* 2015; 2: 93–99.

Silverstein SM, Keane BP. Vision Science and Schizophrenia Research: Toward a Re-view of the Disorder Editors' Introduction to Special Section. *Schizophr Bull* 2011; 37: 681–689.

Taylor MM, Creelman CD. PEST: Efficient Estimates on Probability Functions. *The Journal of the Acoustical Society of America* 1967; 41: 782–787.

Waldo MC, Adler LE, Freedman R. Defects in auditory sensory gating and their apparent compensation in relatives of schizophrenics. *Schizophrenia Research* 1988; 1: 19–24.

Wylie KP, Tregellas JR. The role of the insula in schizophrenia. *Schizophrenia Research* 2010; 123: 93–104.

Yeap S, Kelly SP, Sehatpour P, Magno E, Javitt DC, Garavan H, et al. Early Visual Sensory Deficits as Endophenotypes for Schizophrenia: High-Density Electrical Mapping in Clinically Unaffected First-Degree Relatives. *Arch Gen Psychiatry* 2006; 63: 1180–1188.

Zhang XY, Liu L, Liu S, Hong X, Chen DC, Xiu MH, et al. Short-Term Tropisetron Treatment and Cognitive and P50 Auditory Gating Deficits in Schizophrenia. *AJP* 2012; 169: 974–981.

Table Legends

Table 1 – Group average Statistics (\pm SD) of Schizophrenia Patients, their Unaffected Siblings and Healthy Controls.

Table 2 – Post hoc Group comparisons of GFP amplitudes at the peak latencies, using Bonferroni-Holm correction, for each stimulus condition that yielded a significant main effect of Group (Vernier Only, Long SOA and Short SOA).

Table 3 – Locations (Tailarach Coordinates) of the center of mass of EEG source clusters exhibiting significant interaction effects between Group and Condition, and their corresponding statistics (df 1 and df 2 are the degrees of freedom, Greenhouse-Geisser corrected).

Table 4 – Summary of the best subsets regression analysis for the activity of the center of mass of EEG source clusters predicting the behavioral performance in each of the 3 conditions containing the target vernier.

Figure Legends

Fig. 1 – VBM procedure. In experiment 1 (Adaptive Procedure), for each participant, we determined the vernier duration (VD), for which the vernier discrimination threshold was below 40". Then, for each observer, we used his/hers individual VD and presented a blank screen (ISI) and a mask comprised of 25 aligned verniers. We determined the stimulus-onset asynchrony (SOA=VD+ISI), for which 75% correct responses were reached, using the Parametric Estimation by Sequential Testing (PEST). In experiment 2 (EEG), we fixed the VD (30 ms) and we had 4 stimulus conditions: Vernier Only (only the vernier was presented), Long SOA (the mask followed the vernier with an SOA of 150 ms), Short SOA (the mask followed the vernier with an SOA of 30 ms), and Mask Only (only the mask was presented).

Fig. 2 – Behavioral Results. A) Experiment 1. Mean SOA (stimulus onset asynchrony) for each group. Performance of siblings was significantly in between controls and patients. B) Experiment 2. Mean accuracy for each group for the 4 conditions. Patients were less accurate at discriminating the vernier offset compared to both siblings and controls. This difference in performance increased

with task difficulty (Vernier Only < Long SOA < Short SOA). Siblings and controls performed at the same level. Error bars indicate standard error of the mean.

Fig. 3 – A) Group average Global Field Power (GFP) time series for patients, siblings, and controls, in the 4 stimulus conditions. GFP amplitudes were significantly different for the 3 groups at around 200 ms after stimulus onset (Bonferroni-Holm corrected) for all the conditions containing the target vernier (grey region). B) Group average GFP amplitudes at the peak latencies for all groups and conditions. Patients have decreased GFP peak amplitudes in all conditions with the target vernier. Siblings have higher amplitudes than controls in the Vernier Only and Long SOA conditions. For patients and controls, GFP amplitudes are lower for the Long SOA than the Short SOA condition. For the siblings, the GFP amplitudes remained on a high level. Error bars indicate standard error of the mean.

Fig. 4 – Source imaging results. A) Clusters of significant Group X Condition effects are indicated in red ($p < 0.05$, Bonferroni-Holm corrected). B) Average current density (CD) at the centers of mass for the 6 clusters, indicating the direction of the interaction effects. In general, group differences are larger in the three conditions with the target vernier compared with the Mask Only condition. Group mean CDs for each condition of the six EEG source clusters exhibiting significant Group x Condition interaction effects are shown in [Supplementary Table 8](#).

562 **Tables**

563 Table 1

564

	Patients	Siblings	Controls	Statistics	Post-hoc (<i>p</i> -values)		
					Patients vs Siblings	Patients vs Controls	Relatives vs Controls
Gender (F/M)	15/75	26/29	34/42	$\chi^2(2)=20.290, P<0.001$	<0.001	<0.001	0.774
Age	35.8±8.8	32.7±9.4	34.9±8.1	$F(2,218)=2.662, P=0.144$			
Education	13.2±2.7	14.3±2.9	15.0±2.8	$F(2,218)=8.148, P=0.002$	0.076	<0.001	0.133
Handedness (R/L)	86/4	52/3	71/5	$\chi^2(2)=0.366, P=0.833$			
Visual acuity	1.4±0.4	1.5±0.4	1.6±0.4	$F(2,218)=4.383, P=0.084$			
Vernier duration*	30 [20, 40]	20 [20, 20]	20 [20, 20]	$\chi^2(2)=26.910, P<0.001$	0.015	<0.001	0.190
Illness duration	11.3±8.0						
SANS	10.7±5.3						
SAPS	10.0±8.1						
CPZ equivalent	549.3±398.5						

Abbreviations: SANS, Scale for the Assessment of Negative Symptoms; SAPS, Scale for the Assessment of Positive Symptoms; CPZ, Chlorpromazine; CPT, Continuous Performance Task; WCST, Wisconsin Card Sorting Test

*Median [25th percentile, 75th percentile]

Table 2

Condition	Group I	Group II	<i>t</i> -value	df	<i>p</i> -value	<i>d</i>
Vernier Only	Patients	Siblings	-7.489	143	<0.001	1.252
		Controls	-5.619	164	<0.001	0.878
	Siblings	Controls	2.296	129	0.023	0.404
Long SOA	Patients	Siblings	-7.586	143	<0.001	1.268
		Controls	-5.914	164	<0.001	0.924
	Siblings	Controls	2.129	129	0.034	0.375
Short SOA	Patients	Siblings	-6.236	143	<0.001	1.043
		Controls	-5.966	164	<0.001	0.932
	Siblings	Controls	0.778	129	0.437	0.137

Table 3

Label	Coordinates (x,y,z)	<i>F</i> -value	df 1	df 2	<i>p</i> -value	η^2
Left Middle Temporal Gyrus	-43, -62, 12	20.556	4.380	473.026	<0.001	0.153
Left Insula	-34, -6, 14	12.290	5.349	577.682	<0.001	0.101
Left Precentral Gyrus	-27, -21, 56	6.484	5.798	626.186	0.002	0.055
Right Middle Temporal Gyrus	42, -61, 11	23.766	4.353	470.176	<0.001	0.171
Right Insula	36, -27, 21	8.216	4.795	517.820	<0.001	0.066
Right Precuneus	9, -64, 23	15.812	5.085	549.170	<0.001	0.124

Table 4

Condition	Region	β	SE	<i>t</i> -value	df	<i>p</i> -value
Vernier Only	Right Insula	25.982	5.997	4.333	219	<0.001
Long SOA	Right Insula	25.979	9.617	2.701	219	0.007
	Left Precentral Gyrus	3.025	1.172	2.581	219	0.011
Short SOA	Right Insula	59.876	14.445	4.145	219	<0.001

Figures

Figure 1

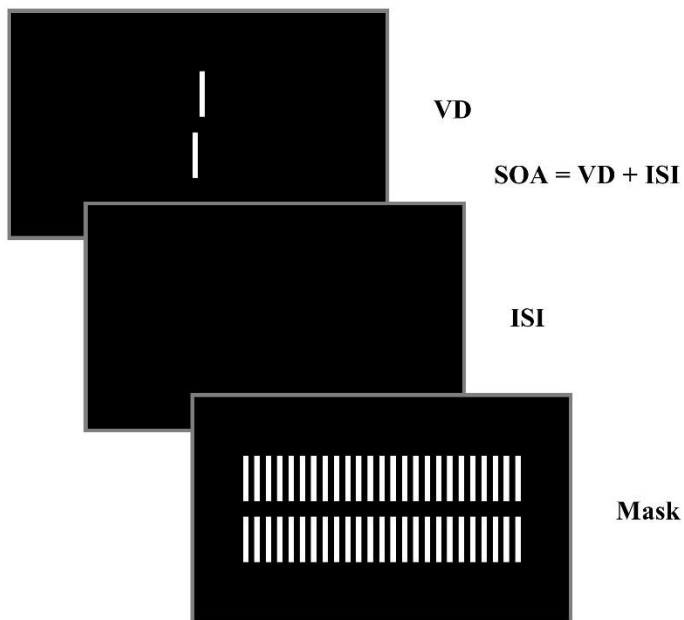
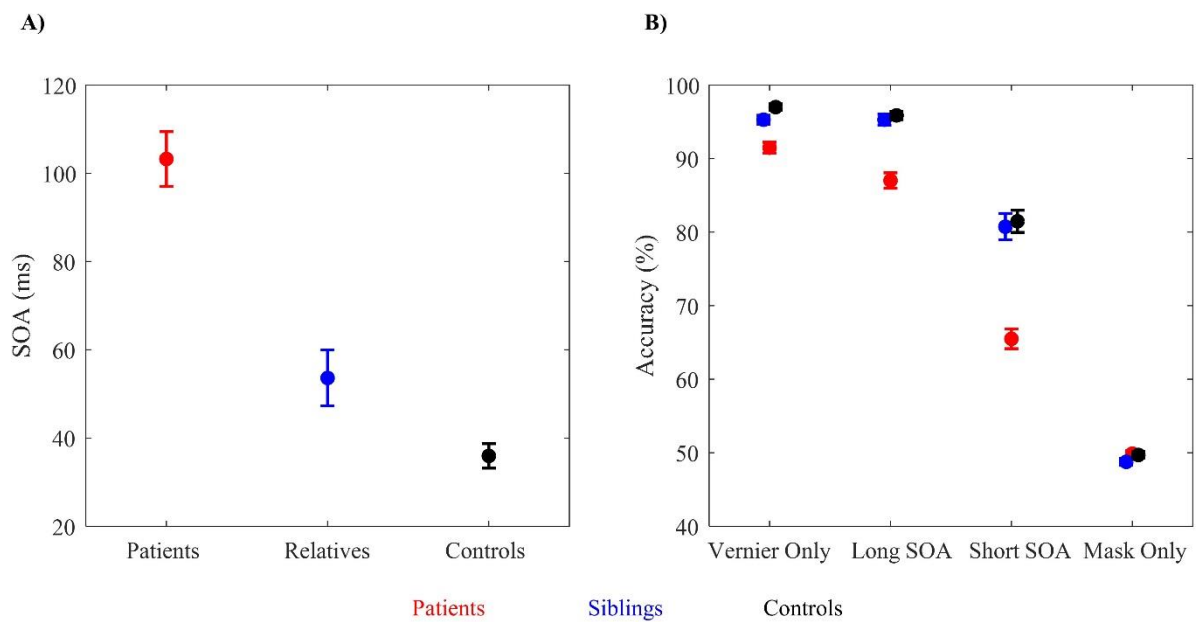
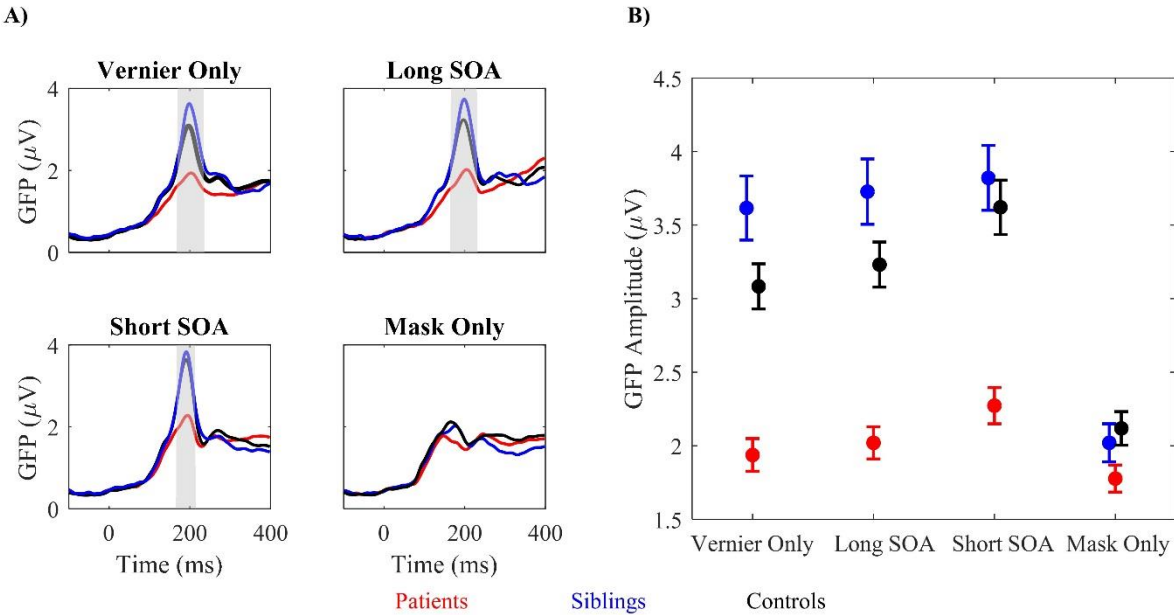
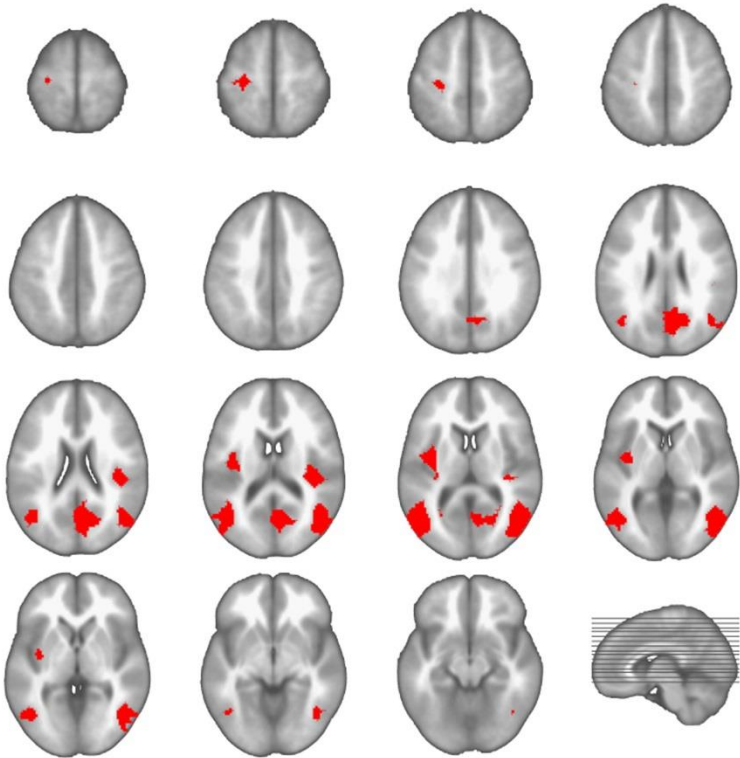


Figure 2

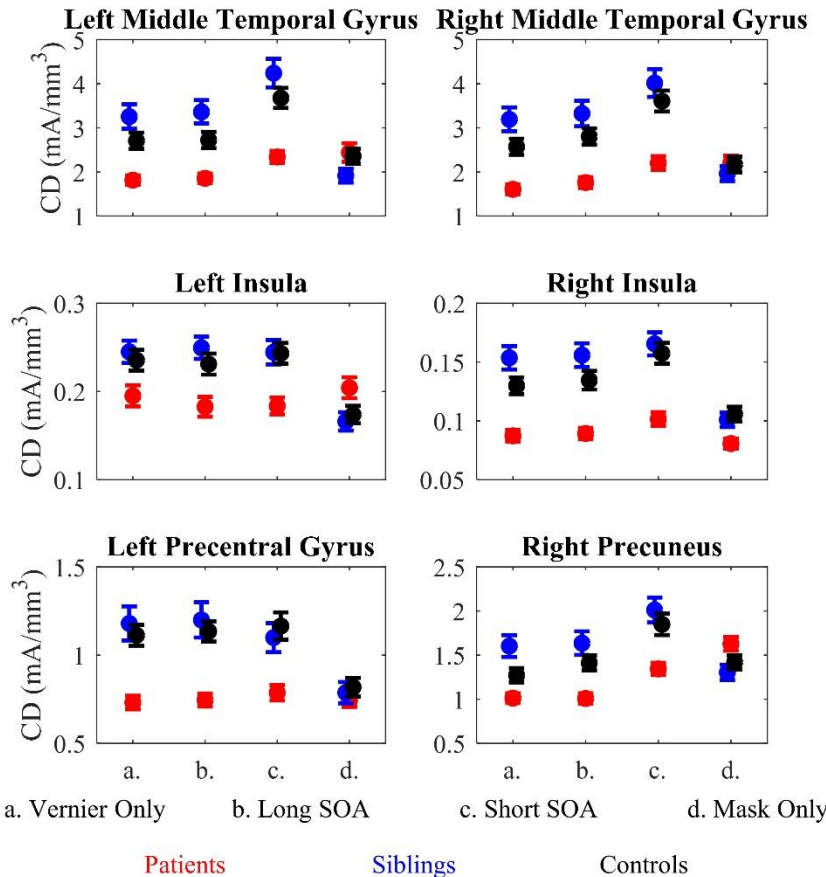




A)



B)



Supplementary Material for

Neural compensation mechanisms of siblings of schizophrenia patients as revealed by high-density EEG

Authors: Janir Ramos da Cruz^{1,2*}, Albulena Shaqiri¹, Maya Roinishvili^{3,4}, Eka Chkonia^{4,5}, Andreas Brand¹, Patrícia Figueiredo², and Michael H. Herzog¹

Affiliations:

¹ Laboratory of Psychophysics, Brain Mind Institute, École Polytechnique Fédérale de Lausanne (EPFL), Switzerland

² Institute for Systems and Robotics – Lisbon (LARSys) and Department of Bioengineering, Instituto Superior Técnico, Universidade de Lisboa, Portugal

³ Laboratory of Vision Physiology, Beritashvili Centre of Experimental Biomedicine, Tbilisi, Georgia

⁴ Institute of Cognitive Neurosciences, Free University of Tbilisi, Tbilisi, Georgia

⁵ Department of Psychiatry, Tbilisi State Medical University, Tbilisi, Georgia

***Corresponding author:**

Janir Ramos da Cruz, Laboratory of Psychophysics, Brain Mind Institute, School of Life Sciences, École Polytechnique Fédérale de Lausanne (EPFL), CH-1015 Lausanne, Switzerland

Phone number: +41 21 693 17 42

Email: janir.amos@epfl.ch

Number of supplementary figures: 4

Number of supplementary tables: 11

Table of Contents

1.	Methods and Materials.....	3
1.1.	Experiment 1 – Adaptive Procedure.....	3
1.2.	Experiment 2 – EEG.....	3
1.2.1.	Topographic Consistency Test.....	3
1.2.2.	Topographic Segmentation Analysis	3
2.	Results.....	5
2.1.	Experiment 1	5
2.2.	Experiment 2	5
2.2.1.	Behavior.....	5
2.2.2.	Topographic Consistency	7
2.2.3.	Topographic Segmentation	8
2.2.4.	GFP	12
2.2.5.	Distributed Electrical Source Imaging.....	16
	References.....	20

1. Materials and Methods

1.1. Experiment 1 – Adaptive Procedure

To assess the test-retest reliability of the paradigm, we computed the Pearson product-moment correlation between the first and the second testing.

1.2. Experiment 2 – EEG

1.2.1. Topographic Consistency Test

An analysis of topographic consistency was conducted to ensure that the EEG was analysed in time periods where there is evidence that the stimulus event consistently activates a set of brain electric sources across within each group of participants for each stimulus condition (1). This test compares the Global Field Power (GFP) of the measured event-related potential (ERP) with the null hypothesis, using randomization techniques. In order to obtain the null distribution of the ERP at each time point, for every participant of an experimental group and condition, the channels are shuffled; in this study we generated 5000 shuffles/randomizations. Subsequently, the group mean of the GFP is calculated for each randomization and compared with the measured GFP. The result of the topographic consistency test shows time periods during which the measured scalp field cannot be explained by the null distribution. The topographic consistency test was performed using the RAGU software (2).

1.2.2. Topographic Segmentation Analysis

We performed a segmentation analysis of the ERPs into microstates to assess the spatial variations of the scalp potential topography over time, of the 3 groups during the 4 conditions.

Group grand average ERP data across all conditions at each time point, after stimulus onset, were subjected to a spatio-temporal clustering method, i.e. topographical atomize-agglomerate hierarchical clustering (3). This analysis allows the identification of scalp potential maps that remain in a quasi-stable configuration for short periods of time – the so-called microstates.

The optimal number of template maps/ microstates was determined by the second peak of an adapted Krzanovski-Lai criterion, as suggested by (4). Template maps with short durations (< 15 ms) were merged with the neighboring map that best correlated with them. We further merged template maps that spatially correlated above 90%. Template maps with similar topographies but inverted voltages were considered as different maps.

After segmenting the grand average ERP data, the microstate template maps were fitted back into the individual ERPs of each subject and condition using a competitive procedure. For each time point after stimulus onset, the scalp topography was correlated to each template map identified in the grand average ERP data by means of normalized spatial correlation. Each time point of data was then labeled with the template map with which it best correlated. From the fitting procedure, we identified the duration during which a given template map was present in each participant and condition. Microstates template map durations were subjected to a two-way repeated measures ANOVA with the factors Group (patients, siblings and controls) and Condition (Vernier Only, Long SOA, Short SOA and Mask Only).

The topographic segmentation analysis was performed using the CARTOOL software (5).

2. Results

2.1. Experiment 1

A good reliability was found between the first and second testing ($r(219)=0.858$, $p<0.001$). The result held true for each group separately: patients ($r(88)=0.788$, $p<0.001$), siblings ($r(53)=0.885$, $p<0.001$), and controls ($r(74)=0.738$, $p<0.001$).

2.2. Experiment 2

2.2.1. Behavior

Performance of the patients was inferior in the 3 conditions that contained the target vernier¹, while siblings and controls achieved similar performances. Group average statistics are shown in Supplementary Table 1. Post hoc pairwise comparisons between groups for each Condition are shown in Supplementary Table 2.

Supplementary Table 1 – Mean accuracy (\pm SD), expressed in %, for each group for each group for the four conditions.

Condition	Group		
	Patients	Siblings	Controls
Vernier Only	91.48 \pm 7.01	96.70 \pm 4.42	97.00 \pm 3.88
Long SOA	87.01 \pm 10.01	95.30 \pm 5.48	95.88 \pm 4.96
Short SOA	65.49 \pm 12.74	80.74 \pm 13.26	81.47 \pm 13.17
Mask Only	49.88 \pm 3.72	48.77 \pm 3.50	49.70 \pm 3.84

¹ No statistics was computed on the performance during the Mask Only condition because no target vernier was present and the accuracy was calculated by comparing the left/right offset response to a randomly chosen notional offset, which was not presented

Supplementary Table 2 - Experiment 2: Post hoc pairwise group comparisons of accuracy using Bonferroni-Holm correction for each stimulus condition that contained the target vernier (Vernier Only, Long SOA, and Short SOA).

Condition	Group I	Group II	<i>t</i> -value	df	<i>p</i> -value	<i>d</i>
Vernier Only	Patients	Siblings	-5.561	143	<0.001	0.847
		Controls	-6.460	164	<0.001	0.953
	Siblings	Controls	-0.308	129	0.758	0.073
Long SOA	Patients	Siblings	-6.415	143	<0.001	0.964
		Controls	-7.547	164	<0.001	1.094
	Siblings	Controls	-0.439	129	0.661	0.113
Short SOA	Patients	Siblings	-6.841	143	<0.001	1.178
		Controls	-7.877	164	<0.001	1.235
	Siblings	Controls	-0.317	129	0.751	0.055

The SOAs in Experiment 1 correlated with the performance in Experiment 2, for each condition containing the target vernier, for all participants together and for each group separately. Pearson correlation coefficients are shown in Supplementary Table 3.

Supplementary Table 3 – Pearson correlation between the SOAs in Experiment 1 and the performance in the 4 conditions of Experiment 2, for all participants together and for patients, siblings, and controls separately (corrected for multiple comparison using Bonferroni-Holm correction). Participants with shorter SOAs are more accurate at discriminating the vernier offset in Experiment 2.

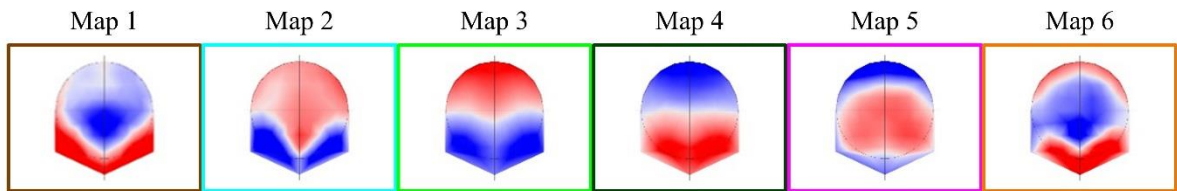
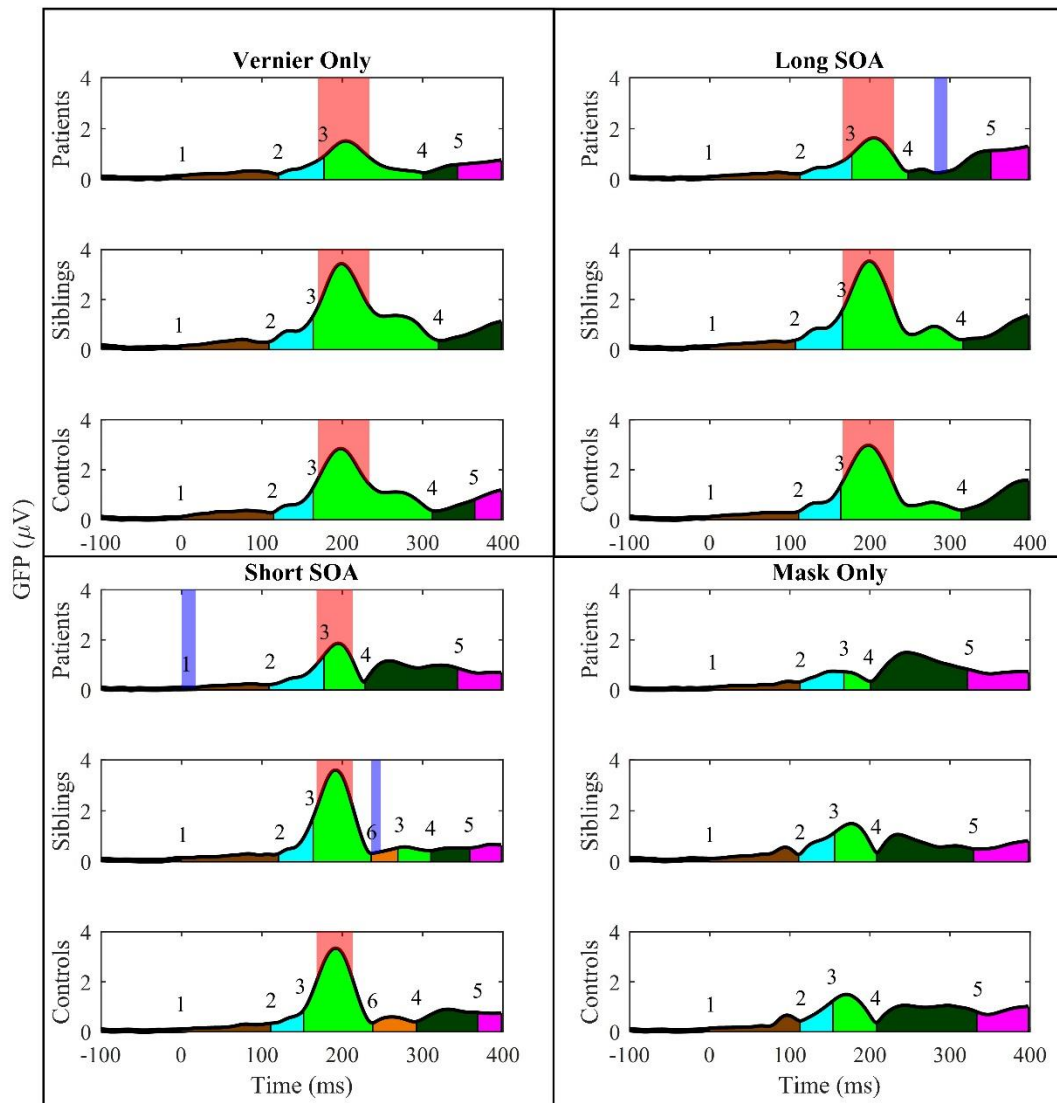
Condition	Group	<i>r</i>	df	<i>p</i> -value
Vernier Only	All	-0.570	219	<0.001
	Patients	-0.447	88	<0.001
	Siblings	-0.428	53	0.003
	Controls	-0.495	74	<0.001
Long SOA	All	-0.662	219	<0.001
	Patients	-0.569	88	<0.001
	Siblings	-0.551	53	<0.001
	Controls	-0.460	74	<0.001
Short SOA	All	-0.663	219	<0.001
	Patients	-0.536	88	<0.001
	Siblings	-0.618	53	<0.001
	Controls	-0.616	74	<0.001
Mask Only	All	0.087	219	0.415
	Patients	0.085	88	0.888
	Siblings	0.011	53	1.000
	Controls	0.125	74	0.590

2.2.2. Topographic Consistency

Topographic consistency test generally showed evidence of common ERP topographies ($p < 0.05$), after stimulus onset, within each group for each condition, but with a few exceptions: patients during Long SOA condition (from 280 to 297 ms), patients during Short SOA condition (from 0 to 18 ms), and siblings during Short SOA condition (from 236 to 248 ms; Supplementary Fig. 1).

2.2.3. *Topographic Segmentation*

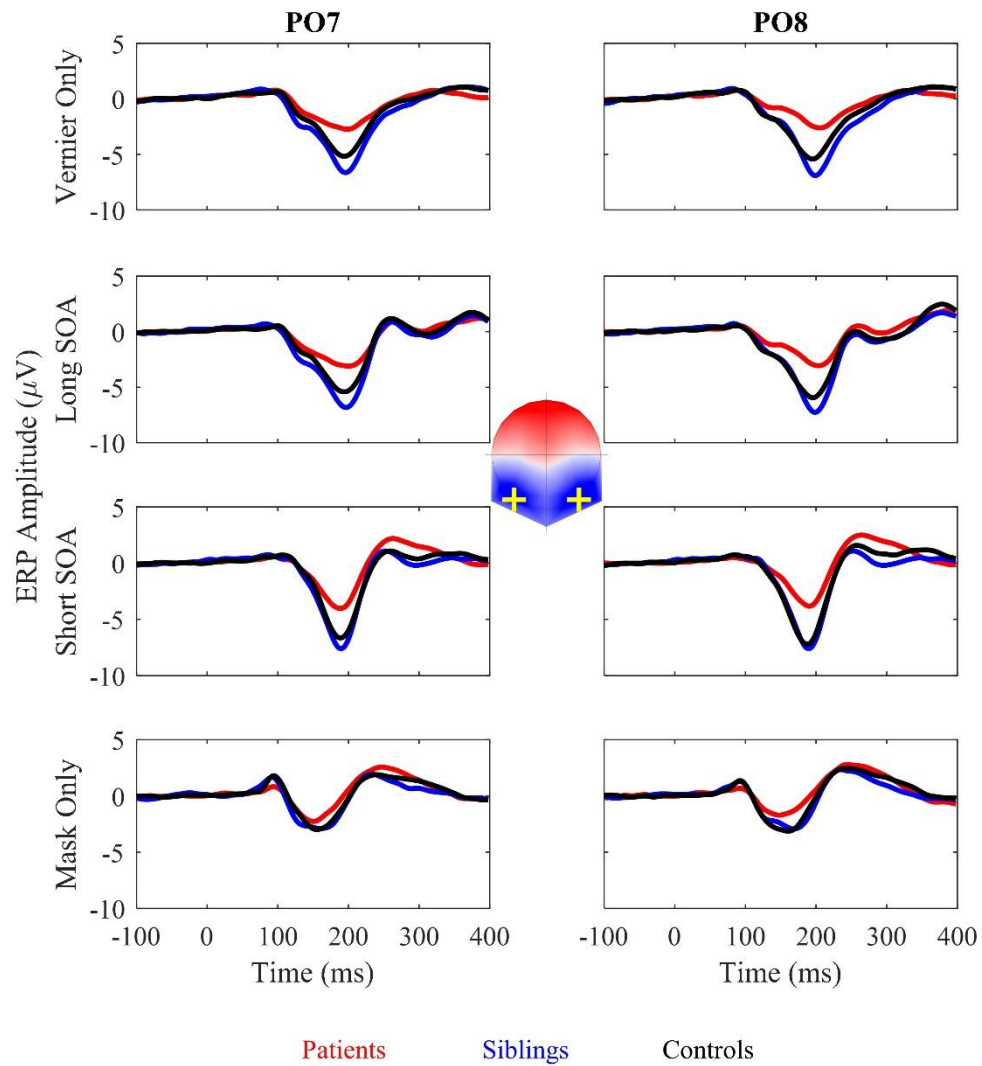
The segmentation analysis identified 6 template maps (microstates) that accounted for around 90.78% of the global explained variance of the data (Supplementary Fig. 1). In general, after stimulus onset, all groups' ERPs followed similar sequence of microstates for all 4 experimental conditions.



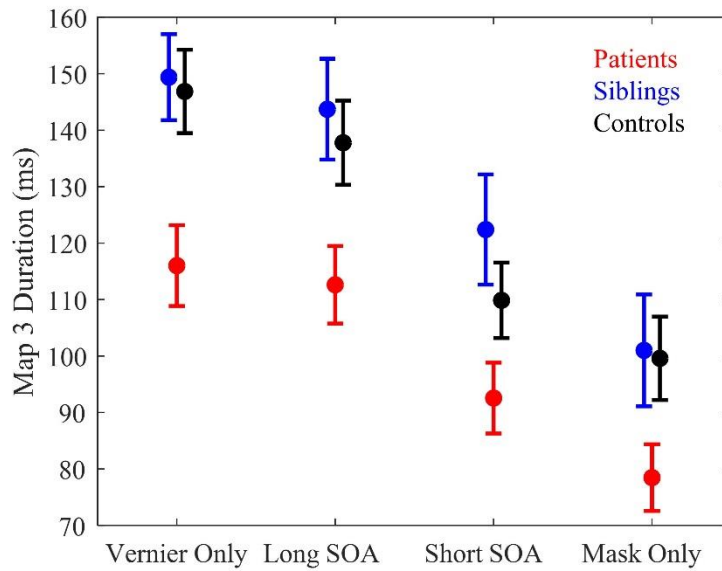
Supplementary Fig. 1 – Topography segmentation results for patients, siblings and controls for each of the 4 stimulus conditions, with the GFP of the grand-average ERPs on the ordinate and time on the abscissa. The vertical lines represent the onset and offset of a given microstate. The colors and numbers correspond to the microstates, which are presented at the bottom as voltage topographies (average reference, nose on top, blue reflecting negative potentials and red positive potentials). In general, after stimulus, all groups follow similar sequences of microstates for all the conditions. Analysis of the GFP amplitudes showed group differences at

around 200 ms after stimulus onset for all the conditions containing the target vernier (light red region). Topographic consistency test showed evidence of common ERP topographies after stimulus onset, within group for each condition, apart from the time periods indicated in light blue region.

Patients showed decreased duration of a microstate (map 3) across all 4 conditions. This microstate occurred at around 200 ms after stimulus onset, for all experimental groups, in each of the 3 conditions containing the target vernier and at around 170 ms for the Mask Only condition. The template map 3 is characterized by a bilateral negativity in the occipital area, reflecting the N1 component (Supplementary Fig. 2). A two-way ANOVA with Greenhouse-Geisser correction of the template map 3 duration showed statistically significant main effects of Group ($F(2,218)=6.304$, $P=0.002$, $\eta^2=0.055$), Condition ($F(2.398,522.799)=58.617$, $P<0.001$, $\eta^2=0.211$), and a nonsignificant interaction ($F(4.796,522.799)=0.652$, $P=0.653$, $\eta^2=0.005$). The summary statistics are shown in Supplementary Fig. 3. Post-hoc analysis of the main effect of Group using Bonferroni-Holm correction, indicated that, on average, patients had decreased map 3 durations compared to siblings ($t(143)=3.152$, $p=0.006$, $d=0.527$) and controls ($t(164)=2.799$, $p=0.011$, $d=0.437$). However, siblings and controls had similar map 3 durations ($t(129)=0.584$, $p=0.560$, $d=0.103$). Post-hoc analysis of the main effect of Condition using Bonferroni-Holm correction, indicated that map 3 durations for Vernier Only and Long SOA conditions were similar ($t(220)=1.967$, $p=0.050$, $d=0.132$), but their map 3 duration were longer than that for Short SOA ($t(220)=7.852$, $p<0.001$, $d=0.528$; $t(220)=6.848$, $p<0.001$, $d=0.461$; Vernier Only and Long SOA, respectively). Map 3 durations in Short SOA condition were longer than the Mask Only condition ($t(220)=4.457$, $p<0.001$, $d=0.300$).



Supplementary Fig. 2 – Grand average ERP traces at PO7 (left) and PO8 (right), in each stimulus conditions, for patients, siblings and controls. Participants showed prominent negative deflections peaking around 200 ms, for conditions containing the target Vernier, and around 170 ms, for Mask Only, resembling the N1 evoked component.



Supplementary Fig. 3 – Average duration of microstate map 3 for patients, siblings and controls, for the 4 experimental conditions. Patients had shorter map 3 durations compared to siblings and controls, independently of the condition. Mean map 3 durations were similar for Vernier Only and Long SOA conditions. However, map 3 durations were shorter in the Short SOA condition, which was longer than the Mask Only condition. Error bars indicate standard error of the mean.

2.2.4. GFP

GFP group mean amplitudes at the peak latencies for each condition are shown in Supplementary Table 4. As shown in Supplementary Table 5, for controls and patients, GFP peak amplitudes increased with task difficulty, i.e., from Vernier Only to Long SOA and to Short SOA conditions.

Supplementary Table 4 – GFP amplitudes at the peak latencies (\pm SD), expressed in μ V, for each group for each group for the four conditions.

Condition	Group		
	Patients	Siblings	Controls
Vernier Only	1.94 \pm 1.05	3.62 \pm 1.61	3.08 \pm 1.34
Long SOA	2.02 \pm 1.04	3.73 \pm 1.65	3.23 \pm 1.04
Short SOA	2.27 \pm 1.67	3.82 \pm 1.64	3.62 \pm 1.61
Mask Only	1.78 \pm 0.88	2.02 \pm 0.96	2.12 \pm 1.00

Supplementary Table 5 – Post hoc pairwise Condition comparisons (for each stimulus condition that contained the target vernier: Vernier Only, Long SOA, and Short SOA) of the GFP peak amplitude using Bonferroni-Holm correction for patients and controls.

Condition I	Condition II	Group	<i>t</i> -value	df	<i>p</i> -value	d
Vernier Only	Long SOA	Patients	-1.997	89	0.048	0.210
		Controls	-2.901	75	0.005	0.333
	Short SOA	Patients	-4.295	89	<0.001	0.453
		Controls	-5.411	75	<0.001	0.621
Long SOA	Short SOA	Patients	-2.902	89	0.009	0.306
		Controls	-3.643	75	<0.001	0.418

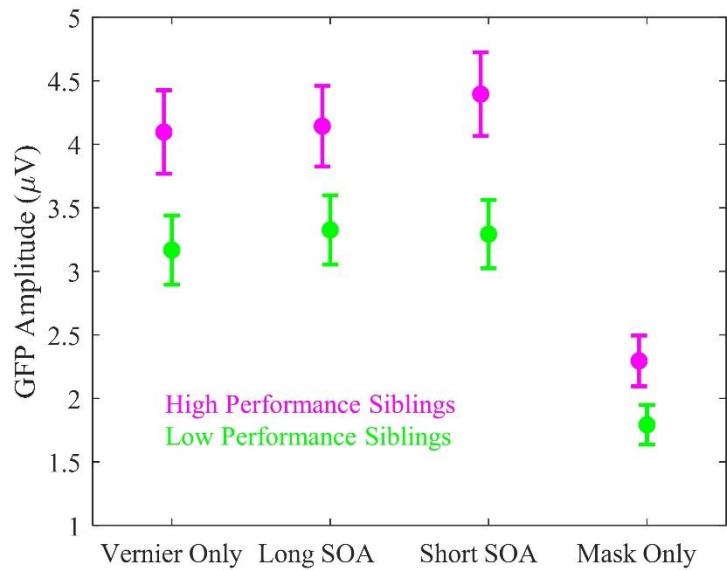
GFP amplitudes at the peak latencies correlated with the performance for all conditions containing the target vernier, when considering all participants. As shown in Supplementary Table 6, this was also the case for the siblings only. For patients and controls, while the individual groups' correlations were not statistically significant, they showed similar trends to the results considering all the participants.

Supplementary Table 6 - Pearson correlation between the GFP amplitudes at the peak latencies and the accuracy in the 4 conditions, for all participants, as well as the groups of patients, siblings, and controls individually.

Condition	Group	<i>r</i>	df	<i>p</i> -value
Vernier Only	All	0.347	219	<0.001
	Patients	0.145	88	0.173
	Siblings	0.355	53	0.008
	Controls	0.168	74	0.147
Long SOA	All	0.386	219	<0.001
	Patients	0.215	88	0.042
	Siblings	0.327	53	0.015
	Controls	0.188	74	0.103
Short SOA	All	0.362	219	<0.001
	Patients	0.164	88	0.123
	Siblings	0.298	53	0.027
	Controls	0.133	74	0.253
Mask Only	All	-0.031	219	1.000
	Patients	0.008	88	1.000
	Siblings	0.030	53	0.825
	Controls	0.034	74	0.772

Aiming at exploring whether different subgroups of siblings had different neural responses across experimental conditions (i.e. GFP peak amplitudes increase with task difficulty), siblings were divided in 2 subgroups by classifying them as either high or low performers, depending on whether their SOA was below (high performer siblings (HPS); $n=27$) or above (low performer sibling (LPS); $n=27$) 45 ms (median SOA of the 55 siblings). The HPS group had on average SOAs around 20.81 ± 11.45 ms and the LPS group around 86.75 ± 46.95 ms. A two-way ANOVA with Greenhouse-Geisser correction of the peak GFP amplitudes showed statistically significant main effects of Group ($F(1,52)=5.499$, $P=0.023$, $\eta^2=0.096$) and Condition ($F(1.945,101.115)=77.200$, $P<0.001$, $\eta^2=0.590$). However, no statistically significant interaction was found ($F(1.945,101.115)=1.694$, $P=0.190$, $\eta^2=0.013$).

Post hoc tests of the main effect of Condition using Bonferroni-Holm showed no statistically significant differences in the GFP peak amplitudes between the 3 conditions containing the target vernier. These results are depicted in Supplementary Fig. 4 and Supplementary Table 7.



Supplementary Fig. 4 – Comparison of the GFP peak amplitudes of high and low performance siblings (HPS and LPS, respectively) for the 4 experimental conditions. No statistically significant interaction was found. Error bars indicate standard error of the mean.

Supplementary Table 7 – Post hoc comparisons of the main effect of Condition of the GFP amplitudes at the peak latencies for the comparison of two groups of siblings (high vs low performers), using Bonferroni-Holm correction.

Condition I	Condition II	<i>t</i> -value	df	<i>p</i> -value	d
Vernier Only	Long SOA	-1.614	53	0.259	0.220
	Short SOA	-1.748	53	0.259	0.238
	Mask Only	9.727	53	<0.001	1.324
Long SOA	Short SOA	-0.850	53	0.399	0.116
	Mask Only	9.669	53	<0.001	1.316
Short SOA	Mask Only	12.283	53	<0.001	1.671

2.2.5. Distributed Electrical Source Imaging

Group mean CDs for each condition of the six EEG source clusters exhibiting significant Group x Condition interaction effects are shown in Supplementary Table 8.

Supplementary Table 8 – Group average current density (CD), expressed in, at the centers of mass for the six clusters

Condition	Region	Group		
		Patients	Siblings	Controls
Vernier Only	Left Middle Temporal Gyrus	1.82 ± 1.01	3.26 ± 2.05	2.71 ± 1.61
	Left Insula	0.20 ± 0.11	0.25 ± 0.09	0.24 ± 0.10
	Left Precentral Gyrus	0.73 ± 0.36	1.18 ± 0.72	1.11 ± 0.51
	Right Middle Temporal Gyrus	1.61 ± 1.05	3.19 ± 2.00	2.57 ± 1.58
	Right Insula	0.09 ± 0.05	0.15 ± 0.07	0.13 ± 0.06
	Right Precuneus	1.01 ± 0.52	1.60 ± 0.91	1.27 ± 0.71
Long SOA	Left Middle Temporal Gyrus	1.86 ± 1.01	3.36 ± 1.97	2.72 ± 1.62
	Left Insula	0.18 ± 0.11	0.25 ± 0.09	0.23 ± 0.10
	Left Precentral Gyrus	0.75 ± 0.35	1.20 ± 0.74	1.13 ± 0.50

	Right Middle Temporal Gyrus	1.76 ± 1.16	3.33 ± 2.14	2.80 ± 1.63
	Right Insula	0.09 ± 0.05	0.15 ± 0.08	0.14 ± 0.07
	Right Precuneus	1.01 ± 0.55	1.64 ± 1.00	1.41 ± 0.75
Short SOA	Left Middle Temporal Gyrus	2.34 ± 1.30	4.24 ± 2.41	3.68 ± 1.99
	Left Insula	0.18 ± 0.09	0.24 ± 0.10	0.24 ± 0.10
	Left Precentral Gyrus	0.79 ± 0.41	1.10 ± 0.61	1.17 ± 0.68
	Right Middle Temporal Gyrus	2.20 ± 1.48	4.02 ± 2.34	3.61 ± 2.06
	Right Insula	0.10 ± 0.06	0.16 ± 0.07	0.16 ± 0.08
	Right Precuneus	1.34 ± 0.65	2.01 ± 1.05	1.85 ± 1.06
Mask Only	Left Middle Temporal Gyrus	2.44 ± 2.00	1.92 ± 1.17	2.36 ± 1.48
	Left Insula	0.20 ± 0.11	0.17 ± 0.08	0.17 ± 0.09
	Left Precentral Gyrus	0.74 ± 0.35	0.79 ± 0.45	0.82 ± 0.46
	Right Middle Temporal Gyrus	2.21 ± 1.51	1.96 ± 1.25	2.17 ± 1.53
	Right Insula	0.08 ± 0.04	0.10 ± 0.05	0.11 ± 0.06
	Right Precuneus	1.63 ± 0.73	1.30 ± 0.65	1.42 ± 0.70

187

188 To identify in which conditions there were statistically significant Group differences of
189 the activity at the center of mass in each region, we performed simple main effects of Group
190 for each of the 4 conditions per identified region (4 Conditions x 6 regions = 24 ANCOVAs)
191 with Bonferroni-Holm correction. The results, listed in Supplementary Table 9, show that
192 group differences tend to be larger in the conditions with the target vernier than in the Mask
193 Only condition.

194

Supplementary Table 9 – Simple main effect of Group, for each of the 4 experimental conditions, of the activity at the center of mass of regions that showed significant interaction effects, with Bonferroni-Holm correction for multiple comparison.

Label	Condition	$F(2,216)$	p -value	η^2
Left Middle Temporal Gyrus	Vernier Only	13.979	<0.001	0.114
	Long SOA	17.023	<0.001	0.135
	Short SOA	17.604	<0.001	0.140
	Mask Only	2.445	0.267	0.022
Left Insula	Vernier Only	3.629	0.112	0.031
	Long SOA	6.248	0.016	0.053
	Short SOA	8.332	0.003	0.069
	Mask Only	4.086	0.090	0.035
Left Precentral Gyrus	Vernier Only	18.995	<0.001	0.148
	Long SOA	21.198	<0.001	0.160
	Short SOA	9.554	0.001	0.081
	Mask Only	1.422	0.488	0.013
Right Middle Temporal Gyrus	Vernier Only	17.265	<0.001	0.135
	Long SOA	16.127	<0.001	0.128
	Short SOA	16.446	<0.001	0.128
	Mask Only	0.815	0.488	0.007
Right Insula	Vernier Only	19.521	<0.001	0.151
	Long SOA	18.251	<0.001	0.143
	Short SOA	17.271	<0.001	0.135
	Mask Only	4.568	0.077	0.040
Right Precuneus	Vernier Only	10.632	<0.001	0.090
	Long SOA	10.896	<0.001	0.092
	Short SOA	7.495	0.006	0.064
	Mask Only	4.569	0.077	0.040

To assess the effect of the activity in each of the 6 brain regions on the behavioral performance for each group, individually, the center of mass activations were used as predictors in separate multiple linear regressions for the dependent variable accuracy for each of 3 the conditions containing the target vernier, for each group. We used the best subsets regression analysis (6) with the Bayesian Information Criterion (BIC) model selection criterion to remove correlated factors. As shown in Supplementary Table 10, similar to results considering all the participants together, the activity of the right insula significantly predicted the accuracy for all groups and conditions, apart for controls in Vernier Only and Long SOA conditions. However, in these two cases, there was a trend.

Supplementary Table 10 – Results with best subsets regression analysis of the activity of the 6 brain regions as predictors of accuracy for each group and condition.

Condition	Group	Region	β	SE	<i>t</i> -value	df	<i>p</i> -value
Vernier Only	Patients	Right Insula	4.423	1.998	2.214	88	0.029
	Siblings	Right Insula	16.71	7.888	2.118	53	0.039
	Controls	Right Insula	11.436	7.137	1.602	74	0.113
Long SOA	Patients	Right Insula	7.872	2.979	2.642	88	0.010
	Siblings	Right Insula	21.167	9.666	2.19	53	0.033
	Controls	Right Insula	16.206	9.097	1.781	74	0.079
Short SOA	Patients	Right Insula	9.767	3.126	3.124	88	0.002
	Siblings	Right Insula	50.604	23.999	2.109	53	0.040
	Controls	Right Insula	73.543	25.02	2.939	74	0.004
		Right Precuneus	-4.907	1.823	-2.692	74	0.009

As shown in Supplementary Table 11, GFP amplitudes at the peak latencies correlated strongly with the center of mass activation of the right insula for all conditions, when considering all participants, as well as when considering each group separately.

Supplementary Table 11 – Pearson correlation between the GFP amplitudes at the peak latencies and the center of mass activation of the right insula in the 4 conditions, for all participants, as well as the groups of patients, siblings, and controls individually.

Condition	Group	<i>r</i>	df	<i>p</i> -value
Vernier Only	All	0.872	219	<0.001
	Patients	0.766	88	<0.001
	Siblings	0.888	53	<0.001
	Controls	0.852	74	<0.001
Long SOA	All	0.880	219	<0.001
	Patients	0.795	88	<0.001
	Siblings	0.900	53	<0.001
	Controls	0.850	74	<0.001
Short SOA	All	0.903	219	<0.001
	Patients	0.876	88	<0.001
	Siblings	0.885	53	<0.001
	Controls	0.887	74	<0.001
Mask Only	All	0.774	219	<0.001
	Patients	0.779	88	<0.001
	Siblings	0.744	53	<0.001
	Controls	0.779	74	<0.001

References

1. Koenig T, Melie-García L (2010): A Method to Determine the Presence of Averaged Event-Related Fields Using Randomization Tests. *Brain Topogr.* 23: 233–242.
2. Koenig T, Kottlow M, Stein M, Melie-García L (2011): Ragu: A Free Tool for the Analysis of EEG and MEG Event-Related Scalp Field Data Using Global Randomization Statistics. *Comput Intell Neurosci.* 2011: e938925.
3. Tibshirani R, Walther G (2005): Cluster Validation by Prediction Strength. *J Comput Graph Stat.* 14: 511–528.
4. Murray MM, Brunet D, Michel CM (2008): Topographic ERP Analyses: A Step-by-Step Tutorial Review. *Brain Topogr.* 20: 249–264.

- 228 5. Brunet D, Murray MM, Michel CM (2011): Spatiotemporal Analysis of Multichannel
229 EEG: CARTOOL. *Intell Neuroscience*. 2011; 2:1–2:15.
- 230 6. Lumley T (2017): *leaps: Regression Subset Selection*. Retrieved from [https://cran.r-](https://cran.r-project.org/web/packages/leaps/leaps.pdf)
231 [project.org/web/packages/leaps/leaps.pdf](https://cran.r-project.org/web/packages/leaps/leaps.pdf).

232

Appendix D

da Cruz, J. R., Favrod, O., Roinishvili, M., Chkonia, E., Brand, A., Mohr, C.,
Figueiredo, P., & Herzog M. H. (under review)

EEG microstates: a candidate endophenotype for schizophrenia

Authors: Janir Ramos da Cruz^{1,2*}, Ophélie Favrod¹, Maya Roinishvili^{3,4}, Eka Chkonia^{4,5}, Andreas Brand¹, Christine Mohr⁶, Patrícia Figueiredo², and Michael H. Herzog¹

Affiliations:

¹ Laboratory of Psychophysics, Brain Mind Institute, École Polytechnique Fédérale de Lausanne (EPFL), Switzerland

² Institute for Systems and Robotics – Lisbon (LARSys) and Department of Bioengineering, Instituto Superior Técnico, Universidade de Lisboa, Portugal

³ Laboratory of Vision Physiology, Beritashvili Centre of Experimental Biomedicine, Tbilisi, Georgia

⁴ Institute of Cognitive Neurosciences, Free University of Tbilisi, Tbilisi, Georgia

⁵ Department of Psychiatry, Tbilisi State Medical University, Tbilisi, Georgia

⁶ Faculté des Sciences Sociales et Politiques, Institut de Psychologie, Bâtiment Geopolis, Lausanne, Switzerland

***Corresponding author:**

Janir Ramos da Cruz, Laboratory of Psychophysics, Brain Mind Institute, School of Life Sciences, École Polytechnique Fédérale de Lausanne (EPFL), CH-1015 Lausanne, Switzerland

Phone number: +41 21 693 17 42

Email: janir.amos@epfl.ch

Running title: Microstates are an endophenotype for schizophrenia (50 characters, max 50)

Keywords: siblings, schizophrenia, schizotypy, endophenotype, microstates, EEG

Number of words in abstract: 247 (max 250)

Number of words in the main text: 3990 (max 4000)

Number of figures: 3

Number of tables: 2

Number of supplementary information: 1

Abstract

Background

Electroencephalogram (EEG) microstates are recurrent scalp potential configurations that remain stable for around 90ms. The temporal dynamics of particular classes of microstates has been suggested as a potential endophenotype for schizophrenia. For an endophenotype, it is important that unaffected relatives of schizophrenia patients also show abnormal patterns compared to controls. No study has yet investigated the dynamics of microstates in relatives of schizophrenia patients.

Methods

We examined EEG microstate dynamics in 5 minutes resting-state recordings of 38 unaffected siblings of schizophrenia patients, 89 schizophrenia patients, 69 healthy controls, 42 healthy students scoring either high or low in schizotypal traits, and 22 patients with first episodes of psychosis (FEP).

Results

Schizophrenia patients showed increased presence of a microstate class labeled C and decreased presence of a microstate class labeled D compared to controls. Siblings showed similar patterns of microstate classes C and D as chronic patients. Surprisingly, siblings showed an increased presence of a microstate class labeled B compared to chronic patients. A similar result was also found in students scoring high in schizotypal traits compared to the ones scoring low. No difference was found between FEP and matched chronic patients.

Conclusions

Our findings support the hypothesis that the dynamics of microstate classes C and D meet the requirements for an endophenotype of schizophrenia. The novel finding of the increased presence of microstates class B in siblings, as well as students scoring high in schizotypal traits, may reflect a compensation mechanism opposing the vulnerability to develop schizophrenia.

1. Introduction

Electroencephalogram (EEG) has evolved into a powerful tool capable of providing spatiotemporal information regarding brain (dys)function (1). One major advancement for characterizing the resting-state activity of the human brain, and particularly sensitive to schizophrenia, is microstate analysis (2, 3). Microstates are global patterns of scalp potential topographies that remain quasi-stable for around 60–120ms before changing to a different topography that remains quasi-stable again, suggesting semi-simultaneity of activity of large-scale brain networks (4).

Four dominant classes of microstates are consistently observed across resting-state EEG studies, explaining 65–84% of the global variance of the data (3). Several studies have attempted to identify the brain sources underlying these microstates (5–10). A recent review paper (3) demonstrated that these four EEG microstates are closely related to resting-state networks (RSNs) commonly found in resting-state functional magnetic resonance imaging (fMRI). The first microstate (class A) was associated with the auditory RSN, the second microstate (class B) with the visual RSN, the third microstate (class C) with the salience RSN, and the last microstate (class D) with the attention RSN.

Numerous studies have reported abnormalities in parameters characterizing the temporal dynamics of EEG microstates measured in schizophrenia patients compared to controls (2, 3). A meta-analysis (11) revealed that microstate class C occurred more frequently and for longer durations in patients than in controls. For microstate class D, it was found that it occurred less frequently and for shorter durations in patients compared to controls. The same meta-analysis reported that microstate class B was shorter in patients than controls, but the effect was not significant after correction for multiple comparisons.

Similar abnormalities were also observed in adolescents with 22q11.2 deletion syndrome, a population that has a 30% risk of developing psychosis (12, 13). These results indicate that the abnormal parameters of EEG microstates may provide an endophenotype for schizophrenia. Endophenotypes are associated with the illness, state-independent, co-segregate within families, and found in unaffected relatives of individuals with the disorder at a higher prevalence than in the general population (14). To the best of our knowledge, no study has analyzed the resting-state dynamics of these four microstate classes in relatives of schizophrenia patients.

Here, we analyzed the microstates dynamics in unaffected siblings of schizophrenia patients, schizophrenia patients, and healthy controls. If microstates dynamics are endophenotypes for schizophrenia, siblings must show abnormalities as patients, compared to controls. To preface our results, siblings showed abnormalities in microstates class C and D, similar to patients. Surprisingly, siblings also showed increased presence of microstate class B compared to patients. We interpreted this increased presence of microstate class B as a compensation signal, which might prevent unaffected siblings to develop the disorder even if there is a genetic predisposition.

These results motivated us to investigate microstates dynamics in healthy people scoring high in schizotypal traits. Schizotypy belongs to the schizophrenia spectrum and reflects the non-clinical equivalent of schizophrenia (15, 16). Schizotypy allows to study the etiology of schizophrenia by promoting a developmental approach (17, 18). Schizotypal traits are measured by self-reporting questionnaires such as the Oxford-Liverpool Inventory of Feelings and Experiences (O-LIFE) (19). As with schizophrenia symptoms, there are three dimensions of symptoms: positive traits, negative traits, and cognitive disorganization, measured with the Unusual Experience (UnExp), Introvertive Anhedonia (IntAn), and Cognitive Disorganization (CogDis) subscales of the O-LIFE. CogDis is more clinically relevant than the other two dimensions since a high CogDis score predicts a high score in the other dimensions (20). Cognitive slippage and associative loosening (reflected by CogDis) are thought to be core features of schizophrenia (20), and elevated CogDis scores are associated with high probability of transition towards psychosis (21). Here, we hypothesized that if an increased prevalence of microstate class B is evidence for a compensation signal, participants scoring high in CogDis should have increased values compared to the ones scoring low. We tested this hypothesis by analyzing microstates in healthy students scoring either high or low in schizotypal traits. In a third experiment, we investigated whether patients with a first episode of psychosis (FEP) show similar microstates dynamics as chronic schizophrenia patients or FEP have the compensation signal (i.e., increased presence of microstate class B).

2. Methods and Materials

2.1. Participants

Schizophrenia patients, their unaffected siblings, their healthy matched controls, and patients with FEP, were recruited in Georgia. Healthy students were recruited in Switzerland. EEG was

recorded under similar conditions in both locations. Participants were no older than 55 years old. General exclusion criteria were alcohol or drug abuse, severe neurological incidents or diagnoses (including head injury), developmental disorders (autism spectrum disorder or intellectual disability) or other somatic mind-altering illnesses, assessed through interview by certified psychiatrists. All Axis I disorders were an exclusion criterion for the non-clinical cohorts. All participants have participated in a previous study on masking and evoked-related potentials (ERPs). Masking and ERP data of some participants have been already published, while data of other participants have not been analyzed yet. All participants signed informed consent and were informed that they could quit the experiments at any time. All procedures complied with the Declaration of Helsinki and were approved by the local ethics committee.

2.1.1. Experiment 1: Patients, Siblings, and Controls

Three groups of participants joined experiment 1: chronic schizophrenia patients (n=89), unaffected siblings of schizophrenia patients (n=38), and healthy controls (n=69). Masking and ERP data of 71 patients, 34 siblings, and 54 controls have already been published (22). Schizophrenia patients and their siblings were recruited from the Tbilisi Mental Health Hospital or the psycho-social rehabilitation center. Patients were invited to participate in the study when they had recovered sufficiently from an acute psychotic episode. 26 were inpatients; 63 were outpatients. Diagnosis was made according to the *Diagnostic and Statistical Manual of Mental Disorders Fourth Edition* (DSM-IV) criteria, based on the SCID-CV (Structured Clinical Interview for DSM-IV, Clinician Version), information from staff, and study of patients' records. Psychopathology of schizophrenia patients was assessed by an experienced psychiatrist using the Scales for the Assessment of Negative Symptoms (SANS) and Scales for the Assessment of Positive Symptoms (SAPS). 76 out of the 89 patients were receiving neuroleptic medication. We included siblings of the schizophrenia patients only when they had no history of psychoses. Controls were recruited from the general population, and they had no family history of psychosis. Group characteristics are presented in **Supplementary Table S1**. Groups differed in terms of gender, age, and education.

2.1.2. Experiment 2: High and Low Schizotypal Traits

49 healthy university students from either the École Polytechnique Fédérale de Lausanne (EPFL) or University of Lausanne (UNIL) participated in the study. Before the EEG experiment, participants filled in the French version of the O-LIFE short questionnaire (23). Masking and ERP data of all participants have been published in previous work (24). Participants were selected based on their CogDis subscale score, which varied from the lowest (0 points) to the highest (11 points). The selection procedure is described in detail in (24). Since we were interested in extreme groups, we removed participants with an intermediate CogDis score (either 5, $n=0$ or 6, $n=7$), ending up with 42 participants separated into two groups. In the Low CogDis group ($n=20$), participants had CogDis scores ranging from 0 to 4, while in the High CogDis group ($n=22$) group, they had CogDis score ranging from 7 to 11. Group characteristics are presented in **Supplementary Table S2**. As aimed for, groups differed only on the CogDis dimension.

2.1.3. Experiment 3: FEP

22 FEP participated in the study. Masking and ERP data of 21 of them have been published in previous work (25). FEP were recruited from the Tbilisi Mental Health Hospital or the Acute Psychiatric Departments of Multiprofile Clinics. FEP selection, exclusion criteria, and psychopathological assessment were the same as for chronic schizophrenia patients, see sub-section 2.1.1. FEP were diagnosed either as having a brief psychotic disorder (DSM-IV 298.8) or as a schizophreniform disorder (DSM-IV 295.40). 20 out of the 22 FEP were receiving neuroleptic medication. 4 were inpatients; 18 were outpatients. From our pool of 89 chronic schizophrenia patients (see sub-section 2.1.1), we pseudo-randomly selected 22 patients (Patients_22), to match the 22 FEP as closely as possible, regarding gender, age, and education. Group characteristics are shown in **Supplementary Table S3**. FEP and Patients_22 groups differed only in terms of illness duration, SANS and SAPS scores.

2.2.EEG Recording and Data Processing

Participants were sitting in a dim lit room. They were instructed to keep their eyes closed and to relax for five minutes. In Georgia, resting-state EEG was recorded before participants participated in a masking experiment and using a BioSemi Active 2 system (Biosemi) with 64 Ag-AgCl sintered active electrodes, referenced to the common mode sense (CMS) electrode. In Switzerland, resting-state EEG was recorded after participants participated in a masking

experiment and the study took place at EPFL in a Faraday Cage using a Biosemi with 192 Ag-AgCl sintered active electrodes, referenced to the CMS. In both locations, the recording sampling rate was 2048Hz. Offline, data were downsampled to 128Hz and pre-processed using an automatic pipeline (APP; for details, see **Supplementary Information 1.4**) (26).

The Global Field Power (GFP) of the pre-processed EEG data was determined for each participant. GFP is an instantaneous reference-independent measure of neuronal activity throughout the brain, and it is calculated as the standard deviation of the electrical potential across all electrodes at each time point (27). Since EEG map topographies remain stable around the GFP peaks and these are the best representatives of the topographic maps regarding signal-to-noise ratio (28), only EEG topographies at the GFP peaks were submitted to further analysis. The GFP-reduced data were submitted to k-means clustering (29, 30) to identify the most dominant topographies as classes of microstates present in the recordings. The clustering analysis was first done at the individual level and then across participants in each group. To have equal contributions of microstates per participant, each participant contributed to the group k-means clustering with his/hers four most dominant microstates. To compare our results with previous studies, we selected four microstates for each group, and labeled them A-D according to their similarities to the previously reported microstate classes (3). To ensure that the four selected microstates were similar across groups, we computed spatial correlation (31) for each of the four microstate classes for each pair of groups. High spatial correlation coefficients indicated that the microstate classes were similar between groups (see **Supplementary Information 2.1, 2.2, and 2.3**).

Subsequently, for each group, we compared the four microstates with the instantaneous scalp potential maps in each participant's artifact-correct EEG using a competitive fitting procedure. For each time point of the individual EEG, the scalp topography was compared to each microstate class using spatial correlation. The time point was then labeled according to the microstate that exhibited the greatest correlation. Temporal smoothing (window (half) size = 5, strength (Besag) = 10, rejection of microstates with durations of 1 time frame) was applied to ensure that noise during low GFP periods did not interrupt segments of quasi-stable topographies (32). For each subject, three per-class microstate parameters were computed: mean duration, time coverage, and frequency of occurrence (occurrence). Mean duration (in ms) is the average time that a given microstate was *uninterruptedly* present. Time coverage (in %) is the percentage of the total analysis

time spent in a given microstate. Occurrence is the mean number of times a given microstate is occurring per second.

Microstates analysis was performed using CARTOOL (29). For each of the computed microstates parameters (mean duration, time coverage, and occurrence), we performed a two-way repeated measures ANOVA, with two factors: group (patients, siblings, and controls, or High CogDis and Low CogDis, or FEP and Patients_22), and microstate class (A, B, C, and D). In experiment 1, since the groups differed in gender, age and education, these three variables were introduced as covariates in the analyses. All simple main effects and post-hoc analyses were Bonferroni-Holm corrected for multiple comparisons.

3. Results

3.1. Patients, siblings, and controls

The four microstate classes for patients, siblings, and controls are shown in **Figure 1a**). The four microstate classes across participants explained 81.60%, 81.12%, and 78.33% of the global variance in the patients, siblings and control group, respectively. In each of the three groups, the four microstates resembled the four class model maps consistently identified in the literature (3): two microstate classes (A and B) with diagonal axis orientations of the topographic map field, one class (C) with anterior-posterior orientation, and one class (D) with a fronto-central extreme location.

Two-way repeated measures ANOVAs yielded significant group \times microstate class interaction for all microstate parameters: mean duration ($F(6,570)=6.455, P<0.001, \eta^2=0.060$), time coverage ($F(6,570)=7.478, P<0.001, \eta^2=0.068$), and occurrence ($F(6,570)=6.516, P<0.001, \eta^2=0.062$). These interactions indicate that group differences depend on the microstate class. Simple main effects of group revealed significant group differences for microstate classes B, C and D for all microstate parameters (**Table 1**). Post-hoc pairwise group comparisons showed that for microstate class B, siblings had increased values compared to patients for all microstate parameters (**Figure 1** and **Table 2**). Patients had decreased mean duration compared to controls. For microstate class C, patients and siblings had increased values compared to controls for all the computed microstates parameters, except for mean duration, which was similar for siblings and controls. For microstate

class D, similar analysis showed that patients and siblings had decreased values compared to controls for all computed microstates parameters.

3.2. High and Low CogDis

The four microstate classes for the High CogDis and Low CogDis groups are shown in **Figure 2a**). The four microstate classes across participants explained 79.06% of the global variance for the High CogDis group and 77.91% for the Low CogDis group. Similarly to patients, siblings, and controls (**Figure 1a**), in the High and Low CogDis groups, the four microstates resembled the four class model maps consistently identified in the literature.

Two-way repeated measures ANOVAs yielded non-significant group \times microstate class interactions for mean duration ($F(3,120)=2.012$, $P=0.116$, $\eta^2=0.023$) and time coverage ($F(3,120)=2.479$, $P=0.064$, $\eta^2=0.026$), as well as a significant group \times microstate class interaction for occurrence ($F(3,120)=2.816$, $P=0.042$, $\eta^2=0.029$). As shown in **Figure 2**, simple main effects of group revealed that High CogDis participants had a higher occurrence ($t(40)=3.519$, $p=0.004$, $g=1.067$) of microstate class B than Low CogDis participants.

3.3. FEP

The four microstate classes for the FEP group are shown in **Figure 3a**). The four microstate classes explained 73.97% of the global variance, across participants. Similarly to patients, siblings, and controls (**Figure 1a**), as well as to the High and Low CogDis groups (**Figure 2a**), the four microstates resembled the four class model maps consistently identified in the literature.

We found no statistically significant differences between the FEP and Patients_22 groups for any of the computed microstates parameters. Two-way repeated measures ANOVAs yielded non-significant group \times microstate class interactions for mean duration ($F(3,126)=0.457$, $P=0.713$, $\eta^2=0.007$), time of coverage ($F(3,126)=0.214$, $P=0.886$, $\eta^2=0.003$), and occurrence ($F(3,126)=0.373$, $P=0.772$, $\eta^2=0.005$), as well as non-significant group differences for mean duration ($F(1,42)=0.583$, $P=0.449$, $\eta^2=0.014$), time of coverage ($F(1,42)=0.057$, $P=0.813$, $\eta^2=0.001$), and occurrence ($F(1,42)=1.093$, $P=0.302$, $\eta^2=0.025$).

4. Discussion

Several studies have consistently identified abnormal temporal dynamics of EEG microstates in schizophrenia patients (13, 33–39). Similar patterns were also found in patients with 22q11.2 deletion syndrome, a population that has a 30% risk of developing psychosis (12). Based on these findings, Tomescu and colleagues suggested that these alterations in the temporal dynamics of EEG microstates are a marker for developing schizophrenia (13), so-called endophenotype. For an endophenotype, it is important that unaffected relatives also show deficits, suggesting a genetic component underpinning the marker (14).

Here, we investigated the resting-state dynamics of EEG microstates in unaffected siblings of schizophrenia patients, schizophrenia patients, and healthy controls. If the microstates dynamics are endophenotypes for schizophrenia, siblings must show similar abnormalities as patients, compared to controls. Siblings and patients showed similar microstates dynamics: increased presence of microstate class C and decreased presence of microstate class D, compared to controls. These results suggest that microstate classes C and D capture some genetic component shared by patients and their unaffected siblings, which might be related to schizophrenia. For microstates class B, patients showed decreased mean durations compared to controls. Surprisingly, microstate class B was more present in siblings compared to patients. We interpret this increased presence of microstate class B in siblings as a compensation signal. More specifically, even though patients and siblings share similar traits, e.g., dynamics of microstates class C and D, which might indicate vulnerability for schizophrenia, siblings can somehow counteract these traits by having an increased presence of microstate class B.

We hypothesized that if this increased presence of microstates class B is a “protective” aspect opposing the vulnerability to develop schizophrenia, healthy people with high schizotypal traits may also show similar microstates class B dynamics. To test this hypothesis, we analyzed the resting-state dynamics of EEG microstates in healthy students scoring high vs. the ones scoring low in the CogDis subscale of the O-LIFE questionnaire (19, 23). High CogDis scores reveal a tendency for the participants to have disorganized or derailed thoughts, and are believed to be more clinically relevant than the UnExp and IntAn subscales of the O-LIFE (20). Our results indeed show an increased occurrence of microstate class B in students scoring high in CogDis scores, supporting the compensation signal hypothesis. The two groups did not differ in the dynamics of

the other microstate classes. Our results mirror the findings of Schlegel and colleagues, who showed that students scoring high in the belief of paranormal phenomena have increased microstate class B time coverage and occurrence compared to students scoring low (40). Even though they measured paranormal belief and not directly schizotypal traits, paranormal belief is one of the features of schizotypal personalities (41, 42). Moreover, paranormal believers and high schizotypal subjects tend to have similar EEG hemispheric asymmetries, which has been proposed as a marker for schizotypal ideation (43).

Considering the evidence for a compensation signal in siblings and high schizotypal students, we conjectured whether this increased presence of microstate class B existed in patients with FEP since the disorder has not fully blown. We analyzed the EEG microstates of 22 FEP patients and a subset of 22 chronic schizophrenia patients, selected pseudo-randomly to match the FEP patients' demographics as close as possible. We found no evidence for differences between the two groups in any of the microstates parameters of any of the microstate classes, suggesting that FEP patients do not have the compensation signal. We re-tested FEP patients two other times, separated by six months, and found that the microstates dynamics remained stable (see **Supplementary Information 1.1.** and **2.3**). However, this interpretation should be taken with care since only a subset of the initial 22 FEP (16 in the second testing and 11 in the third testing) participated in the three tests. Nevertheless, these results suggest that the microstates abnormalities are present at the beginning of the disease and remain stable until chronicity is established, which is important for fulfilling the requirements of an endophenotype (14). Moreover, we found no evidence for a compensation mechanism in FEP patients compared to chronic schizophrenia patients, which suggests that the increased presence of microstate class B might be a distinctive feature of a subset of population prone to schizophrenia, but that does not develop the disease.

We updated the meta-analysis of Rieger et al. (11), by including two old studies (37, 38), which were not included in their meta-analysis, and a recent study (39) as well as our results. We also removed one study (12) from their meta-analysis, since it includes only 22q11.2 deletion syndrome patients and not schizophrenia patients (see **Supplementary Information 1.5.** and **2.4**). Our meta-analysis yielded similar results as the ones reported in (11). Namely, increased presence of microstate class C and decreased presence of microstate class D in patients compared to controls, with medium effect sizes. Decreased mean duration of microstates class B in patients compared to

controls, with small effect size. All these effects were significant after correction for multiple comparisons.

In sum, the dynamics of resting-state EEG microstates, particularly classes C and D, is a potential endophenotype for schizophrenia since it meets most of the major criteria proposed by Gottesman and Gould (14) and further practicability and explicability criteria proposed by Turetsky and colleagues (44), discussed one-by-one below. *Association with the disease*: abnormalities in the temporal metrics of microstate classes C and D have been associated with schizophrenia for almost 20 years, with meta-analyses yielding medium effect sizes (11). *Relatives*: here, we showed that unaffected siblings show similar abnormalities as their ill relatives. *State independency*: here, we showed that FEP show similar microstates dynamics as chronic patients and that the dynamics remain stable throughout one year. We did not directly compare the FEP against healthy controls or the effects of medication, but several other studies have done so and found that FEP and un-medicated chronic patients also show similar microstates class C and D deviations (11, 33–35, 37, 38, 45). *Practicability*: resting-state EEG is easily recorded in a 5 minutes session, and EEG montages with as low as 19 electrodes can be used for microstates analysis (28). However, the use of microstates analysis in clinical settings might be limited by the lack of expertise to record EEG, analyze the data and interpret the results. *Explicability*: the abnormal microstates dynamics in schizophrenia are viewed as an imbalance between processes that load on saliency (microstate class C), which are increased, and processes that integrate contextual information (microstate class D), which are reduced (11). This interpretation goes in line with the view of schizophrenia as a state of abnormal assignment of saliency (46) and a disorder affecting attentional processes, context update, and executive control (47). *Heritability*: We currently have no information on the heritability of the patterns of microstate dynamics.

We speculate that EEG microstates dynamics are not only a candidate endophenotype, but also, as our results suggest, they reveal a potential compensation signal that unaffected siblings and healthy people with high schizotypal traits have that might prevent them to develop the disorder. We associate this compensation signal with the increased presence of microstate class B present in these populations. Little is known about microstate class B. It has been related to a resting-state visual network in fMRI (5, 9). In healthy participants, it is the shortest and least frequent microstate from adolescence on (28, 48). Moreover, the visual network is expected to reach maturation much earlier than higher order cognitive networks (49). Combined together, these observations suggest

that the dynamics of microstate class B might be an early marker to discriminate people that are at risk to develop schizophrenia from those that might compensate for their vulnerability.

There are several considerations that should be taken into account regarding our results. First, there are demographics differences between schizophrenia patients, their siblings, and controls. Tomescu and colleagues (48) showed evidence for age and sex-specific effects on the microstates dynamics. Here, we tried to minimize these effects by using them as co-variates in the analyses. Second, schizophrenia is a heterogeneous disease and our samples are small to cover the full schizophrenia spectrum. Third, we cannot exclude the potential effects of treatment in the microstate class B differences between siblings and patients. Fourth, the resting-state EEG was recorded in a protocol that included visual tasks and we cannot exclude potential confoundings. Fifth, EEG was recoded in two different locations, which might be a source of bias. However, there is evidence that EEG findings reproduce well across locations (50). Additionally, we used similar set-ups at both locations.

In conclusion, this is the first study on the temporal dynamics of the four canonical EEG microstates in siblings of schizophrenia patients. Results indicate that the dynamics of resting-state EEG microstates, particularly classes C and D, is a potential endophenotype for schizophrenia. Since the dynamics of microstates can be altered by neurofeedback (51) and transcranial magnetic stimulation (52), these results open avenues for the development of new treatments for the disorder.

Acknowledgments

This work was partially funded by the Fundação para a Ciência e a Tecnologia under grant FCT PD/BD/105785/2014 and the National Centre of Competence in Research (NCCR) Synapsy (The Synaptic Basis of Mental Diseases) under grant 51NF40-158776.

Disclosures

The authors report no biomedical financial interests or potential conflicts of interest.

References

1. Michel CM, Murray MM (2012): Towards the utilization of EEG as a brain imaging tool. *NeuroImage*. 61: 371–385.
2. Khanna A, Pascual-Leone A, Michel CM, Farzan F (2015): Microstates in resting-state EEG: Current status and future directions. *Neuroscience & Biobehavioral Reviews*. 49: 105–113.
3. Michel CM, Koenig T (2018): EEG microstates as a tool for studying the temporal dynamics of whole-brain neuronal networks: A review. *NeuroImage*. 180: 577–593.
4. Lehmann D, Ozaki H, Pal I (1987): EEG alpha map series: brain micro-states by space-oriented adaptive segmentation. *Electroencephalography and Clinical Neurophysiology*. 67: 271–288.
5. Britz J, Van De Ville D, Michel CM (2010): BOLD correlates of EEG topography reveal rapid resting-state network dynamics. *NeuroImage*. 52: 1162–1170.
6. Musso F, Brinkmeyer J, Mobascher A, Warbrick T, Winterer G (2010): Spontaneous brain activity and EEG microstates. A novel EEG/fMRI analysis approach to explore resting-state networks. *NeuroImage*. 52: 1149–1161.
7. Yuan H, Zotev V, Phillips R, Drevets WC, Bodurka J (2012): Spatiotemporal dynamics of the brain at rest — Exploring EEG microstates as electrophysiological signatures of BOLD resting state networks. *NeuroImage*. 60: 2062–2072.
8. Pascual-Marqui RD, Lehmann D, Faber P, Milz P, Kochi K, Yoshimura M, *et al.* (2014): The resting microstate networks (RMN): cortical distributions, dynamics, and frequency specific information flow. *arXiv:1411.1949 [q-bio]*. . Retrieved November 16, 2018, from <http://arxiv.org/abs/1411.1949>.

9. Custo A, Van De Ville D, Wells WM, Tomescu MI, Brunet D, Michel CM (2017): Electroencephalographic Resting-State Networks: Source Localization of Microstates. *Brain Connectivity*. 7: 671–682.
10. Milz P, Pascual-Marqui RD, Achermann P, Kochi K, Faber PL (2017): The EEG microstate topography is predominantly determined by intracortical sources in the alpha band. *NeuroImage*. 162: 353–361.
11. Rieger K, Diaz Hernandez L, Baenninger A, Koenig T (2016): 15 Years of Microstate Research in Schizophrenia – Where Are We? A Meta-Analysis. *Front Psychiatry*. 7. doi: 10.3389/fpsyt.2016.00022.
12. Tomescu MI, Rihs TA, Becker R, Britz J, Custo A, Grouiller F, *et al.* (2014): Deviant dynamics of EEG resting state pattern in 22q11.2 deletion syndrome adolescents: A vulnerability marker of schizophrenia? *Schizophrenia Research*. 157: 175–181.
13. Tomescu MI, Rihs TA, Roinishvili M, Karahanoglu FI, Schneider M, Menghetti S, *et al.* (2015): Schizophrenia patients and 22q11.2 deletion syndrome adolescents at risk express the same deviant patterns of resting state EEG microstates: A candidate endophenotype of schizophrenia. *Schizophrenia Research: Cognition*. 2: 159–165.
14. Gottesman II, Gould TD (2003): The Endophenotype Concept in Psychiatry: Etymology and Strategic Intentions. *AJP*. 160: 636–645.
15. Claridge G, Beech T (1995): Fully and quasi-dimensional constructions of schizotypy. In: Raine A, Lencz T, Mednick SA, editors. *Schizotypal Personality*. Cambridge University Press.

16. Nelson MT, Seal ML, Pantelis C, Phillips LJ (2013): Evidence of a dimensional relationship between schizotypy and schizophrenia: A systematic review. *Neuroscience & Biobehavioral Reviews*. 37: 317–327.
17. Ettinger U, Meyhöfer I, Steffens M, Wagner M, Koutsouleris N (2014): Genetics, Cognition, and Neurobiology of Schizotypal Personality: A Review of the Overlap with Schizophrenia. *Frontiers in Psychiatry*. 5. doi: 10.3389/fpsyt.2014.00018.
18. Kwapil TR, Barrantes-Vidal N (2015): Schizotypy: Looking Back and Moving Forward. *Schizophrenia Bulletin*. 41: S366–S373.
19. Mason O, Linney Y, Claridge G (2005): Short scales for measuring schizotypy. *Schizophrenia Research*. 78: 293–296.
20. Polner B, Faiola E, Urquijo MF, Meyhöfer I, Steffens M, Rónai L, *et al.* (2018): The Network Structure of Schizotypy in the General Population. . doi: 10.31234/osf.io/p389m.
21. Demjaha A, Valmaggia L, Stahl D, Byrne M, McGuire P (2012): Disorganization/Cognitive and Negative Symptom Dimensions in the At-Risk Mental State Predict Subsequent Transition to Psychosis. *Schizophr Bull*. 38: 351–359.
22. da Cruz JR, Shaqiri A, Roinishvili M, Chkonia E, Brand A, Figueiredo P, Herzog MH (submitted): Neural compensation mechanisms of siblings of schizophrenia patients as revealed by high-density EEG. .
23. Sierro G, Rossier J, Mason OJ, Mohr C (2016): French Validation of the O-LIFE Short Questionnaire. *European Journal of Psychological Assessment*. 32: 195–203.
24. Favrod O, Sierro G, Roinishvili M, Chkonia E, Mohr C, Herzog MH, Cappe C (2017): Electrophysiological correlates of visual backward masking in high schizotypic personality traits participants. *Psychiatry Research*. 254: 251–257.

25. Favrod O, Roinishvili M, da Cruz JR, Brand A, Okruashvili M, Gamkrelidze T, *et al.* (2018): Electrophysiological correlates of visual backward masking in patients with first episode psychosis. *Psychiatry Research: Neuroimaging*. . doi: 10.1016/j.pscychresns.2018.10.008.
26. da Cruz JR, Chicherov V, Herzog MH, Figueiredo P (2018): An automatic pre-processing pipeline for EEG analysis (APP) based on robust statistics. *Clinical Neurophysiology*. 129: 1427–1437.
27. Lehmann D, Skrandies W (1980): Reference-free identification of components of checkerboard-evoked multichannel potential fields. *Electroencephalography and Clinical Neurophysiology*. 48: 609–621.
28. Koenig T, Prichep L, Lehmann D, Sosa PV, Braeker E, Kleinlogel H, *et al.* (2002): Millisecond by Millisecond, Year by Year: Normative EEG Microstates and Developmental Stages. *NeuroImage*. 16: 41–48.
29. Brunet D, Murray MM, Michel CM (2011): Spatiotemporal Analysis of Multichannel EEG: CARTOOL. *Intell Neuroscience*. 2011: 2:1–2:15.
30. Murray MM, Brunet D, Michel CM (2008): Topographic ERP Analyses: A Step-by-Step Tutorial Review. *Brain Topogr*. 20: 249–264.
31. Brandeis D, Naylor H, Halliday R, Callaway E, Yano L (1992): Scopolamine Effects on Visual Information Processing, Attention, and Event-Related Potential Map Latencies. *Psychophysiology*. 29: 315–335.
32. Pascual-Marqui RD, Michel CM, Lehmann D (1995): Segmentation of brain electrical activity into microstates: model estimation and validation. *IEEE Transactions on Biomedical Engineering*. 42: 658–665.

33. Koenig T, Lehmann D, Merlo MCG, Kochi K, Hell D, Koukkou M (1999): A deviant EEG brain microstate in acute, neuroleptic-naïve schizophrenics at rest. *European Archives of Psychiatry and Clinical Neuroscience*. 249: 205–211.
34. Lehmann D, Faber PL, Galderisi S, Herrmann WM, Kinoshita T, Koukkou M, *et al.* (2005): EEG microstate duration and syntax in acute, medication-naïve, first-episode schizophrenia: a multi-center study. *Psychiatry Research: Neuroimaging*. 138: 141–156.
35. Kikuchi M, Koenig T, Wada Y, Higashima M, Koshino Y, Strik W, Dierks T (2007): Native EEG and treatment effects in neuroleptic-naïve schizophrenic patients: Time and frequency domain approaches. *Schizophrenia Research*. 97: 163–172.
36. Andreou C, Faber PL, Leicht G, Schoettle D, Polomac N, Hanganu-Opatz IL, *et al.* (2014): Resting-state connectivity in the prodromal phase of schizophrenia: Insights from EEG microstates. *Schizophrenia Research*. 152: 513–520.
37. Strelets V, Faber PL, Golikova J, Novototsky-Vlasov V, Koenig T, Gianotti LRR, *et al.* (2003): Chronic schizophrenics with positive symptomatology have shortened EEG microstate durations. *Clinical Neurophysiology*. 114: 2043–2051.
38. Irisawa S, Isotani T, Yagyu T, Morita S, Nishida K, Yamada K, *et al.* (2006): Increased Omega Complexity and Decreased Microstate Duration in Nonmedicated Schizophrenic Patients. *NPS*. 54: 134–139.
39. Giordano GM, Koenig T, Mucci A, Vignapiano A, Amodio A, Di Lorenzo G, *et al.* (2018): Neurophysiological correlates of Avolition-apathy in schizophrenia: A resting-EEG microstates study. *NeuroImage: Clinical*. 20: 627–636.
40. Schlegel F, Lehmann D, Faber PL, Milz P, Gianotti LRR (2012): EEG Microstates During Resting Represent Personality Differences. *Brain Topogr*. 25: 20–26.

41. Meehl PE (1962): Schizotaxia, schizotypy, schizophrenia. *American Psychologist*. 17: 827–838.
42. Eckblad M, Chapman LJ (1983): Magical ideation as an indicator of schizotypy. *Journal of Consulting and Clinical Psychology*. 51: 215–225.
43. Pizzagalli D, Lehmann D, Gianotti L, Koenig T, Tanaka H, Wackermann J, Brugger P (2000): Brain electric correlates of strong belief in paranormal phenomena: intracerebral EEG source and regional Omega complexity analyses. *Psychiatry Research: Neuroimaging*. 100: 139–154.
44. Turetsky BI, Calkins ME, Light GA, Olincy A, Radant AD, Swerdlow NR (2007): Neurophysiological Endophenotypes of Schizophrenia: The Viability of Selected Candidate Measures. *Schizophr Bull*. 33: 69–94.
45. Nishida K, Morishima Y, Yoshimura M, Isotani T, Irisawa S, Jann K, *et al.* (2013): EEG microstates associated with salience and frontoparietal networks in frontotemporal dementia, schizophrenia and Alzheimer’s disease. *Clinical Neurophysiology*. 124: 1106–1114.
46. Kapur S (2003): Psychosis as a State of Aberrant Salience: A Framework Linking Biology, Phenomenology, and Pharmacology in Schizophrenia. *AJP*. 160: 13–23.
47. Fioravanti M, Bianchi V, Cinti ME (2012): Cognitive deficits in schizophrenia: an updated metaanalysis of the scientific evidence. *BMC Psychiatry*. 12: 64.
48. Tomescu MI, Rihs TA, Rochas V, Hardmeier M, Britz J, Allali G, *et al.* (2018): From swing to cane: Sex differences of EEG resting-state temporal patterns during maturation and aging. *Developmental Cognitive Neuroscience*. 31: 58–66.

49. Gogtay N, Giedd JN, Lusk L, Hayashi KM, Greenstein D, Vaituzis AC, *et al.* (2004): Dynamic mapping of human cortical development during childhood through early adulthood. *Proc Natl Acad Sci U S A.* 101: 8174–8179.
50. John ER (1977): *Neurometrics: Clinical Applications of Quantitative Electrophysiology.* John Wiley & Sons.
51. Hernandez LD, Rieger K, Baenninger A, Brandeis D, Koenig T (2016): Towards Using Microstate-Neurofeedback for the Treatment of Psychotic Symptoms in Schizophrenia. A Feasibility Study in Healthy Participants. *Brain Topogr.* 29: 308–321.
52. Sverak T, Albrechtova L, Lamos M, Rektorova I, Ustohal L (2018): Intensive repetitive transcranial magnetic stimulation changes EEG microstates in schizophrenia: A pilot study. *Schizophrenia Research.* 193: 451–452.
53. Stäblein M, Storchak H, Ghinea D, Kraft D, Knöchel C, Prvulovic D, *et al.* (2018): Visual working memory encoding in schizophrenia and first-degree relatives: neurofunctional abnormalities and impaired consolidation. *Psychological Medicine.* 1–9.
54. Cappe C, Herzog MH, Herzig DA, Brand A, Mohr C (2012): Cognitive disorganisation in schizotypy is associated with deterioration in visual backward masking. *Psychiatry Research.* 200: 652–659.
55. Chkonia E, Roinishvili M, Makhatadze N, Tsverava L, Stroux A, Neumann K, *et al.* (2010): The Shine-Through Masking Paradigm Is a Potential Endophenotype of Schizophrenia. *PLoS ONE.* 5: e14268.
56. Plomp G, Roinishvili M, Chkonia E, Kapanadze G, Kereselidze M, Brand A, Herzog MH (2013): Electrophysiological Evidence for Ventral Stream Deficits in Schizophrenia Patients. *Schizophr Bull.* 39: 547–554.

57. Braff DL, Freedman R, Schork NJ, Gottesman II (2007): Deconstructing Schizophrenia: An Overview of the Use of Endophenotypes in Order to Understand a Complex Disorder. *Schizophr Bull.* 33: 21–32.

Table Legends

Table 1 – Simple main effects of group, Bonferroni-Holm corrected, for each microstate parameter (mean duration, time coverage, and occurrence). Results show evidence for group differences in microstate classes B, C, and D, for all microstate parameters. Statistically significant differences are indicated in bold.

Table 2 – Post-hoc group comparisons (Group I vs Group II) of all microstate parameters (mean duration, time coverage, and occurrence), using Bonferroni-Holm correction, for each microstate class that yielded a significant simple main effect of group (microstate classes B, C, and D). Statistically significant differences are indicated in bold.

Figure Legends

Figure 1 – Results of the microstate analysis for patients (red), siblings (blue) and controls (black). a) The spatial configuration of the four microstate classes (A, B, C, D) for the three groups. Statistically significant group differences, Bonferroni-Holm corrected, were found for all computed microstates parameters: b) mean duration, c) time coverage, and d) occurrence. Error bars indicate standard error of the mean. (* $p < 0.05$, ** $p < 0.01$, *** $p < 0.001$). Group average statistics are also shown in **Supplementary Table S7**.

Figure 2 – Results of the EEG microstate analysis for High Schizotypal (red) and Low Schizotypal (black) groups. a) The spatial configuration of the four microstate classes (A, B, C, D) for the two groups. Statistically significant group differences, Bonferroni-Holm corrected, were found in microstate class B for d) occurrence. No group differences were

found for b) mean duration, and c) time coverage. Error bars indicate standard error of the mean. (** $p < 0.01$). Group average statistics are shown in **Supplementary Table S8**.

Figure 3 – Results of the microstate analysis for the patients with first episode of psychosis (FEP, in green) and their matched schizophrenia patients (Patients_22, in red). a) The spatial configuration of the four microstate classes (A, B, C, D) for the two groups. No statistically significant group differences were found for any of the computed microstates parameters: b) mean duration, c) time coverage, and d) occurrence. Error bars indicate standard error of the mean. Group average statistics are also shown in **Supplementary Table S9**.

Tables

Table 1

Microstate Class	Mean Duration	Time Coverage	Occurrence
A	$P=0.259, \eta^2=0.014$	$P=0.212, \eta^2=0.016$	$P=0.219, \eta^2=0.016$
B	$P<0.001, \eta^2=0.076$	$P=0.001, \eta^2=0.074$	$P=0.005, \eta^2=0.059$
C	$P<0.001, \eta^2=0.087$	$P<0.001, \eta^2=0.140$	$P<0.001, \eta^2=0.108$
D	$P<0.001, \eta^2=0.126$	$P<0.001, \eta^2=0.133$	$P=0.001, \eta^2=0.084$

Table 2

Parameter	Group I	Group II	Class B	Class C	Class D
Mean Duration	Patients	Siblings	$p<0.001, g=0.738$	$p=0.152, g=0.288$	$p=0.916, g=0.023$
		Controls	$p=0.043, g=0.381$	$p<0.001, g=0.716$	$p<0.001, g=0.752$
	Siblings	Controls	$p=0.063, g=0.365$	$p=0.152, g=0.394$	$p<0.001, g=0.724$
Time Coverage	Patients	Siblings	$p<0.001, g=0.734$	$p=0.064, g=0.346$	$p=0.670, g=0.090$
		Controls	$p=0.073, g=0.340$	$p<0.001, g=0.913$	$p<0.001, g=0.795$
	Siblings	Controls	$p=0.073, g=0.405$	$p=0.017, g=0.50$	$p<0.001, g=0.724$
Occurrence	Patients	Siblings	$p=0.002, g=0.649$	$p=0.139, g=0.327$	$p=0.527, g=0.118$
		Controls	$p=0.105, g=0.281$	$p<0.001, g=0.767$	$p<0.001, g=0.653$
	Siblings	Controls	$p=0.105, g=0.391$	$p=0.034, g=0.429$	$p=0.017, g=0.560$

Figures

Figure 1

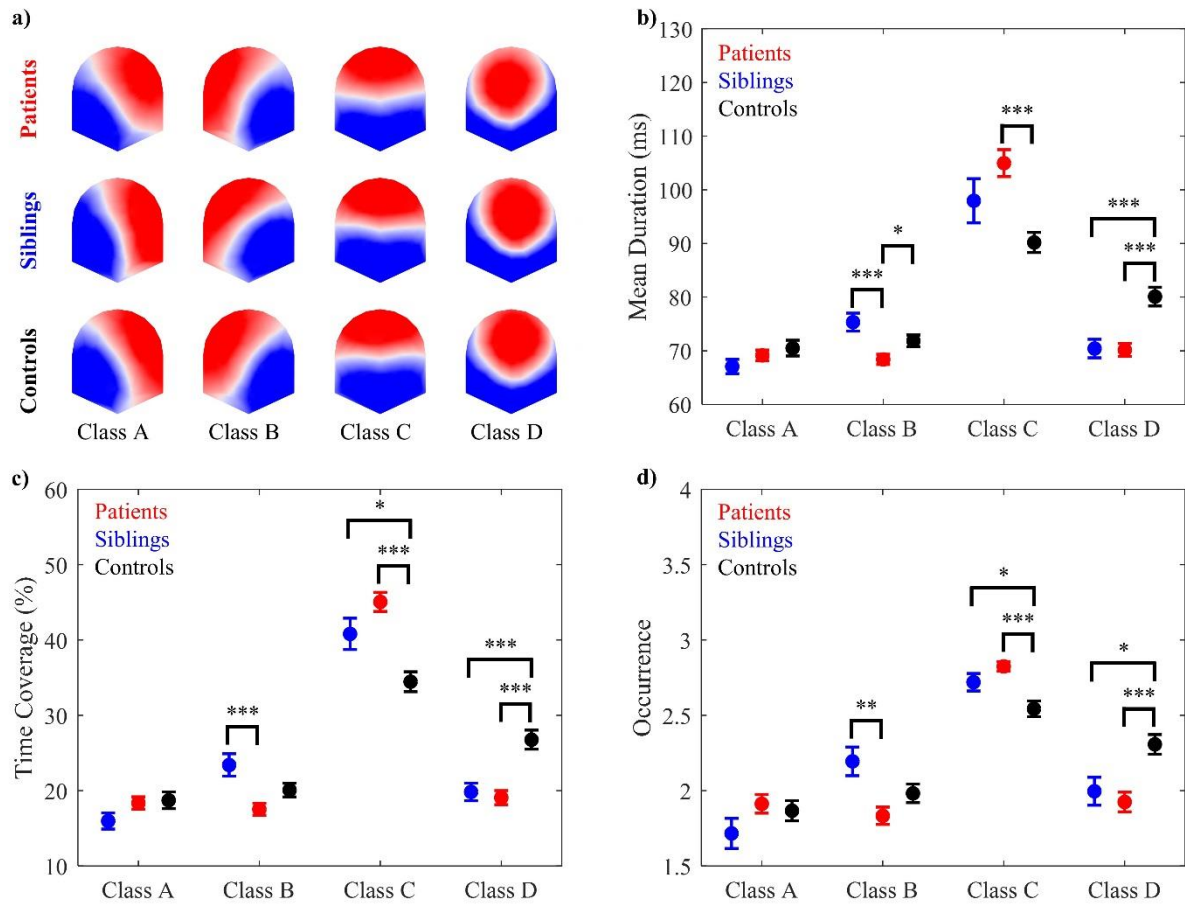


Figure 2

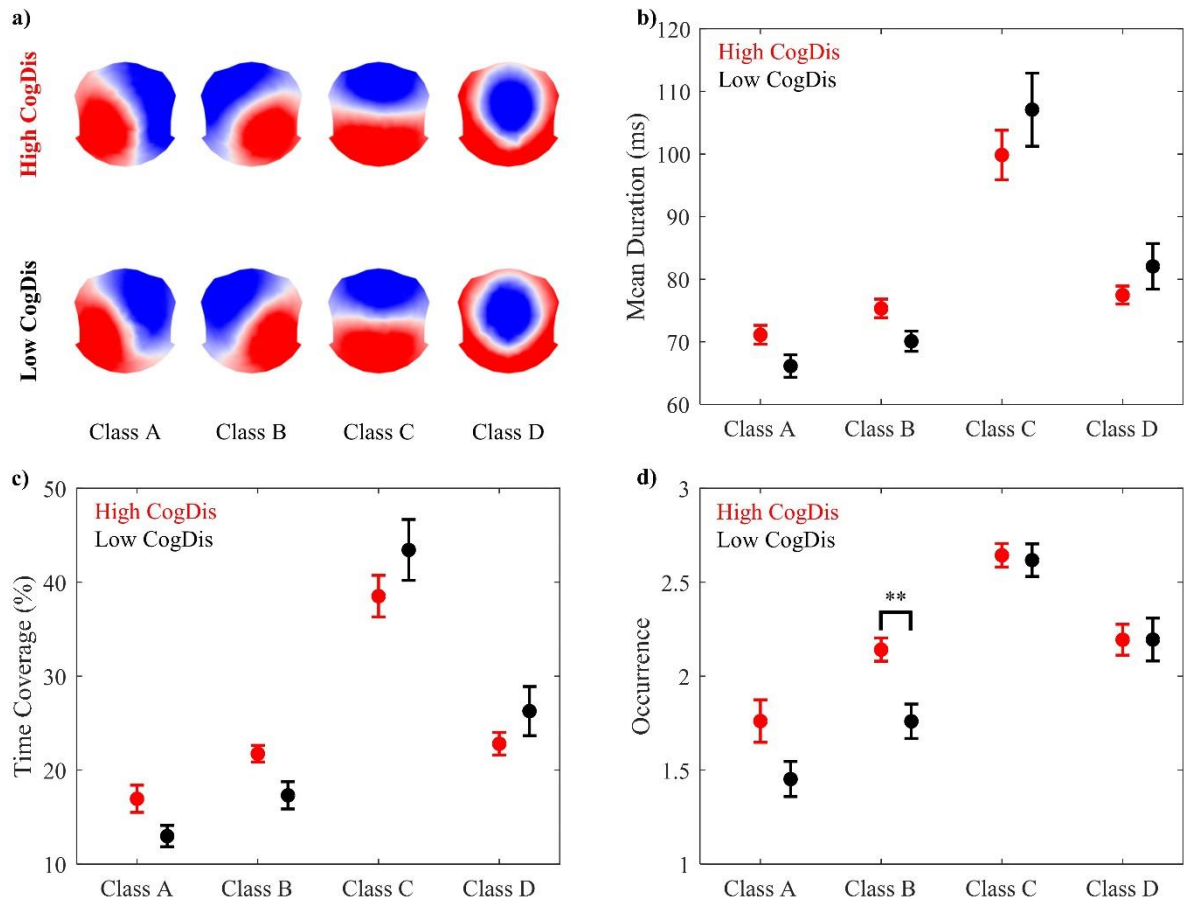
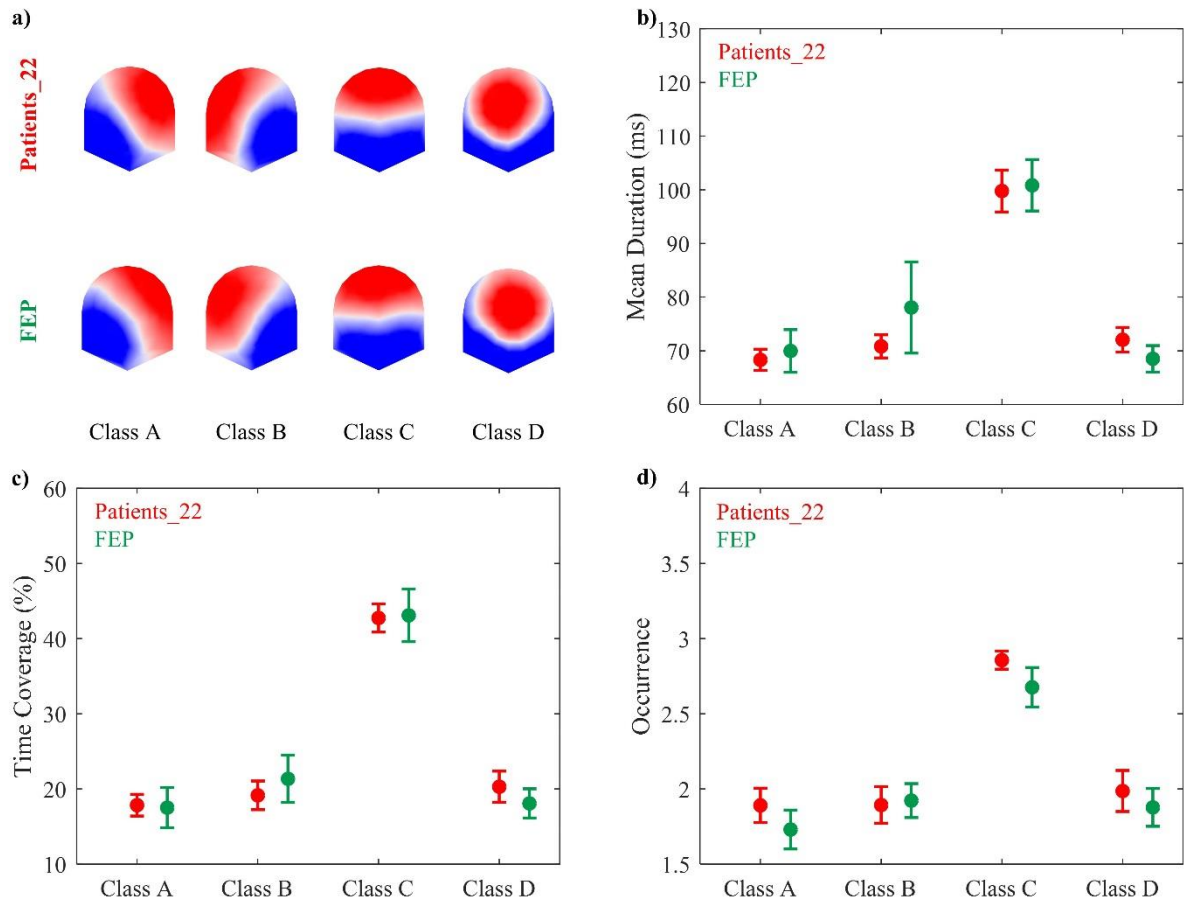


Figure 3



Supplementary Information

EEG microstates: a candidate endophenotype for schizophrenia

Authors: Janir Ramos da Cruz^{1,2*}, Ophélie Favrod¹, Maya Roinishvili^{3,4}, Eka Chkonia^{4,5}, Andreas Brand¹, Christine Mohr⁶, Patrícia Figueiredo², and Michael H. Herzog¹

Affiliations:

¹ Laboratory of Psychophysics, Brain Mind Institute, École Polytechnique Fédérale de Lausanne (EPFL), Switzerland

² Institute for Systems and Robotics – Lisbon (LARSys) and Department of Bioengineering, Instituto Superior Técnico, Universidade de Lisboa, Portugal

³ Laboratory of Vision Physiology, Beritashvili Centre of Experimental Biomedicine, Tbilisi, Georgia

⁴ Institute of Cognitive Neurosciences, Free University of Tbilisi, Tbilisi, Georgia

⁵ Department of Psychiatry, Tbilisi State Medical University, Tbilisi, Georgia

⁶ Faculté des Sciences Sociales et Politiques, Institut de Psychologie, Bâtiment Geopolis, Lausanne, Switzerland

***Corresponding author:**

Janir Ramos da Cruz, Laboratory of Psychophysics, Brain Mind Institute, School of Life Sciences, École Polytechnique Fédérale de Lausanne (EPFL), CH-1015 Lausanne, Switzerland

Phone number: +41 21 693 17 42

Email: janir.amos@epfl.ch

1. Supplementary Methods

1.1. Experiment 1: Patients, Siblings, and Controls

Group characteristics of schizophrenia patients, their unaffected siblings, and healthy controls are presented in **Table S1**.

Table S1 – Group average statistics (\pm SD) of Schizophrenia Patients, their Unaffected Siblings, and Healthy Controls

	Patients	Siblings	Controls	Statistics
Gender (F/M)	10/79	17/21	36/33	$\chi^2(2)=33.290, P<0.001$
Age (years)	36.5 ± 8.9	30.7 ± 10.2	35.3 ± 7.7	$F(2,193)=5.762, P=0.004$
Education (years)	13.5 ± 2.7	14.1 ± 3.0	15.1 ± 2.8	$F(2,193)=6.867, P=0.001$
Handedness (L/R)	4/85	2/36	4/65	$\chi^2(2)=0.139, P=0.933$
Illness duration (years)	12.5 ± 8.1			
SANS	10.2 ± 5.2			
SAPS	9.8 ± 8.1			
CPZ	573.3 ± 402.2			

Abbreviations: SANS, Scale for the Assessment of Negative Symptoms; SAPS, Scale for the Assessment of Positive Symptoms; CPZ, Chlorpromazine

1.2. Experiment 2: High and Low Schizotypal Traits

Group characteristics of healthy students scoring either high or low in the cognitive disorganization (CogDis) subscale of the Oxford-Liverpool Inventory Experiences (O-LIFE) short questionnaire are presented in **Table S2**. As aimed for, there was a significant group \times O-LIFE subscales interaction ($F(2,80)=48.65$, $P<0.001$, $\eta^2=0.266$). Bonferroni-Holm corrected simple main effects, revealed that the groups differed only on the CogDis dimension.

Table S2 – Group average statistics (\pm SD) of the High and Low CogDis groups

	High CogDis	Low CogDis	Statistics
Gender (F/M)	18/4	16/4	$\chi^2(1)=0.022$, $p=0.881$
Age (years)	21.2 ± 2.7	20.9 ± 2.8	$t(40)=0.394$, $p=0.696$
Handedness (L/R)	1/21	3/17	$\chi^2(1)=1.329$, $p=0.249$
CogDis	8.5 ± 1.2	2.6 ± 1.0	$t(40)=17.150$, $p<0.001$
UnExp	2.5 ± 2.3	2.2 ± 2.0	$t(40)=0.377$, $p=0.71$
IntAn	1.7 ± 1.5	1.0 ± 0.9	$t(40)=2.066$, $p=0.091$

Abbreviations: CogDis, Cognitive Disorganization; UnExp, Unusual Experiences; IntAn, Introvertive Anhedonia

1.3.Experiment 3: FEP

Group characteristics of patients with a first episode of psychosis (FEP) and a sub-group of chronic schizophrenia patients (Patients_22), pseudo-randomly selected to match the FEP as closely as possible, are shown in **Table S3**.

Table S3 – Group average statistics (\pm SD) of the FEP and Patients_22 groups

	FEP	Patients_22	Statistics
Gender (F/M)	12/10	8/14	$\chi^2(1)=1.467, p=0.226$
Age (years)	29.6 ± 9.1	31.3 ± 10.1	$t(42)=0.563, p=0.576$
Education (years)	12.9 ± 2.5	13.5 ± 2.7	$t(42)=0.780, p=0.440$
Handedness (L/R)	1/21	1/21	$\chi^2(1)=0.000, p=1.000$
Illness duration (years)	0.7 ± 0.4	7.2 ± 5.2	$t(42)=5.838, p<0.001$
SANS	7.6 ± 4.8	10.7 ± 4.2	$t(42)=2.271, p=0.028$
SAPS	6.7 ± 3.1	9.0 ± 3.0	$t(42)=2.433, p=0.019$
CPZ	465.3 ± 312.6	495.0 ± 285.5	$t(36)=0.305, p=0.762$

Abbreviations: SANS, Scale for the Assessment of Negative Symptoms; SAPS, Scale for the Assessment of Positive Symptoms; CPZ, Chlorpromazine

We tested the FEP group three times throughout one year to assess whether the microstates dynamics change with the progression of the disease. Out of the 22 patients, 16 participated six months later on a second session. Out of these 16, 11 were tested six months later on a third session. All the 22 FEP were invited to participate in all three session but six of them decided to quit the study after the first session and the other five patients opted to leave the study after the second session. Group characteristics of the FEP that participated in the first and second testing sessions (FEP_2) and all the three testing sessions (FEP_3) are shown in **Table S4**.

To investigate whether the computed microstates parameters changed throughout one year, for the FEPs, we used *lme4* (1) to perform a linear mixed effect analysis of the relationship between the testing session and each of the three computed microstate parameters. As fixed effects, we used testing session (first, second, and third) and microstate class (A, B, C, and D; with the interaction term) into each model. As random effects, we had intercepts for subjects and by-subject slopes for the effect of testing session and microstate class. *P*-values were obtained by likelihood ratio tests

of the full model with the interaction term against the model with additive effects of testing session and microstate class. In case of no significant differences between the two above-mentioned models, the model with additive effects was compared against a reduced model without the effect of testing session, by means of likelihood ratio tests.

Table S4 – Group average statistics (\pm SD) of the patients with first episode of psychosis that participated in the first testing session (FEP), first and second (FEP_2), and all the three testing sessions (FEP_3)

	FEP	FEP_2	FEP_3
Gender (F/M)	12/10	10/6	6/5
Age (years)	29.6 \pm 9.1	29.1 \pm 9.1	29.4 \pm 10.9
Education (years)	12.9 \pm 2.5	12.6 \pm 2.4	12.7 \pm 2.3
Handedness (L/R)	1/21	1/15	0/11
Illness duration (months)	0.7 \pm 0.4	0.7 \pm 0.4	0.8 \pm 0.4
SANS	7.6 \pm 4.8	10.5 \pm 5.7	9.8 \pm 6.4
SAPS	6.7 \pm 3.1	6.2 \pm 3.3	6.7 \pm 2.5
CPZ	465.3 \pm 312.6	412.5 \pm 378.64	239.8 \pm 191.9

Abbreviations: SANS, Scale for the Assessment of Negative Symptoms; SAPS, Scale for the Assessment of Positive Symptoms; CPZ, Chlorpromazine

1.4. EEG Pre-processing

Offline, data were downsampled to 128Hz and processed using an automatic pre-processing pipeline (APP) (2): filtering with a bandpass of 1–40Hz; removal of powerline noise; re-referencing to the biweight estimate of the mean of all channels; removal and 3D spline interpolation of bad channels; removal of bad EEG periods; independent component analysis (ICA) to remove eye movement-, muscular- and bad channel-related artifacts; re-referencing to common average-reference. The proportion of interpolated electrodes was less than 5% for each participant.

1.5. Meta-analysis

We updated the meta-analysis of Rieger et al. (3). We included two old studies (4, 5), which were not included in the first meta-analysis and we added two recent studies: Giordano et al. (6), and the current one (da Cruz et al.). Moreover, we removed one study (7) from the original meta-analysis, since it includes only 22q11.2 deletion syndrome patients and not schizophrenia patients.

For each study, we calculated Cohen's d as the mean difference between patients and controls divided by the pooled standard deviation. Standardized effect sizes (Hedges' g) were calculated using Cohen's d multiplied by the coefficient J , which is a correction for small samples. In studies where the group average statistics were not reported, p -values were converted to Hedges' g using equivalent statistics as suggested by Francis (8).

Hedges' g s were introduced as a generic effect size in the OpenMeta Analyst software (<http://www.cebm.brown.edu/openmeta/>) with the corresponding variance (SE). We used the continuous random-effect analysis with the DerSimonian-Laird (DL) method. The meta-analysis software computed the effect sizes, with 95% confidence intervals (C.I.) and the pooled effect size g^* . P -values were corrected for multiple comparisons using Bonferroni-Holm correction.

2. Supplementary Results

2.1. Patients, siblings, and controls

High spatial correlation coefficients indicated that the microstate classes were similar between groups (**Table S5**). Additionally, we performed topographical ANOVAs (TANOVAs) (9, 10) to investigate whether there were systematic group differences in the microstates classes. The resulting p -values of the TANOVA (not corrected for multiple comparisons) are shown in **Table S6**. The only statistical significant group difference was found between siblings and controls for microstate class A ($p=0.036$). However, this difference disappears after correcting for multiple comparisons using Bonferroni-Holm ($p=0.144$).

Table S5 – Spatial correlation coefficients between microstate class topographies in each pair of groups. The high coefficients indicate that the microstate classes were similar between groups.

Microstate class	Patients vs Siblings	Patients vs Controls	Controls vs Siblings
A	0.94	0.97	0.97
B	0.97	0.99	0.97
C	0.99	0.99	0.99
D	0.91	0.93	0.98

Table S6 – TANOVA results between microstate class topographies in each pair of groups (p -values are not corrected for multiple comparisons).

Microstate class	Patients vs Siblings	Patients vs Controls	Controls vs Siblings
A	0.308	0.448	0.036
B	0.778	0.769	0.396
C	0.279	0.302	0.364
D	0.519	0.131	0.147

Table S7 – Group average statistics (\pm SD) of the Schizophrenia Patients, their Unaffected Siblings and Healthy Controls for all the computed microstates parameters and classes.

Microstate Parameter	Microstate Class	Group		
		Patients	Siblings	Controls
Mean Duration (ms)	A	69.14 \pm 9.51	67.07 \pm 8.16	70.50 \pm 12.15
	B	68.39 \pm 8.94	75.34 \pm 10.28	71.84 \pm 9.07
	C	105.00 \pm 23.71	97.95 \pm 25.41	90.18 \pm 15.51
	D	70.16 \pm 11.55	70.41 \pm 10.64	80.10 \pm 14.52
Time Coverage (%)	A	18.36 \pm 7.71	15.96 \pm 6.62	18.71 \pm 9.18
	B	17.51 \pm 7.42	23.40 \pm 9.16	20.07 \pm 7.56
	C	45.06 \pm 11.98	40.81 \pm 12.82	34.46 \pm 10.98
	D	19.07 \pm 8.86	19.83 \pm 7.20	26.76 \pm 10.54
Occurrence	A	1.91 \pm 0.58	1.72 \pm 0.61	1.87 \pm 0.56
	B	1.83 \pm 0.54	2.19 \pm 0.59	1.98 \pm 0.51
	C	2.83 \pm 0.30	2.72 \pm 0.36	2.54 \pm 0.44
	D	1.92 \pm 0.61	2.00 \pm 0.57	2.31 \pm 0.54

2.2. High and Low CogDis

High spatial correlation coefficients were found between the microstate classes of the High and Low CogDis groups: 0.91 (A-A), 0.96 (B-B), 0.99 (C-C), and 0.98 (D-D). In addition, we performed TANOVA for each microstate class between the two groups and we found no statistical significant differences (A-A, $p=0.871$; B-B, $p=0.457$; C-C, $p=0.395$; D-D, $p=0.051$; no correction for multiple comparisons).

Table S8 – Group average statistics (\pm SD) of the High and Low CogDis groups for all the computed microstates parameters and classes.

Microstate Parameter	Microstate Class	Group	
		High CogDis	Low CogDis
Mean Duration (ms)	A	71.12 \pm 7.06	66.14 \pm 7.97
	B	75.33 \pm 6.91	70.09 \pm 7.23
	C	99.84 \pm 18.53	107.1 \pm 26.15
	D	77.47 \pm 6.77	82.06 \pm 16.28
Time Coverage (%)	A	16.94 \pm 6.77	12.97 \pm 5.07
	B	21.74 \pm 4.17	17.32 \pm 6.48
	C	38.51 \pm 10.34	43.43 \pm 14.49
	D	22.80 \pm 5.62	26.28 \pm 11.68
Occurrence	A	1.76 \pm 0.53	1.45 \pm 0.42
	B	2.14 \pm 0.29	1.76 \pm 0.41
	C	2.64 \pm 0.29	2.62 \pm 0.39
	D	2.19 \pm 0.38	2.19 \pm 0.51

Since a two-way repeated measures ANOVA yielded a marginally significant group (High and Low CogDis) \times microstate class (A, B, C, and D) interaction for time coverage ($F(3,120)=2.479$, $P=0.064$, $\eta^2=0.026$), we re-analyzed the data by estimating Bayes factors. A JZS Bayes factor two-way repeated measures ANOVA (11) with default prior scales revealed that the interaction model was preferred to the main effects model by a Bayes factor of 2.312. Therefore, the data provide only weak evidence to the hypothesis that group and microstate class interact in the time coverage of microstates.

2.3. FEP

High spatial correlation coefficients were found between the microstate classes of the FEP and patients: 0.97 (A-A), 0.96 (B-B), 0.99 (C-C), and 0.91 (D-D). Additionally, we performed TANOVA for each microstate class between the two groups and we found no statistical significant differences (A-A, $p=0.518$; B-B, $p=0.245$; C-C, $p=0.450$; D-D, $p=0.174$; no correction for multiple comparisons).

Table S9 – Group average statistics (\pm SD) of the FEP and Patients_22 groups for all the computed microstates parameters and classes.

Microstate Parameter	Microstate Class	Group	
		FEP	Patients_22
Mean Duration (ms)	A	69.97 \pm 18.62	68.31 \pm 9.26
	B	78.07 \pm 39.85	70.82 \pm 10.12
	C	100.80 \pm 22.48	99.78 \pm 18.33
	D	68.50 \pm 11.55	72.06 \pm 10.73
Time Coverage (%)	A	17.51 \pm 12.58	17.83 \pm 6.77
	B	21.34 \pm 14.75	19.14 \pm 8.97
	C	43.08 \pm 16.43	42.74 \pm 8.79
	D	18.07 \pm 9.10	20.29 \pm 9.71
Occurrence	A	1.73 \pm 0.61	1.89 \pm 0.53
	B	1.92 \pm 0.53	1.89 \pm 0.57
	C	2.68 \pm 0.62	2.86 \pm 0.28
	D	1.88 \pm 0.59	1.99 \pm 0.64

Summary statistics of the computed microstates parameters for the FEP group for the three measurements throughout one year (FEP, FEP_2, FEP_3) is shown in **Figure S1** and **Table S10**. No statistically significant interaction was found for any of the three microstates parameters: mean duration ($\chi^2(6)=4.338$, $p=0.631$), time of coverage ($\chi^2(6)=3.494$, $p=0.745$), and occurrence ($\chi^2(6)=4.069$, $p=0.667$). Similarly, no statistically significant effect of testing session was found for any of the three microstate parameters: mean duration ($\chi^2(2)=1.363$, $p=0.506$), time of coverage ($\chi^2(2)=0.877$, $p=0.645$), and occurrence ($\chi^2(2)=0.748$, $p=0.688$).

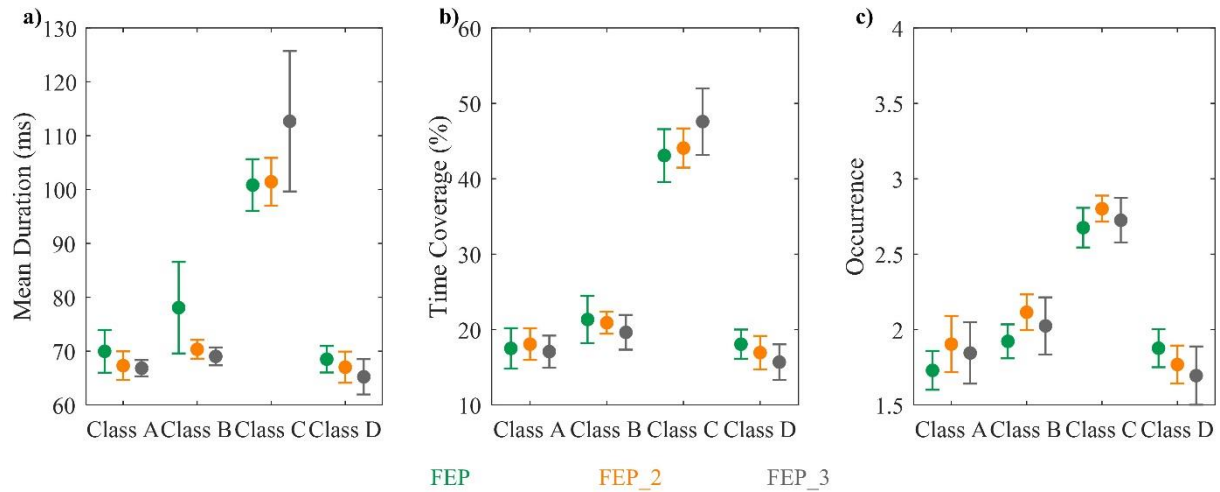


Figure S1 – Results of the microstate analysis for the patients with first episode of psychosis, for the three testing sessions: first session (FEP, in green), second session (FEP_2, in orange), and third session (FEP_3, in grey). No statistically significant testing session differences were found for any of the computed microstates parameters: a) mean duration, b) time coverage, and c) occurrence. Error bars indicate standard error of the mean. Group average statistics are also shown in **Table S10**.

Table S10 – Group average statistics (\pm SD) of the patients with first episode of psychosis for the three testing sessions (FEP, FEP_2, and FEP_3) for all the computed microstates parameters and classes.

Microstate Parameter	Microstate Class	Group		
		FEP (n=22)	FEP_2 (n=16)	FEP_3 (n=11)
Mean Duration (ms)	A	69.97 \pm 18.62	67.31 \pm 10.61	66.84 \pm 5.00
	B	78.07 \pm 39.85	70.34 \pm 6.99	69.03 \pm 5.53
	C	100.80 \pm 22.48	101.44 \pm 17.68	112.68 \pm 43.22
	D	68.50 \pm 11.55	67.02 \pm 11.59	65.24 \pm 10.87
Time Coverage (%)	A	17.51 \pm 12.58	18.07 \pm 8.38	17.09 \pm 7.03
	B	21.34 \pm 14.75	20.91 \pm 5.83	19.64 \pm 7.66
	C	43.08 \pm 16.43	44.08 \pm 10.40	47.58 \pm 14.62
	D	18.07 \pm 9.10	16.95 \pm 8.83	15.69 \pm 7.81
Occurrence	A	1.73 \pm 0.61	1.90 \pm 0.75	1.85 \pm 0.68
	B	1.92 \pm 0.53	2.12 \pm 0.47	2.03 \pm 0.63
	C	2.68 \pm 0.62	2.80 \pm 0.35	2.73 \pm 0.49
	D	1.88 \pm 0.59	1.77 \pm 0.50	1.70 \pm 0.64

2.4. Meta-analysis

The forest plots of the significant mean effect sizes are shown in **Figure S2 - Figure S6**. Similar to Rieger et al. (3), we found consistently increased time coverage ($g=0.593$, $p<0.001$) and occurrence ($g=0.745$, $p<0.001$) of microstate class C in schizophrenia patients compared to controls, as well as decreased time coverage ($g=-0.643$, $p<0.001$) and mean duration ($g=-0.557$, $p<0.001$) of microstate class D in schizophrenia patients compared to controls. Contrary to the above-mentioned meta-analysis, as shown in **Figure S2**, we also found consistently decreased mean duration of microstate class B in schizophrenia patients compared to controls ($g=-0.403$, $p=0.024$).

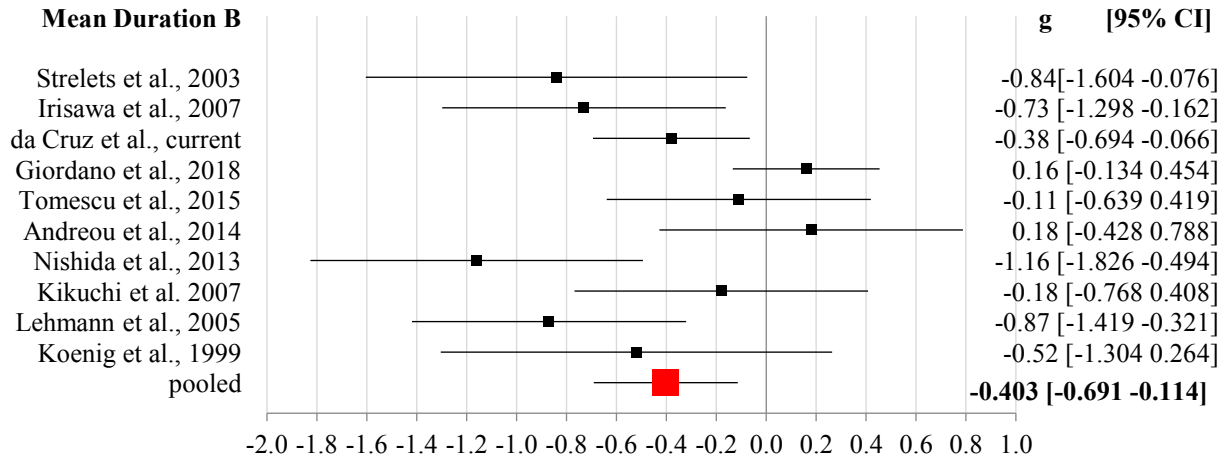


Figure S2 - Forest plot of studies considering the mean duration of microstates class B (N=694, k=10, $g=-0.403$, $p=0.024$). We found that schizophrenia patients have significant shorter microstate class B mean durations than controls. (Heterogeneity $I^2=67\%$, $p=0.001$).

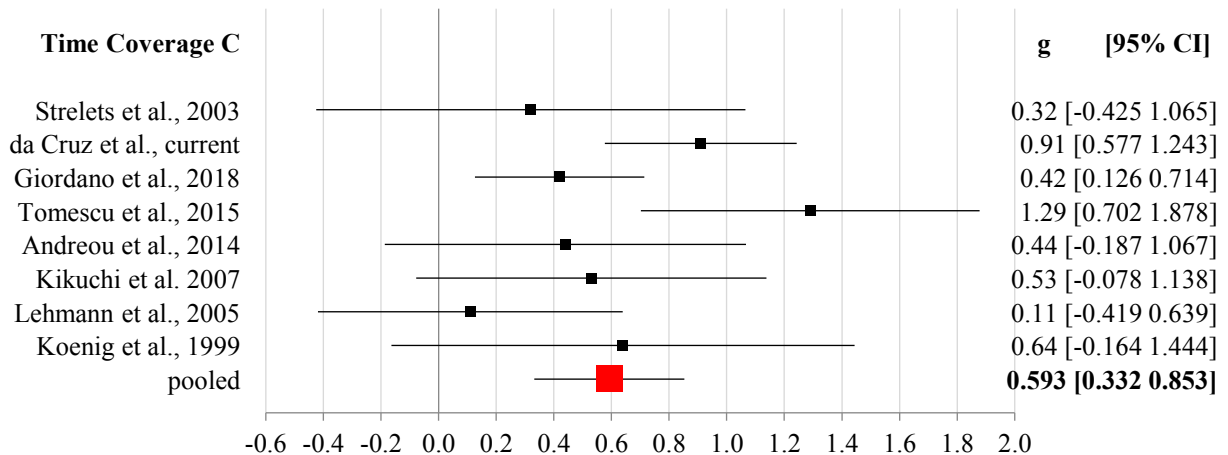


Figure S3 - Forest plot of studies considering the time coverage of microstates class C (N=608, k=8, $g=0.593$, $p<0.001$). We found that schizophrenia patients have significant longer microstate class C time coverage than controls. (Heterogeneity $I^2=51\%$, $p=0.048$)

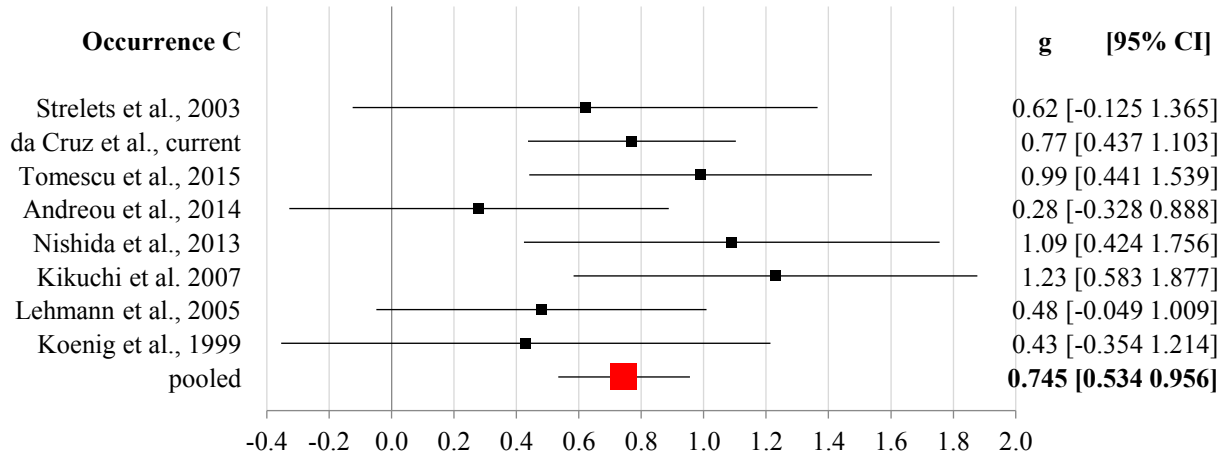


Figure S4 - Forest plot of studies considering the occurrence of microstates class C (N=440, k=8, $g=0.745$, $p<0.001$). We found that microstates class C occurs significantly more in schizophrenia patients than controls. (Heterogeneity $I^2=12\%$, $p=0.340$)

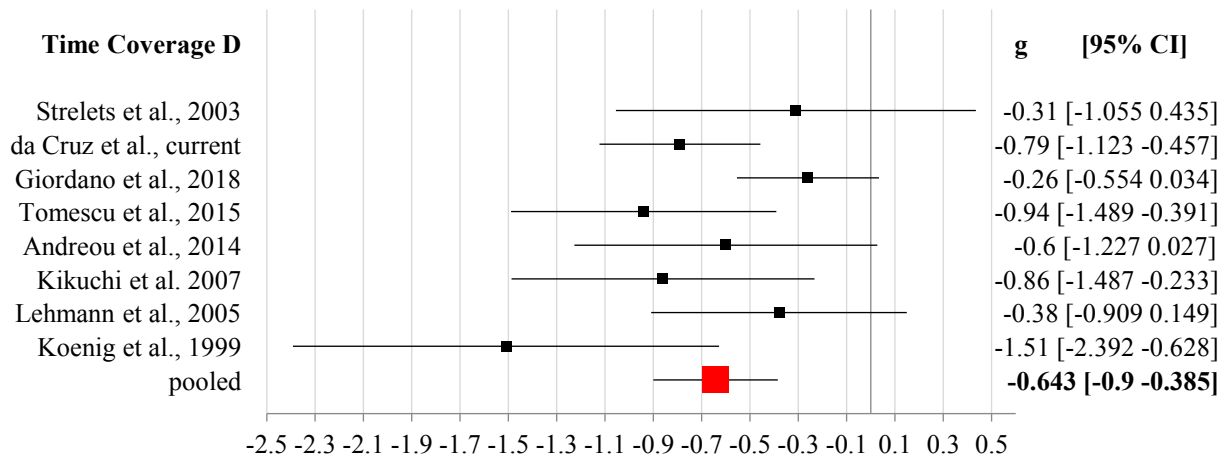


Figure S5 - Forest plot of studies considering the time coverage of microstates class C (N=608, k=8, $g=-0.643$, $p<0.001$). We found that schizophrenia patients have significant shorter microstate class C time coverage than controls. (Heterogeneity $I^2=49\%$, $p=0.054$)

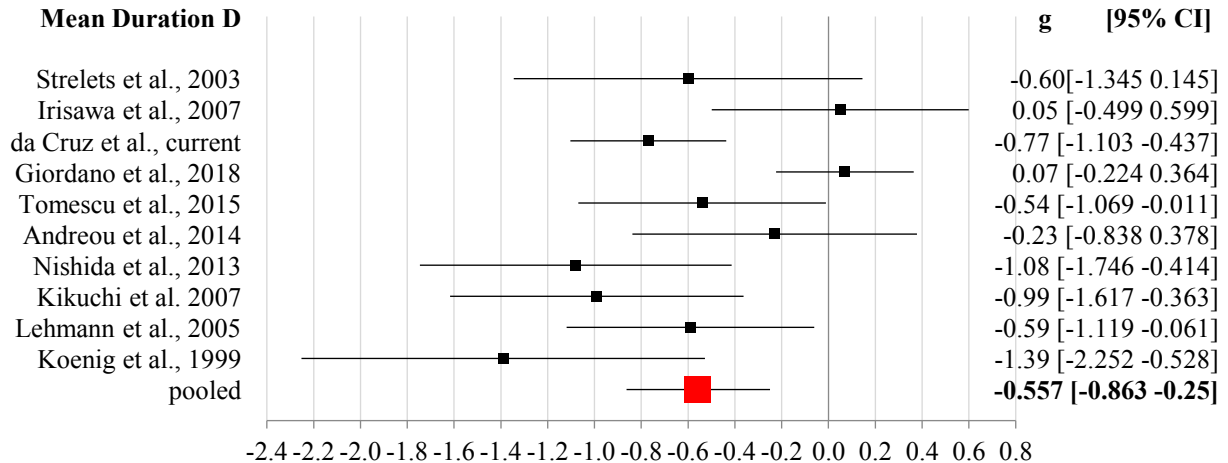


Figure S6 - Forest plot of studies considering the mean duration of microstates class D (N=694, k=10, $g=-0.557$, $p<0.001$). We found that schizophrenia patients have significant shorter microstate class D mean durations than controls. (Heterogeneity $I^2=71\%$, $p<0.001$)

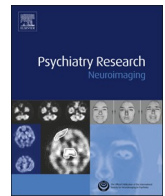
References

1. Bates D, Mächler M, Bolker B, Walker S (2015): Fitting Linear Mixed-Effects Models Using **lme4**. *Journal of Statistical Software*. 67. doi: 10.18637/jss.v067.i01.
2. da Cruz JR, Chicherov V, Herzog MH, Figueiredo P (2018): An automatic pre-processing pipeline for EEG analysis (APP) based on robust statistics. *Clinical Neurophysiology*. 129: 1427–1437.
3. Rieger K, Diaz Hernandez L, Baenninger A, Koenig T (2016): 15 Years of Microstate Research in Schizophrenia – Where Are We? A Meta-Analysis. *Front Psychiatry*. 7. doi: 10.3389/fpsy.2016.00022.
4. Irisawa S, Isotani T, Yagyu T, Morita S, Nishida K, Yamada K, *et al.* (2006): Increased Omega Complexity and Decreased Microstate Duration in Nonmedicated Schizophrenic Patients. *NPS*. 54: 134–139.

5. Strelets V, Faber PL, Golikova J, Novototsky-Vlasov V, Koenig T, Gianotti LRR, *et al.* (2003): Chronic schizophrenics with positive symptomatology have shortened EEG microstate durations. *Clinical Neurophysiology*. 114: 2043–2051.
6. Giordano GM, Koenig T, Mucci A, Vignapiano A, Amodio A, Di Lorenzo G, *et al.* (2018): Neurophysiological correlates of Avolition-apathy in schizophrenia: A resting-EEG microstates study. *NeuroImage: Clinical*. 20: 627–636.
7. Tomescu MI, Rihs TA, Becker R, Britz J, Custo A, Grouiller F, *et al.* (2014): Deviant dynamics of EEG resting state pattern in 22q11.2 deletion syndrome adolescents: A vulnerability marker of schizophrenia? *Schizophrenia Research*. 157: 175–181.
8. Francis G (2017): Equivalent statistics and data interpretation. *Behav Res*. 49: 1524–1538.
9. Murray MM, Brunet D, Michel CM (2008): Topographic ERP Analyses: A Step-by-Step Tutorial Review. *Brain Topogr*. 20: 249–264.
10. Koenig T, Stein M, Grieder M, Kottlow M (2014): A Tutorial on Data-Driven Methods for Statistically Assessing ERP Topographies. *Brain Topogr*. 27: 72–83.
11. Rouder JN, Morey RD, Speckman PL, Province JM (2012): Default Bayes factors for ANOVA designs. *Journal of Mathematical Psychology*. 56: 356–374.

Appendix E

Favrod, O., Roinishvili, M., da Cruz, J. R., Brand, A., Okruashvili, M., Gramkrelidze, T., Figueiredo, P., Herzog, M. H., Chkonia, E., & Shaqiri, A. (2018)



Electrophysiological correlates of visual backward masking in patients with first episode psychosis

Ophélie Favrod^{a,*}, Maya Roinishvili^{b,c}, Janir R. da Cruz^{a,d}, Andreas Brand^a, Mariam Okruashvili^e, Tinatin Gamkrelidze^e, Patrícia Figueiredo^d, Michael H. Herzog^a, Eka Chkonia^{c,f}, Albulena Shaqiri^a

^a Laboratory of Psychophysics, Brain Mind Institute, École Polytechnique Fédérale de Lausanne (EPFL), Switzerland

^b Laboratory of Vision Physiology, Beritashvili Centre of Experimental Biomedicine, Tbilisi, Georgia

^c Institute of Cognitive Neurosciences, Agricultural University of Georgia, Tbilisi, Georgia

^d Institute for Systems and Robotics - Lisboa, Department of Bioengineering, Instituto Superior Técnico, Universidade de Lisboa, Portugal

^e Tbilisi Mental Health Center, Tbilisi, Georgia

^f Department of Psychiatry, Tbilisi State Medical University, Tbilisi, Georgia

ARTICLE INFO

KeyWords:

Global field power
Schizophrenia
Longitudinal
N1 component
Event-related potential

ABSTRACT

Visual backward masking is strongly impaired in patients with schizophrenia. Masking deficits have been proposed as potential endophenotypes of schizophrenia. Masking performance deficits manifest as strongly reduced amplitudes in the electroencephalogram (EEG). In order to fulfill the criteria of an endophenotype, masking deficits should not vary substantially across time and should be present at the first psychotic event. To verify whether these conditions are met for visual backward masking, we tested patients with first episode psychosis ($n = 21$) in a longitudinal study. Patients were tested with visual backward masking and EEG three times every six months over a period of one year. We found that the EEG amplitudes of patients with first episode psychosis were higher as compared to those of patients with schizophrenia but lower as compared to those of unaffected controls. More interestingly, we found that the EEG amplitudes of patients with first episode psychosis remained stable over the course of one year. Since chronic schizophrenia patients have strongly reduced amplitudes, we speculate that the neural correlates of masking deficits (EEG amplitudes) continue to decrease as the disease progresses.

1. Introduction

Schizophrenia is strongly influenced by genetic and environmental factors. Even though heritability is about 50%, genome-wide association studies have not found individual single-nucleotide polymorphisms (SNPs) that are strongly associated with the disease. For this reason, endophenotypes - which test for abnormal factors that lie between the genetic underpinnings and the clinical phenotype - are crucial (Gottesman and Gould, 2003). Visual masking performance is deteriorated in patients as compared to controls (Green et al., 2011; Herzog and Brand, 2015; Kéri et al., 2000, 2001; Rund, 1993; Saccuzzo and Braff, 1981, 1986) and is thought to be an endophenotype of psychosis (Chkonia et al., 2010; Green and Nuechterlein, 1999; Nuechterlein

et al., 1994). In the last decade, we established a particularly sensitive visual backward masking (VBM) technique, the Shine-Through paradigm, which is both temporally and spatially challenging. In the Shine-Through paradigm, a vernier (two vertical bars separated by a horizontal offset) is presented, followed by a grating mask composed of 25 aligned verniers (Fig. 1A). The lower bar of the vernier is offset either to the left or to the right. Participants are asked to indicate the offset direction. Performance is only slightly deteriorated in patients with schizophrenia (pSZ) when the vernier is presented alone, i.e., without the mask (Roinishvili et al., 2008; Schütze et al., 2007). However, performance strongly deteriorates when the vernier is followed by the mask. Performance is measured as the stimulus onset asynchrony (SOA), which is the time between the onset of the vernier and the mask.

Abbreviations: CogDis, Cognitive disorganization; CTRL, healthy control participants; GFP, Global field power; MMN, Mismatch negativity; pFEP, Patients with first episode psychosis; pSZ, Patients with schizophrenia; SNP, Single-nucleotide polymorphism; SOA, Stimulus onset asynchrony; VBM, Visual backward masking; VD, Vernier duration; VEP, Visual evoked potential

* Corresponding author.

E-mail address: ophelie.favrod@epfl.ch (O. Favrod).

<https://doi.org/10.1016/j.psychresns.2018.10.008>

Received 7 June 2018; Received in revised form 19 September 2018; Accepted 29 October 2018

Available online 30 October 2018

0925-4927/ © 2018 Elsevier B.V. All rights reserved.

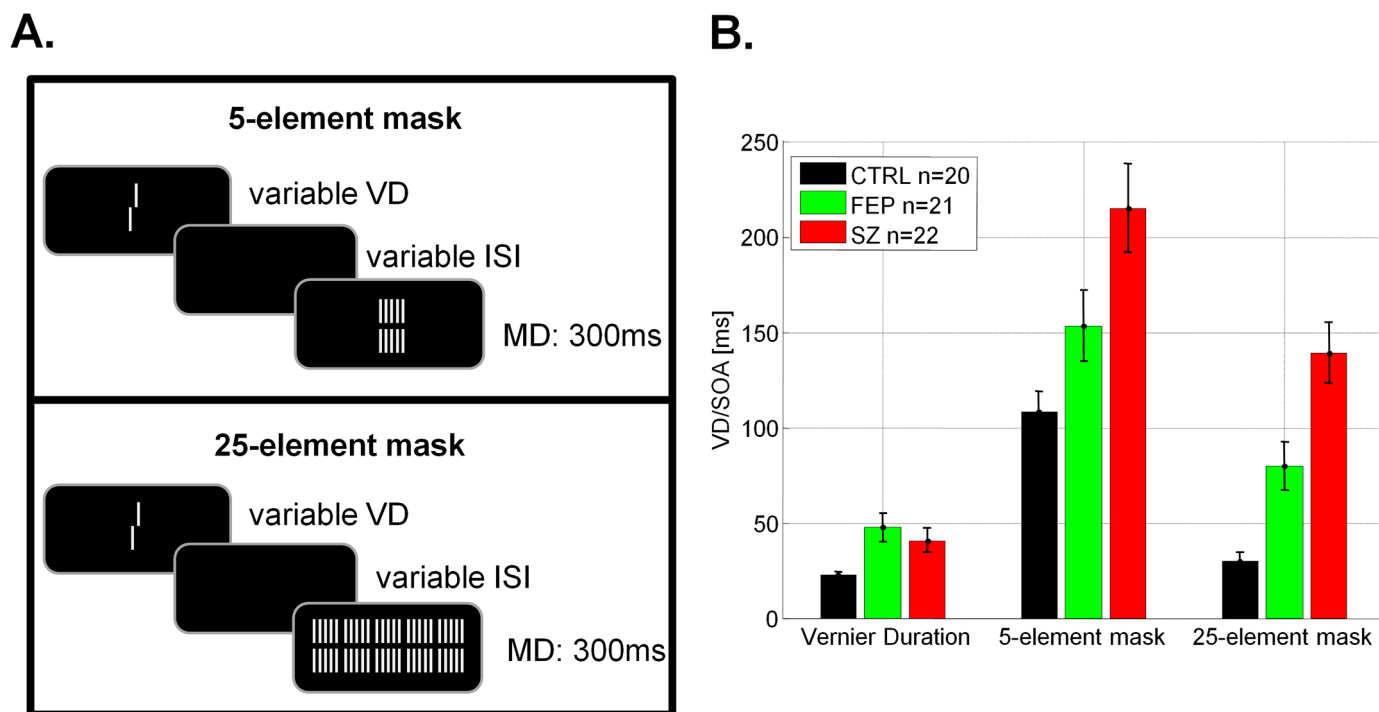


Fig. 1. Adaptive procedure: A. Stimulus display: The vernier duration (VD) was determined for each observer individually. The vernier was then followed by a mask with a variable inter-stimulus interval (ISI). The mask was composed of either 5- or 25-element. The mask duration (MD) was 300 ms. Note: SOA = VD + ISI. B. Behavioral results: vernier duration (VD) and thresholds (SOA) for the two types of mask. Masking performance (SOA threshold) of pFEP is higher as compared to controls (longer SOAs = stronger deficits) but lower as compared to pSZ. VD of pFEP is higher compared to controls. Error bars represent the standard error of the mean. For the VD, a ceiling level was set to 100 ms (5 pFEP had longer duration).

The SOAs in the pSZ are five times longer as compared to those of unaffected controls (Herzog et al., 2004). The Shine-Through paradigm meets the main criteria of an endophenotype (Gottesman and Gould, 2003). First, the first-order relatives of the patients need longer SOAs than controls but shorter SOAs than patients (Chkonia et al., 2010). Second, masking deficits do not change over the course of one year in chronic patients, indicating that the Shine-Through paradigm is a trait rather than a state marker (Chkonia et al., 2010). Third, patients with functional psychosis, such as schizoaffective patients and bipolar patients, show masking deficits but depressive patients and abstinent alcoholics do not (Chkonia et al., 2012). Fourth, adolescents with psychosis show masking deficits, suggesting that deficits are already present at early stages of the disease (Holzer et al., 2009). Fifth, students scoring high in cognitive disorganization (CogDis), a schizotypal personality trait, are impaired in VBM as compared to those with low CogDis scores, but to a much smaller degree than patients (Cappe et al., 2012). Sixth, we were able to identify a SNP related to the cholinergic nicotinic receptor ($\alpha 7$), which was correlated with masking performance in patients (Bakanidze et al., 2013). Finally, we could identify neural correlates of masking deficits in schizophrenia: patients have reduced EEG amplitudes in the N1 component, 200 ms after stimulus onset (Plomp et al., 2013) and the same holds true for participants scoring high in CogDis as compared to those with low CogDis scores (Favrod et al., 2017).

As mentioned above, adolescents with psychosis show masking deficits indicating that deficits are present even before the disease fully develops (Holzer et al., 2009). On average, masking deficits are much weaker in adolescents with psychosis than in adult patients. One reason for the weaker deficits is that not all adolescents will develop schizophrenia during their lifetime. Here, we hypothesized that the patients with a first episode of psychosis (pFEP) show similar patterns of deficits as adolescents. We determined performance and neural correlates with the VBM task in pFEP in a longitudinal study. Our main questions were: first, what is the magnitude of masking deficits at the onset of the

psychotic breakdown? Second, are the deficits expressed in the EEG correlates? Third, does performance change over the course of one year?

2. Methods and materials

2.1. Participants

All participants had normal or corrected-to-normal vision with a visual acuity of ≥ 0.8 determined for both eyes with the Freiburg Visual Acuity test (FrAct; Bach, 1996). All participants signed informed consent and were informed that they could quit the experiments at any time. All procedures complied with the Declaration of Helsinki and were approved by the local ethics committee.

2.2. Patients with First Episode Psychosis (pFEP)

Twenty-one pFEP participated in a first session. Out of these 21 patients, 16 participated six months later in a second session. Finally, 11 out of the 16 participants were tested a third time, again six months later. We invited all patients to participate in all three sessions but 5 patients opted to leave the study after the first session and 5 additional patients left the study after the second session.

Patients were recruited either from the Tbilisi Mental Health Hospital or from the Acute Psychiatric Departments of Multiprofile Clinics. General exclusion criteria were drug or alcohol abuse and neurological or other somatic illnesses influencing subjects' mental state. Patients were diagnosed according to the Diagnostic and Statistical Manual of Mental Disorders IV/V by means of an interview based on the Structured Clinical Interview, information of the staff, and the study of the records. Psychopathology of patients was assessed by an experienced psychiatrist (EC) by the Scales for the assessment of negative and positive symptoms (SANS, Andreasen 1984a; SAPS, Andreasen 1984b). At the first contact, patients were diagnosed either

Table 1

Demographics for the three groups of participants: controls (CTRL), patients with first episode psychosis (pFEP) for the three EEG sessions and patients with schizophrenia (pSZ). Abbreviations: F=female, M=male, SD=standard deviation, SANS= scales for the assessment of negative symptoms, SAPS= scales for the assessment of positive symptoms, CPZ=chlorpromazine, L=left, R=right, * data collected during the first session, ** during the second session, *** during the third session.

	CTRL	pFEP who participated in the 1st session	pFEP who participated in the 1st and 2nd sessions	pFEP who participated in all three sessions	pSZ
<i>n</i>	20	21	16	11	22
Gender (F/M)	8/12	12/9	10/6	6/5	7/15
Age (years) \pm SD	35 \pm 10	30 \pm 9*	29 \pm 9*	29 \pm 11*	33 \pm 8
Education (years) \pm SD	15 \pm 3	13 \pm 2	13 \pm 2*	13 \pm 2*	13 \pm 2
Illness Duration (months) \pm SD		8 \pm 4*	8 \pm 4*	9 \pm 4*	98 \pm 77
SANS \pm SD		7 \pm 5*	8 \pm 5*, 9 \pm 6**	9 \pm 6*, 9 \pm 7**, 9 \pm 7***	11 \pm 5
SAPS \pm SD		6 \pm 3*	7 \pm 3*,	7 \pm 3*, 6 \pm 3**, 7 \pm 2***	13 \pm 17
CPZ equivalent \pm SD		429 \pm 334*	6 \pm 3** 452 \pm 339*, 258 \pm 359**	452 \pm 376*, 220 \pm 262**, 131 \pm 185***	618 \pm 408
Handedness (L/R)	2/18	1/20	1/15	0/11	1/21
Visual acuity \pm SD	1.6 \pm 0.5	1.4 \pm 0.4*	1.5 \pm 0.3*	1.5 \pm 0.4*	1.4 \pm 0.3

as brief psychotic disorder (DSM-IV 298.8) or as schizophreniform disorder (DSM-IV 295.40). At the second contact, patients were diagnosed with schizophrenia, except one patient who had a first bipolar I episode. This patient's data is similar to the data of the other patients. In addition, we have previously shown that masking deficits are similar in schizophrenia and bipolar patients (Chkonia et al., 2012). Results that include this patient are almost identical to the results when the patient is omitted (supplementary material Fig.S1).

We prefer to use the term first episode psychosis rather than first episode schizophrenia, because the former term is more heterogeneous, including all types of psychotic disorders. Subtypes of diagnosis are shown in Tab.S1 of the supplementary material for all three sessions. Group characteristics are depicted in Table 1. All patients were receiving neuroleptic medication before our experiment.

2.3. Stimuli and Apparatus

Stimuli were displayed on a Siemens Fujitsu P796-1 monitor with a refresh rate of 100 Hz. The screen resolution was 1024 \times 768 pixels. Patients sat 3.5 m away from the monitor in a weakly illuminated room. The stimuli were white, with a luminance of 100 cd/m² on a black background (< 1 cd/m²).

We presented vernier stimuli consisting of two vertical bars separated by a vertical gap of 1' (arc min). The lower bar was slightly offset either to the left or to the right compared to the upper one. The horizontal vernier offset was 1.2'. The mask consisted of either five or twenty-five aligned vernier stimuli. The horizontal spacing between mask elements was 3.33'.

Observers responded by pushing one of the two hand-held buttons. Participants were instructed to be as accurate as possible. Two-way rm-ANOVAs with Greenhouse-Geisser corrections (when necessary) were performed.

2.4. Adaptive procedure

We determined the vernier duration (VD) necessary to reach 75% of correct responses. For each observer, we found the VD, for which the threshold of vernier offset discrimination was below 0.6'. Afterwards, we used the individual VD with a fixed vernier offset of 1.2' and determined the SOA threshold for each participant through an adaptive strategy (Parametric Estimation by Sequential Testing; Taylor, 1967) in order to reach 75% of correct responses. Hence, we did not determine performance by an examination of a set of SOAs separately but directly

determined the masking effect via the psychophysical threshold. The protocol was similar to previous studies (Cappe et al., 2012; Herzog et al., 2004; Shagiri et al., 2015). We used two types of masks: a 5- and a 25-element grating mask (Fig. 1A).

2.5. EEG experiment design

As in previous EEG studies (Favrod et al., 2017; Plomp et al., 2013), we tested four conditions: Vernier Only, Long SOA, Short SOA, and Mask Only (Fig. 2A). In the Vernier Only condition, the vernier was presented alone for 30 ms. In the Short and Long SOA conditions, the vernier was presented for 30 ms followed by the 25-element mask for 300 ms with an SOA of either 30 or 150 ms, respectively. The 30 ms SOA is the mean performance level of controls and the 150 ms SOA is that of pSZ. In the Mask Only condition, the mask was presented for 300 ms; there was no vernier.

In each session, 8 blocks of 80 trials (20 trials / condition) were presented. The condition order was randomized within a block. In total, there were 160 trials per condition.

2.6. EEG recordings and pre-processing

We used the EEG BioSemi Active Two system with 64 Ag-AgCl sintered active electrodes distributed across the scalp according to the 10/20 layout system. The sampling frequency was 2048 Hz. EEG data were pre-processed offline in Matlab (R2012a, The MathWorks Inc., Natick, MA) with EEGLAB (Delorme and Makeig, 2004) and using an in-house, automated pre-processing pipeline (The APP; da Cruz et al., 2018). The signal was down-sampled to 512 Hz, band-passed filtered from 1 to 40 Hz and the 50 Hz line noise was removed using CleanLine (Mullen, 2012). The signal was re-referenced to the biweight estimate of the mean of all electrode-channels (Hoaglin et al., 1983, 1985). Unstable and noisy electrodes were removed and interpolated with a 3D spline function. The proportion of interpolated electrodes was about one channel per EEG recording. EEG epochs were extracted from 100 ms before the stimulus onset (baseline) to 400 ms after stimulus onset. Noisy trials (with artifacts such as eye blinks) were also removed. The rejected trials constituted about 4% of each EEG recording (Tab.S2 in the supplementary material). We did not apply any exclusion criterion based on reaction time. Hit and miss trials were averaged for each condition and each participant. The individual averages were baseline corrected.

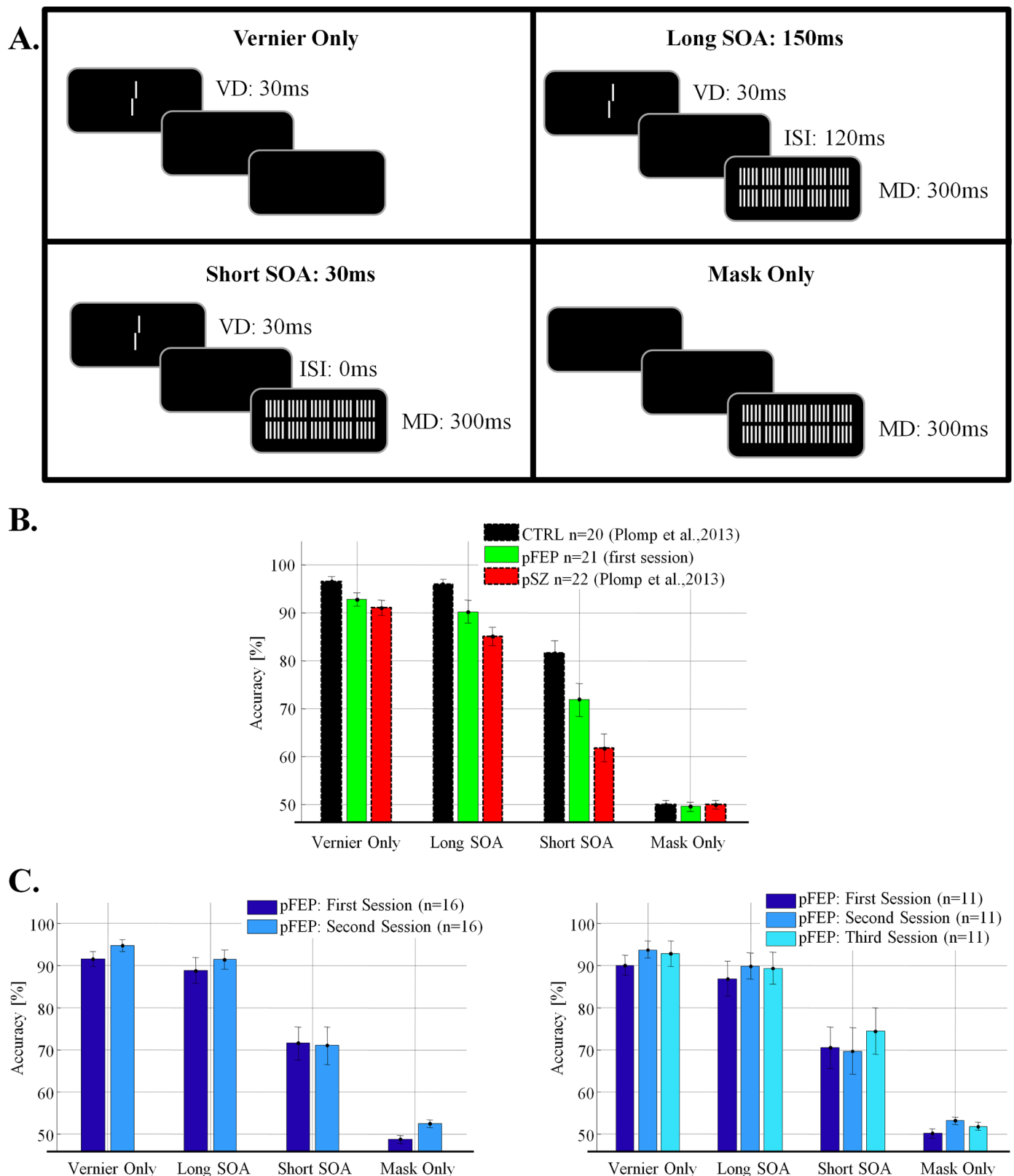


Fig. 2. EEG experiment: A. Stimulus display: In the Vernier Only condition, the vernier was presented alone for 30 ms. In the Short and Long SOA conditions, the vernier was followed by a mask with an SOA of either 30 or 150 ms, respectively. In the Mask Only condition, only the mask was presented. VD = vernier duration, ISI = Inter-Stimulus Interval, SOA = Stimulus Onset Asynchrony, MD = mask duration. SOA = VD + ISI. B. Accuracy for the four conditions (Vernier Only, Long SOA, Short SOA and Mask Only). The performance of pFEP (green, $n = 21$) is lower as compared to controls (black, $n = 20$) but higher as compared to pSZ (red, $n = 22$), in particular for the Long and Short SOA conditions. For the Vernier Only condition, the three groups are at ceiling. For the Mask Only condition, the three groups are at chance level, as expected. Error bars represent the standard error of the mean. C. Left panel: accuracy across the two sessions for the four conditions and the 16 pFEP. There was a slight improvement between the two sessions. Right panel: accuracy across the three sessions for the four conditions and the 11 pFEP. Performance did not change over the three sessions. (For interpretation of the references to colour in this figure legend, the reader is referred to the web version of this article.)

2.7. EEG analysis

The individual visual evoked potentials (VEP) were analyzed in MATLAB (R2010b, The MathWorks Inc., Natick, MA). Signal from one occipital electrode (Oz) was extracted in order to visualize the positive and negative components of the VEPs (supplementary material Fig.S2). The Global Field Power (GFP) is computed as the standard deviation across all electrodes at each time point for each participant and each condition separately (Lehmann and Skrandies, 1980). GFP is an overall measure of brain activity taking into account all EEG sources. Grand averages of GFPs were computed for each condition, each session and each group of participants.

Statistical analysis for the GFPs was performed using the Statistical Toolbox for Electrical Neuroimaging (STEN) developed by Jean-François Knebel (<http://www.unil.ch/line/Sten>). We performed between- and within-subject rm-ANOVAs for each timeframe with the factor Group and Condition (between-group design) or Session and Condition (within-group design). For the main effects, we considered intervals that yielded significant effects for more than 10 consecutive time frames (about 20 ms and 13 time frames, about 26 ms for post-hoc) in order to remove short significant time intervals in the baseline or unrealistic effects (too early). This approach has been shown to partially control for multiple comparisons and false positives in EEG analyses (Blair and Karniski, 1993; Knebel et al., 2011; Knebel and Murray, 2012). We performed a Bayesian rm-ANOVA for an interval around 200 ms (190–215 ms, arbitrarily chosen to have all grand average peaks included) using JASP (<https://jasp-stats.org/>, version 0.8.1.1). We used the averaged GFP during this time window to compute the statistics.

2.8. Controls (CTRL) and Patients with Schizophrenia (pSZ)

We compared data of pFEP with data of pSZ and controls that were previously published in (Plomp et al., 2013). The equipment and testing location of the former and the current study were exactly the same. In the past (i.e., Plomp et al., 2013), data were analyzed semi-automatically (i.e., through visual inspection of the data). Recently, we developed an automatic pre-processing pipeline (the APP, da Cruz et al., 2018). Here, we used the APP to analyze the pFEP data set and re-analyzed the pSZ and controls dataset of (Plomp et al., 2013). Both datasets are pre-processed exactly the same way, avoiding any subjective bias from the EEG expert.

3. Results

3.1. Adaptive procedure

The VD of the controls was significantly lower compared to that of the pFEP (Fig. 1B, left). There was no significant difference between the VD of pFEP and pSZ (main effect of Group: $F(2,60) = 4.588$, $p = 0.014$, $\eta^2 = 0.133$, post-hoc: CTRL vs pFEP: $t(39) = -2.931$, $p_{\text{tukey}} = 0.013$, pFEP vs pSZ: $t(41) = 0.802$, $p_{\text{tukey}} = 0.703$ and CTRL vs pSZ: $t(40) = -2.172$, $p_{\text{tukey}} = 0.084$).

For the masking conditions, the performance of pFEP laid between that of controls and pSZ (significant main effect of Group: $F(2,60) = 14.51$, $p < 0.001$, $\eta^2 = 0.326$). Post-hoc tests revealed no significant difference between CTRL and pFEP: $t(80) = -2.343$, $p_{\text{tukey}} = 0.058$, but significant differences between the performance of pFEP and pSZ: $t(84) = -3.032$, $p_{\text{tukey}} = 0.010$ and CTRL vs pSZ: $t(82) = -5.363$, $p_{\text{tukey}} < 0.001$. Masking was stronger with the 5-element as compared to the 25-element mask (significant main effect of Mask: $F(1,60) = 100.840$, $p < 0.001$, $\eta^2 = 0.627$). There was no significant Group x Mask interaction: $F(2,60) = 0.030$, $p = 0.971$, $\eta^2 = 0.000$ (Fig. 1B, right).

3.2. EEG experiment

Using the 25-element mask, we first compared the three groups (pSZ, pFEP-1st session and CTRL). Second, we recorded EEG for the pFEP over the course of one year (after 6 months: 2nd session, after 12 months: 3rd session).

The adaptive procedure is very sensitive and allows for the exploration of individual differences. With EEG, we cannot use the adaptive procedure because conditions have to be the same across all observers. For this reasons, we selected the averaged SOA values (30 ms corresponding to the performance of controls and 150 ms for patients) based on previous experiments. The performance of pFEP laid between that of controls and pSZ, especially in the two masking conditions (Long and Short SOAs, Fig. 2B). pSZ had the lowest performance. There was a main effect of Group: $F(2,60) = 9.884$, $p < 0.001$, $\eta^2 = 0.248$, main effect of Condition: $F(1.729,103.759) = 494.508$, $p < 0.001$, $\eta^2 = 0.869$ and interaction Group x Condition: $F(3.459, 103.759) = 7.318$, $p < 0.001$, $\eta^2 = 0.026$.

Longitudinally, the performance of pFEP slightly improved for the second session compared to the first session (Fig. 2C, left, $n = 16$). However, the performance of pFEP did not change over the course of one year when comparing all three sessions (Fig. 2C, right, $n = 11$). For the sample size of $n = 16$: significant main effect of Session: $F(1,15) = 4.576$, $p = 0.049$, $\eta^2 = 0.234$ (average statistics in the supplementary material Tab.S3), significant main effect of Condition: $F(1.529, 22.941) = 101.264$, $p < 0.001$, $\eta^2 = 0.871$ and no significant interaction Session x Condition: $F(2.040, 30.597) = 1.751$, $p = 0.19$, $\eta^2 = 0.105$. For the sample size of $n = 11$: no significant main effect of Session: $F(2,20) = 1.517$, $p = 0.244$, $\eta^2 = 0.132$, a significant main effect of Condition: $F(1.433,14.335) = 61.946$, $p < 0.001$, $\eta^2 = 0.861$ and no significant interaction Session x Condition: $F(6,60) = 1.513$, $p = 0.189$, $\eta^2 = 0.131$.

3.2.1. Neural correlates: Group Study

GFP amplitudes of the pFEP were between those of controls and pSZ in the Vernier Only and Mask Only conditions (Fig. 3). We found a significant main effect of Group around 200 ms corresponding to the N1 component (for the time interval 170–218 ms with the highest significance at 192 ms $F(2,60) = 5.78$, $p = 0.005$). Post-hoc analysis showed that N1 amplitudes of pFEP were significantly lower compared to controls in the Short SOA condition (before 200 ms). pFEP had significantly higher amplitudes compared to pSZ in the Long SOA condition (after 200 ms) and in the Vernier Only condition (Fig. 3). F-values and main effects of condition/interaction are shown in the supplementary material (Fig.S3A).

To ensure that the group differences are not restricted to visual areas (but are indeed global) we plotted the topographic maps for the main effect of Group interval in the supplementary material (Fig.S4). The three groups show similar voltage maps around 200 ms which differ only in intensity as reflected by the GFP.

3.2.2. Neural correlates: Longitudinal study

We compared the 16 pFEP who underwent the two first sessions over the course of six months and the 11 pFEP who underwent all of the three sessions over the course of one year.

GFPs traces of the 16 patients who participated in the two sessions are mainly overlapping (Fig. 4A). We found a significant main effect of Session after 300 ms (for the time interval 347–377 ms with the highest significance at 356 ms; $F(1,15) = 6.72$, $p = 0.02$). We did not find any significant effect of Session around 200 ms (GFP peak, N1 component). In order to test whether the GFP amplitude remained stable at 200 ms across the two sessions, we computed within-subject rm-Bayesian ANOVA for the averaged time window 190–215 ms. We found a Bayesian factor (BF_{10}) for the main effect of Session of 0.220 indicating 4.5 times more evidence in favor of the null hypothesis (no difference across sessions) as compared to the alternative (there was a difference

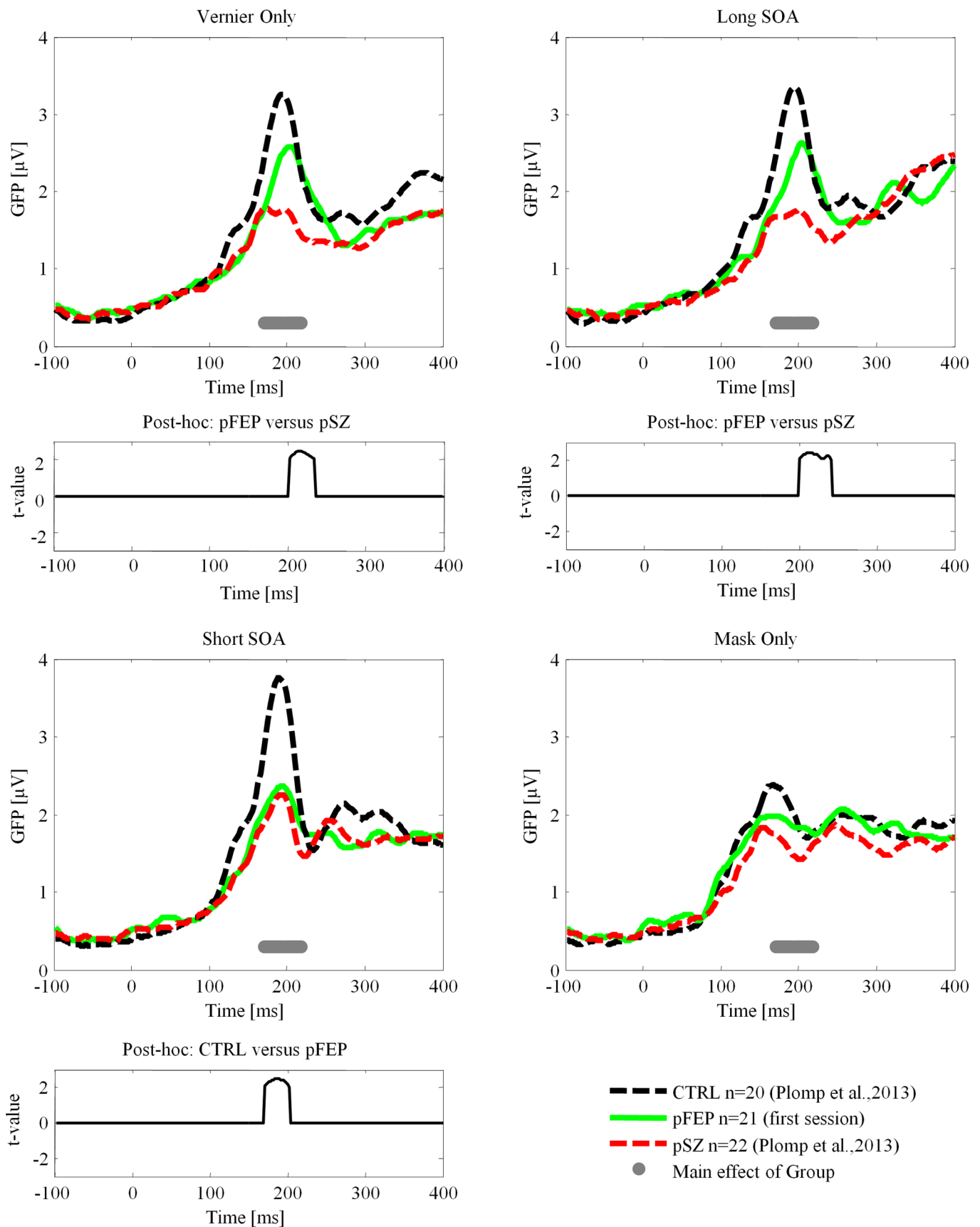


Fig. 3. Global Field Power (GFP) for the three groups: pFEP (green), controls (black) and pSZ (red). The amplitudes at 200 ms are strongly reduced for pSZ but to a lesser degree for pFEP as compared to CTRL. The bottom line shows the results of the timewise rm-ANOVA for the main effect of Group (gray). Post-hoc statistics (t-values) are shown as black lines at the bottom of the panels. There is a significant difference around 200 ms between CTRL and pFEP in the Short SOA condition and between pFEP and pSZ in the Vernier Only and Long SOA conditions. The other comparisons with pFEP were null. (For interpretation of the references to colour in this figure legend, the reader is referred to the web version of this article.)

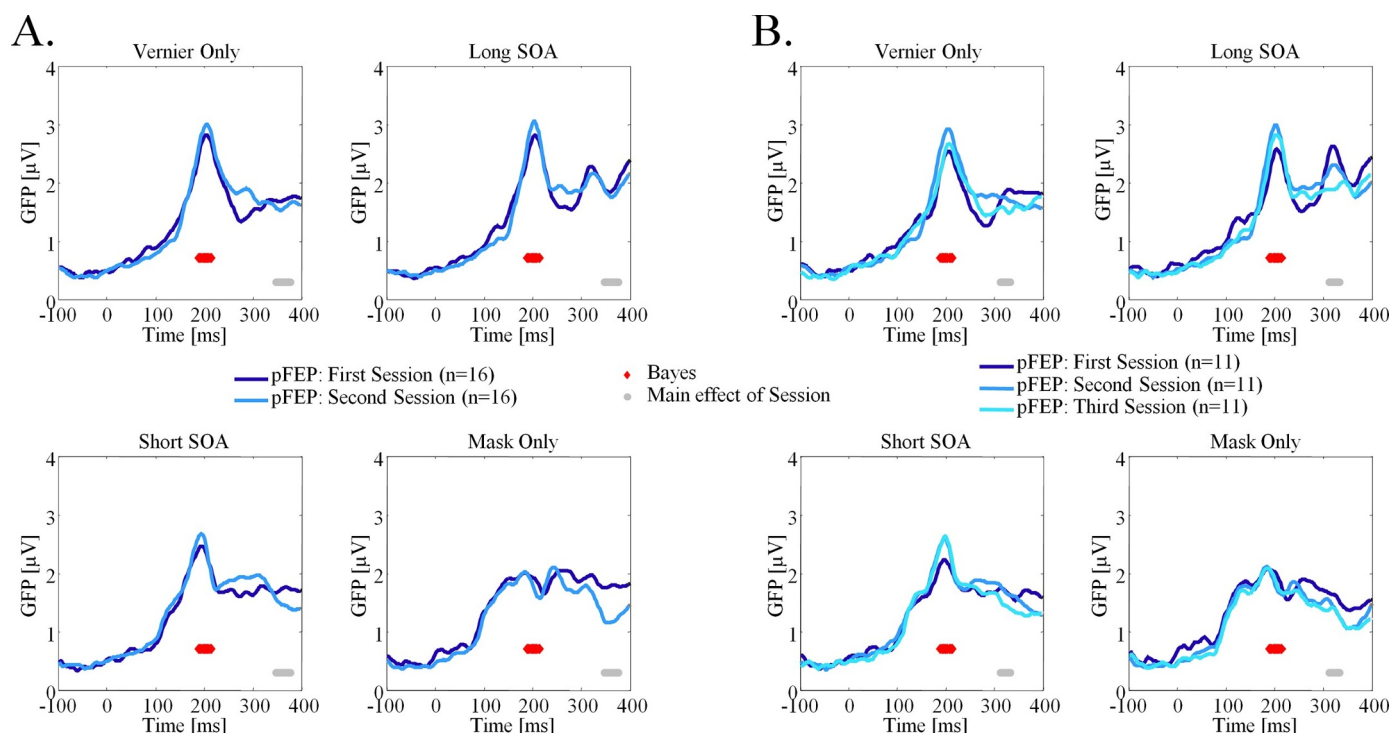


Fig. 4. A. Global Field Power (GFP) for the 16 pFEP who performed the first (dark blue) and second (medium blue) session. The horizontal lines show the results of the timewise rm-ANOVA for the main effect of Session (gray) and the time interval of interest (190–215 ms) selected for the Bayesian rm-ANOVA (red). B. Similarly, GFP for the 11 pFEP who performed all three sessions: grand average for the first session (dark blue), second session (medium blue) and third session (light blue). The horizontal lines show the results of the timewise rm-ANOVA for the main effect of Session (gray) and the time interval of interest (190–215 ms) selected for the Bayesian rm-ANOVA (red). (For interpretation of the references to colour in this figure legend, the reader is referred to the web version of this article.)

across sessions). F-values for the main effects of condition/interaction are shown in the supplementary material (Fig.S3B).

GFPs traces of the 11 patients who participated in the three sessions are overlapping (Fig. 4B). We found a significant main effect of Session after 300 ms (time interval: 312–334 ms with the highest significance at 323 ms $F(2,20) = 6.36$, $p = 0.007$). We did not find any significant effect of Session around 200 ms. To test whether the GFP amplitude remained stable at 200 ms across the three sessions, we computed a within-subject rm-Bayesian ANOVA for the averaged time window 190–215 ms. We found a BF_{10} for the main effect of Session of 0.204 indicating 4.9 times more evidence in favor of the null hypothesis. F-values for the main effects of condition/interaction are shown in the supplementary material (Fig.S3C).

4. Discussion

Schizophrenia is strongly influenced by genetic dispositions. However, genetic studies have found only weak associations between SNPs and the disease (Bernardo et al., 2017; Kavanagh et al., 2015; Kendler, 2015). For this reason, endophenotypes are of crucial interest. VBM is a sensitive endophenotype, in particular the Shine-Through masking paradigm, which has a high sensitivity of 87% and specificity of 89% (Chkonia et al., 2010). Masking deficits are found in the siblings of patients (Chkonia et al., 2010), in students scoring high in CogDis (Cappe et al., 2012; Favrod et al., 2017) and in adolescents with psychosis (Holzer et al., 2009). The latter result shows that deficits are present even before the disease fully develops. In addition, masking deficits are well reflected in the EEG, with GFP amplitudes around 200 ms reduced as compared to controls (Plomp et al., 2013). Here, we asked the question whether adult pFEP show fully blown deficits in the EEG as chronic pSZ and how results change over the course of one year.

First, we conducted a behavioral experiment with an adaptive method and found that the performance levels of pFEP were between

those of controls and pSZ with the 5- and 25-element grating mask (Fig. 1B). When only the vernier was presented, there were only small differences between the three groups ($\eta^2 = 0.133$). This is in accordance with previous results showing that masking ($\eta^2 = 0.326$), and not vernier acuity, is the sensitive endophenotype. Also, relatives of pSZ have masking deficits compared to controls but no VD deficits (Chkonia et al., 2010). The same is true for adolescents with psychosis (Holzer et al., 2009). It is the combination of a spatially (fine offset discrimination) and temporally (short SOAs) challenging task that makes the strong differences between patients and controls visible. Importantly, deficits vary greatly from 15 to 141 ms in SOA thresholds with the 25-element mask (Table 2). VD do not vary as much between the populations from 10 to 55 ms. Interestingly, the masking deficits of pFEP ($79.8 \text{ ms} \pm 57.7$) were similar to those of adolescents with psychosis ($70.6 \text{ ms} \pm 52.4$; Holzer et al., 2009, see Table 2). The slight difference might be explained by the fact that only a subset of the adolescents will develop schizophrenia and that the adolescents were much younger than the pFEP (16 years old vs. 30 years; masking performance deteriorates with age: Plomp et al., 2012; Roinishvili et al., 2011). Hence, deficits in the Shine-Through paradigm are present at the onset of the psychotic event but are not yet fully developed. Similar behavioral results were also true in the EEG experiment (Fig. 2B). It remains an open question why deficits further deteriorate when the disease progresses.

For the EEG results, pFEP exhibited clearly reduced amplitudes in the Short SOA condition compared to controls, showing that masking deficits are present at the first psychotic event. However, in the Vernier Only and Long SOA conditions, amplitudes were intermediate, showing that it is only under the most challenging condition (Short SOA) that deficits are fully visible (Fig. 3). These results go hand in hand with the behavioral results.

Interestingly, masking deficits are also present in healthy people scoring high in CogDis, but again, this is only true under challenging

Table 2

Summary of the behavioral studies using the 25-element mask: vernier durations (VD; mean \pm SD) and stimulus onset asynchrony thresholds (SOA; mean \pm SD) for each population.

Group	n	age [years]	VD [ms]	SOA threshold [ms]	Study
Schizophrenia	22	33.5 \pm 7.9	40.9 \pm 30.1	139.1 \pm 73.9	Current study
First episode Psychosis	21	30.0 \pm 9.2	47.6 \pm 35.7	79.8 \pm 57.7	Current study
Controls	20	35.4 \pm 10.5	22.5 \pm 9.1	29.7 \pm 23.0	Current study
Participants scoring high in CogDis	22	21.1 \pm 2.0	10.0 \pm 0.0	18.6 \pm 6.6	Cappe et al., 2012
Participants scoring low in CogDis	18			15.1 \pm 3.0	Cappe et al., 2012
Bipolar	22	34.1 \pm 10.1	41.8 \pm 30.3	124.4 \pm 90.6	Chkonia et al., 2012
Schizoaffective	20	35.1 \pm 8.9	54.5 \pm 33.3	140.7 \pm 74.6	Chkonia et al., 2012
Relatives	39	35.0 \pm 15.9	27.7 \pm 19.0	74.0 \pm 62.3	Chkonia et al., 2010
Adolescent with psychosis	15	16.4 \pm 1.4	19.9 \pm 20.5	70.6 \pm 52.4	Holzer et al., 2009
Controls	19	16.0 \pm 1.6	14.4 \pm 19.2	22.83 \pm 16.7	Holzer et al., 2009

conditions (Cappe et al., 2012). These masking deficits are also reflected in EEG by lower amplitudes (Favrod et al., 2017). Hence, masking deficits and the corresponding electrophysiological correlates are present in the unmedicated populations of healthy controls with schizotypal traits (Favrod et al., 2017), the unmedicated siblings of pSZ (although EEG correlates are not lower, da Cruz et al., 2019.), medicated pFEP and chronic pSZ (Plomp et al., 2013). The N1 peak is always around 200 ms, independently of the SOAs or the number of elements in the mask (supplementary material Tab.S4). Taken together, these results show that masking deficits are trait markers and that the EEG amplitudes decrease after the beginning of the disease.

In the longitudinal study, we found no evidence that behavioral performance decreases (there is even a slight improvement, which we attribute to learning, Fig. 2C) and, respectively, amplitudes of the EEG did not further decrease (there is also a slight increase, if at all, Fig. 4). Hence, performance and EEG signals are rather unaffected during the year following a first episode, which is well in line with an endophenotype.

With the Shine-Through paradigm, the amplitude of the N1 component for pFEP is between the ones of the controls and pSZ. There are other endophenotypes of psychosis that show a similar pattern. For example, the Mismatch Negativity (MMN), which is a measure of the brain response to a deviant tone in a sequence of repetitive tones, is deficient in chronic pSZ compared to controls (Salisbury et al., 2018). Interestingly, there was no or only a weak difference in the MMN amplitude between pFEP compared to controls (see also Erickson et al., 2016; Haigh et al., 2017). The MMN has even been proposed to be a measure for disease progression (Umbrecht and Krljes, 2005). Similar results were found for the auditory P3, an attention-related component. The P3 amplitude is reduced in all electrodes in chronic pSZ, while the amplitudes are reduced only in the frontal electrodes in pFEP (Demiralp et al., 2002), possibly because the deficits of pFEP are not yet fully developed compared to chronic patients. The P50 suppression (for paired sound stimuli), measuring sensory gating, is also impaired in schizophrenia (no suppression). The mechanisms for the underlying P50 reduction are potentially similar to those observed with the Shine-Through paradigm in the sense that they are both related to the dysfunction of the cholinergic system, in particular the nicotinic receptor $\alpha 7$ (Bakanidze et al., 2013; Turetsky et al., 2012). Deficits in different sensory modalities may result from a common mechanism. We proposed that masking deficits are the expression of a more general deficit related to target enhancement (Herzog et al., 2013).

There is a long debate as to whether schizophrenia is a neurodevelopmental disorder or whether the brain starts to deteriorate only with the beginning of the disease (Anderson et al., 1998; Knoll et al., 1998; Lewis and Levitt, 2002; Murray et al., 2017; Rapoport et al., 2012). Our results are compatible with both theories, since deficits are already present with the first signs of psychosis (even in unaffected relatives) and deteriorate across the course of the illness. It seems that pFEP are in an in-between state where the neural correlates are not yet fully reduced as in chronic pSZ.

PFEP were medicated. However, masking deficits are unlikely due to medication (Brody et al., 1980; Butler et al., 1996) because healthy high CogDis participants also show masking deficits (Cappe et al., 2012). Furthermore, medication often normalizes performance and/or brain activity, as shown for instance with P50 suppression deficits (Light et al., 2000; Nagamoto et al., 1996).

This work suffers from a few limitations. First, sample sizes are small. Second, patients were followed up only for a short duration (one year). A longer monitoring of patients is needed to determine how deficits evolve over time. Finally, medication was highly heterogeneous, introducing a confounding factor. We could not investigate the effects of atypical versus typical medication, which influence the performance in visual tasks (Fernandes et al., 2019).

In conclusion, masking deficits are present when the first psychotic event occurs in pFEP but are not yet fully developed. Performance of pFEP is between the ones of controls and chronic patients. The behavioral results are well reflected in the reduced EEG amplitudes. In addition, pFEP show almost no behavioral or electrophysiological differences compared to controls when the task is easy, while they do show differences when the task is challenging. Importantly, masking performance and neural correlates do not change over the course of one year. These results add further evidence that masking is a sensitive endophenotype for the psychosis spectrum.

Funding

This work was supported by the NCCR Synapsy from the Swiss National Science Foundation SNF (51NF40-158776), by the Portuguese Fundação para a Ciência e a Tecnologia, (FCT PD/BD/105785/2014) and by the “Knowledge Foundation” of Georgia. The authors have declared that there are no conflicts of interest in relation to the subject of this study.

Disclosures

Authors declare no conflict of interest.

Acknowledgments

We would like to thank Marc Repnow for his precious comments and his technical support. We thank Maya Jastrzębowska for proof-reading the manuscript.

Supplementary materials

Supplementary material associated with this article can be found, in the online version, at doi:10.1016/j.psychres.2018.10.008.

References

Anderson, J.E., O'Donnell, B.F., McCarley, R.W., Shenton, M.E., 1998. Progressive

- changes in schizophrenia: do they exist and what do they mean. *Restor. Neurol. Neurosci.* 12 (2, 3), 175–184.
- Andreasen, N.C., 1984a. Scale for the Assessment of Negative Symptoms (SANS). University of Iowa, Iowa City.
- Andreasen, N.C., 1984b. Scale for the Assessment of Positive Symptoms (SAPS). University of Iowa, Iowa City.
- Bach, M., 1996. The Freiburg visual acuity test-automatic measurement of visual acuity. *Optom. Vis. Sci.* 73, 49–53.
- Bakanidze, G., Roinishvili, M., Chkonia, E., Kitzrow, W., Richter, S., Neumann, K., Herzog, M.H., Brand, A., Puls, I., 2013. Association of the nicotinic receptor $\alpha 7$ subunit gene (CHRNA7) with schizophrenia and visual backward masking. *Front. Psychiatry* 4, 133.
- Bernardo, M., Bioque, M., Cabrera, B., Lobo, A., González-Pinto, A., Pina, L., Corripio, I., Sanjuan, J., Mané, A., Castro-Fornieles, J., Vieta, E., 2017. Modelling gene-environment interaction in first episodes of psychosis. *Schizophr. Res.* 189, 181–189.
- Blair, R.C., Karniski, W., 1993. An alternative method for significance testing of waveform difference potentials. *Psychophysiology* 30, 518–524.
- Brody, D., Saccuzzo, D.P., Braff, D.L., 1980. Information processing for masked and unmasked stimuli in Schizophrenia and old age. *J. Abnorm. Psychol.* 89 (5), 617.
- Butler, P.D., Harkavy-Friedman, J.M., Amador, X.F., Gorman, J.M., 1996. Backward masking in schizophrenia: relationship to medication status, neuropsychological functioning, and dopamine metabolism. *Biol. Psychiatry* 40 (4), 295–298.
- Cappe, C., Herzog, M.H., Herzog, D.A., Brand, A., Mohr, C., 2012. Cognitive disorganisation in schizotypy is associated with deterioration in visual backward masking. *Psychiatry Res.* 200 (2), 652–659.
- Chkonia, E., Roinishvili, M., Makhatadze, N., Tserava, L., Stroux, A., Neumann, K., Herzog, M.H., Brand, A., 2010. The shine-through masking paradigm is a potential endophenotype of schizophrenia. *PLoS One* 5 (12), e14268.
- Chkonia, E., Roinishvili, M., Reichard, L., Wurch, W., Puhlmann, H., Grimsen, C., Herzog, M.H., Brand, A., 2012. Patients with functional psychoses show similar visual backward masking deficits. *Psychiatry Res.* 198 (2), 235–240.
- da Cruz, J.R., Chicherov, V., Herzog, M.H., Figueiredo, P., 2018. An automatic pre-processing pipeline for EEG analysis (APP) based on robust statistics. *Clin. Neurophysiol.* 129 (7), 1427–1437.
- da Cruz, J.R., Shaqiri, A., Roinishvili, M., Chkonia, E., Brand, A., Figueiredo, P., Herzog, M.H., 2019. In preparation. Neural compensation mechanisms of siblings of schizophrenia patients as revealed by high-density EEG.
- Delorme, A., Makeig, S., 2004. EEGLAB: an open source toolbox for analysis of single-trial EEG dynamics including independent component analysis. *J. Neurosci. Methods* 134 (1), 9–21.
- Demiralp, T., Üçok, A., Devrim, M., Isoglu-Alkaç, Ü., Tecer, A., Polich, J., 2002. N2 and P3 components of event-related potential in first-episode schizophrenic patients: scalp topography, medication, and latency effects. *Psychiatry Res.* 111 (2), 167–179.
- Erickson, M.A., Ruffle, A., Gold, J.M., 2016. A meta-analysis of mismatch negativity in schizophrenia: from clinical risk to disease specificity and progression. *Biol. Psychiatry* 79 (12), 980–987.
- Favrod, O., Sierro, G., Roinishvili, M., Chkonia, E., Mohr, C., Herzog, M.H., Cappe, C., 2017. Electrophysiological correlates of visual backward masking in high Schizotypic personality traits participants. *Psychiatry Res.* 254, 251–257.
- Fernandes, T.P., Shaqiri, A., Brand, A., Nogueira, R.L., Herzog, M.H., Chkonia, E., Santos, N.A., Roinishvili, M., 2019. In revision. Schizophrenia patients using atypical medication perform better in visual tasks than patients using typical medication. *Psychiatry Res.*
- Gottesman, I.I., Gould, T.D., 2003. The endophenotype concept in psychiatry: etymology and strategic intentions. *Am. J. Psychiatry* 160 (4), 636–645.
- Green, M.F., Nuechterlein, K.H., 1999. Backward masking performance as an indicator of vulnerability to schizophrenia. *Acta Psychiatrica Scandinavica* 99 (s395), 34–40.
- Green, M.F., Lee, J., Wynn, J.K., Mathis, K.I., 2011. Visual masking in schizophrenia: overview and theoretical implications. *Schizophr. Bull.* 37 (4), 700–708.
- Haigh, S.M., Coffman, B.A., Salisbury, D.F., 2017. Mismatch negativity in first-episode schizophrenia: a meta-analysis. *Clin. EEG Neurosci.* 48 (1), 3–10.
- Herzog, M.H., Kopmann, S., Brand, A., 2004. Intact figure-ground segmentation in schizophrenia. *Psychiatry Res.* 129 (1), 55–63.
- Herzog, M.H., Roinishvili, M., Chkonia, E., Brand, A., 2013. Schizophrenia and visual backward masking: a general deficit of target enhancement. *Front. Psychology* 4, 254.
- Herzog, M.H., Brand, A., 2015. Visual masking & Schizophrenia. *Schizophr. Res.* 2 (2), 64–71.
- Hoaglin, D.C., Mosteller, F., Tukey, J.W., 1983. Understanding robust and exploratory data analysis. Wiley, New York.
- Hoaglin, D.C., Mosteller, F., Tukey, J.W., 1985. Exploring Data Tables, Trends, and Shapes, 1st edition. Wiley, New York.
- Holzer, L., Jauguey, L., Chinot, L., Herzog, M.H., 2009. Deteriorated visual backward masking in the shine-through effect in adolescents with psychosis. *J. Clin. Exp. Neuropsychol* 31 (6), 641–647.
- Kavanagh, D.H., Tansey, K.E., O'donovan, M.C., Owen, M.J., 2015. Schizophrenia genetics: emerging themes for a complex disorder. *Mol. Psychiatry* 20 (1), 72.
- Kendler, K.S., 2015. A joint history of the nature of genetic variation and the nature of Schizophrenia. *Mol. Psychiatry* 20 (1), 77–83.
- Kéri, S., Antal, A., Szekeres, G., Benedek, G., Janka, Z., 2000. Visual information processing in patients with Schizophrenia: evidence for the impairment of central mechanisms. *Neurosci. Lett.* 293 (1), 69–71.
- Kéri, S., Kelemen, O., Benedek, G., Janka, Z., 2001. Different trait markers for schizophrenia and bipolar disorder: a neurocognitive approach. *Psychol. Med.* 31 (5), 915–922.
- Knebel, J.F., Javitt, D.C., Murray, M.M., 2011. Impaired early visual response modulations to spatial information in chronic Schizophrenia. *Psychiatry Res. – Neuroimaging* 193, 168–176.
- Knebel, J.F., Murray, M.M., 2012. Towards a resolution of conflicting models of illusory contour processing in humans. *Neuroimage* 59, 2808–2817.
- Knoll IV, J.L., Garver, D.L., Ramberg, J.E., Kingsbury, S.J., Croissant, D., McDermott, B., 1998. Heterogeneity of the psychoses: is there a neurodegenerative psychosis. *Schizophr. Bull.* 24 (3), 365.
- Lehmann, D., Skrandies, W., 1980. Reference-free identification of components of checkerboard-evoked multichannel potential fields. *EEG Clin. Neurophysiol.* 48 (6), 609–621.
- Lewis, D.A., Levitt, P., 2002. Schizophrenia as a disorder of neurodevelopment. *Ann. Rev. Neurosci.* 25 (1), 409–432.
- Light, G.A., Geyer, M.A., Clementz, B.A., Cadenhead, K.S., Braff, D.L., 2000. Normal P50 suppression in schizophrenia patients treated with atypical antipsychotic medications. *Am. J. Psychiatry* 157 (5), 767–771.
- Mullen, T., 2012. CleanLine. NITRC. <https://www.nitrc.org/projects/cleanline/>.
- Murray, R.M., Bhavsar, V., Tripoli, G., Howes, O., 2017. 30 Years on: how the neurodevelopmental hypothesis of schizophrenia morphed into the developmental risk factor model of psychosis. *Schizophr. Bull.* 43 (6), 1190–1196.
- Nagamoto, H.T., Adler, L.E., Hea, R.A., Griffith, J.M., McRae, K.A., Freedman, R., 1996. Gating of auditory P50 in schizophrenics: unique effects of clozapine. *Biol. Psychiatry* 40 (3), 181–188.
- Nuechterlein, K.H., Dawson, M.E., Green, M.F., 1994. Information-processing abnormalities as neuropsychological vulnerability indicators for schizophrenia. *Acta Psychiatrica Scandinavica* 384, 71–79 Suppl.
- Plomp, G., Kunchulia, M., Herzog, M.H., 2012. Age-related changes in visually evoked electrical brain activity. *Hum. Brain Mapp.* 33 (5), 1124–1136.
- Plomp, G., Roinishvili, M., Chkonia, E., Kapanadze, G., Kereselidze, M., Brand, A., Herzog, M.H., 2013. Electrophysiological evidence for ventral stream deficits in Schizophrenia patients. *Schizophr. Bull.* 39, 547–554.
- Rapoport, J.L., Giedd, J.N., Gogtay, N., 2012. Neurodevelopmental model of Schizophrenia: update. *Mol. Psychiatry* 17 (12), 1228–1238.
- Roinishvili, M., Chkonia, E., Brand, A., Herzog, M.H., 2008. Contextual suppression and protection in schizophrenic patients. *Eur. Arch. Psychiatry Clin. Neurosci.* 258 (4), 210–216.
- Roinishvili, M., Chkonia, E., Stroux, A., Brand, A., Herzog, M.H., 2011. Combining vernier acuity and visual backward masking as a sensitive test for visual temporal deficits in aging research. *Vis. Res.* 51 (4), 417–423.
- Rund, B.R., 1993. Backward-masking performance in chronic and nonchronic schizophrenics, affectively disturbed patients, and normal control subjects. *J. Abnorm. Psychol.* 102 (1), 74.
- Saccuzzo, D.P., Braff, D.L., 1981. Early information processing deficit in schizophrenia. New findings using Schizophrenic subgroups and manic control subjects. *Arch. Gen. Psychiatry* 38 (2), 175–179.
- Saccuzzo, D.P., Braff, D.L., 1986. Information-processing abnormalities: trait- and state-dependent components. *Schizophr. Bull.* 12 (3), 447–459.
- Salisbury, D.F., McCathern, A.G., Coffman, B.A., Murphy, T.K., Haigh, S.M., 2018. Complex mismatch negativity to tone pair deviants in long-term schizophrenia and in the first-episode schizophrenia spectrum. *Schizophr. Res.* 191, 18–24.
- Schütze, C., Bongard, I., Marbach, S., Brand, A., Herzog, M.H., 2007. Collinear contextual suppression in Schizophrenic patients. *Psychiatry Res.* 150 (3), 237–243.
- Shaqiri, A., Willemin, J., Sierro, G., Roinishvili, M., Iannantuoni, L., Rürup, L., Chkonia, E., Herzog, M.H., Mohr, C., 2015. Does chronic nicotine consumption influence visual backward masking in Schizophrenia and Schizotypy. *Schizophr. Res.* 2 (2), 93–99.
- Taylor, M.M., 1967. PEST: efficient estimates on probability functions. *J. Acoust. Soc. Am.* 41 (4A), 782.
- Turetsky, B.I., Dent, G., Jaeger, J., Zukin, S.R., 2012. P50 amplitude reduction: a nicotinic receptor-mediated deficit in first-degree relatives of schizophrenia patients. *Psychopharmacology* 221 (1), 39–52.
- Umbrecht, D., Krjjes, S., 2005. Mismatch negativity in Schizophrenia: a meta-analysis. *Schizophr. Res.* 76 (1), 1–23.

Supplementary Material

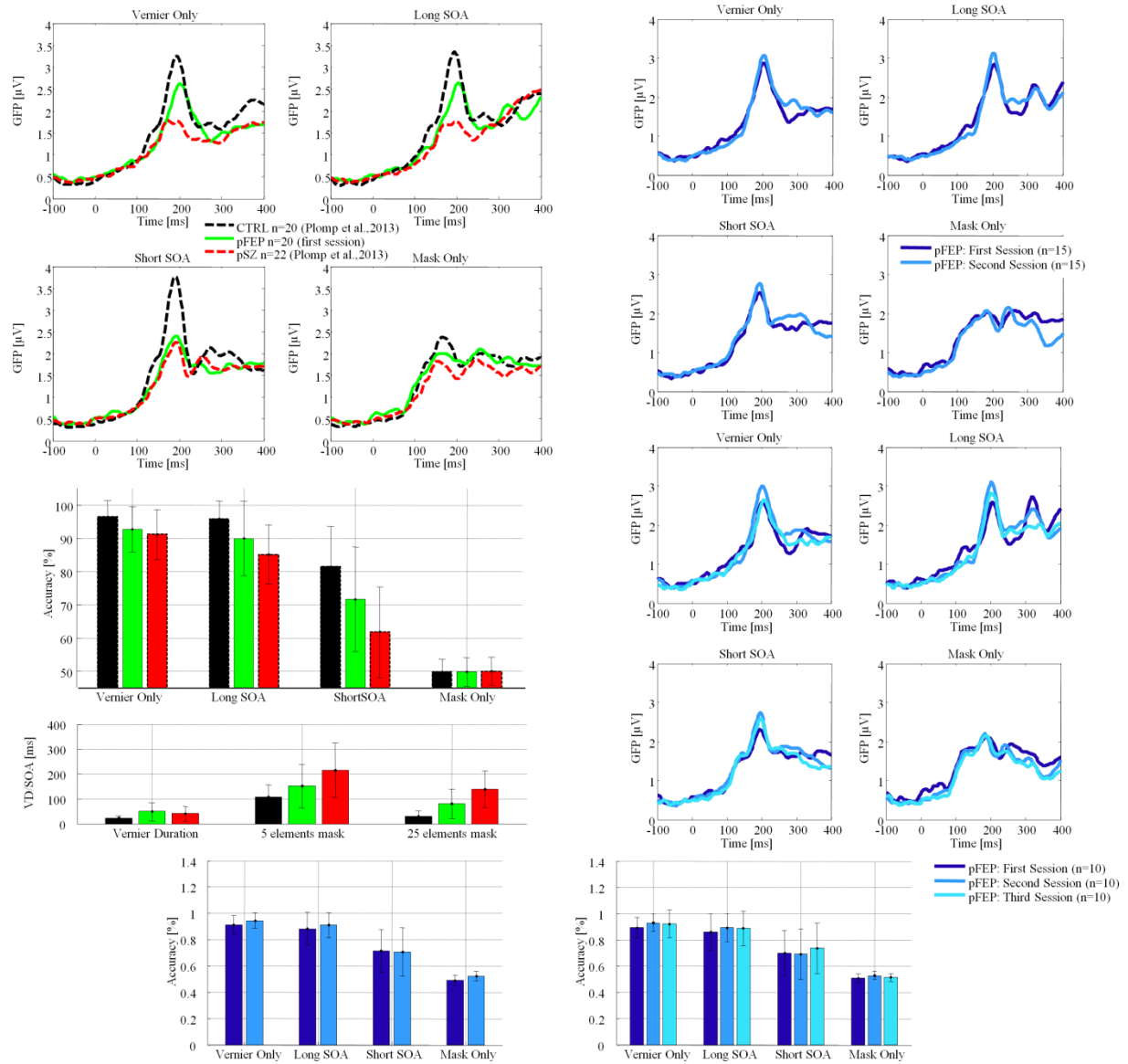


Figure S1| Replication of the manuscript figures without the bipolar I patient. Patients with FEP sample size: $n=20$ in the first session, $n=15$ in the second session and $n=10$ in the third session.

Table S1 | *Subtypes of diagnosis according to the DSM-IV for all three sessions.*

n	Diagnosis (DSM-IV)
First Session (n total=21)	
2	Schizophrenia, Disorganized Type (295.1)
15	Schizophrenia, Paranoid Type (295.3)
3	Schizophrenia, Undifferentiated Type (295.9)
1	Bipolar I Disorder, Most Recent Episode Depressed, In Partial Remission (296.55)
Second Session (n total=16)	
1	Schizophrenia, Disorganized Type (295.1)
8	Schizophrenia, Paranoid Type (295.3)
2	Schizoaffective Disorder (295.7)
3	Schizophrenia, Undifferentiated Type (295.9)
1	Bipolar I Disorder, Most Recent Episode Depressed, Mild (296.51)
1	Bipolar I Disorder, Most Recent Episode Depressed, In Partial Remission (296.55)
Third Session (n total=11)	
8	Schizophrenia, Paranoid Type (295.3)
2	Schizophrenia, Undifferentiated Type (295.9)
1	Bipolar I Disorder, Most Recent Episode Depressed, In Partial Remission (296.55)

Table S2 | *EEG pre-processing detailed information: Average per EEG recording for each group, patients with schizophrenia (pSZ), patients with first episode psychosis (pFEP) and controls (CTRL).*

	Number of Bad Channels (64 total)	Excluded Trials [%]	Groups	n
Average	1.09	5.13	pSZ	22
SD	0.68	3.53	pSZ	22
Average	0.58	3.88	pFEP 1 st session	21
SD	0.60	2.23	pFEP 1 st session	21
Average	0.70	3.75	pFEP 2 nd session	16
SD	0.59	2.22	pFEP 2 nd session	16
Average	0.82	3.75	pFEP 3 rd session	11
SD	0.78	1.55	pFEP 3 rd session	11
Average	0.70	3.57	CTRL	20
SD	0.80	2.40	CTRL	20

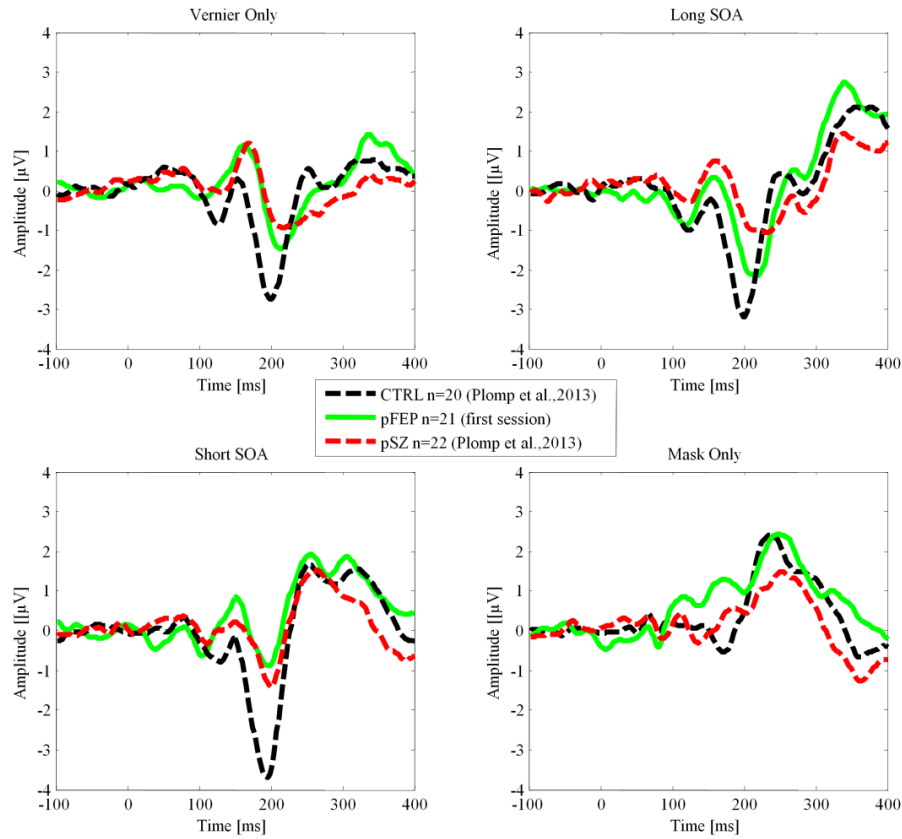


Figure S2 | Visual evoked response of the occipital electrode *Oz* for the three groups of participant: the controls (CTRL, dashed black), the patients with first episode psychosis (pFEP, solid green) during the first session and the patients with schizophrenia (pSZ, dashed red). A first positive component (P1) appears around 150 ms followed by a strong negative deflection (N1) around 200 ms for each condition with a target vernier.

Table S3 | Average statistics for Figure 2C left, $n=16$

Condition	Session	Mean	SD
Vernier Only	First	0.916	0.071
	Second	0.947	0.058
Long SOA	First	0.889	0.122
	Second	0.914	0.092
Short SOA	First	0.715	0.159
	Second	0.71	0.179
Mask Only	First	0.487	0.042
	Second	0.524	0.035

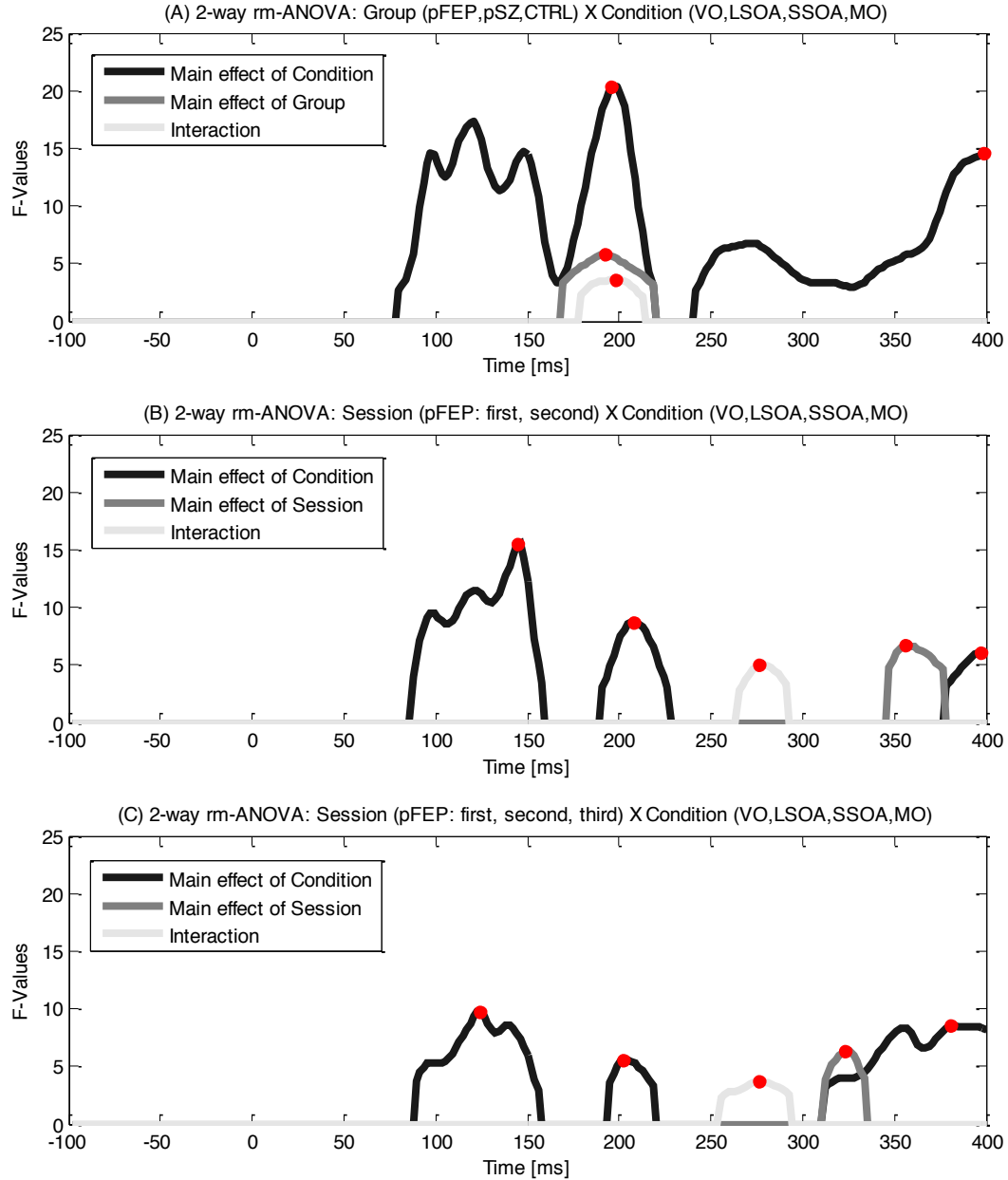


Figure S3 | *F-values for the main effects of the rm-ANOVAs. Red dots indicate the highest F -values (for each time interval) which are reported in the main text. **A.** The two main effects of Condition lasted for almost the entire epoch (first for the time interval 80-218 ms with the highest significance at 196 ms $F(3,180)=20.40$, $p<0.001$ and second for the time interval 242-400 ms with the highest significance at 399 ms $F(3,180)=14.65$, $p<0.001$). We also found an*

*interaction Group x Condition in an interval around 200 ms (179-212 ms with the highest significance at 198 ms $F(6,180)=3.62$, $p=0.002$). **B.** There were main effects of Condition for three time intervals (the first interval started from 87 to 158 ms with the highest significance at 145 ms $F(3,45)=15.51$, $p<0.001$, the second interval started from 191 to 226 ms with the highest significance at 208 ms $F(3,45)=8.73$, $p<0.001$ and the last interval started from 379 to 400 ms with the highest significance at 397 ms $F(3,45)=6.12$, $p=0.001$). There was an interaction Session x Condition for an interval before 300 ms (265-291 ms with the highest significance at 276 ms $F(3,45)=5.06$, $p=0.004$). **C.** There were main effects of Condition for three time intervals (the first interval started from 89 to 156 ms with the highest significance at 124 ms $F(3,30)=9.76$, $p<0.001$, the second interval started from 195 to 218 ms with the highest significance at 202 ms $F(3,30)=5.62$, $p=0.003$ and the last interval started from 312 to 400 ms with the highest significance at 381 ms $F(3,30)=8.54$, $p<0.001$). There was an interaction Session x Condition for an interval before 300 ms (255-293 ms with the highest significance at 276 ms $F(6,60)=3.72$, $p=0.003$).*

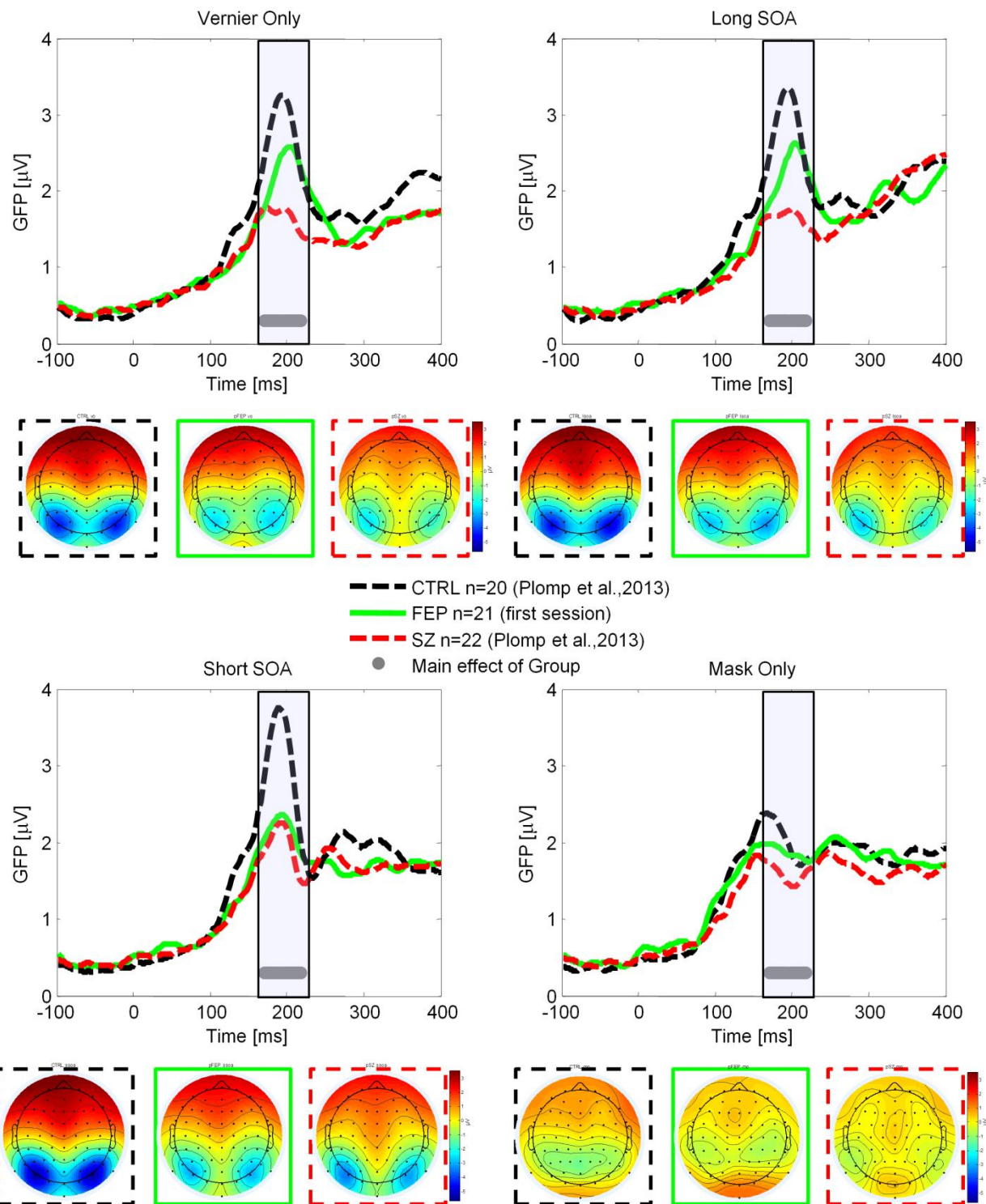


Figure S4 | Voltage maps for the time interval highlighted in gray (main effect of Group). The topographies are similar across groups (except for the Mask Only condition). The maps differ in intensity between groups.

Table S4 | EEG studies: Percent correct (mean \pm SD), maximal EEG amplitudes (N1; mean \pm SD) and the corresponding latencies for the grand average of each population. An EEG condition is defined by the vernier duration (VD) and the SOA duration (SOA). Accuracy does not differ between the current study and the Plomp et al., 2013 study while EEG does since data were re-analyzed with the App (27).

Group	n	VD [ms]	Mask	SOA [ms]	Correct responses [%]	N1 amplitude [ms]	N1 latency [ms]	Study
Schizophrenia	22	30	25 elements	30	61.8 \pm 13.6	2.2 \pm 1.0	193	Current study
First Episode Psychosis	21	30	25 elements	30	71.9 \pm 15.4	2.4 \pm 1.6	193	Current study
Controls	20	30	25 elements	30	81.5 \pm 12.0	3.8 \pm 2.1	191	Current study
Schizophrenia	22	30	25 elements	150	85.1 \pm 8.9	1.8 \pm 0.8	199	Current study
First Episode Psychosis	21	30	25 elements	150	90.2 \pm 11.0	2.6 \pm 1.6	205	Current study
Controls	20	30	25 elements	150	95.9 \pm 5.3	3.3 \pm 1.8	195	Current study
Participants scoring high in CogDis	25	10	5 elements	60	63.4 \pm 12.5	1.8 \pm 0.7	191	Favrod et al., 2017
Participants scoring low in CogDis	20	10	5 elements	60	64.7 \pm 12.1	2.2 \pm 0.9	196	Favrod et al., 2017
Participants scoring high in CogDis	25	10	5 elements	80	67.4 \pm 13.6	2.0 \pm 0.8	184	Favrod et al., 2017
Participants scoring low in CogDis	20	10	5 elements	80	68.0 \pm 13.4	2.4 \pm 1.1	195	Favrod et al., 2017
Schizophrenia	10	30	5 elements	110	70.5 \pm 12.1	1.6 \pm 0.8	218	Favrod et al., 2017
Schizophrenia	10	30	5 elements	230	83.2 \pm 13.3	1.7 \pm 0.8	216	Favrod et al., 2017
Schizophrenia	22	30	25 elements	30	idem	2.1 \pm 0.9	197	Plomp et al., 2013
Controls	20	30	25 elements	30	idem	3.6 \pm 2.0	193	Plomp et al., 2013
Schizophrenia	22	30	25 elements	150	idem	1.6 \pm 0.7	205	Plomp et al., 2013
Controls	20	30	25 elements	150	idem	3.2 \pm 1.7	199	Plomp et al., 2013

Masking is always stronger with the 5-element compared to the 25-element mask. N1 amplitude is the lowest for the chronic patients. Amplitude difference is smaller between the high and low schizotypy healthy populations compared to clinical versus non-clinical populations.

Appendix F

Favrod, O., da Cruz, J. R., Roinishvili, M., Brand, A., Figueiredo, P., Herzog, M. H., & Chkonia, E. (under review)

Electrophysiological Correlates of Visual Backward Masking in Patients with Major Depressive Disorder

Ophélie Favrod^a, Janir R. da Cruz^{a,b}, Maya Roinishvili^{c,d}, Ekaterine Berdzenishvili^e, Andreas Brand^a, Patrícia Figueiredo^b, Michael H. Herzog^a, Eka Chkonia^{d,e}

^a Laboratory of Psychophysics, Brain Mind Institute, École Polytechnique Fédérale de Lausanne (EPFL), Switzerland

^b Institute for Systems and Robotics - Lisboa, Department of Bioengineering, Instituto Superior Técnico, Universidade de Lisboa, Portugal

^c Laboratory of Vision Physiology, Beritashvili Centre of Experimental Biomedicine, Tbilisi, Georgia

^d Institute of Cognitive Neurosciences, Agricultural University of Georgia, Tbilisi, Georgia

^e Department of Psychiatry, Tbilisi State Medical University, Tbilisi, Georgia

Corresponding author: Ophélie Favrod, LPSY, BMI, SV, EPFL - Station 19, CH-1015 Lausanne, +41 21 693 17 43, ophelie.favrod@epfl.ch

Running Title: EEG correlates of visual masking in depression

Key Words: Global Field Power; N1 component; Event-Related Potential, Endophenotype of Schizophrenia

Number of words in the abstract: 199/200

Number of words in the main text: 3615/4000 (without figures/tables captions)

Number of figures: 4

Number of tables: 4

Supplemental information: one word file containing 2 tables and 3 figures

Abbreviations:

CPT: Continuous Performance Test, CTRL: control participants, GFP: global field power, DEP: depressive patients, SZ: schizophrenia patients, SNP: single-nucleotide polymorphism, SOA: stimulus onset asynchrony, VBM: visual backward masking, VD: vernier duration, VEP: visual evoked potential, VFT: Verbal Fluency Test, WCST: Wisconsin Card Sorting Test.

Abstract

Depression and schizophrenia are two psychiatric diseases with different psychopathology but shared features and high co-morbidity. Mind diseases are costly for our society and a burden for the patients. There is an urge to find sensitive endophenotypes which can disentangle these disorders. Visual backward masking is such a potential endophenotype for schizophrenia. Masking is strongly deteriorated in schizophrenia patients, reflected in reduced amplitudes in the EEG. Here, we tested whether masking deficits and associated EEG changes were also expressed in patients with major depressive disorder (n=21). Performance and neural correlates were compared with those from a sample of schizophrenia patients (n=90) and healthy controls (n=76). First, we replicated results showing that depressive patients had no masking deficits. Second, we found that the EEG amplitudes of depressive patients were reduced compared to controls and at the level of schizophrenia patients. However, depressive patients did not show an increase in amplitude as the task became more challenging whereas controls and schizophrenia patients did. Finally, we showed that the masking paradigm outperformed other cognitive tests such as the degraded continuous performance test, the verbal fluency, and (to a lesser extent) the Wisconsin card sorting test, to discriminate between schizophrenia, depression and controls.

Introduction

Depression and schizophrenia are two major psychiatric diseases with different psychopathology but shared features and high co-morbidity. For example, negative symptoms of schizophrenia, such as poverty of speech or physical anergia, are also present in depressive patients (Andreasen, 1982). Likewise, depressive patients exhibit psychotic symptoms, such as delusions (Sax et al., 1996). In addition, genetic correlations are found between schizophrenia and major depressive disorder, even though only of moderate magnitude (Lee et al., 2013). Although disorders overlap, treatment for depression and schizophrenia largely differ. Therefore, it is important to be able to distinguish the schizophrenia-related components from the depressive ones. The present study aims at disentangling the neural correlates of a well-defined endophenotype for schizophrenia from those of depression.

An endophenotype must be state-independent, inheritable, present at a higher rate within at risk population and be associated to one disease only (Gottesman and Gould, 2003). Visual backward masking (and particularly the Shine-Through paradigm, where a target vernier is followed by a grating mask) is a potential endophenotype of schizophrenia (Chkonia et al., 2010a) and therefore must be different from depression.

The masking deficits of schizophrenia patients are well reflected in electroencephalography (EEG) by a strongly reduced N1 component of evoked-related potentials (ERPs) as measured by the global field power (GFP; Plomp et al., 2013; da Cruz et al., submitted). These masking deficits are also present in first-episode psychosis patients but to a weaker extent. The neural correlates are in an intermediate state: GFP traces are similar to controls when the task is easy and similar to chronic schizophrenia patients when the task is challenging (Favrod et al., 2018).

Comparably, high schizotypes show reduced GFP amplitudes (Favrod et al., 2017). Siblings of schizophrenia patients show attenuated masking deficits, but their GFP amplitudes are surprisingly increased compared to controls, suggesting a compensation mechanism (da Cruz et al., submitted).

It has already been shown that the Shine-Through paradigm can differentiate schizophrenia patients from depressive patients and that the performance of depressive patients is not different from the healthy controls (Chkonia et al., 2012). However, little is known about the underlying neural correlates, and the electrophysiological signature of visual backward masking in depressive patients is the missing piece to the endophenotype rationale. We have no prior expectation, except that it would be different from schizophrenia patients in order to be able to differentiate the two diseases. According to the ERP literature on depression, we expect a decrease in amplitude compared to controls since this is found for example for the P3 amplitude in oddball and challenging tasks (large effect sizes), and also for the auditory N1 amplitude, although the results are more heterogeneous in this case (see Bruder et al., 2012 for a review, e.g., not all patients show the ERP reduction effect because it is state-dependent; remission versus relapse). Interestingly, ERP reduction in depressive patients is more pronounced in patients with psychotic features (Karaaslan et al., 2003; Kaustio et al., 2002). Altered P50 suppression (increased amplitude) is also found in depression (and bipolarity; Olbrich and Arns, 2013 for a review). Interestingly, P50 suppression reflecting sensory gating is known to be impaired in schizophrenia (Bramon et al., 2004). Hence, the primary goal of this study is to quantify the magnitude of the potential amplitude reduction in depression as compared to schizophrenia and test whether there are also qualitative differences.

As a second normative goal, we also compare the Shine-Through paradigm to other cognitive tasks such as the degraded continuous performance test (CPT), the Wisconsin card sorting test (WCST) and a verbal fluency test (VFT). These tasks are often believed to be a marker for psychiatric diseases, despite controversial results (Chkonia et al., 2010b; relatives do not show deficits in CPT). Here, we investigate the extent of the deficits in depression as compared to schizophrenia.

Methods

Visual Backward Masking

Stimuli were displayed on a Siemens Fujitsu P796-1 monitor with a refresh rate of 100 Hz. The screen resolution was 1024x768 pixels. Patients sat at 3.5 m away from the monitor in a weakly illuminated room. The stimuli were white with a luminance of 100 cd/m² on a black background (<1 cd/m²).

We presented vernier stimuli consisting of two vertical bars separated by a vertical gap of 1' (arc min). The lower bar was slightly offset either to the left or to the right compared to the upper one. The horizontal vernier offset was 1.2'. After the vernier, a mask was presented which

consisted of either five or twenty-five aligned vernier stimuli. The horizontal spacing between mask elements was 3.33°. An illustration of the stimuli display can be found in the supplementary material (Figure S1). Observers reported the offset direction of the lower bar by pushing one of the two hand-held buttons.

Behavioral experiment (adaptive)

For each observer, we found the vernier duration (VD) for which the threshold of offset discrimination was below 0.6°. Afterwards, we used the individual VD with a fixed vernier offset of 1.2° and determined the stimulus onset asynchrony (SOA) threshold for each participant with an adaptive strategy (Parametric Estimation by Sequential Testing; Taylor, 1967) to reach 75% of correct responses. The protocol was similar to previous studies (Cappe et al., 2012; Herzog et al., 2004; Shaqiri et al., 2015, Favrod et al., 2018). We used two types of mask: a 5- and a 25-element grating mask.

EEG experiment

For the EEG experiment, we used only the 25-elements mask. As in previous EEG studies (Favrod et al., 2017; Favrod et al., 2018; Plomp et al., 2013), we tested four conditions: Vernier Only, Long SOA, Short SOA and Mask Only. In the Vernier Only condition, the vernier was presented alone for 30 ms which is about the mean duration of schizophrenia patients in previous studies. In the Short and Long SOA conditions, the vernier was presented for 30 ms followed by a mask for 300 ms with an SOA of either 30 or 150 ms, which are the average SOAs for controls and schizophrenia patients, respectively. In the Mask Only condition, the mask was presented for 300 ms, there was no vernier.

For each observer, 8 blocks of 80 trials (20 trials / condition) were presented. The conditions order was randomized within each block. In total, there were 160 trials per condition.

EEG recordings and pre-processing

We used the EEG BioSemi Active Two system with 64 Ag-AgCl sintered active electrodes distributed across the scalp according to the 10/20 layout system. The sampling frequency was 2048 Hz. EEG data were pre-processed offline in Matlab (R2012a, The MathWorks Inc., Natick, MA) with EEGLAB (Delorme and Makeig, 2004) and using an automated pre-processing pipeline (APP; da Cruz et al., 2018). The signal was down-sampled to 512 Hz, band-passed filtered from 1 to 40 Hz and the 50 Hz line noise was removed using CleanLine (Mullen, 2012). Signal was re-referenced to the biweight estimate of the mean of all electrode-channels (Hoaglin et al., 1983, 1985). Unstable and noisy electrodes were removed and interpolated with a 3D spline function. Eye blink artefacts were removed through an independent component analysis (ICA). EEG epochs were extracted from 100 ms before the stimulus onset (baseline) to 400 ms after stimulus onset and then re-referenced to the common average. We applied an exclusion

criterion on reaction time [300 ms - 3 s]. Hits and missed trials were averaged for each condition and each participant. The individual averages were baseline corrected.

EEG analysis

The individual visual evoked potentials (VEP) were analyzed in MATLAB (R2018b, The MathWorks Inc., Natick, MA). Signal from two occipital electrodes (PO7 and PO8) were extracted to visualize the positive and negative components of the VEPs (supplementary material Figure S2). The Global Field Power (GFP) was computed as the standard deviation across all electrodes at each time point for each participant and each condition separately (Lehmann and Skrandies, 1980). We selected this measure to avoid the problem of selecting an electrode arbitrarily. Grand averages of GFPs were computed for each condition, each session, and each group of participants.

CPT, WCST, and VFT

We administered a computerized version of the Nelson Test (Nelson, 1976), which was a modified Wisconsin Card Sorting Test (WCST, Berg, 1948) with 48 cards. We recorded the number of categories that participants went through, the number of correct responses, errors and preservative errors. We also administered a degraded Continuous Performance Test (CPT, Rosvold et al., 1956). We reported d' . Methodological details can be found in Chkonia et al., 2010a. The Verbal Fluency Test (VBF) was derived from the Controlled Oral Word Association Test (COWAT, Bechtold et al., 1962). We asked the participants to report as many words as they could belong to either the animal or fruit/vegetables category. The number of words for each category was reported.

Statistical analysis

Repeated measures ANOVAs were performed using JASP (<https://jasp-stats.org/>, version 0.9.1.0). Statistical tests were Greenhouse-Geisser corrected when necessary.

Participants

All participants had normal or corrected-to-normal vision; with a visual acuity of ≥ 0.8 determined for both eyes with the FrAct (Bach, 1996). All participants signed informed consent and were informed that they could quit the experiments at any time. All procedures complied with the Declaration of Helsinki and were approved by the local ethics committee.

Depressive patients

Patients were recruited either from the Tbilisi Mental Health Hospital or from the Acute Psychiatric Departments of Multiprofile Clinics. General exclusion criteria were drug or alcohol abuse, neurological, or other somatic illnesses influencing subjects' mental state. Patients were diagnosed with major depressive disorder according to the Diagnostic and Statistical Manual of

Mental Disorders IV/V (296.31; 296.32; 296.33) by means of an interview based on the Structured Clinical Interview, information of the staff, and the study of the records. Psychopathology was assessed by an experienced psychiatrist (EC) through the Brief Psychiatric Rating Scale (BPRS; Overall and Gorham, 1962) and the Hamilton scale (Hamilton, 1960).

In total, there were 33 depressive patients. Not all of them participated in each task for various reasons (e.g., did not want to, etc.). Thirty-two performed the WCST. Thirty-one performed the CPT degraded test. Thirty performed the VFT. Twenty-eight performed the adaptive masking paradigm. Finally, twenty-one of them performed the masking paradigm with EEG. Group characteristics are depicted in Table 1. Out of the 33 patients, 23 patients were receiving neuroleptic medication. Out of the 21 patients who performed the EEG, 16 were receiving neuroleptic medication.

Table 1 | *Demographics for the controls, the depressive patients (two groups: all of them and the EEG subgroup) and schizophrenia patients*

	Controls	Depression (all)	Depression (EEG)	Schizophrenia
<i>N</i>	76	33	21	90
Gender (F/M)	34/42	21/12	12/9	15/75
Age (years) \pm SD	34.9 \pm 8.1	34.9 \pm 10.4	31.4 \pm 9.1	35.8 \pm 8.8
Education (years) \pm SD	15.0 \pm 2.8	14.5 \pm 2.6	14.7 \pm 2.5	13.2 \pm 2.7
Illness Duration (months) \pm SD		6.8 \pm 7.1	5.7 \pm 5.5	11.3 \pm 8.0
SANS \pm SD				10.7 \pm 5.3
SAPS \pm SD				10.0 \pm 8.1
BPRS		31.7 \pm 7.3	30.2 \pm 5.0	
Hamilton		15.1 \pm 6.0	14.8 \pm 5.9	
CPZ equivalent \pm SD		286.6 \pm 319.9	198.4 \pm 199.3	549.3 \pm 398.5
Handedness (L/R)	5/71	1/32	1/20	4/86
Visual Acuity \pm SD	1.6 \pm 0.4	1.2 \pm 0.4	1.3 \pm 0.4	1.5 \pm 0.4

Note: Visual acuity was missing for one depressive patient in the n=33 set. Only 26 of the 33 depressive patients were assessed with the Hamilton scale (and 17 for the EEG dataset). 72 of the 90 schizophrenic patients received neuroleptic medication.

Controls and Schizophrenia patients

Controls and schizophrenia patients were the same participants as in da Cruz et al., submitted. We used them here for comparison purposes with the depressive patients group and re-plotted them. The EEG data for three groups were collected and analyzed using the same experimental setup and pre-processing pipeline as described in a previous section (APP; da Cruz et al., 2018). Psychopathology was assessed by the Scales for the assessment of negative and positive

symptoms (SANS, Andreasen 1984a; SAPS, Andreasen 1984b). Out of the 76 controls, 75 performed the CPT, 74 the WCST and 48 the VFT. Out of the 90 patients, 89 of them did the WCST, 88 the CPT and 23 the VFT. All of them were taken into account for the masking experiments (adaptive and EEG).

Results

Visual Backward Masking

The VD was significantly lower for controls compared to both groups of patients Figure 1a, Table 2.

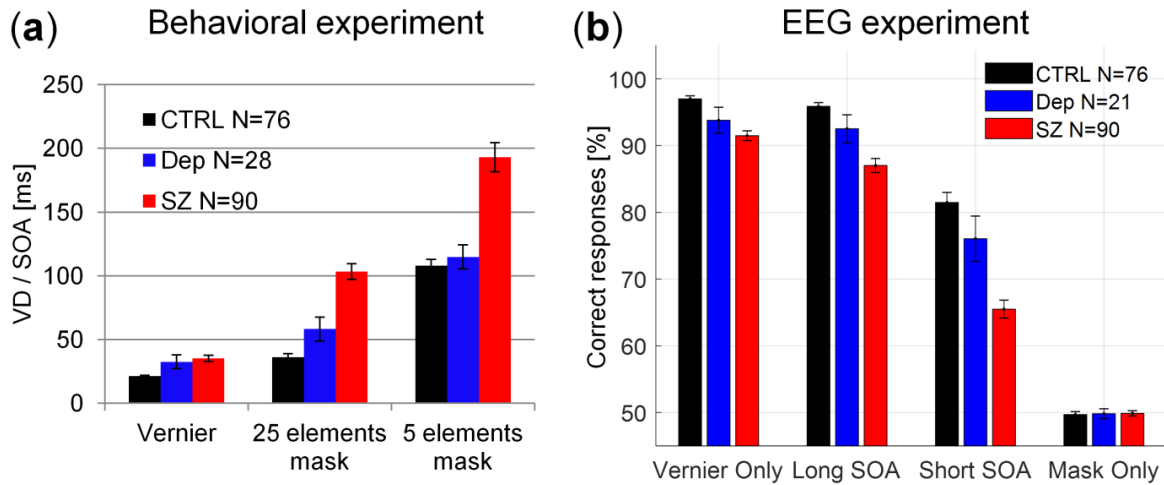


Figure 1| (a) Psychophysical thresholds obtained with the adaptive procedure, for the controls (Ctrl), depressive patients (Dep) and schizophrenia patients (Sz): Vernier duration (VD) for the Vernier condition and SOA for the two masking conditions with the 5- and 25-element mask (b) Percent correct responses in each condition of the EEG experiment (25-element mask) for the Ctrl, Dep, and Sz groups.

The 5-element mask led to stronger masking. Most importantly, schizophrenia patients performed significantly worse compared to both depressive patients and controls (Figure 1a). There was no significant difference between controls and depressive patients (Table 2).

In the EEG experiment, we found a strong behavioral difference between controls and schizophrenia patients, a smaller difference between depressive and schizophrenia patients and no significant difference between controls and depressive patients (Table 2). The performance of depressive patients was in between the performance of controls and schizophrenia patients, though closer to controls Figure 1b.

In summary, depressive patients performed better than schizophrenia patients and rather similarly to controls in the masking conditions.

Table 2 | *Statistical analysis for the visual backward masking performance: adaptive masking experiment (Vernier, 5- and 25-element mask) and EEG experiment.*

Vernier Duration				Comments
group	F(2,191)=10.10, p<0.001, $\eta^2=0.096$			
post-hoc	Ctrl vs Dep	Ctrl vs Sz	Dep vs Sz	
	t(102)=-2.516, d=-0.723, p _{holm} =0.025	t(164)=-4.403, d=-0.753, p _{holm} <0.001	t(116)=-0.600, d=-0.103, p _{holm} =0.549	
5-element and 25-element mask (SOA)				
mask	F(1,191)=197.987, p<0.001, $\eta^2=0.500$			
SOA5 vs SOA25	t(192)=-16.93, d=1.216, p _{holm} <0.001			
mask*group	F(2,191)=3.492, p=0.032, $\eta^2=0.018$			simple main effects and post-hoc statistics are reported in the supplementary material (Table S2)
group	F(2,191)=36.71, p<0.001, $\eta^2=0.278$			
post-hoc	Ctrl vs Dep	Ctrl vs Sz	Dep vs Sz	
	t(206)=-1.114, d=-0.080, p _{holm} =0.267	t(330)=-8.277, d=-0.594, p _{holm} <0.001	t(234)=-4.821, d=-0.346 p _{holm} <0.001	
EEG experiment				
condition	F(1.809,332.828)=1110.55, p<0.001, $\eta^2=0.832$			simple main effects and post-hoc statistics are reported in the supplementary material (Table S2)
condition*group	F(3.618,332.828)=20.36, p<0.001, $\eta^2=0.030$			
group	F(2,184)=30.59, p<0.001, $\eta^2=0.250$			
post-hoc	Ctrl vs Dep	Ctrl vs Sz	Dep vs Sz	
	t(386)=1.933, d=0.141, p _{holm} =0.055	t(662)=7.782, d=0.569, p _{holm} <0.001	t(442)=3.037, d=0.222, p _{holm} =0.005	

Visual Backward Masking: Global Field Power

We computed the repeated measure ANOVA at the peak location of the grand average Figure 2 for each group and each condition, (Table S1, in the supplementary material).

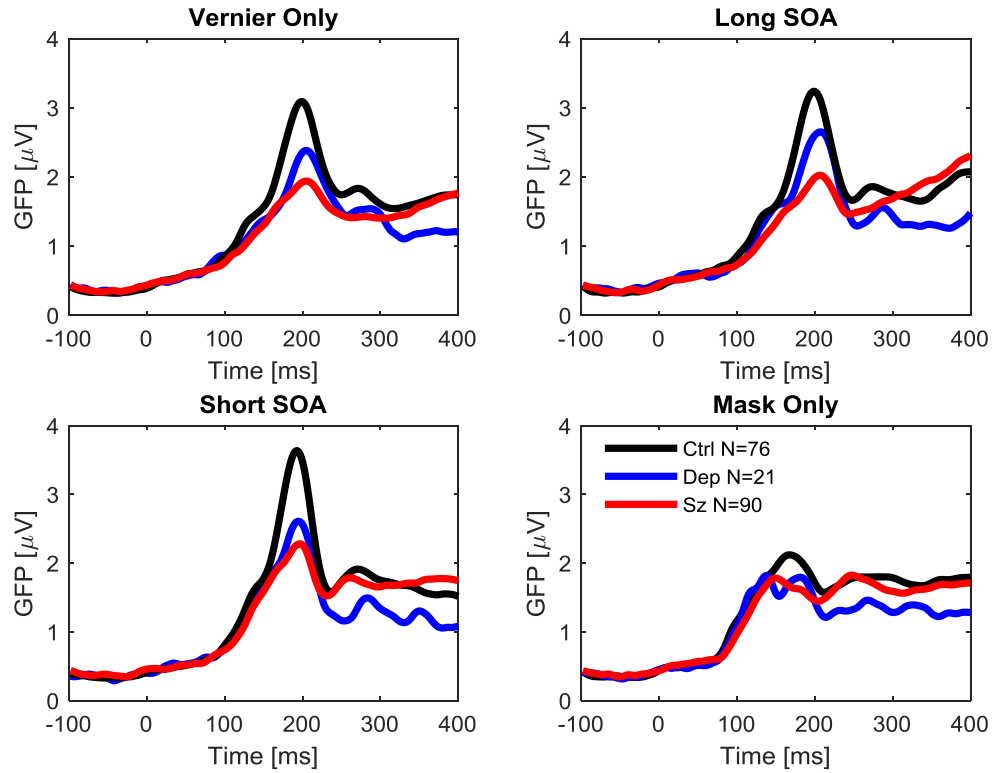


Figure 2 | Global Field Power (GFP) for the four EEG conditions with the 25-element mask. Black: controls (Ctrl); Blue: depressive patients (Dep), and Red: schizophrenia patients (Sz). In all four conditions with a vernier, the N1 peak is observed around 200 ms.

We found a strong difference between controls and schizophrenia patients, no difference between depressive and schizophrenia patients and a small difference between controls and depressive patients. In particular, the differences were due to the conditions where there was a target vernier. Statistics are reported in Table 3.

For comparative analysis with previous studies (Favrod et al., 2017; 2018; da Cruz et al., submitted), statistics across the whole epoch (i.e., computed at each time frame) are shown in the supplementary material Figure S3.

Considering only the three conditions with a vernier, we found a main effect of condition for the schizophrenia group: $F(1.357, 120.788) = 12.37$, $p < 0.001$, $\eta^2 = 0.122$, and for the controls group: $F(1.352, 101.433) = 20.27$, $p < 0.001$, $\eta^2 = 0.213$, as it was shown in da Cruz et al., submitted. However, here we found no difference for the depressive group: $F(2, 40) = 2.274$, $p = 0.116$, $\eta^2 = 0.102$.

In summary, the N1 amplitudes of depressive patients were reduced compared to controls and closer to those of schizophrenia patients. In addition, we found that depressive patients did not show a difference in amplitude across conditions whereas controls and schizophrenia patients

did, in line with previous studies (da Cruz et al., submitted). The amplitude of schizophrenia patients and controls increased in the Short SOA condition compared to the Vernier Only condition (same with Long SOA), suggesting a bigger allocation of the neural resources when the task became more challenging (da Cruz et al., submitted). Here, we did not find this pattern for the depressive patients: the N1 amplitudes remained constant across the conditions when a vernier was present.

Table 3 | Statistical analysis for the GFP N1 peak measured in the EEG experiment.

N1 peak (~200 ms)				Comments
group	F(2,184)=20.21, $p<0.001$, $\eta^2=0.180$			
post-hoc	Ctrl vs Dep	Ctrl vs Sz	Dep vs Sz	
	t(386)=2.590, d=0.189, $p_{holm}=0.021$	t(662)=6.342, d=0.464, $p_{holm}<0.001$	t(442)=1.442, d=0.105, $p_{holm}=0.151$	
condition	F(2.136,393.098)=49.70, $p<0.001$, $\eta^2=0.194$			post-hoc statistics are shown in the supplementary material (Table S2)
condition*group	F(4.273,393.098)=11.22, $p<0.001$, $\eta^2=0.088$			simple main effects show a difference for all the conditions with a Vernier
post-hoc	Ctrl vs Dep	Ctrl vs Sz (da Cruz et al., submitted)	Dep vs Sz	
Vernier Only	t(95)=2.450, d=0.558, $p_{holm}=0.030$	t(164)=6.300, d=0.951, $p_{holm}<0.001$	t(109)=1.558, d=0.436, $p_{holm}=0.121$	F(2,184)=19.89, $p<0.001$, $\eta^2=0.178$
Long SOA	t(95)=2.030, d=0.458, $p_{holm}=0.058$	t(164)=6.633, d=1.011, $p_{holm}<0.001$	t(109)=2.199, d=0.610, $p_{holm}=0.058$	F(2,184)=22.03, $p<0.001$, $\eta^2=0.193$
Short SOA	t(95)=3.051, d=0.677, $p_{holm}=0.005$	t(164)=6.378, d=0.967, $p_{holm}<0.001$	t(109)=0.995, d=0.286, $p_{holm}=0.321$	F(2,184)=20.76, $p<0.001$, $\eta^2=0.184$
Mask Only	F(2,184)=3.046, $p=0.050$, $\eta^2=0.032$			

CPT, VFT, and WVCST

For the CPT, we found a group difference due to the performance difference between controls and schizophrenia patients as shown by the post-hoc tests (Table 4). Depressive patients were marginally different from schizophrenia patients (Figure 3a).

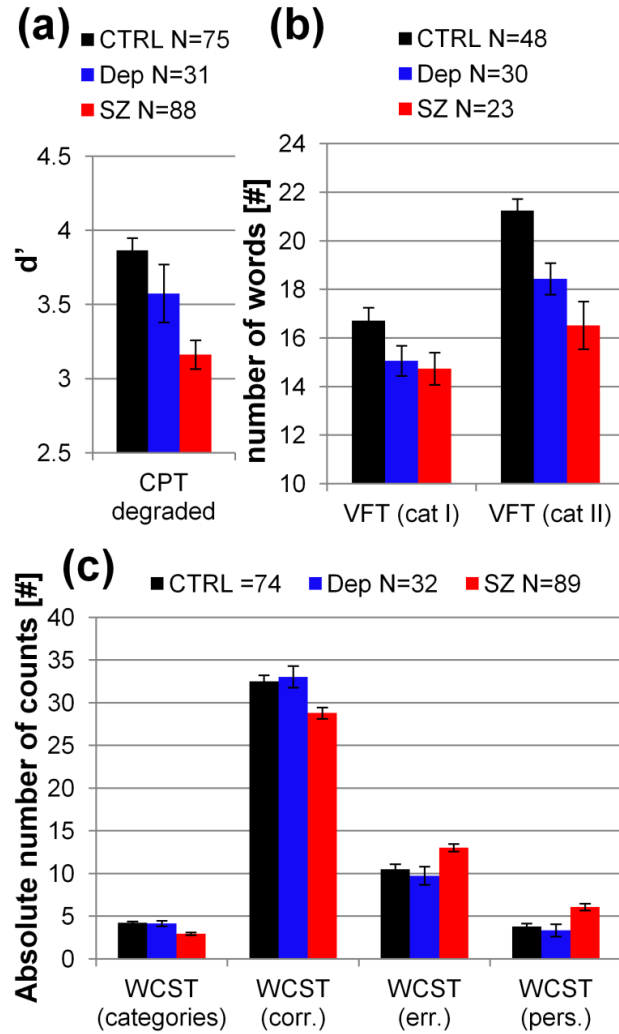


Figure 3 | Performance for the Continuous Performance Test (CPT), the Verbal Fluency Test (VFT) and the Wisconsin Card Sorting Test (WCST), in the three groups (CTRL, DEP and SZ). (a) d' for the CPT (b) number of words for the VFT - category I: animals, category II: vegetables/fruits (c) the four different measures for the WCST: the categories, the number of correct responses, the number of errors and the perseverative errors.

In the VFT, we found a group difference with the controls performing better than schizophrenia patients and also better compared to depressive patients (Table 4). Depressive and schizophrenia patients were not performing significantly differently (Figure 3b).

For the WCST, we found a significant interaction measure*group showing that patients with schizophrenia were making more mistakes, were less accurate, and were going through fewer categories compared to controls (Figure 3c). We found that schizophrenia patients underwent fewer categories than controls and depressive patients. They were also making less correct responses. We did not find any significant differences between controls and depressive patients for either measure. The most interesting and widely reported measures are the number of errors

and the preservative errors. We found that schizophrenia patients were making more errors than controls for both types of error. Schizophrenia patients were also making more errors than depressive patients. We found no difference in performance between controls and depressive patients. Post-hoc tests were reported in Table 4.

In summary, we found a significant difference between controls and schizophrenia patients for all tasks. We found a significant difference between controls and depressive patients for the VD, the peak amplitude and the VFT. Finally, we found a significant difference between depressive and schizophrenia patients for the SOAs (adaptive masking) and the WCST (the CPT only marginally).

Table 4 | *Statistical analysis for the three tasks: degraded continuous performance test (CPT), verbal fluency test (VFT), and Wisconsin card sorting test (WCST).*

CPT				Comments
group	F(2,191)=13.18, p<0.001, $\eta^2= 0.121$			
post-hoc	Ctrl vs Dep	Ctrl vs Sz	Dep vs Sz	
	t(104)=1.550, d=0.343, p _{holm} =0.123	t(161)=5.108, d=0.846, p _{holm} <0.001	t(117)=2.258, d=0.431, p _{holm} =0.050	
VFT				
group	F(2,98)=10.78, p<0.001, $\eta^2= 0.180$			
post-hoc	Ctrl vs Dep	Ctrl vs Sz	Dep vs Sz	
	t(154)=3.130, d=0.311, p _{holm} =0.005	t(140)=4.315, d=0.429, p _{holm} <0.001	t(104)=1.320, d=0.131 p _{holm} =0.190	
category	F(1,98)=64.172, p<0.001, $\eta^2= 0.377$			simple main effects and post-hoc tests are reported in the supplementary material (Table S2)
category*group	F(2,98)=4.004, p=0.021, $\eta^2= 0.047$			
WCST				
group	(F(2,192)=1.329, p=0.267, $\eta^2= 0.014$			
measure	F(1.305,250.527)=1027.667, p<0.001, $\eta^2= 0.830$			post-hoc tests are found in the supplementary material (Table S2)
measure*group	F(2.610,250.527)=9.338, p<0.001, $\eta^2= 0.015$			all simple main effects were significant
post-hoc	Ctrl vs Dep	Ctrl vs Sz	Dep vs Sz	
category	t(104)=0.218,	t(161)=5.167,	t(119)=3.720,	

	d=0.044, p _{holm} =0.828	d=0.839, p _{holm} <0.001	d=0.763 p _{holm} <0.001	
correct response	t(104)=-0.394, d=-0.083, p _{holm} =0.694	t(161)=3.697, d=0.597, p _{holm} <0.001	t(119)=3.226, d=0.649, p _{holm} =0.003	
error	t(104)=0.742, d=0.140, p _{holm} =0.459	t(161)=-3.281, d=-0.544 p _{holm} =0.004	t(119)=-3.266, d=-0.705, p _{holm} =0.004	
perseverative error	t(104)=0.593, d=0.131 p _{holm} =0.554	t(161)=-4.011, d=-0.652, p _{holm} <0.001	t(119)=-3.670, d=-0.703, p _{holm} <0.001	

Discussion

Our primary goal is to investigate the neural correlates of the well defined masking endophenotype for schizophrenia in depression. Behaviourally, depressive patients perform better than schizophrenia patients in the masking conditions, almost at the level of controls. This is in line with the criterion for an endophenotype, as it must co-segregate with other disorders. Schizophrenia and depression symptoms sometimes overlap, and here the masking paradigm distinguishes well the two diseases, which is essential to an endophenotype. Electrophysiologically, depressive patients have reduced EEG N1 amplitudes compared to controls and are similar to schizophrenia patients. Quantitatively, these neural correlates of the masking paradigm are not different between the two diseases: $d_{\text{dep-sz}}=0.105$, even though the difference between controls and schizophrenia is about 2.5 times larger ($d_{\text{ctrl-sz}}=0.464$) than between controls and depressive ($d_{\text{ctrl-dep}}=0.189$). Qualitatively, however, we would like to emphasize a small difference. ERP amplitudes at around 200 ms have been shown to be susceptible to task difficulty (Philiastides et al., 2006). Indeed, in previous studies, we find that controls and schizophrenia patients show higher GFP amplitudes in the Short SOA condition (the Shine-Through condition, which is challenging) compared to the Long SOA and Vernier Only conditions (comparatively easier), and similarly in the Long SOA condition compared to the Vernier Only (da Cruz et al., submitted). For the depressive patients, we find that the N1 amplitudes are similar in all three conditions with a vernier. There is no N1 increase associated with condition difficulty. We speculate that depressive patients are not able to allocate more resources (over-shoot) when the task becomes challenging, whereas all other populations do. The neural signature of depressive patients stays in a “constant state” independently of the task difficulty.

We have to mention we do not find this difference across conditions for patients with first episode psychosis: main effect of condition with a vernier (VO, LSOA, SSOA): $F(1.237, 24.749)=1.391$, $p=0.257$, $\eta^2=0.065$ (the amplitudes values are reported in the supplementary material in Favrod et al., 2018). It makes the first episode psychosis patients “electrophysiologically equivalent” to depressive patients. However, we speculate that the

underlying mechanisms are different, although they may look similar. Patients with first episode psychosis are in an intermediate and unstable state where their neural correlates are not fully developed, whereas depressive patients are in an un-modulated and monotonous state where they are not able to take into account the task difficulty (e.g., VO compared to LSOA or SSOA). Speculatively, depressive patients show a “motivational” deficit rather than the attentional deficit observed in schizophrenia (Herzog et al., 2013). There is something different in the neural correlates of depressive patients as their EEG amplitudes tend to be inversely associated with their behaviour (Figure 4). The opposite is true for all other populations studied, namely schizophrenia patients, unaffected siblings of schizophrenia patients, first episode psychosis, bipolar and controls: N1 amplitudes are positively associated with the correct responses (not significantly though, because the sample is small and the sensitivity of the measure is low in the EEG experiment (i.e., percent correct responses as compared to the psychophysical threshold in the adaptive masking experiment). The negative associations disappear when one outlier is discarded (but r is close to 0). Sample sizes have to be increased to draw any strong conclusions.

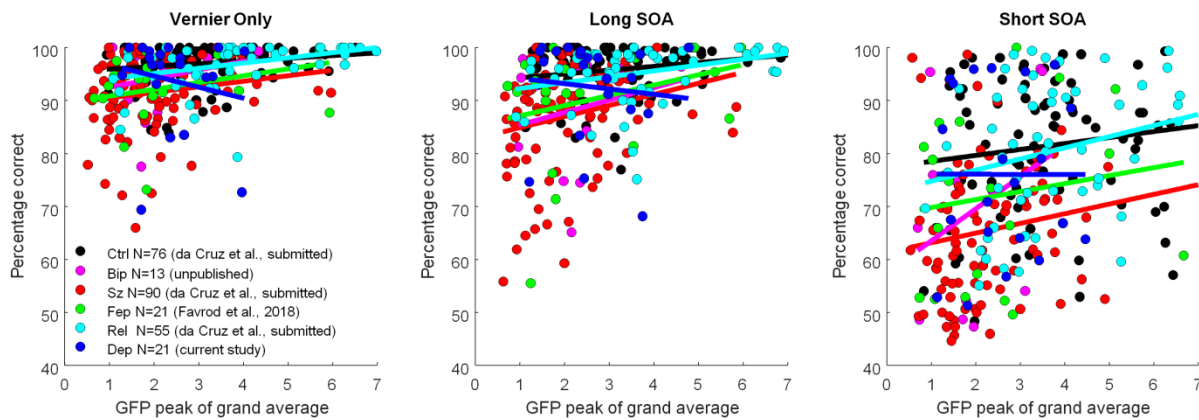


Figure 4 | Scatter plots between the behaviour (percent correct responses) and the EEG N1 amplitude, for all populations tested with a 25-element mask. There is a positive association for the controls (Ctrl, black), the bipolar patients (Bip, pink), the schizophrenia patients (Sz, red), the first episode psychosis patients (Fep, green) and the relatives/siblings of schizophrenia patients (Rel, cyan) while there is a negative association for the depressive patients (Dep, blue) in all three conditions (VO, LSOA, and SSOA). The lines represent the best linear fit. Note: Pearson correlations are not significant (except for LSOA: Sz and Rel).

Reduced P3 amplitudes in depressive are found to be state dependent (Bruder et al., 2012) and it is not surprising that amplitudes are highly heterogeneous. Reduced P3 amplitudes in depression are also associated with increased P3 latencies. Patients with anxiety disorders show increased P3 amplitudes and those with depressive-anxiety co-morbidity show no difference with controls (Bruder et al., 2002). It indicates that co-morbidity plays an important role. Interestingly, a study found that schizophrenia and depression differ in processing latencies to positive affect stimulus. Schizophrenia patients show an increase in gamma band activity in an early time period post

stimulus presentation while depressive patients show an increase at a later time period (Martin et al., 2018). However, social anhedonia and self-reported depression in schizophrenia are related to decrease gamma band activity in general, highlighting once again the interference of co-morbidity and how it produces heterogeneous results.

As a secondary goal, we wish to emphasize the low-level masking endophenotype in comparison to other cognitive tasks. The endophenotype is neither the vernier duration (because first, we find difference between controls and depressive which should not be the case for a schizophrenia endophenotype and, second, healthy siblings of schizophrenia patients have no VD deficits and an endophenotype must be present in healthy people carrying the genes) nor the EEG correlates (which just shed light on the underlying mechanisms). The only marker sensitive enough is the adaptive procedure with the 25-element mask, known as the Shine-Through paradigm, which is one of the most consistent and reliable endophenotypes for schizophrenia.

Comparatively, the CPT shows no difference between depressive patients and schizophrenia patients (we only find a marginal difference). In addition, in a previous study (Chkonia et al., 2010a/b), there is no difference between controls and relatives for the CPT, discarding this test from being an endophenotype. Depressive patients perform differently from controls on the VFT, also discarding this test from being a marker for schizophrenia, as depressive patients are impaired. Finally, the WCST could be a marker for schizophrenia (as there is no difference between controls and depressive) but as for the CPT there is no difference between controls and relatives (for the number of errors at least, Chkonia et al., 2010a). In addition, the WCST has repeatedly shown its bad inheritability in twin studies, also discarding this test from being a potential biomarker (Kremen et al., 2007; Taylor, 2007).

In conclusion, we find reduced EEG N1 amplitudes in depressive patients similarly to schizophrenia patients. However, we speculate that this finding is explained by a different strategy in vernier discrimination. Depressive patients show a lack of modulation. They are unable to over-shoot the signal in a challenging condition (Short SOA) as compared to an easy condition (Vernier Only), whereas schizophrenia patients, their unaffected sibling (not shown here) and controls can. Finally, we have shown again that the Shine-Through paradigm is a very reliable marker for schizophrenia but not for depression and that it outperforms most of others potential cognitive markers.

Acknowledgements

Funding

This work was supported by an NCCR Synapsy grant from the Swiss National Science Foundation (51NF40-158776), by the Portuguese Fundação para a Ciência e a Tecnologia, grant # FCT PD/BD/105785/2014 and by the “Knowledge Foundation” of Georgia. The authors have declared that there are no conflicts of interest in relation to the subject of this study.

References

- Andreasen, N. C. (1982). Negative symptoms in schizophrenia: definition and reliability. *Archives of general psychiatry*, 39(7), 784-788.
- Andreasen, N. C. (1984a). The scale for the assessment of negative symptoms (SANS). *Rinsho Seishin Igaku*, 13, 999-1010.
- Andreasen, N. C. (1984b). Scale for the assessment of positive symptoms (SAPS) University of Iowa College of Medicine. *Iowa City*.
- Bach, M. (1996). The Freiburg Visual Acuity Test-automatic measurement of visual acuity. *Optometry and vision science*, 73(1), 49-53.
- Bechtoldt, H. P., Benton, A. L., & Fogel, M. L. (1962). An application of factor analysis in neuropsychology. *The Psychological Record*, 12(2), 147-156.
- Berg, E. A. (1948). A simple objective technique for measuring flexibility in thinking. *The Journal of general psychology*, 39(1), 15-22.
- Bramon, E., Rabe-Hesketh, S., Sham, P., Murray, R. M., & Frangou, S. (2004). Meta-analysis of the P300 and P50 waveforms in schizophrenia. *Schizophrenia research*, 70(2-3), 315-329.
- Bruder, G. E., Kayser, J., Tenke, C. E., Leite, P., Schneier, F. R., Stewart, J. W., & Quitkin, F. M. (2002). Cognitive ERPs in depressive and anxiety disorders during tonal and phonetic oddball tasks. *Clinical Electroencephalography*, 33(3), 119-124.
- Bruder, G. E., Kayser, J., & Tenke, C. E. (2012). Event-related brain potentials in depression: clinical, cognitive and neurophysiologic implications. *The Oxford handbook of event-related potential components*, 2012, 563-592.
- Cappe, C., Herzog, M. H., Herzig, D. A., Brand, A., & Mohr, C. (2012). Cognitive disorganisation in schizotypy is associated with deterioration in visual backward masking. *Psychiatry Research*, 200(2-3), 652-659.
- Chkonia, E., Roinishvili, M., Makhatadze, N., Tsverava, L., Stroux, A., Neumann, K., ... & Brand, A. (2010a). The shine-through masking paradigm is a potential endophenotype of schizophrenia. *PLoS One*, 5(12), e14268.
- Chkonia, E., Roinishvili, M., Herzog, M. H., & Brand, A. (2010b). First-order relatives of schizophrenic patients are not impaired in the Continuous Performance Test. *Journal of clinical and experimental neuropsychology*, 32(5), 481-486.
- Chkonia, E., Roinishvili, M., Reichard, L., Wurch, W., Puhlmann, H., Grimsen, C., ... & Brand, A. (2012). Patients with functional psychoses show similar visual backward masking deficits. *Psychiatry Research*, 198(2), 235-240.

- da Cruz, J. R., Chicherov, V., Herzog, M. H., & Figueiredo, P. (2018). An automatic pre-processing pipeline for EEG analysis (APP) based on robust statistics. *Clinical Neurophysiology*, 129(7), 1427-1437.
- da Cruz J.R., Shaqiri A., Roinishvili M., Chkonia E., Brand A., Figueiredo P., Herzog, M.H., (submitted). Neural compensation mechanisms of siblings of schizophrenia patients as revealed by high-density EEG. *Brain*
- Delorme, A., & Makeig, S. (2004). EEGLAB: an open source toolbox for analysis of single-trial EEG dynamics including independent component analysis. *Journal of neuroscience methods*, 134(1), 9-21.
- Favrod, O., Sierro, G., Roinishvili, M., Chkonia, E., Mohr, C., Herzog, M. H., & Cappe, C. (2017). Electrophysiological correlates of visual backward masking in high schizotypic personality traits participants. *Psychiatry research*, 254, 251-257.
- Favrod, O., Roinishvili, M., da Cruz, J. R., Brand, A., Okruashvili, M., Gamkrelidze, T., ... & Shaqiri, A. (2018). Electrophysiological correlates of visual backward masking in patients with first episode psychosis. *Psychiatry Research: Neuroimaging*, 282, 64-72.
- Gottesman, I. I., & Gould, T. D. (2003). The endophenotype concept in psychiatry: etymology and strategic intentions. *American Journal of Psychiatry*, 160(4), 636-645.
- Hamilton, M. (1960). A rating scale for depression. *Journal of neurology, neurosurgery, and psychiatry*, 23(1), 56.
- Herzog, M. H., Kopmann, S., & Brand, A. (2004). Intact figure-ground segmentation in schizophrenia. *Psychiatry research*, 129(1), 55-63.
- Herzog, M. H., Roinishvili, M., Chkonia, E., & Brand, A. (2013). Schizophrenia and visual backward masking: a general deficit of target enhancement. *Frontiers in psychology*, 4, 254.
- Hoaglin, D. C., Mosteller, F., & Tukey, J. W. (1983). Understanding robust and exploratory data analysis. *Wiley Series in Probability and Mathematical Statistics*, New York: Wiley, 1983, edited by Hoaglin, David C.; Mosteller, Frederick; Tukey, John W.
- Hoaglin, D. C., Mosteller, F., & Tukey, J. W. (Eds.). (2011). *Exploring data tables, trends, and shapes* (Vol. 101). John Wiley & Sons.
- Karaaslan, F., Gonul, A. S., Oguz, A., Erdinc, E., & Esel, E. (2003). P300 changes in major depressive disorders with and without psychotic features. *Journal of Affective Disorders*, 73(3), 283-287.

- Kaustio, O., Partanen, J., Valkonen-Korhonen, M., Viinamäki, H., & Lehtonen, J. (2002). Affective and psychotic symptoms relate to different types of P300 alteration in depressive disorder. *Journal of Affective Disorders*, 71(1-3), 43-50.
- Kremen, W. S., Eisen, S. A., Tsuang, M. T., & Lyons, M. J. (2007). Is the Wisconsin Card Sorting Test a useful neurocognitive endophenotype?. *American Journal of Medical Genetics Part B: Neuropsychiatric Genetics*, 144(4), 403-406.
- Lee, S. H., Ripke, S., Neale, B. M., Faraone, S. V., Purcell, S. M., Perlis, R. H., ... & Absher, D. (2013). Genetic relationship between five psychiatric disorders estimated from genome-wide SNPs. *Nature genetics*, 45(9), 984.
- Lehmann, D., & Skrandies, W. (1980). Reference-free identification of components of checkerboard-evoked multichannel potential fields. *Electroencephalography and clinical neurophysiology*, 48(6), 609-621.
- Martin, E. A., Siegle, G. J., Steinhauer, S. R., & Condray, R. (2018). Timing matters in elaborative processing of positive stimuli: Gamma band reactivity in schizophrenia compared to depression and healthy adults. *Schizophrenia research*.
- Mullen, T., CleanLine. NITRC. 2012; <https://www.nitrc.org/projects/cleanline/>
- Nelson H (1976) A modified card sorting response sensitive to frontal lobe defects. *Cortex* 12: 313–324.
- Olbrich, S., & Arns, M. (2013). EEG biomarkers in major depressive disorder: discriminative power and prediction of treatment response. *International Review of Psychiatry*, 25(5), 604-618.
- Philiastides, M. G., Ratcliff, R., & Sajda, P. (2006). Neural representation of task difficulty and decision making during perceptual categorization: a timing diagram. *Journal of Neuroscience*, 26(35), 8965-8975.
- Plomp, G., Roinishvili, M., Chkonia, E., Kapanadze, G., Kereselidze, M., Brand, A., & Herzog, M. H. (2013). Electrophysiological evidence for ventral stream deficits in schizophrenia patients. *Schizophrenia bulletin*, 39(3), 547-554.
- Rosvold H, Mirsky A, Sarason I, Bransome E, Beck L (1956) A continuous performance test of brain damage. *J Consul Clin Psychol* 20: 343–350.
- Sax, K. W., Strakowski, S. M., Keck, J. P., Upadhyaya, V. H., West, S. A., & McElroy, S. L. (1996). Relationships among negative, positive, and depressive symptoms in schizophrenia and psychotic depression. *The British journal of psychiatry: the journal of mental science*, 168(1), 68-71.

Shaqiri, A., Willemin, J., Sierro, G., Roinishvili, M., Iannantuoni, L., Rürup, L., ... & Mohr, C. (2015). Does chronic nicotine consumption influence visual backward masking in schizophrenia and schizotypy?. *Schizophrenia Research: Cognition*, 2(2), 93-99.

Taylor, J. (2007). Heritability of Wisconsin Card Sorting Test (WCST) and Stroop Color-Word Test performance in normal individuals: implications for the search for endophenotypes. *Twin Research and Human Genetics*, 10(6), 829-834.

Taylor, M., & Creelman, C. D. (1967). PEST: Efficient estimates on probability functions. *The Journal of the Acoustical Society of America*, 41(4A), 782-787.

Curriculum Vitae

Personal Information

Name: Janir Nuno Ramos Antunes da Cruz

Date of Birth: 25th January 1990

Citizenship: Cape Verdean

Address: EPFL SV BMI LPSY, Station 19
1015 Lausanne, Switzerland

Tel.: +41 21 693 1742

E-mail: janir.ramos@epfl.ch

Education

Ph.D. in Neuroscience, École Polytechnique Fédérale de Lausanne (EPFL), Switzerland,
2015 - 2019

Ph.D. in Biomedical Engineering, Instituto Superior Técnico (IST), Universidade de
Lisboa, Portugal, 2015 - 2019

M. Sc. in Electrical and Computer Engineering, University of Macau, Macau, 2013 - 2015

Certificate of Honours College, Honours College, University of Macau, Macau, 2010 - 2013

B. Sc. in Electrical and Electronics Engineering, University of Macau, Macau, 2009 - 2013

Research Interests

Data science, human vision, schizophrenia, neuroimaging, brain-computer interface, neurofeedback training, and decision-making

Research Expertise

EEG (EEGLAB, FieldTrip, Cartool, and BCI2000)

Design, setup and perform experiments

Pre-processing and analysis of evoked-related potentials and resting-state data

Psychophysical experiments (Matlab and PsychToolbox)

Statistical analysis (Matlab, R, Python, SPSS, and JASP)

Frequentist and Bayesian

Machine learning

Writing manuscripts and research proposals (MS Word, Latex and Bibtex)

Language Skills

Portuguese (mother tongue), Creole (mother tongue), English (fluent), French (fluent), Spanish (good comprehension), and Mandarin (elementary)

Journal Articles

- da Cruz**, Shaqiri, Roinishvili, Chkonia, Brand, Figueiredo, and Herzog (submitted). Neural compensation mechanisms of siblings of schizophrenia patients as revealed by high-density EEG.
- da Cruz**, Favrod, Roinishvili, Chkonia, Brand, Mohr, Figueiredo, and Herzog (submitted). EEG microstates: a candidate endophenotype for schizophrenia.
- Favrod, **da Cruz**, Roinishvili, Brand, Figueiredo, Herzog, and Chkonia (submitted). Electrophysiological correlates of visual backward masking in patients with depression.
- Favrod, Roinishvili, **da Cruz**, Brand, Okruashvili, Gramkrelidze, Figueiredo, Herzog, Chkonia, and Shaqiri (2018). Electrophysiological correlates of visual backward masking in patients with first episode psychosis. *Psychiatry Research: Neuroimaging*, 282, 64-72.
- da Cruz**, Rodrigues, Thoresen, Chicherov, Figueiredo, Herzog, and Sandi (2018). Dominant men are faster in decision-making situations and exhibit a distinct neural signal for promptness. *Cerebral Cortex*, 28(10), 3740-3751.
- da Cruz**, Chicherov, Herzog, and Figueiredo (2018). An automatic pre-processing pipeline for EEG analysis (APP) based on robust statistics. *Clinical Neurophysiology*, 129(7), 1427-1437.
- Wan, **da Cruz**, Nan, Wong, Vai, and Rosa (2016). Alpha neurofeedback training improves SSVEP-based BCI performance. *Journal of Neural Engineering*, 13(3), 036019.
- da Cruz**, Wan, Wong, and Cao (2015). Adaptive time-window length based on online performance measurement in SSVEP-based BCIs. *Neurocomputing*, 149, 93-99.
- Cao, Wan, Wong, **da Cruz**, and Hu (2014). Objective evaluation of fatigue by EEG spectral analysis in steady-state visual evoked potential-based brain-computer interfaces. *Biomedical Engineering Online*, 13(1), 28.

Conference Papers

- Wang, **da Cruz**, and Wan (June 2015). Adaptive Fourier decomposition approach for lung-heart sound separation. *IEEE International Conference on Intelligence and Virtual Environments for Measurement Systems and Applications (CIVEMSA)*. Shenzhen, China.

- Wong, Tang, **da Cruz**, and Wan (June 2015). A multi-channel SSVEP-based BCI for computer games with analogue control. *IEEE International Conference on Intelligence and Virtual Environments for Measurement Systems and Applications (CIVEMSA)*. Shenzhen, China.
- Qu, Tang, Yang, Nan, **da Cruz**, Wan, Mou, Mak, Mak, Vai, Hu, and Rosa (June 2015). How mental strategy affects beta/theta neurofeedback training. *World Congress on Medical Physics and Biomedical Engineering*. Toronto, Canada.
- da Cruz**, Wang, Wong, and Fan (December 2014). Single-trial detection of error-related potential by one-unit SOBI-R in SSVEP-based BCI. *International Symposium on Neural Networks*. Hong Kong & Macau.
- Wang, Wong, **da Cruz**, Wan, Mak, Mak, and Vai (October 2014). Muscle and electrode motion artifacts reduction in ECG using adaptive Fourier decomposition. *IEEE International Conference on Systems, Man, and Cybernetics*. San Diego, CA, USA.
- da Cruz**, Wong, Cao, and Wang (November 2013). Patterned visual stimuli for enhancement of SSVEP-based BCI performance. *IEEE/EMBS Conference on Neural Engineering*. San Diego, CA, USA.
- da Cruz**, Wong, and Wang (July 2013). An SSVEP-based BCI with adaptive time-window length. *International Symposium on Neural Networks*. Dalian, China.

Selected Conference Abstracts

- da Cruz**, Favrod, Roinishvili, Chkonia, Brand, Mohr, Figueiredo, Herzog (June 2019). EEG microstates and the schizophrenia spectrum: evidence for compensation mechanisms. *Organization for Human Brain Mapping Annual Meeting*. Rome, Italy.
- da Cruz**, Favrod, Johnston, Figueiredo, and Herzog (May 2019). Neural correlates of target enhancement. *Vision Sciences Society Annual Meeting*. St. Pete Beach, FL, USA.
- da Cruz**, Roinishvili, Chkonia, Figueiredo, and Herzog (May 2018). Cholinergic dysfunction might affect backward masking performance: evidence from schizophrenia. *Vision Sciences Society Annual Meeting*. St. Pete Beach, FL, USA.
- da Cruz**, Roinishvili, Chkonia, Figueiredo, and Herzog (September 2017). Visual backward masking in siblings of schizophrenia patients: evidence for a compensation mechanism. *International Conference on Basic Clinical Multimodal Imaging*. Bern, Switzerland.

- da Cruz**, Favrod, Shaqiri, Roinishvili, Chkonia, Figueiredo, and Herzog (June 2017). Visual backward masking and the schizophrenia spectrum: EEG correlates. *Organization for Human Brain Mapping Annual Meeting*. Vancouver, Canada.
- da Cruz**, Thoresen, Rodrigues, Chicherov, Figueiredo, Herzog, and Sandi (May 2017). Social dominance orientation influences the perception of facial expressions. *Vision Sciences Society Annual Meeting*. St. Pete Beach, FL, USA.
- da Cruz**, Chicherov, Herzog, and Figueiredo (June 2016). A novel automatic pre-processing pipeline for EEG analysis based on robust statistics. *Organization for Human Brain Mapping Annual Meeting*. Geneva, Switzerland.
- da Cruz**, Roinishvili, Chkonia, Figueiredo, and Herzog (May 2016). Higher N1 responses in relatives of schizophrenia patients than controls in visual backward masking. *Vision Sciences Society Annual Meeting*. St. Pete Beach, FL, USA.

Awards

- Fonds Jean Falk-Vairant Prize for Best Clinical Neuroscience Poster or Presentation at the NeuroLeman Doctoral Schools Meeting, Les Diablerets, Switzerland, May 2019
- Best Clinical Poster at the National Centre of Competence in Research - Synapsy Annual Meeting, Villars-sur-Ollon, Switzerland, March 2018
- Best Behavior and Cognition Poster at the 2nd PhD Students Meeting of the Mind-Brain College, Universidade de Lisboa, Lisbon, Portugal, November 2016
- Companhia de Electricidade Macau (CEM) Academic Prize for Best Student Graduate in Electrical and Electronics Engineering, University of Macau, 2013
- First Prize IEEE Competition for Best Graduating Student Project for universities of Macau and Hong Kong, 2013
- Best Graduating Student Project of Faculty of Science and Technology, University of Macau, Academic Year 2012/2013
- Best Graduating Student Project of Department of Electrical and Computer Engineering, Academic Year 2012/2013
- Dean's Honor List, University of Macau, from 1st and 2nd Semester of Academic Year of 2012/2013
- Dean's List, University of Illinois at Urbana-Champaign, Spring 2012

Dean's Honor List, University of Macau, from 1st Semester of Academic Year of 2009/2010 to 1st Semester of Academic Year 2011/2012

Teaching experience

Bachelor project supervision - project: "EEG correlates of backward masking", EPFL, 03/2019 - 06/2019

Master project supervision - project: "Investigation of resting-state EEG patterns in schizophrenia patients and their non-affected relatives", IST, 02/2017 - 11/2017

Summer project supervision - project: "Neural correlates of target enhancement", EPFL, 07/2016 - 08/2016

Teaching Assistant for "Understanding Statistics and Experimental Design", EPFL, Fall 2015 and Fall 2017

Teaching Assistant for "Neuroimaging", IST, Fall 2016

Teaching Assistant for "Controls Systems", University of Macau, Fall 2013 and Fall 2014

Teaching Assistant for "Digital Signal Processing", University of Macau, Spring 2014

